

GEOLOGY, COLLAPSE MECHANISMS AND PREDICTION
OF COLLAPSIBLE SOILS IN EL LLANO, NEW MEXICO

By

Richard F. Reimers

Submitted in partial fulfillment
of the Master of Science degree
in Geology

New Mexico Institute of Mining and Technology

Socorro, New Mexico

January, 1986

ABSTRACT

Structural damage to private homes and public buildings in El Llano, New Mexico, prompted a geotechnical investigation by the New Mexico Bureau of Mines and Mineral Resources to study the possible causes. Ground subsidence and cracking around the damaged structures were attributed to collapsible soils--loose, dry, low density, fine to medium-grained sediment that compacts appreciably upon wetting either by man-induced or natural moisture intrusion.

El Llano rests on a low-gradient coalescing alluvial fan surface above complexly interbedded Holocene sediments. The principal processes of sedimentation on this surface are braided and arroyo channel, sheetflow and mudflow deposition. Silty and poorly graded sands interfinger with minor amounts of silt, clay and gravel lenses.

Most collapsible soils have dry densities ranging from 80 to 100 pcf, low moisture contents (1-10%), low Atterberg limits, and are poorly graded to silty sands with only minor amounts of clay (1-3%). Their soil structure is characterized by delicate grain point contacts, clay and silt aggregates that bond the larger sand grains together, clay coated sand grains (cutans), and high porosities from 30 to 40%.

Geologic cross-sections and fence diagrams across the study area reveal both the continuous and patchy nature of surface and subsurface collapsible soils. These sediments can be delineated using depth profiles of blow counts, moisture content and saturation, and dry density and density at liquid limit. Seismic refraction velocities and depth to the ground water table are also helpful in outlining collapsible zones.

The collapse mechanism of collapsible soils is evaluated on two levels: the "macro-mechanism" of surface subsidence and cracking; and the "micro-mechanism" of grain slippage and clay aggregate shear failure. Surface subsidence and cracking are caused by a loss of vertical support beneath the wetted area, soil hydrocompaction, the weight of the injected water itself, and by a small amount of true consolidation. Cracking around the subsidence area is characterized by sets of concentric tensional cracks, with offsets up to 15 inches, and by slight tilting of blocks in between each set of cracks. Zones of tensional and compressional strain develop around the cracks and blocks and cause differential settlement.

The process of collapse within the soil structure involves a reduction of shear strength from saturation. Clay and silt aggregates, loosely binding the sand grains, also lose their strength when wetted which enhances grain slippage and volume reduction. The dissolution of soluble

salts and cements in the soil by intruding water may also weaken the bonds between sand grains. A collapse mechanism experiment, in which four specimens were loaded to four different stresses and then wetted, showed the effect of saturation on collapse decreases with increasing overburden load. Another experiment demonstrated that these soils need not be 100% saturated to collapse but can exhibit large volume reductions at saturations less than 70%.

The collapse ratio, R , is used as the independent variable in a multiple, stepwise regression analysis. A logarithmic regression equation models El Llano soils the best. Liquid limit, plasticity index, dry density and per cent fines (silt and clay) control 96% of the variance in the collapse ratio.

The results of the discriminant function analysis show there is no significant difference between soil properties and collapsibility between soils located east and west of the El Llano acequia unless the level of significance is raised to 0.10.

TABLE OF CONTENTS

Abstract.....	ii
List of Figures.....	vi
List of Tables.....	viii
List of Appendices.....	ix
1.0 INTRODUCTION.....	1
1.1 Scope of completed NMBM&MR project.....	3
2.0 SCOPE OF THIS STUDY	8
3.0 TOPOGRAPHIC SETTING.....	9
4.0 CULTURAL SETTING.....	12
4.1 Climatic precipitation.....	16
4.2 Vegetation.....	16
5.0 REGIONAL STRATIGRAPHY.....	17
5.1 Pre-Santa Fe Group Rocks.....	17
5.2 Santa Fe Group Rocks.....	17
5.3 Post-Santa Fe Group sediments.....	20
6.0 STRUCTURE AND EVOLUTION OF ESPANOLA BASIN.....	23
7.0 PREVIOUS WORK ON COLLAPSIBLE SOILS.....	26
7.1 In the United States and abroad.....	26
7.2 In New Mexico.....	28
7.3 In El Llano and vicinity.....	30
8.0 GEOLOGIC CONDITIONS OF COLLAPSIBLE SOILS IN EL LLANO.....	31
8.1 Alluvial fan sedimentation.....	31
8.1.1 Mudflows.....	31
8.1.2 Textural characteristics of mudflows.....	36
8.1.3 Water-laid deposits.....	41
8.1.4 Eolian processes.....	42
8.1.5 Soil development.....	43
8.2 Alluvial fan morphology.....	45
8.3 General distribution and factors affecting the formation of collapsible soils.....	50
9.0 GEOTECHNICAL CONDITIONS IN EL LLANO.....	53
9.1 Description of laboratory field tests.....	53
9.2 Discussion of laboratory test results.....	57
9.2.1 Dry density.....	57
9.2.2 Moisture content and saturation.....	60
9.2.3 Atterberg limits and liquid limit vs.	

dry density criterion.....	62
9.2.4 Grain-size distribution and thin-section analyses.....	67
9.2.5 Modified and double consolidation tests and collapse potential.....	71
9.3 Analysis of cross-sections AA' to FF'-- surface and subsurface distribution of collapsible soils.....	77
9.3.1 Cross-section AA' (Plates 3A-3E).....	78
9.3.2 Cross-section BB' (Plates 4A-4E).....	81
9.3.3 Cross-section CC' (Plates 5A-5E).....	83
9.3.4 Geotechnical Ground Stabilization Study (GGSS)--fence diagram of GGSS Area 4 (Plates 6A-6F) and cross-section FF' (Plates 7A-7E).....	85
10.0 COLLAPSE MECHANISM.....	88
10.1 GGSS Areas 1-4 water-injection experiments...	89
10.2 Macro-mechanism.....	96
10.3 Micro-mechanism.....	106
10.3.1 Undisturbed, dry sample.....	109
10.3.2 Undisturbed, saturated sample.....	112
10.3.3 0.31 to 5.06 tsf, saturated samples....	116
10.3.4 Effect of varying moisture content and saturation at constant load.....	119
10.3.5 The role of clay and silt aggregates....	123
10.3.6 The role of clay mineralogy.....	125
10.3.7 The influence of soluble salts and cements.....	129
10.3.8 The hydrodynamic effect.....	132
11.0 EXISTING COLLAPSE PREDICTION CRITERIA.....	132
11.1 Denisov's (1951) coefficient of subsidence, K.....	135
11.2 Beles and Stanculescu's (1961) coefficient of collapse, τ	135
11.3 Prinklonskij's (1952) collapse criterion, K_d , for saturated soils.....	136
11.4 Feda's (1966) subsidence index, K_l	137
11.5 Gibbs and Bara's (1967a) collapse ratio, R.....	139
11.6 Comparison of criteria.....	142
12.0 REGRESSION AND DISCRIMINANT FUNCTION ANALYSIS-- SUGGESTED CRITERION FOR COLLAPSIBLE SOILS IN EL LLANO.....	142
12.1 Pearson Correlations.....	143
12.2 Stepwise Regression Analysis.....	143
12.3 Discriminant Function Analysis.....	147
13.0 CONCLUSIONS.....	150
ACKNOWLEDGEMENTS.....	156
REFERENCES.....	157

LIST OF FIGURES

FIGURE 1--	Location map of El Llano and vicinity.....	2
FIGURE 2--	Oblique aerial view of El Llano, New Mexico, showing area of most concentrated geotechnical activities.....	5
FIGURE 3--	Vertical aerial view of El Llano taken in 1949.....	7
FIGURE 4--	Regional topographic map.....	10
FIGURE 5--	Total number of structures in El Llano.....	13
FIGURE 6--	Geologic map of Española Basin.....	18
FIGURE 7--	Composite stratigraphic section and correlation chart of the Santa Fe Group in the vicinity of the study area.....	21
FIGURE 8--	Idealized mudflow showing lobate shape and thin margins.....	33
FIGURE 9--	Typical collapsible soil structures.....	37
FIGURE 10--	Scanning electron micrograph of a collapsible soil showing sand grains bonded loosely together by clay and silt aggregates.....	39
FIGURE 11--	Stereo SEM photograph of sand grains coated with clay (cutans).....	44
FIGURE 12--	Thin section photograph showing partial weathering of feldspars and rock fragments and hematitic staining.....	46
FIGURE 13--	Photograph of a Soiltest, Inc. medium- capacity consolidation apparatus and fixed- ring consolidometer.....	55
FIGURE 14--	Criterion for evaluating soil collapse.....	64
FIGURE 15--	Liquid limit vs. dry density criterion for soils located east and west of the El Llano acequia.....	66
FIGURE 16--	Cumulative grain-size distribution curves of collapsible soils of different origin.....	70
FIGURE 17--	Range of grain-size distributions for El Llano soils based on collapse ratio, R.....	72
FIGURE 18--	Typical El Llano collapsible soil consolidation curve showing its collapse potential.....	73
FIGURE 19--	Photograph of GGSS Area 3 showing extensive cracking and surface subsidence.....	92
FIGURE 20--	Photograph of GGSS Area 4 before collapse occurred.....	92
FIGURE 21--	Map of GGSS Area 4 (concrete foundations) showing well locations.....	93
FIGURE 22--	Photograph of GGSS Area 4 showing incipient surface subsidence and ground cracks on May 29, 1985.....	95

FIGURE 23--	Photograph of GGSS Area 4 showing near-to-maximum surface settlement and ground cracks on June 10, 1985.....	95
FIGURE 24--	Photograph of crack scarps and radial cracks at GGSS Area 4.....	97
FIGURE 25--	Diagrammatic sections showing a possible explanation of subsidence cracks.....	101
FIGURE 26--	Photograph of primary and secondary cracks at GGSS Area 3.....	103
FIGURE 27--	Idealized sketch of tensional, compressional and strain-free zones at GGSS Area 4.....	105
FIGURE 28--	Deformation of soil structure in tensional and compressional zones bordering a wetted area.....	105
FIGURE 29--	Void ratio vs. log stress consolidation curves and collapse potentials for the Collapse Mechanism Experiment samples.....	108
FIGURE 30--	Stereo SEM photograph of the undisturbed, dry sample from GGSSS-17, 4-6 ft.....	110
FIGURE 31--	Thin-section photograph of same sample as in Figure 30.....	111
FIGURE 32--	Stereo SEM photograph of the undisturbed, saturated sample.....	113
FIGURE 33--	SEM photograph of a point contact between two sand grains and the forces transmitted between them.....	114
FIGURE 34--	Model of a fine silty sand.....	114
FIGURE 35--	Mohr circles and failure envelope for a dry partially saturated soil (Circle 1) and a saturated, collapsed soil (Circle 2).....	117
FIGURE 36--	SEM photograph of the 5.06 tsf, saturated sample showing a honeycomb structure.....	118
FIGURE 37--	Void ratio vs. log stress consolidation curves for varying saturations of GGSSS-21, 9-11 ft. samples showing collapse potentials.....	121
FIGURE 38--	Relationship between collapse and saturation for soils compacted at the same dry density at different moisture contents.....	122
FIGURE 39--	Stereo SEM photograph of clay and silt particles in a loose "cardhouse" structure flocculated between two sand grains.....	124
FIGURE 40--	Schematic diagram of a soil microfabric and macrofabric.....	128
FIGURE 41--	Dynamic study of the failure of a clay aggregate.....	130
FIGURE 42--	Metastability evaluation graph.....	140
FIGURE 43--	Scatterplot of Collapse Ratio, R, vs. liquid limit displaying their relation to $\ln R = 0.6114 - 0.02039LL$	144

LIST OF TABLES

TABLE	1--Quantitative geomorphic properties of alluvial fans in California (Bull, 1964) and in El Llano.....	49
TABLE	2--Mean values, standard deviations, ranges and number of cases analysed for El Llano soil properties.....	58
TABLE	3--Means and standard deviations of properties for soils located east and west of the acequia.....	59
TABLE	4--Consolidation test data.....	75
TABLE	5--Water-injection and settlement data for the GGSS Areas.....	90
TABLE	6--Soil properties of the Collapse Mechanism Experiment samples.....	107
TABLE	7--Means, standard deviations and ranges of other workers' collapse criteria applied to El Llano soils for the entire study area.....	134
TABLE	8--Means, standard deviations and two-tailed probabilities at a 0.01 level of significance of other workers' collapse criteria applied to soils east and west of the El Llano acequia.....	134
TABLE	9--Unstandardized canonical discriminant function coefficients for soils located east and west of the acequia.....	148
TABLE	11--Classification results of soils located both east and west of the El Llano acequia showing percentages of correctly classified and misclassified cases.....	149

LIST OF APPENDICES

APPENDIX I.....	Plates 1-7
APPENDIX II.....	Climatic precipitation data
APPENDIX III.....	Trench logs
APPENDIX IV.....	Contour and crack maps of GGSS Areas 1-4
APPENDIX V.....	Pearson correlations of soil properties
APPENDIX VI.....	Laboratory data compilation tables

Late in November 1984 geologists from the New Mexico Bureau of Mines and Mineral Resources (NMBM&MR) investigated utility and structural damage and ground subsidence in the community of El Llano, northeast of Española, New Mexico (Fig. 1). After considering many possible causes, it was concluded that the large subsidence cracks around many of the houses and public buildings were due to collapsible soils. In response to Executive Order 84-76 (signed by Governor Toney Anaya in December 1984), which declared southern Rio Arriba and northern Santa Fe Counties within the Santa Cruz Grant a disaster area due to the ground subsidence, the NMBM&MR and its subcontractors began an extensive geotechnical investigation. This NMBM&MR study lasted until June 28, 1985, when the final report (Johnpeer and others, 1985b) was submitted to the Civil Emergency Preparedness Division in Santa Fe, New Mexico.

The purpose of the NMBM&MR investigation was to make data available for soil-stabilization recommendations around the condemned houses and public buildings as well as in areas yet to be developed. This study was not site specific but attempted to describe the geological, geotechnical, hydrologic and seismic conditions as they

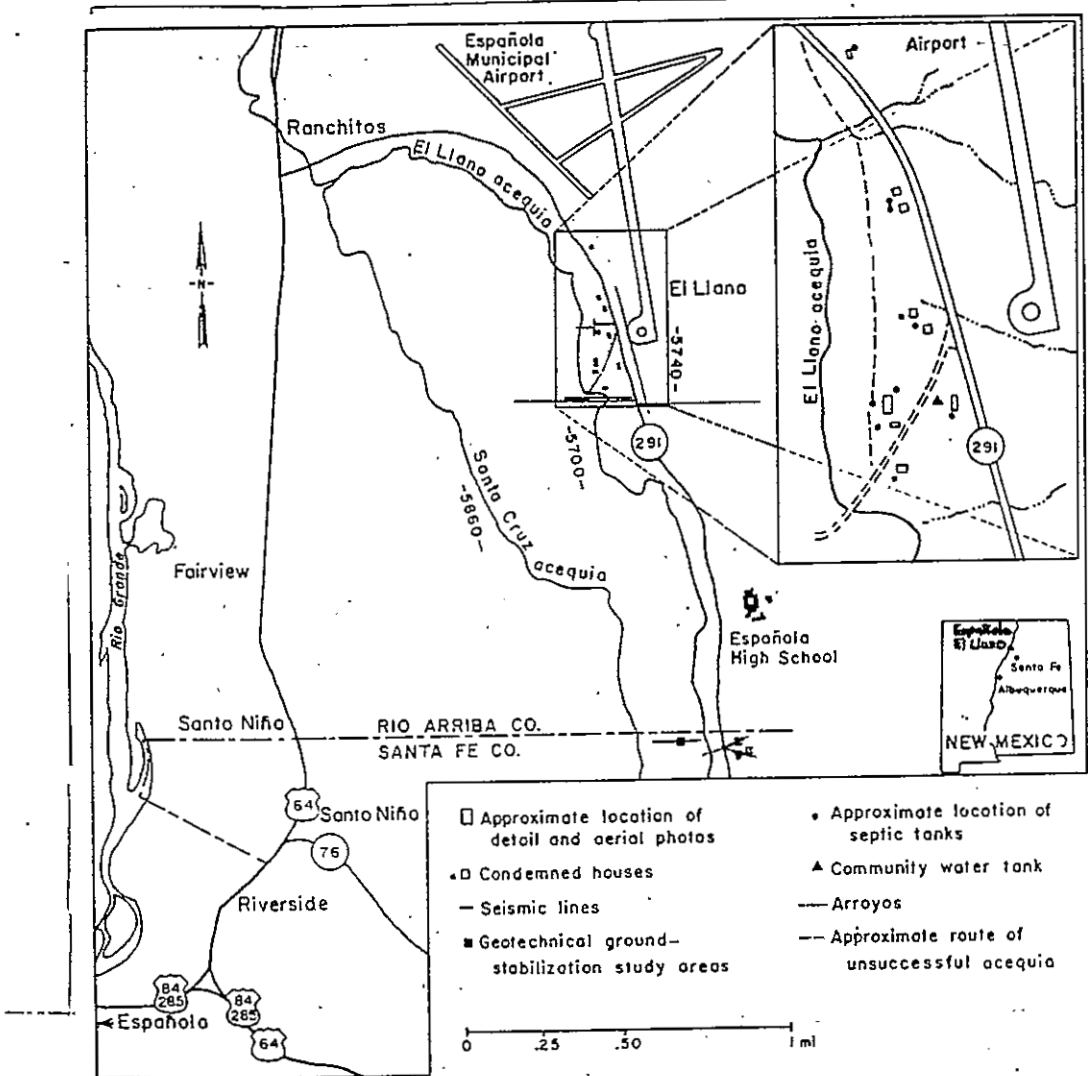


FIGURE 1--Location map of El Llano and vicinity (from Johnpeer and others, 1985b).

pertained to collapsible soils in the El Llano vicinity.

1.1 Scope of completed NMBM&MR project

Work conducted during the NMBM&MR study is described by Johnpeer and others (1985b). It consisted of an extensive literature review of existing maps, aerial photographs in the study area and other collapsible soil reports around New Mexico, the United States and the world. Detailed aerial and infra-red photographs and topographic maps of the study area were made. Geologic mapping of the surrounding area was conducted with special emphasis given to delineation of collapsible and non-collapsible units and to suspected faults.

The subsurface investigation consisted of drilling 102 wells to depths between 10 to 125 ft. A total of 560 disturbed (split-spoon) and 397 undisturbed (Shelby tube and continuous sampler) samples were obtained and later tested for grain size distribution, moisture content, dry density, Atterberg limits, consolidation, clay mineralogy and soil structure under a scanning electron microscope (Section 9.2).

The first forty-two boreholes were drilled in the El Llano area to investigate the subsurface conditions, to determine ground water levels and to monitor settlement around selected areas (Appendix I, Plate 1). The remainder of the boreholes drilled were a part of the Geotechnical Ground Stabilization Study (GGSS). In this separate study, water was injected through injection wells into the soil to induce subsidence at four different areas south of

Española High School (Appendix I, Plate 2). Boreholes around these four areas served for monitoring settlement, moisture content, and density and for identifying subsurface conditions and water injection.

Eleven trenches, ranging in depth from 7 to 12 ft, were excavated, shored, gridded and logged in detail to identify shallow subsurface conditions, soil type, and subsidence cracks at depth (Appendix III, Figs. 1-11). These trenches, all located in El Llano, served to pinpoint the depth of man-induced wetting of the soils from leaking septic tanks and broken water lines. Several soil and charcoal samples were also obtained from the trenches for age dating using carbon-14 methods. All samples tested gave ages younger than 3,000 years and confirmed the very young, Holocene age of these collapsible soils.

Seismic reflection and refraction surveys were conducted to enhance knowledge of subsurface conditions, to locate the ground water table and to delineate deep, buried faults in the Tertiary and older rocks. The locations of these surveys are shown in Plates 1 and 2. Identification of near-surface low velocity layers that may correlate with collapsible soils helped to outline critical areas of possible future subsidence.

Topographic and cultural surveys using a Lietz TM20H theodolite and stadia rod were performed at the subsidence depression west of the Moya residence (Fig. 2). This area was surveyed five times over a four-month period to detect any elevation changes. GGSS Area 2 was surveyed in a similar

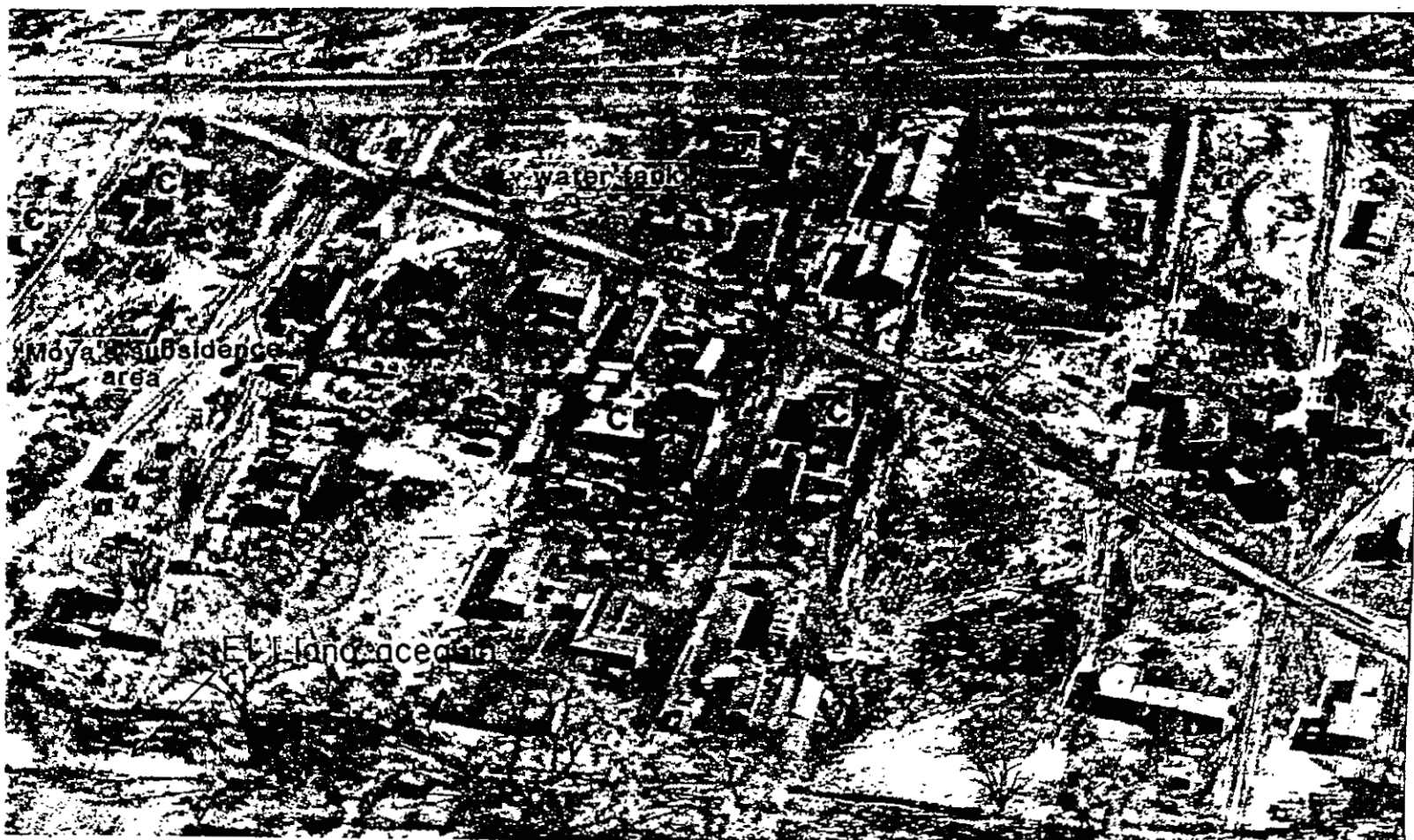


FIGURE 2--Oblique aerial photograph of El Llano, New Mexico showing area of most concentrated geotechnical activities. C=condemned house. View to east (from Johnpeer and others, 1985b). Photograph by J. Hawley, January 3, 1985.

manner. At GGSS Areas 1, 3 and 4 a string grid was established across each subsidence pit so that elevations from a datum could be more accurately recorded over time. Subsidence cracks in each area were also monitored and drawn at different times to see what effect water injection had on crack dimensions and rate of propagation (Appendix IV, Figs. 1-7).

A separate study to predict soil consolidation from consolidation observed in a controlled field experiment was conducted by Dr. Dan Stephens and Robert Knowlton of New Mexico Tech (Stephens and Knowlton, 1985). This experiment was conducted at GGSS Area 3.

Charles Carrillo, a historian from Albuquerque, was contracted to document the history and use of the acequias that transect El Llano. One active acequia runs roughly north-south through the study area (Fig. 2). Aerial photographs of El Llano show a faint presence of a smaller acequia located just east of the active one (Figs. 1 and 3), (Carrillo and Mirabel, 1985, p. 15). Because water in the acequias wets the soils to the west more than those located to the east on the alluvial fan surface, it is suspected that soil collapsibility may be partially dependent on the location and size of the acequias.

Dr. Robert McNeill and Mr. Robert Holt assessed the structural damage of the nine condemned houses in El Llano. For the most part, structural damage consisted of cracked foundation slabs and walls, separations between the stem wall and the rest of the building, corner-down-type



FIGURE 3--Vertical aerial view of El Llano taken in 1949. Note lack of development east of El Llano acequia (arrow) and extensive irrigation west of the acequia. The box represents the approximate location of Figure 2.

failures, and cracking near windows and doors where large stress concentrations are located (McNeill, 1985). Structural damage also occurred as upward heaving near the middle of the walls, slight rotation of the stem walls, horizontal translation outward and slight rotation of the corners about a vertical axis. All housing damage was photo-documented by Mr. Neil Hollander and the NMBM&MR staff.

Finally, monthly weather records over the past 90 years were compiled to assess the effect of rainfall on the study area. Preliminary investigation suggested that the increase in rainfall intensity and accumulation in the fall of 1984 contributed to increased soil saturation and subsidence in El Llano.

2.0

SCOPE OF THIS STUDY

The New Mexico Bureau of Mines and Mineral Resources final report (Johnpeer and others, 1985b) and subsequent lab testing of the remaining undisturbed soil samples released an enormous amount of data. However, due to time constraints and objectives of that emergency study, emphasis was placed on determining causes of subsidence and possible remedial measures. The main objective of this thesis, therefore, is to describe the geologic and engineering properties of collapsible soils in El Llano. This is done using detailed cross-sections and fence diagrams and laboratory

data statistical analyses. The collapse mechanism of collapsible soils both on the micro-and macro-scales is described using stereo scanning electron microscope photographs, clay mineralogy and content, consolidation tests and from analysis of surface cracks and subsidence at GGSS Areas 1, 3 and 4.

Finally, and perhaps most important, a collapse criterion is generated from a stepwise multiple regression analysis and compared with criteria of previous workers. Discriminant function analysis and T-tests using laboratory data from soils located both east and west of the El Llano acequia are conducted to determine if there is actually a difference in soil collapsibility between the two areas.

3.0

TOPOGRAPHIC SETTING

The study area is located in the central Espanola Basin at elevations from 5600 to 5800 ft (Fig. 4). The Espanola Basin is bounded by Precambrian-cored uplifts, the Nacimiento uplift along with the eastward-sloping, dissected Pajarito Plateau to the west and the southern Sangre de Cristo Mountains to the east. The western half of the basin is filled with volcanic rocks of the Jemez Mountains which define the western edge of the topographic basin that is only 20 mi wide. To the north and south, the Espanola Basin terminates near the basalts of the Servilleta Formation and

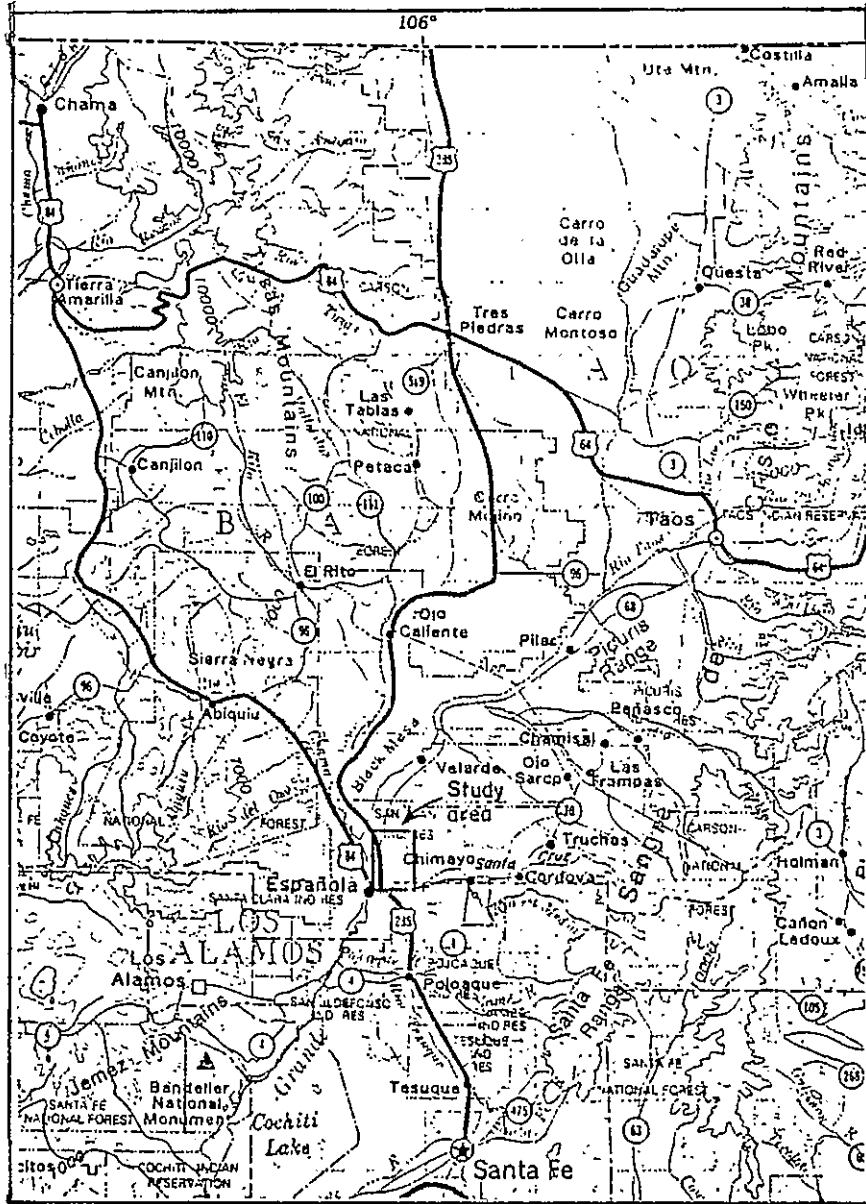


FIGURE 4--Regional topographic map.

the Cerros del Rio volcanic field, respectively.

The Española Valley is about 25 miles long and extends from Velarde to White Rock Canyon. The Rio Grande flows to the south with an average gradient of 11 ft per mi. The present Rio Grande floodplain is 1 to 3 mi wide.

The Rio Chama empties into the Rio Grande from the northwest just below San Juan Pueblo. The Santa Cruz River has an average gradient of 50 ft per mi and has most of its water diverted for irrigation. The Rio Chama and Santa Cruz River are the only perennial streams flowing into the Rio Grande near the study area. Numerous arroyos are tributary to the Rio Grande but these flow only a few hours on a few days during the year when heavy thunderstorms occur in the adjacent mountains. Large quantities of sand and silt and some gravel from the bordering alluvial fans and valley uplands are swept into the Rio Grande by the flash floods of sudden summer storms (Galusha and Blick, 1971, p. 98).

On the eastern side of the Española Basin are dissected foothills sloping westward toward the Rio Grande. A badland-type topography consisting of highly eroded Chamita and Tesuque Formations (Miocene) extends from an unconformable contact with the Precambrian granite of the Sangre de Cristos near Truchas and Chimayo to 2-3 mi east of the Rio Grande. Between the most western edge of these badlands and the Rio Grande floodplain are gently sloping (55-125 ft per mi) coalescing alluvial fans. The study area is located on the proximal and medial

reaches of these fans. On this surface river terraces occur discontinuously along both the Rio Grande and Santa Cruz River from San Juan Pueblo to La Plaza south of Española. Numerous incised and broad arroyos extend from the valley uplands westward across the study area.

The community of El Llano and GGSS Area 2 are located west of Airport Road (NM-291), and GGSS Areas 1, 3 and 4 are located east of this road (Plates 1 and 2). Acequias run subparallel to the Rio Grande from the north of San Juan Pueblo through El Llano to the agricultural areas of the Rio Grande floodplain. Two acequias from the Santa Cruz River, the Santa Cruz and El Llano acequias, trend northwest from Santa Cruz to Ranchitos (Fig. 1).

4.0

CULTURAL SETTING

To assess the impact of human activity and of the increased use of irrigation water from the acequias on the El Llano area two separate studies were conducted. The first involved counting the number of structures over the past 50 years using aerial photographs taken since 1935 (Fig. 5). The second study by Carrillo and Mirabal (1985) involved researching the history of the acequia systems.

The first Spanish explorers in northern New Mexico arrived in 1539 and their first settlement was established in 1598 on the west side of the Rio Grande across from San

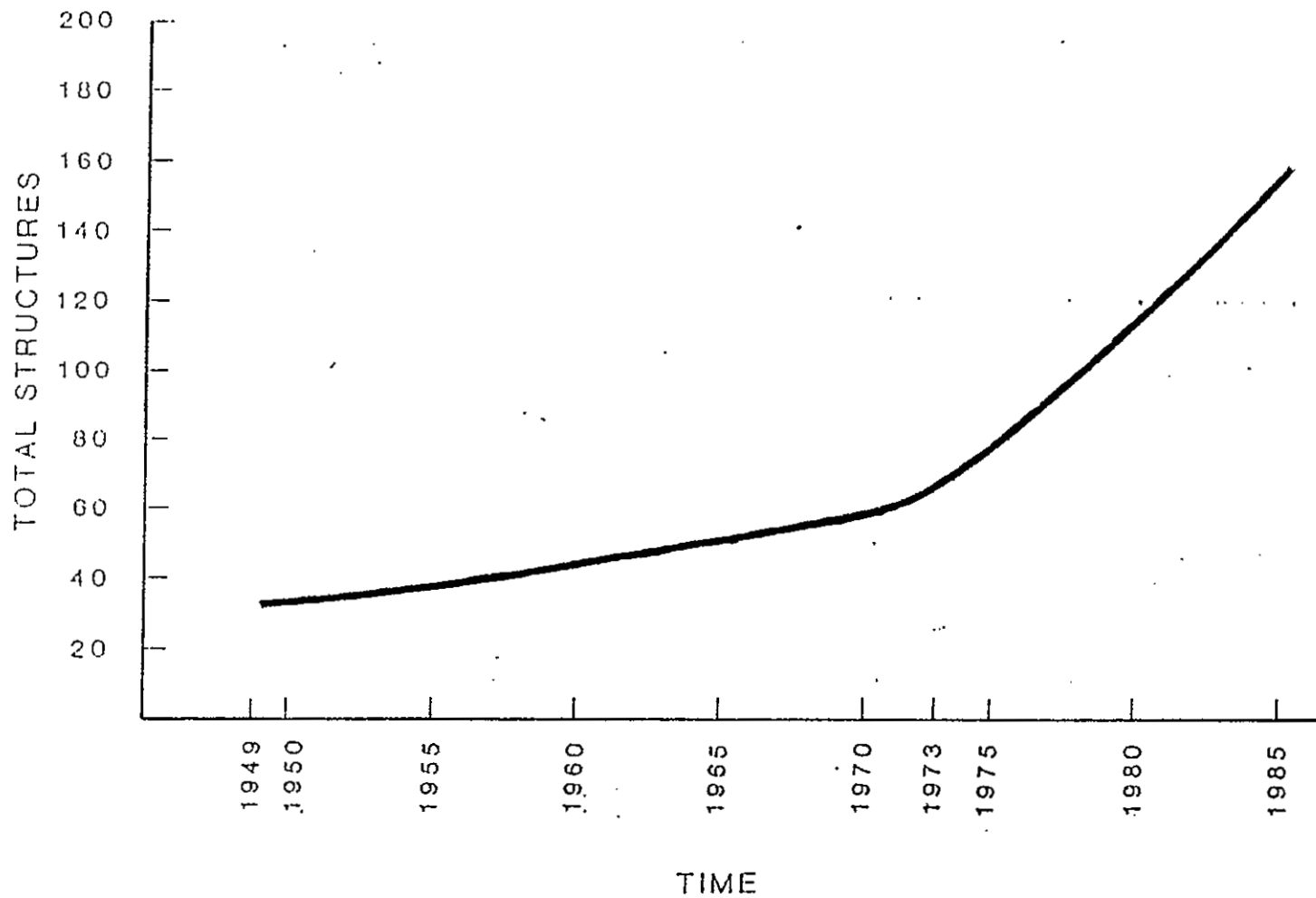


FIGURE 5--Total number of structures in El Llano (from Johnpeer and others, 1985b).

Juan Pueblo. Although there are no indications of any settlements in El Llano, the Spanish population continued to grow in the Española Valley during the 17th century. Both Indian and Spanish irrigation systems were in use in the study area prior to the Pueblo Revolt in 1680 (Carrillo and Mirabal, 1985, p. 3).

As settlements grew along the semi-arid Española Valley, the people constructed an irrigation ditch sufficiently large to convey water to their lands for the irrigation of crops. Individuals owned and cultivated a specific tract of land which was perpendicular to the acequia. The development of the study area in recent years may have contributed to the ground subsidence. Individual tracts of land were divided among male and female heirs according to Hispanic custom (Carrillo and Mirabal, 1985, p. 16-17). Thus each strip of land became narrower with time. Leaking septic tanks, broken utility lines and other causes of local soil moisture now affects many houses due in part to their close proximity.

Although the entire Santa Cruz acequia was lined with concrete in 1964 (Carrillo and Mirabal, 1985, p. 13), most of the El Llano acequia remains unlined to allow water infiltration. In addition to the Santa Cruz and El Llano acequias, there are literally hundreds of small sangrias (veins) that divert water to various fields. Water in both acequias follows the contour of the land from the Santa Cruz River to El Llano. Water is usually diverted into the two acequias from spring through late fall.

In addition to the two older acequias, another built by the Mormons in the late 19th century extended from Velarde southward along the talus slopes east of the Rio Grande into El Llano. The remains of this abandoned acequia are slightly visible on aerial photographs going back to 1935 (Fig. 3). This acequia was short-lived due to numerous washouts where it crossed arroyos. Therefore soils east of the main El Llano acequia on this westward sloping alluvial plain are undisturbed. This is also the area where most of the reported structural damage and ground subsidence has occurred. In contrast, soils west of El Llano acequia have been irrigated and saturated for about 300 years. Consequently, these soils have already largely collapsed. The GGSS Area 2 water-injection study further supports this assumption (Sec. 10.1). No incidences of structural damage due to collapsible soils have been confirmed west of the acequia.

The El Llano community water well was dug sometime between 1936 and 1949. A small reservoir tank is located just west of one of the condemned houses (Fig. 2). Residents report that the tank periodically overflows, allowing water to saturate the foundation soils. As a result, the tank has settled and leaned significantly, rupturing water pipes leading to and from it (Johnpeer and others, 1985b, p. 5-2). In borehole ESPDH-4, located just west of the tank, soil-moisture contents were exceptionally high down to 56 ft.

Most houses in El Llano are adobe with conventional slab foundations, have no rain gutters and downspouts, and

are not landscaped to accommodate surface runoff well. Ponding of water is common around many houses and some residents sprinkle their lawns during the summer months. Furthermore, several arroyos extending westward down the alluvial fan surface intersect Airport Road (NM-291) and occasionally cause water ponding in the study area during summer cloudbursts.

4.1 Climatic precipitation

Rainfall data collected over the past five years (Gabin and Lesperance, 1977) display a normal monthly precipitation pattern increasing from January to June, a sharp increase in July and August, and a gradual decrease from September to December (Appendix II, Fig. 1). However, in 1984 the wettest month occurred in October when 2.93 inches of rain were recorded (Appendix II, Fig. 2). On three days during that month precipitation was greater than 0.5 inches. Shortly thereafter, in November, much of the structural damage due to differential settlement from collapsible soils was reported.

4.2 Vegetation

Although most of the study area is developed and/or cultivated, the surrounding alluvial aprons to the east support native grasses, rabbitbrush, yucca, prickly pear and other types of cactus. Cottonwood trees line the El Llano and Santa Cruz acequias.

5.0

REGIONAL STRATIGRAPHY

5.1 Pre-Santa Fe Group Rocks

El Llano is located in north-central Española Basin, one of a series of north-south aligned Cenozoic structural and topographic basins comprising the Rio Grande rift from central Colorado to southern New Mexico (Chapin, 1971; Manley, 1978a). The southern Sangre de Cristo Range on the east and Nacimiento and Jemez Mountains on the west border the Española Basin. Regional uplift surrounding the basin has occurred over the past 10-12 m.y. (Chapin, 1971).

The Sangre de Cristo Mountains consist of crystalline rocks older than one b.y. They are overlain by thick sequences of Paleozoic and Mesozoic sedimentary rocks which dip gently westward beneath the Española Basin. The Precambrian core of the Nacimiento uplift on the western margin of the Española Basin is covered with volcanic rocks ranging in age from 9.1 m.y. to about 100,000 yrs (Fig. 6).

5.2 Santa Fe Group Rocks

In the vicinity east of the study area, lower to upper Miocene rocks of the Tesuque and Chamita Formations (Santa Fe Group) are exposed. The Tesuque Formation in the north-central Española Basin is composed of three Members: the Nambé, Skull Ridge and Pojoaque. These sediments were deposited between 20 and 8 m.y. as basin-fill alluvial deposits shed from the uplifting Sangre de Cristo

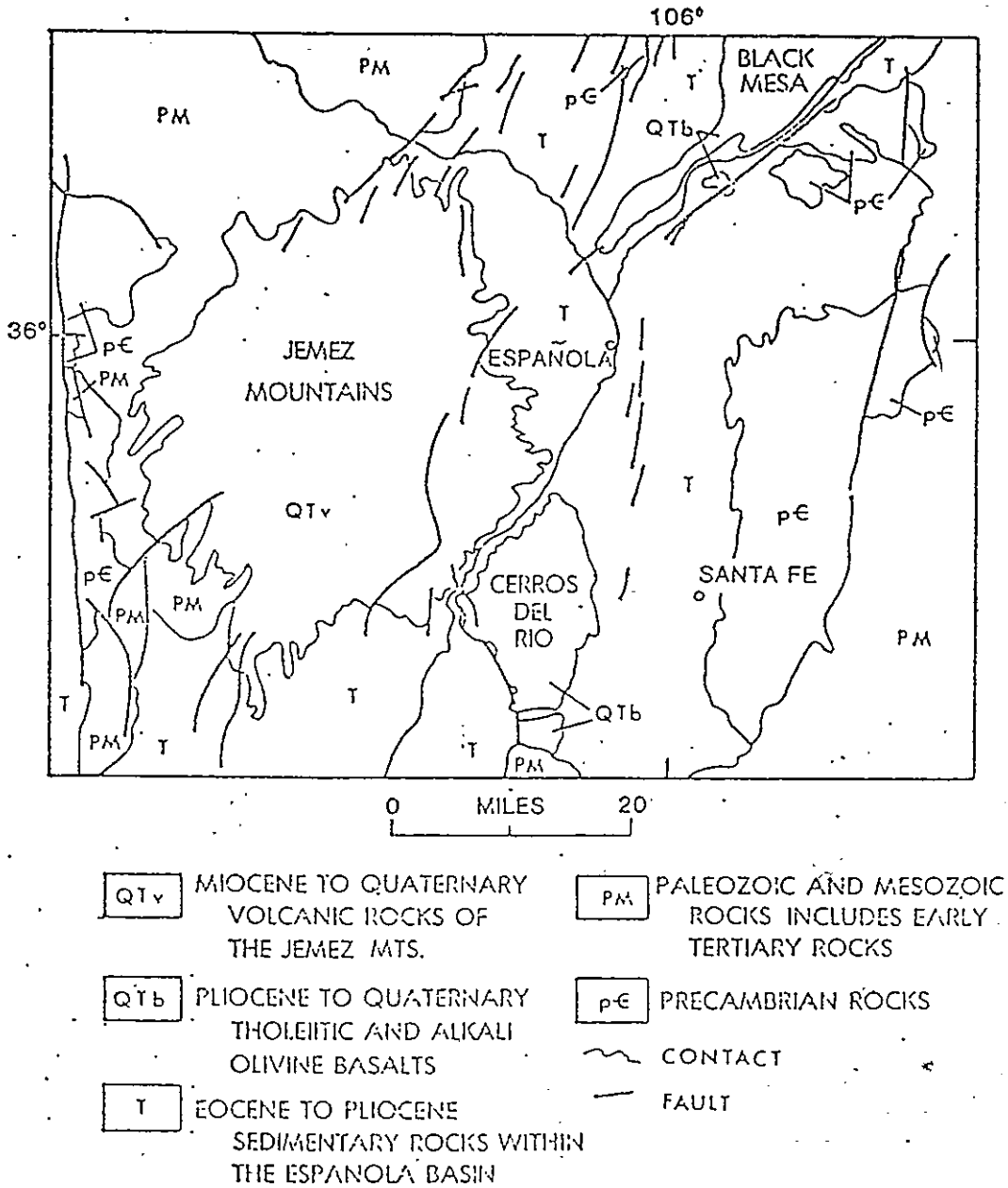


FIGURE 6--Geologic map of Española Basin (from Manley, 1978a, p. 4).

Mountains. East of the study area the Pojoaque Member of the Tesuque Formation and the Chamita Formation are exposed in a badland-type topography and form high bluffs and mesas that are dissected by numerous arroyos.

The Pojoaque Member is a salmon or pink to buff, tan to grey sequence of partially consolidated sandstone, siltstone and mudstone with conglomeratic lenses. Numerous white to grey ash beds derived from the Jemez Mountains provide good correlation markers in the Pojoaque Member. In general, these rocks are exposed in a great semicircular belt of isolated groups from Chimayo, north of Santa Cruz, Espanola, to Pojoaque, New Mexico (Galusha and Blick, 1971, p. 64).

North and west of the study area the Chama-el rito Member (which is a time equivalent to the Pojoaque Member) is exposed. This sequence consists of well-rounded pebble-to cobble-sized volcanic clasts interbedded in buff to pinkish, coarse to fine, soft sandstone and siltstone. These rocks were derived from volcanic source terrain in northern New Mexico and the San Juan Region in Colorado.

The late Miocene Chamita Formation unconformably overlies the Pojoaque Member and Ojo Caliente Sandstone of the Tesuque Formation east and north of the study area. This formation consists of coarse sands and gravelly sandstones interlayered with two distinct zones of tuffaceous beds. The lower zone has 80 ft of coarse sand and gravel layers with 4 to 5 dark ashy layers, while the upper zone consists of 100 ft of white to pink tuffaceous

beds intercalated with quartzitic sands and gravels (Manley, 1978a; Galusha and Blick, 1971).

Both the Chamita and Tesuque Formations strike roughly northeast and dip 4° to 6° northwest. Nearly 5000 ft of these Santa Fe Group basin-fill sediments have been measured in the Española Basin (Galusha and Blick, 1971; Fig. 7). Seismic reflection work done during the NMBM&MR study revealed that these Santa Fe rocks are at least 2700 ft thick beneath El Llano.

5.3 Post-Santa Fe Group sediments

Over the past five million yrs the Rio Grande and its tributaries have shaped the present landscape in the Española Valley. The ancestral Rio Grande originally flowed near the level of the high mesas where the Chamita and Tesuque Formations are exposed around the outer rim of the Española Valley. The inner valley comprises the modern Rio Grande floodplain and alluvial fans built by tributary arroyos, mudflows and sheetflows. On the present alluvial aprons are remnants of former valley-floor deposits of the ancestral Rio Grande. These sands and gravels are located north of the study area near San Juan Pueblo, beneath Black Mesa and along terraces of the Santa Cruz River. The tremendous erosive power of the ancestral Rio Grande not only left these elevated, remnant terrace gravels, but also removed several cubic mi of sediment in the Española Valley (Hawley, 1978).

Several boreholes in the study area penetrated

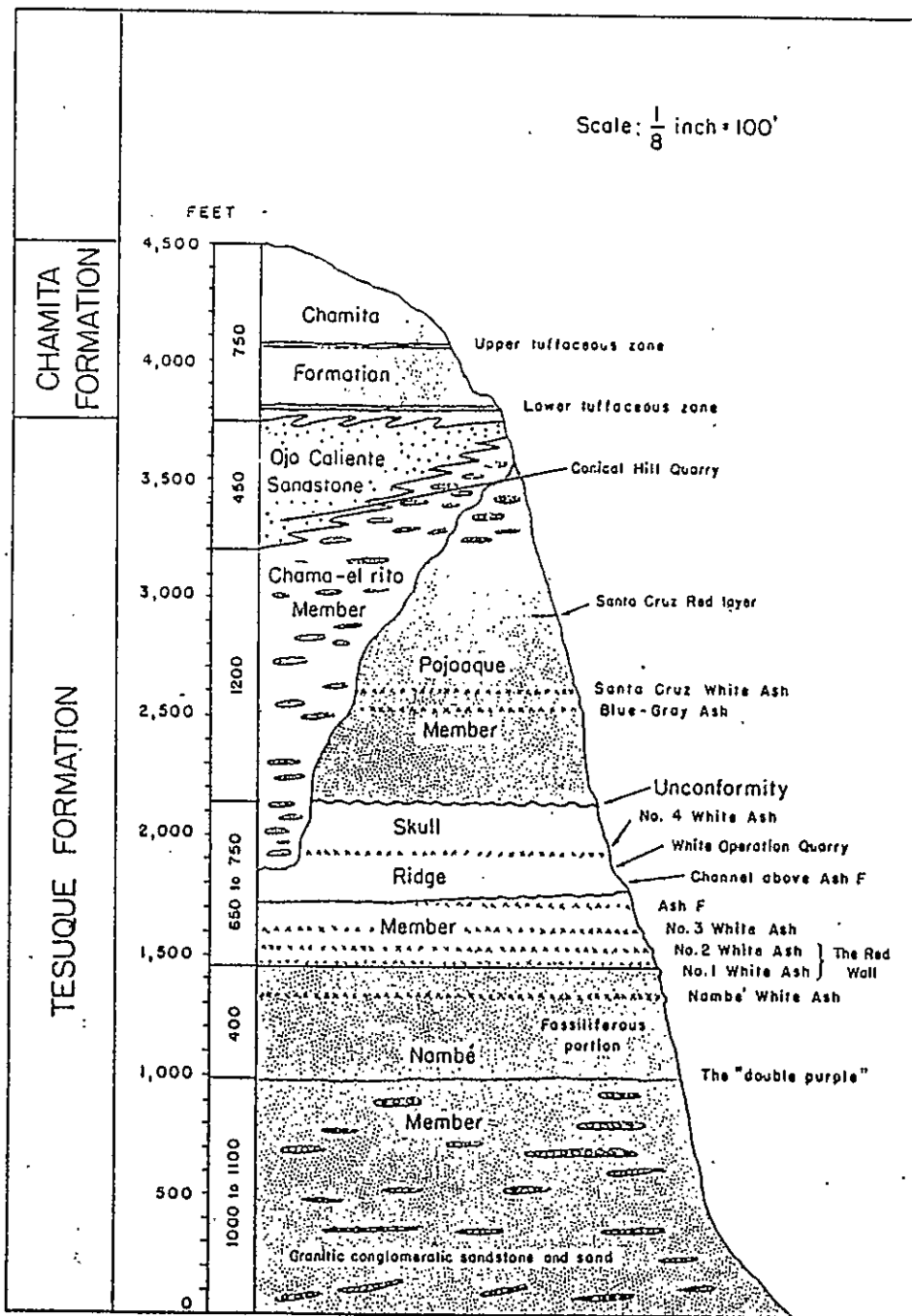


FIGURE 7--Composite stratigraphic section and correlation chart of the Santa Fe Group in the vicinity of the study area (from Galusha and Blick, p. 31).

the ancestral Rio Grande sands and gravels (Qrg) at an average elevation of 5610 ft. These sediments dip 11 ft/mi to the south and closely approximate the present Rio Grande gradient. The sediments consist of sandy gravels and gravelly sands (GP and SP-SW in the Unified Classification System) with local lenses of silt and clay. Blow counts (obtained from standard penetration tests during drilling) are commonly greater than 50 in these deposits. In addition, the deposits are near or below the water table and thus are saturated (see Plates 3A, 4A and 5A). All of these properties indicate these sands and gravels have a high bearing capacity with little susceptibility to consolidate further.

The main geologic unit of concern in this study of collapsible soils is the young (<10,000 yrs) Holocene alluvium that supports most of the structures in El Llano. These alluvial fan deposits were emplaced by ephemeral streams, mudflows and sheetflows emanating from the high mesas to the east. A discussion of these depositional processes and the types of collapsible soils they produce is given in Section 8.0.

Silty sands (SM) and poorly graded sands (SP) interbedded with gravel, silt and clay lenses characterize these alluvial deposits. Thicknesses of the young alluvium range from 100 to 125 ft beneath El Llano to as little as 8 ft near GGSS Areas 1, 3 and 4 (see Plates 3A-7A). Dips vary from 1° to 2° following the present alluvial fan surface. These sediments are well above the water table,

which is located below the study area at elevations between 5600 and 5650 ft. Their porous, dry, unsaturated and loose nature makes them highly vulnerable to consolidation upon wetting and/or loading.

6.0 STRUCTURE AND EVOLUTION OF ESPAÑOLA BASIN

The Española Basin is a sagged and faulted syncline with tilted fault blocks that are collapsed parts of a broad area of the Laramide structural uplift (Chapin, 1971). The western limb of the basin is broken by the Pajarito fault zone, a series of down-to-the-east faults concealed by volcanic rocks of the Jemez Mountains, into eastward-tilting blocks of Santa Fe rocks.

The eastern limb of the Española Basin appears to lack a graben-style border, but instead merges with the west-tilted Santa Fe block of the Sangre de Cristo uplift. In many locations Santa Group sedimentary rocks nonconformably overlie Precambrian or unconformably overlie Pennsylvanian rocks of the Sangre de Cristo Range suggesting an onlap relationship; there is no thick deposit of Tertiary sediment abutting the Sangre de Cristo uplift (Manley, 1978a, p. 12). Thus it appears that either the eastern border is a series of step faults or is not a fault-controlled border.

High angle, normal, intrabasinal faults cutting

Santa Fe Group rocks in the eastern half of the basin are of limited extent (traces less than two mi) with displacements less than 300 ft. Most faults strike north to northeast, following the trend of the Española Valley. The average angle of dip is about 70° . Fault traces show a marked sinuosity with dip directions both east and west. This results in closely spaced horsts and grabens within the Santa Fe Group rocks (Galusha and Blick, 1971).

In particular, the faulting just east of the study area in the high mesas of Santa Fe Group rocks is mostly post-Tesuque in age. Only two faults can be traced northwest along exposures of bedrock east of Española. One well exposed fault trends northwest through the Española landfill. Dipping southwest, this fault has offsets of 10 to 20 ft. Another fault east of the landfill trends N. 20° W. and dips 65° to 85° to the southwest with approximately 60 ft of displacement. This eastern fault zone is 20 ft wide and actually consists of a number of small faults. The fault surfaces are coated with clay or calcium carbonate making them more resistant to erosion than the surrounding beds. Fault traces are associated with topographic highs and adjacent eroded areas between these highs are partially filled with Holocene alluvium that has not been offset by the fault. This fault zone is buried by ancient terrace gravels north of the Santa Cruz River (Johnpeer and others, 1985b, p. 6-14). According to D. Love (pers. comm., 1985) the last fault movement probably occurred more than

one million years ago.

Two other fault zones intersect the Tesuque and Chamita Formations east of Española Municipal Airport. The first, more prominent zone trends N. 41° W. and dips 73° northeast to vertical with an offset between 10 and 30 ft. The fault trace is buried by alluvium which it does not offset. The second fault zone trends N. 38° E., dipping between 51° and 86° to the southeast. Both fault zones form part of a faulted monocline with a faulted syncline in their downthrown blocks (Johnpeer and others, 1985b, p. 6-15).

A seismic reflection profile across the El Llano area (Plate 1) indicates that the Santa Fe beds are located at depths between 50 and 125 ft below the ground surface. The major structural features affecting these Miocene rocks are, from east to west: a shallow syncline overlying an apparently deeper graben; a gentle anticline draped over a deeper horst approximately beneath the center of seismic line ES-1; and a slight rise centered beneath the end of seismic line ES-1, which may be a buried hill or ridge. On seismic line ES-2 and cross-section AA' (Plate 3A) there is evidence of a minor east-dipping fault with offset less than 25 ft and a second fault dipping west with slightly greater displacement. Neither fault penetrates the overlying Holocene alluvium (Reynolds, 1985).

If the faults east and west of the Española landfill are projected northwestward towards El Llano, they generally correspond to those faults interpreted on seismic

reflection line ES-2. However, the sense of movement on the eastern fault is interpreted seismically as being down to the east, whereas the fault, exposed to the south of the study area, displays a down-to-the-west direction.

7.0 PREVIOUS WORK ON COLLAPSIBLE SOILS

7.1 In the United States and abroad

Collapsible soils generally consist of loose, dry, low density, medium-to fine-grained material that compacts appreciably when wetted. They have long been known in the San Joaquin Valley, California, Arizona, the midwestern United States, South Africa, Romania, Bulgaria, Australia, Russia and China. Bull (1961, 1964, 1972), Bara (1972, 1975), Curtin (1973), Gibbs and Bara (1967a, 1967b), Johnson and Moston (1968), and Prokopovich (1963, 1975, 1984) have exhaustively studied subsidence due to hydrocompaction along the San Luis Canal in the San Joaquin Valley, California. Some of the first water injection studies to induce soil collapse were conducted in this area. Some workers developed collapse criteria to predict the occurrence of collapsible soils.

Other workers who have studied collapsible soils in Tucson and Phoenix, Arizona include Alfi (1984), Anderson (1968), Crossley (1968), Platt (1963), and Sultan (1969, 1971). Lobdell (1981) reported on the collapsible Palouse loess in southeastern Washington.

A water flooding study to induce soil collapse along Interstate 70 in western Colorado was conducted by Shelton and others (1975). The U.S. Bureau of Reclamation (1980) and Arman and Thorton (1973) studied collapsible loessical sediments in Missouri and Louisiana, respectively.

Internationally, collapsible soils have been widely researched for over forty years in Russia by Denisov (1946, 1951), Krutov and others (1984), Litvinov (1961), Minkoy (1984), and Prinklonskij (1952). The Russians pioneered some of the first chemical and thermal stabilization methods for collapsible loessical soils. They also devised a number of collapse index equations used for evaluating the collapsibility of loessical and alluvial deposits (Section 11.0). Fedá (1966) did much of his work in Bulgaria and Romania and also invented a useful collapse index equation. In northern China, Lin and Liang (1979) reported on the engineering properties and geographic distribution of collapsible loess and alluvial fan sediments. Finally, Haq (1976) researched the hydrocompaction around the Chashma Right Bank Canal in India.

Much of the work on the geology, engineering properties, collapse mechanism, effect of clay, microstructure and hydrology of collapsible alluvial fan and residual granite soils has been done in South Africa by the following authors: Aitchison (1973), Booth (1975), Bishop and Blight (1963), Brink and Kantey (1961), Ingles (1964), Ingles and Aitchison (1969), Jennings and Burland

(1962), Jennings and Knight (1956, 1957, 1975), Knight (1959, 1961, 1963), and Knight and Dehlen, (1963).

7.2 In New Mexico

Only within the last 20 yrs have collapsible soils taken on major importance in road and building construction in New Mexico. One of the first discoveries of collapsible soils occurred in the late 1960's at a maintenance patrol yard in Alcade between Española and Velarde, about 3 miles north of El Llano. Several inches of differential settlement took place at the west end of the maintenance building following landscaping and lawn watering (Lovelace and others, 1982, p. 2). Since this time several other cases of structural damage due to collapsible soils have been reported in New Mexico.

The paucity of literature pertaining to collapsible soils in New Mexico clearly marks the need for more geotechnical investigations and laboratory testing of these sediments. Beckwith (1976) outlined the occurrence of collapsible soils along the Rio Grande rift. He described their deposition from mudflows emanating from the bordering mountains. He also noted that other weakly cemented dune sands, sodium-rich dispersive clayey silts, and residual granite soils weathered from the Sandia granite also collapsed when wetted.

Clary (1980) and Clary and others (1984) briefly delineated the collapsible soils found around Albuquerque's Northeast Heights. These sediments were derived from mud and

debris flows originating from the canyon mouths of the Sandia Mountains. More specifically, buildings in the area bounded by Juan Tabo, Comanche, Morris and Candelaria Boulevards, Tanoan Village and Montessa Police Park have experienced differential settlement and structural damage apparently due to collapsible soils.

Woodward-Clevenger and Associates (1973) performed a geotechnical investigation on the Montessa Police Park south of Albuquerque to determine the character and extent of the collapsible soils and to try to stabilize the buildings there. Augercast piles were first installed to 30 ft to underpin the cracking foundations but were unsuccessful in arresting the differential settlement. The firm recommended underpinning the foundation to a depth of 125 ft because borehole data indicated that collapsible soils existed to well below 100 ft.

In 1979 the New Mexico State Highway Department conducted a collapsible-soil compaction study on a three-mile stretch of Interstate 25 near Algodones, New Mexico. This part of the highway lies on loosely consolidated, dry alluvial apron deposits ranging in thickness from 20 to 25 ft. Soon after the interstate opened in 1955 sags and waviness developed on its surface. Subsurface soil investigation revealed the sediments had a consolidation potential of 31 inches throughout a 20 ft depth. The New Mexico State Highway Department tested several soil stabilization methods in the area: dynamic compaction; vibrofloatation; ponding with reverse sand drains; and

compacting and wetting the soils above their optimum moisture content (Lovelace and others, 1982).

7.3 In El Llano and vicinity

Most of the geotechnical work done around El Llano has been conducted at the Vista del Rio subdivision located only a few hundred yards south of GGSS Areas 1, 3 and 4. In 1979 Valdez Engineering & Testing drilled six exploratory borings, collected soil samples and did standard penetration tests in the proposed subdivision area. They found the subsurface conditions consisted of silty to clayey sands (SM, SC) and poorly graded sands (SP) to a depth of 15 ft. The foundation and footing recommendations stressed the importance of preventing any wetting of the subsurface soils, which, if occurred, would lead to consolidation and differential settlement underneath the structures (Valdez, 1979).

The most recent geotechnical work in the Vista del Rio subdivision was in early 1985 by Albuquerque Testing Laboratory, Inc. Engineers drilled thirteen 10 to 35-ft test borings, performed standard penetration tests and took soil samples for laboratory testing. They also found the subsurface soils to be silty to clayey sands (SM, SC) and sandy silts (ML) which were very loose and dry. They noted the extreme soil collapse potential from any moisture intrusion. Recommendations for construction included soil prewetting to 5 ft, proof rolling, positive drainage and the use of continuous reinforced concrete

footings (BRAB slab), (Clary and Korecki, 1985).

8.0 GEOLOGIC CONDITIONS OF COLLAPSIBLE SOILS IN EL LLANO

8.1 Alluvial fan sedimentation

El Llano rests on Holocene alluvium consisting mostly of silty to clayey sands (SM, SC) interbedded with poorly graded and gravelly sands (SP, SW); sandy gravels, (GP); and silt and clay lenses (ML, MH, CL, CH). The alluvium ranges in thickness from 30 to 120 ft in the vicinity of the study area. This wedge-shaped layer of alluvium was deposited primarily as coalescing alluvial fans by tributary arroyos, small braided channels, mudflows and sheetflows.

The increase in precipitation and decrease in temperature during the last glacial age (>15,000 yrs) augmented runoff from the bordering mountains into the Española Basin. Coalescing alluvial fans grew toward the axis of the Española Basin. During post-glacial times runoff decreased and drainage channels aggraded and were filled with mostly fine to medium-grained silty sands derived from the Tesuque and Chamita Formations.

8.1.1 Mudflows

Intense flooding on the alluvial apron and on the valley uplands near El Llano caused numerous mudflows-- each layer was deposited by an individual flash flood. One

layer was largely dried before another layer was deposited. Furthermore, each layer was buried by subsequent flows without ever being wetted or consolidated under its own weight. This process produces a very porous, low density, dry, under-consolidated and moisture-sensitive soil that when subject to water infiltration can reduce drastically in volume.

Mudflows have been described by Blackwelder (1928, p. 467) as "a thick film of muddy slim viscously rolling over a gentle rolling plain" (Fig. 8). They are lobate in shape with thin layers and steep margins commonly containing twigs, shrubs, branches, and sometimes uprooted trees. Some of the soil samples taken from shallow depths in trenches and boreholes around El Llano contained decaying vegetative matter. Some samples even displayed open root casts and channels.

Several conditions favor mudflows: steep slopes in the source area to induce rapid erosion; unconsolidated to loosely consolidated material that contains enough clay to make the mass flow when wet; short periods of intense rainfall; and insufficient vegetative protection (Bull, 1964, p. A22). Some of these conditions prevailed in the valley uplands and on the alluvial fan surface east of El Llano over the past 10,000 yrs. The "ideal" material for a mudflow is a gravelly, sandy mass containing enough swelling clay so that when swelling occurs the internal cohesion of the mass decreases to allow movement. The loosely consolidated sandstones and siltstones of the



FIGURE 8--Idealized mudflow showing lobate shape and thin margins
(Drawn by M. Wooldridge).

Chamita and Tesuque Formations interbedded with conglomeratic, clayey and bentonitic volcanic-ash layers were good source rocks for mudflows east of the study area.

If more than half of the solid fraction of a mudflow consists of material larger than sand size (> 4.76 mm), it is termed a debris flow (Bates and Jackson, 1980). An insignificant number of gravel layers were encountered either in the boreholes or in the trenches compared with the abundance of fine-to medium-grained silty sand layers. Stringers of gravel penetrated were probably buried arroyo-channel bottoms consisting of lag deposits. The lack of abundant coarse-grained material in the source area as well as the lack of any steep gradient on the fan surface probably inhibited formation of debris flows. Mudflows, stream channel and sheetflow deposits were probably the most active depositional processes building the alluvial wedge in the vicinity of the study area.

Even though conditions favoring mudflows may only occur every several hundred years, mudflow deposits are ubiquitous throughout the study area. Single mudflow units often overlap and bury sinuous threads of stream sand and gravel (Plates 3A, 4A and 5A). Small amounts of poorly graded stream sands and gravels are surrounded by fine-to medium-grained silty and clayey mudflow sands. These individual mudflow units vary from less than one ft to several ft in thickness. Examination of trenches BH-1 to BH-11 (Appendix III) shows that most silty to clayey sand,

silt and clay units are thin to very thick with interstratification of gravel lenses.

The varied thickness of these mudflow deposits indicates that flow viscosities changed during the course of the alluvial fan construction. Viscosity controls the competence and extent of the mudflow: the thinnest flow is the most fluid; the least competent transporting only clay, silt and fine sand; and the most extensive reaching the distal parts of the fan surface. Based on the overall fine-grained sandy nature of the sediments and their wide extent of deposition in the study area, low-viscosity mudflows probably were the most common type of flow during Holocene time. On cross-section AA' (Plate 3A), which runs east-west from the medial to distal parts of the fan surface, sediment layers generally become finer grained and thinner down-fan.

Fluid mudflows commonly follow the shallow arroyos that already dissect the fan. Once the mudflow fills these channels it spreads out onto the interfluvial areas as overbank deposits in a series of lobes that suggest a pattern of oak leaves (Blackwelder, 1928, p. 475). Long, thin stringers of these clays and silts are common in cross-sections AA', BB' and CC' (Plates 3A-5A).

Thicker, more viscous mudflows occur in the proximal parts of the fan. Due to the lack of abundant gravel-, cobble- and boulder-sized material in any of the sediment around the study area, it is doubtful that viscous mudflows occurred since the construction of the

alluvial fan east of El Llano. Furthermore, the low clay content (less than 10 %) of the source rocks and the Holocene alluvium most likely restricted any viscous mudflows. The most common mudflows emanating from the valley uplands probably consisted of low viscosity, water-laden masses of silt, fine-to medium-grained sand with only small amounts of clay as evidenced by the mean grain sizes of all samples tests in Table 2 (Sec. 9.2).

8.1.2 Textural characteristics of mudflows

It is the textural characteristics of mudflow deposits which enable them to collapse upon wetting. Large intergranular voids result from particles settling into a low-density packing arrangement in which the grains are held together by weak clay bonds after drying. Figure 9 shows some typical collapsible soil structures of mudflow deposits. The clay bonds preserve the void space that would otherwise be lost if no clay were present to resist the increasing overburden load from subsequent deposition. Similar collapsible soils derived from alluvial fan deposition in the San Joaquin Valley, California, averaged 12% clay. Bull (1964, p. A56) discovered that mudflow deposits with large amounts of clay (>30%) were non-collapsible because the abundant clay filled the voids. Soils with less than 6% clay were also non-collapsible because the lack of clay bonds between the grains enhanced compaction from the overburden.

The textural properties of collapsible mudflow

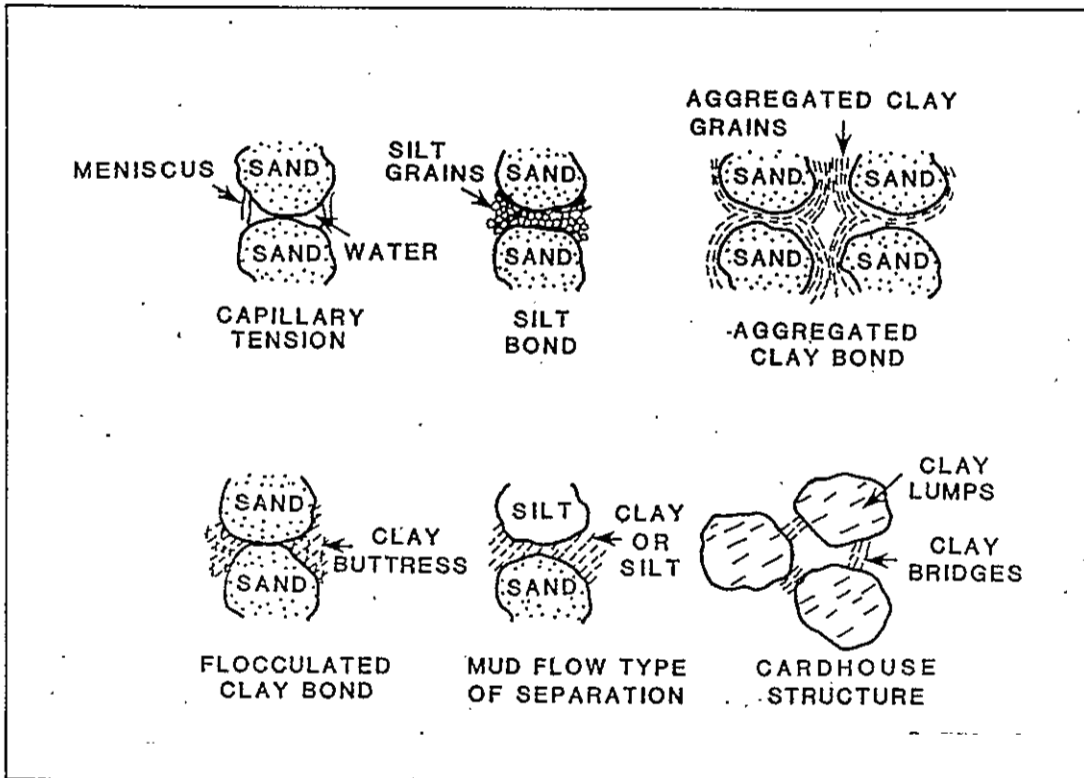


FIGURE 9--Typical collapsible soil structures (adapted from Barden, 1971).

deposits in El Llano are different from those in California because the former's intergranular bonds consist of only minor amounts clay (1-3%) and silt delicately holding the larger sand grains together (Fig. 10). Sieve and pipette analyses of El Llano silty and poorly graded sands showed mean clay percentages of only 3.3. However, the mean percentage of fines (silt and clay) for all soils was 27.5 indicating that most of the fine fraction bonding between sand grains is medium to fine silt. A more thorough discussion on the effect of silt and clay on the collapse mechanism is presented in Section 10.3.5.

Significant volumes of bubble cavities, formed when air is trapped during and after mudflow deposition, also creates a very loose, open-structured collapsible soil. Mudflows pick up air in two ways: during rapid movement down the fan surface and by trapping air after the flow stops. Air in the underlying soil moves upward and becomes trapped in the mudflow deposit to form bubble cavities (Bull, 1964, p. A31). These cavities in El Llano soils tend to be irregular in shape and about 1/16 inch in diameter.

Buried cracks or open fissures in mudflow deposits also contribute to their open structure and low density. As the mudflow dries polygonal dessication cracks form at the surface. Several cracks were encountered at or near the surface during backhoe trenching in the study area. Most are open or partially filled with sand. These buried cracks commonly form in mudflow deposits which dried and cracked with later sand deposition in the cracks before



FIGURE 10--Scanning electron micrograph of a collapsible soil showing sand grains bonded loosely together by clay and silt aggregates. Note the extremely porous and delicate structure. (Mag. 400X, 1mm = 2.5 microns, GGSSS-17, 4-6 ft.)

the underlying mudflow dried. Since the sand has enough dry strength to bridge the gap between the cracks it is preserved in the mudflow deposit. In El Llano some cracks extend 6 to 7 ft below the ground surface. They are probably not related to mudflow deposition but to post-depositional wetting and drying cycles and possibly to pre-historic soil collapse. However, geotechnical studies of collapsible soils in Tucson, Arizona and in the San Joaquin Valley, California revealed the presence of large fissures resembling desiccation cracks that extended 10 ft from the surface (Sultan, 1969; Bull, 1972).

Other cracks, locally called "sótanos" (Valdez, pers. comm, 1985), were reported at widespread localities in the study area and seemed to be related to desiccation and/or shrinkage of expansive clay minerals in near-surface clay layers. As the clays become saturated by surface runoff or by man-induced wetting they expand and cause the cracks to close. During drier periods, the clays desiccate and surface cracks appear. Sótanos have been widely documented in other parts of New Mexico and the southwest where similar clay-rich expansive soils occur (Maker and others, 1974; Soil Conservation Service, 1975). They are not considered to be closely related to the collapse phenomenon.

Other large voids created in mudflow deposits are formed from decaying vegetation that has been transported by the mudflow. Many of the soils within 15 ft of the surface in the study area displayed both fresh and

decaying vegetative matter. Where roots and grasses have decayed there are fairly continuous channels and cavities in several soil samples with diameters as large as 1/16 inch.

8.1.3 Water-laid deposits

Two types of water-laid sediments occur in the study area: those consisting of sheets of sand and silt deposited by a network of intermittent braided streams; and those made up of clay, silt, sand and gravel deposited in arroyos and on overbank areas. Sheetfloods develop into shallow sheetflows which generally develop under upper flow-regime conditions near the mouths of canyons. They deteriorate into patterns of braided channels and bars which dissect the alluvial fan surface. The resulting deposit consists of well-sorted sands and gravels with small-scale internal lenticularity, scouring and cut and fill structures (Collinson, 1978, p. 18). Some of these sedimentary structures can be observed in trenches BH-5, 6, 9, 10 and 11 (Appendix III, Figs. 5, 6, 9, 10 and 11).

Braided channels on the fan surface east of El Llano repeatedly divide and join. Most of these channels are less than six inches deep and are separated by low bars or islands. The sheets of sand in these channels have no distinct margins; each individual deposit usually decreases in thickness until it is a thin film that merges with the underlying soil.

The water-laid sediments in the bottoms of arroyos are usually coarser grained and more poorly sorted than the

braided channel deposits. Fine material from subsequent mudflows may fill the interstices of these arroyo sediments to make them poorly sorted.

Sieve deposits are the product of sheetflows which probably occurred in the study area as evidenced by the thin interbedded gravel lenses detected in several boreholes and trenches. The sediment load of sheetflows is deficient in fine-grained material by the time the sheetflow reaches the medial to distal parts of the alluvial fan. Beneath the sheetflow a highly permeable older deposit causes the sheetflow to diminish rapidly as water infiltration occurs. This results in a clast-supported sand and gravel lobe deposited amidst other finer grained sandy and silty mudflow and braided channel sediments. With burial sieve deposits are slowly filled with fines to give the final sediment a markedly bimodal distribution.

8.1.4 Eolian processes

Because most surficial deposits on the El Llano alluvial fan are loose and dry, the sand is probably subject to eolian erosion, transportation and deposition. No actual dunes exist on the fan surface but there is evidence of eolian transport from the knolls and ridges. Wind deposited sands and silts maintain their loose grain-supported structure unless they are subsequently wetted by intermittent flows. After burial these eolian deposits retain their porous structure and can be very collapsible

if later wetted.

Eolian transport carries only silt and sand-sized particles and deposits them in a loosely packed arrangement. Eolian collapsible soils have very little clay. Compaction and soil collapse can take place with or without wetting as there are no clay aggregates supporting the structure. More petrographic analyses are required to determine the abundance of eolian deposits in the study area. They are most likely minor in abundance compared with the mudflow and water-laid sediments.

8.1.5 Soil development

Some water-laid and mudflow deposits in the study area have sand grains coated with oriented clay (Fig. 11). These coatings, or cutans, are probably the result of illuviation during pedogenic development of the Bt horizon on the fan surface. Although it is beyond the scope of this study to describe pedogenesis in El Llano, it should be noted that some argillic and cambic horizons were observed during trenching. However, most soil horizons were very thin due to the young age of near-surface sediments. Some soils have no pedogenic soil development.

The fact that most clay in these soils is coated on sand grains and is not present as clay aggregates between the grains suggests that the clays are illuvial and are not a product of chemical weathering. Formation of such clay coatings requires prior disaggregation of the clay during illuviation when the clay is brought into suspension and

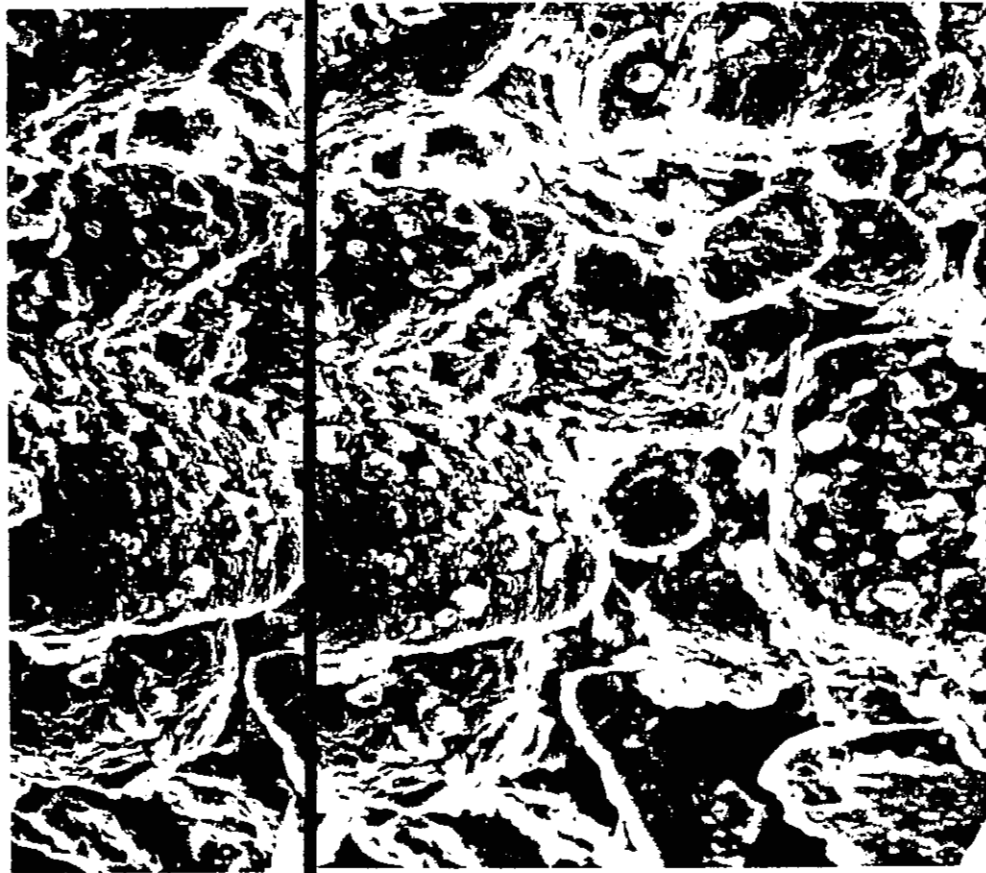


FIGURE 11--Stereo SEM photographs of sand grains coated with clay (cutans). (Mag. 1000X, 1mm = 1 micron, GGSSS-17, 4-6 ft.)

moves through the soil as individual particles (Gile and others, 1981, p. 72).

If chemical weathering is present it is at a very early stage and is not apparent from scanning electron microscope results. In thin section, however, many of the feldspars and sedimentary and granitic rock fragments show partial weathering to clay. In addition, many of the grains display hematite rims (Fig.12).

Calcium carbonate precipitation is present in many of the soil samples collected and analysed under the scanning electron and petrographic microscopes. Calcium carbonate was also present in some of the near-surface soils exposed in the trenches and probably acts as a cementing agent between the sand grains. Subsequent dissolution may contribute to the collapse of the soil structure. This will be discussed more thoroughly in Section 10.3.7.

A buried soil horizon was penetrated just above the Tesuque and Chamita Formation contact with the young alluvium at GGSS Areas 1, 3 and 4 (see Plates 5A, 6A). Here the top of the Santa Fe Group rocks is difficult to pinpoint because there is approximately 3-5 ft of buried clayey and silty soil with calcium carbonate veins and nodules above the suggested Santa Fe contact at 35 ft.

8.2 Alluvial fan morphology

Gradients on the alluvial fan surface east of El Llano range from 1° to 2°. The surface is dissected by numerous arroyo systems; some with wide and shallow channels

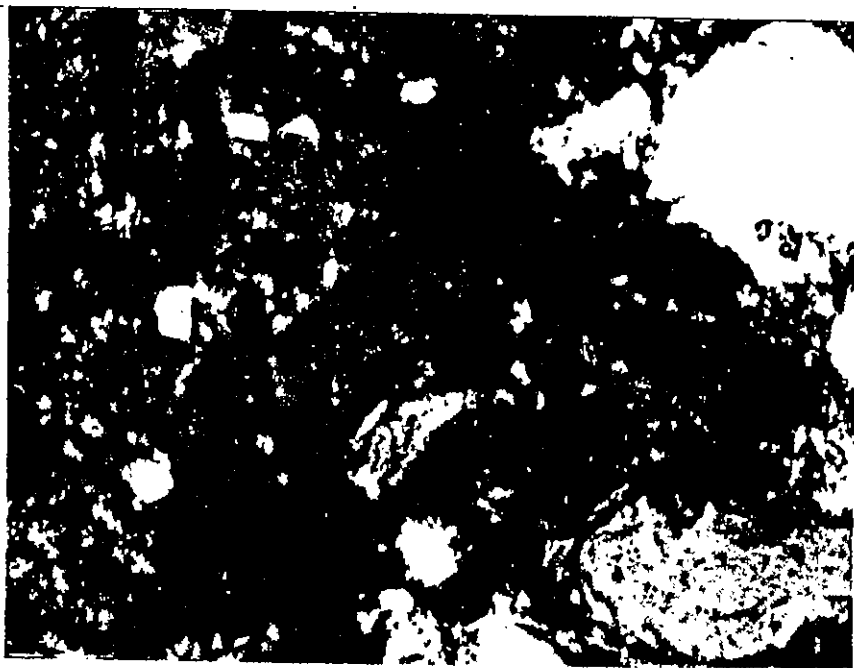


FIGURE 12--Thin section photograph showing partial weathering of feldspars and rock fragments and hematitic staining. (Polarized light, mag. 200X, 1mm = 0.02mm, GGSSS-17, 4-6 ft.)

and others with deep channels entrenched to 10 ft. Bull (1964) examined the drainage area, relief ratio and mean slope of several non-subsiding and subsiding alluvial fans in the San Joaquin Valley, California. He found that subsiding fans have smaller drainage areas and greater relief ratios and mean slopes than non-subsiding fans. This indicated that subsiding fans have greater overall gradients and drainage densities than non-subsiding fans. The study showed that subsiding fans were associated with clay-rich and acid-igneous rocks and with sparse vegetative cover.

The El Llano drainage area covers approximately 10 square mi. The average relief ratio is calculated by dividing the total relief of the alluvial fan by the longest dimension parallel to the principal drainage line. The relief ratio around El Llano averaged 0.110.

The mean slope of a drainage basin is the average slope of all the land within the basin. It is calculated by measuring the area between two specific contour lines. Then the length of this contour belt is measured by averaging the length of the contour lines across the fan surface. A rough mean width between the contour lines can be obtained by dividing the area by the length of the contour lines. The height of the area is the vertical distance between the two contour lines. Thus the mean slope is the ratio of the contour interval and the mean width of the contour belt. It reflects the drainage density of an alluvial fan. East of El Llano the area between two specific contour lines and their

length were obtained to determine the mean width of this contour belt. The mean slope here was 0.052 ft/ft using a 5-ft contour interval.

Comparing the drainage area, relief ratio and mean slope values with those of subsiding fans studied by Bull (1964, Table 1) shows that both drainage areas are relatively small (10 and 11.4 square mi). Similarly, relief ratios were fairly close: 0.110 for El Llano and 0.073 for the Californian alluvial fans. However, the mean slope in El Llano was very low (0.052) compared with that of subsiding fans in California (0.360). This suggests a very low drainage density in the study area, which is apparent from aerial photographs and topographic maps. Although these results are not conclusive evidence for the collapsibility of El Llano soils, they do confirm a typical subsiding fan morphology according to Bull (1964).

Another useful method of identifying potential subsiding fans is aerial infra-red photography. Different soils and rocks can be identified based upon the vegetative pattern they exhibit. Because of its high absorption of photographic infra-red radiation, healthy vegetation has a red signature. Rock outcrops of the Santa Fe Group appear as shades of yellow. An advantage of this method is that damp, subsiding areas with lush vegetation can be easily recognized. Thicker vegetative cover usually outlines older mudflows and water-laid deposits while younger flows have little or no cover (Fuqua and Richter, 1960, p. 452).

Over the past several hundred years water has

TABLE 1--Quantitative geomorphic properties of alluvial fans in California (Bull, 1964) and in El Llano.

	Drainage area (sq. miles)	Relief ratio (ft/ft)	Mean slope (ft/ft)
Subsiding alluvial fans of Bull (1964)	11.4	0.073	0.360
El Llano alluvial fan	10.0	0.110	0.052

deposited a thin fan-shaped blanket of silty sand in El Llano where most of the damaged structures are located (Figs. 2 and 3, Plate 1). East of Airport Road (NM-291) near this arroyo, several natural depressions have resulted from water ponding and subsequent soil collapse. Carbon-14 age dating of these very young sheetflows and channel deposits revealed they are less than 3000 years old (Johnpeer and others, 1985b).

8.3 General distribution and factors affecting the formation of collapsible soils

Because of their diverse depositional origin collapsible soils in El Llano occur from the proximal to distal parts of the alluvial fan. Patches of collapsible soil occur near the tops of knolls and ridges but seldom in hollows or in arroyo bottoms. Generally they are neither found on the Rio Grande floodplain nor, but with some exceptions, west of the El Llano acequia because the river and crop irrigation have saturated and collapsed these soils. The deep water table in the study area has not collapsed the overlying alluvial sediments east of the El Llano acequia. Therefore as much as 85 ft of collapsible sediment remains beneath El Llano.

Factors influencing the distribution and formation of collapsible soils in El Llano are: 1) the ratio of water to solids; 2) meteorologic conditions; 3) the time between successive mudflows or water-laid deposits; 4) local variations in topography; and 5) the amount of vegetation.

Many of these factors are interrelated. For example, landscape position, micro-relief and soil morphology are all important factors affecting soil moisture which may in turn either enhance or inhibit the formation of collapsible soil. Landscape position affects runoff and infiltration. Runoff from higher areas markedly increases the depth of wetting in soils located in topographic lows and in stream channels thus rendering them non-collapsible. Conversely, such runoff decreases moisture in the soils upslope and on topographic highs producing moisture deficient collapsible soils.

Micro-relief can greatly affect moisture infiltration. In small depressions the depth of moisture infiltration is greater than in soils located on knolls and ridges. Consequently, the depth of wetting to precompact the soil can vary significantly within a few feet laterally (Gile and others, 1981, p. 65). Therefore the distribution of moisture-deficient, collapsible soils and wetted non-collapsible soils is also variable.

The degree of pedogenic development on the alluvial fan surface depends in part on the frequency of mudflow and water-laid deposition. A high frequency (every few hundred years) inhibits soil development and prevents the soil from compacting under its own weight. This relatively rapid soil burial preserves textural features such as bubble cavities, mud cracks and vegetation casts and enhances collapse potential. In contrast, a low frequency of deposition (every several thousand years) gives the soil

time to compact and to form soil horizons which reduces collapse potential.

Mudflow and water-laid sediments with high water to solids ratios in semi-arid to arid alluvial fan environments generally produce highly collapsible soils. Some of these deposits may have initial moisture contents as high as 60% with their clay, silt and sand grains supported by water. As the deposit dries clay and silt bind the larger sand grains (Figs. 9-11). This preserves the initial high void ratio, and the loose, dry and delicate structure of the soil.

Another factor possibly involved in collapsible soil formation in the study area is freezing and thawing of surficial soils. A "puffy" and loose character of the surface sediments was noticed during the investigation, especially after freezing temperatures. As these soils go through several freezing and thawing cycles their structure expands and contracts depending in part upon the amount of expansive clays and the amount of moisture held in the soil. Wet soils will exhibit this loose, puffy character particularly well. This process has probably been operative since the alluvial fans in the study area first began to aggrade. If this process was present, the result would be many buried, loose layers of collapsible soil throughout the entire Holocene alluvial wedge (Love, pers. comm., 1985).

9.0 GEOTECHNICAL CONDITIONS IN EL LLANO

9.1 Description of laboratory and field tests

During and after the NMBM&MR investigation laboratory tests were conducted on all of the 397 undisturbed and most of the 560 disturbed samples collected during drilling activities. These tests included dry and wet density, moisture content, Atterberg limits, sieve and pipette analyses for grain-size distribution, consolidation, and thin-section and scanning electron microscope (SEM) analyses for observation of soil structure, grain shape and mineralogy. X-ray diffraction analysis was conducted to identify clay mineralogy. These tests are regarded as the best indicators of collapsible soils.

Wet density of undisturbed samples was determined by cutting off the bottom part of each Shelby tube, weighing the tube and the soil, weighing the tube without the soil and then measuring the length and the diameter of the tube to obtain its volume. Densities could not be determined for disturbed samples.

Moisture content and Atterberg limit tests were conducted on all samples according to ASTM procedures D2216 and D423-424, respectively (American Society for Testing and Materials, 1984). Disturbed samples were bagged and sealed at the drill site and were sent to the soil laboratory as soon as possible.

Particle size analyses were performed using U.S. Standard sieves No. 4, No. 10, No. 20, No. 40, No. 60, No. 80, No. 100, No. 140, and No. 200. Most samples were dry sieved but samples with appreciable clay and silt were

wet sieved by first dispersing them in distilled water overnight, mixing them in a blender, then pouring the solution over a No. 200 sieve and pan. The material retained on the No. 200 sieve was then oven-dried and dry sieved in the normal manner. The clays and silts in the pan were oven-dried and weighed.

Twenty-seven pipette analyses on the material smaller than the No. 200 sieve were performed according to the method described by Folk (1980, p. 33-37). This test was only done on the suspected collapsible silty and clayey sands (SM, SC) and poorly graded sands (SP).

Modified and double consolidation tests were conducted on 35 undisturbed samples according to the method described in the Army Engineering and Design Laboratory Soils Manual (1965) and by Lambe (1951). A Soiltest Inc. medium-capacity lever-type model C-280 consolidation apparatus with a model C-250 fixed-ring consolidometer and an LC-9 strain gauge were used to test samples for their consolidation properties (Fig. 13). During the Collapse Mechanism Experiment (Section 11.0) four undisturbed samples from borehole GGSSS-17, 4-6 ft were saturated at different loads to determine what the effect of load had on collapsibility at 100% saturation. Next, three undisturbed samples from borehole GGSSS-21, 9-11 ft were tested under the same load but at different moisture contents to determine whether there was some moisture content and degree of saturation at which collapse was greatest.

Scanning electron microscope (SEM) analyses for soil

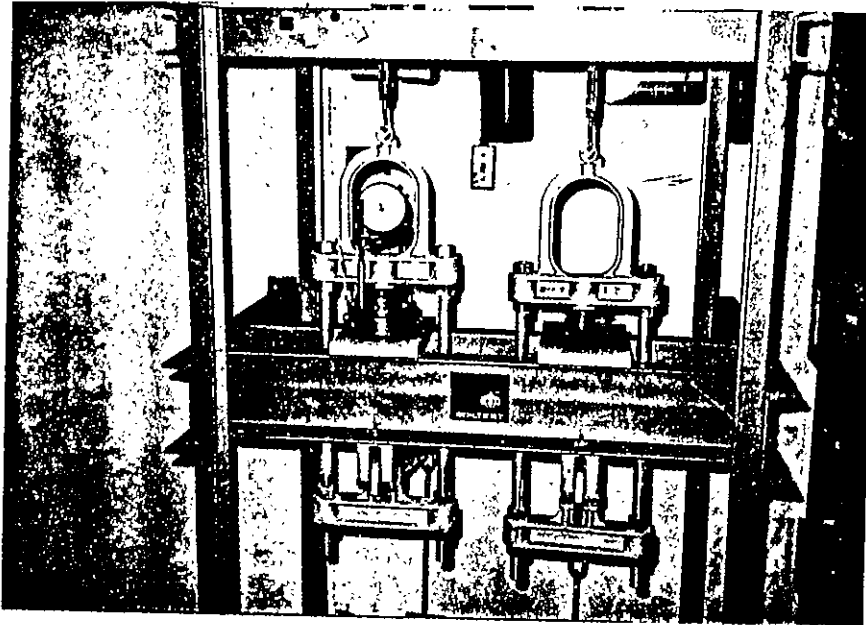


FIGURE 13--Photograph of Soiltest, Inc. medium-capacity consolidation apparatus and fixed-ring consolidometer. Photograph by G. Johnpeer.

structure were conducted on six different soil pedes from the GGSSS-17 samples for the Collapse Mechanism Experiment. The first ped was left undisturbed and allowed to air-dry; the second ped was saturated with distilled water and allowed to air-dry. The other four samples were incrementally loaded to 0.31, 0.63, 1.26, and 5.06 tsf and saturated at their respective loads. Each sample was then air-dried and prepared for SEM analysis. A Hitachi HH-2R scanning electron microscope with a Tracor Northern 5400 Energy Dispersive Spectrometer (EDS) was used. Stereo SEM photographs were taken to better observe the soil structure.

To analyze clay mineralogy of the GGSSS-17 samples, x-ray diffraction was performed using a Rigaku Geigerflex x-ray diffractometer with a Cu fine-focused radiation source and a graphic monochromator. Clays were mounted using the pipette-on-glass-slide method (Gipson, 1966; Austin, written comm., 1985). The slide was run on the x-ray diffractometer four ways: 1) no treatment, 2° to 35° 2θ at 2° 2θ per min; 2) no treatment, 24° to 26° 2θ at 0.4° 2θ per min; 3) after 24 hours in an ethylene glycol atmosphere, 2° to 15° 2θ at 2° 2θ per min; and 4) after heating 30 min at 375° C, 2° to 15° 2θ at 2° 2θ per min. Semi-quantitative analyses using peak intensities for relative abundance of various clay minerals were done using the method described by Austin (written comm., 1985).

Petrographic thin-section analyses were conducted to complement the SEM studies. Thin section analyses allowed determination of mineralogy, grain shape, sorting,

porosity, extent of diagenesis and nature of grain contacts. This was done on the four GGSSS-17 samples: 1) undisturbed dry, 2) 0.31 tsf saturated, 3) 1.26 tsf saturated, and 4) 5.06 tsf saturated. All of these samples were impregnated with epoxy and then mounted on glass slides.

9.2 Discussion of laboratory test results

All laboratory test values are listed in Appendix VI. These test values were tabulated and means, standard deviations and ranges for them were calculated (Table 2). The same parameters were calculated for two groups of soil samples based upon their location either east or west of the El Llano acequia (Table 3). All statistics were calculated using SPSS-X (Statistical Package for the Social Sciences, SPSS, Inc. 1983). In addition, regression analyses, T-tests, Pearson correlations and discriminant function analyses were run on the laboratory data (Sec. 12.0).

9.2.1 Dry density

Dry density is a partial indicator of soil collapse potential because soils will increase in density as they consolidate. A mean value of 96.9 pcf for all El Llano soils tested denotes their overall loose and porous character. As expected the mean dry density west of the acequia (99.2) is greater than the mean east of the acequia (96.4). The data show enough evidence to suggest there is a substantial difference in dry densities

TABLE 2--Mean values, standard deviations, ranges and number of samples analysed for El Llano soil properties.

SOIL PROPERTY	MEAN	S.D.	MIN.	MAX.	SAMPLES
Dry density (pcf)	96.9	9.2	72.0	126.0	370
Moisture content (%)	9.3	7.3	1.0	41.0	630
Liquid limit (%)	28.1	13.9	12.0	82.0	258
Plasticity index (%)	13.4	10.8	0.0	47.0	124
% passing No.4 sieve (gravel)	97.8	6.7	37.0	100.0	478
% passing No.40 sieve (fine sand)	87.1	15.2	14.0	100.0	478
% passing No.200 sieve (silt and clay)	27.5	20.8	0.0	99.0	478
% clay (< 0.002 mm)	3.3	2.7	1.0	13.0	27
% total consolidation with wetting	14.8	7.0	5.0	28.0	24
Collapse potential (%)	4.5	3.5	1.0	13.0	21
% total consolidation without wetting	10.8	5.3	4.0	21.0	9
Blow counts	19.9	12.3	4.0	90.0	256

TABLE 3--Means and standard deviations of properties for soils located east and west of the El Llano acequia.

SOIL PROPERTY	LOCATION	MEAN	S.D.	2-TAILED PROBABILITY*
Dry density (pcf)	East	96.4	9.1	0.014
	West	99.2	9.1	
Moisture content (%)	East	8.5	6.6	0.000
	West	11.5	8.7	
Liquid limit (%)	East	27.8	12.6	0.624
	West	28.8	17.5	
Plasticity Index (%)	East	12.6	9.6	0.104
	West	16.6	14.7	
% passing No.4 sieve (gravel)	East	97.8	6.1	0.991
	West	97.9	8.6	
% passing No.40 sieve (fine sand)	East	86.9	15.1	0.586
	West	87.8	15.6	
% passing No.200 sieve (silt and clay)	East	28.0	20.6	0.326
	West	25.7	21.1	
% clay (< 0.002 mm)	East	3.6	3.0	0.400
	West	2.5	1.2	
% total consolidation with wetting	East	14.9	6.8	0.735
	West	14.0	8.7	
Collapse potential(%)	East	5.1	3.7	0.218
	West	2.8	2.5	
% total consolidation without wetting	East	9.6	4.2	0.221
	West	15.0	8.5	
Blow counts	East	20.8	13.7	0.036
	West	17.9	7.7	

*The two-tailed probability at a 0.01 level of significance indicates whether each mean property value is different or the same between the two areas. If the two-tailed probability is less than the level of significance then there is a difference in values between the two areas.

between the two areas. This is true because the T-test demonstrated there was a low two-tailed probability of 0.014 at a 0.01 level of significance (Table 3).

Because soils west of the El Llano acequia had previously been collapsed (owing to irrigation practice) their dry densities should be greater than the unirrigated dry soils east of the acequia. However, their dry density standard deviations and ranges (Table 3) reveal that some collapsible soils with low densities do occur west of the acequia. Conversely, non-collapsible soils with very high densities are also located east of the acequia.

Testing collapsible loess in Romania, Thortcn and Arulanadan (1975) reported dry densities from 65-105 pcf with 35-45% porosity. Haq (1976) studied alluvial collapsible soils in India and found a similar density range of 85 to 100 pcf. In New Mexico Beckwith (1976, p. 5) reported that most Holocene alluvial fan collapsible soils have dry densities less than 95 pcf while older, more consolidated fan deposits ranged in density from 112-117 pcf. This is also true in El Llano: the ancestral Rio Grande sandy gravels and older alluvium below 100 ft generally have dry densities over 110 pcf and are not collapsible.

9.2.2 Moisture content and saturation

Soil moisture contents for the entire study area averaged 9.3%; they were expectedly higher west of the El Llano acequia (11.5%) than east of it (8.5%).

A two-tailed probability of 0.001 at an 0.01 level of significance from the T-test indicates there is a large difference in soil moisture content between the two areas (Table 3).

Moisture content is a partial indicator of pre-collapsed or post-collapsed conditions in the study area. For example, some soils from boreholes east of El Llano acequia near known collapsed areas had an average moisture content of 16.8% to a depth of 50 ft. This was true for ESPDH-1 near Moya's leaking septic tank and broken water line and for ESPDH-4 near the leaky water community water tank (Plate 1). In contrast, soils from boreholes ESPDH-18, 25, 35 and 37, all located near Airport Road (NM-291) where collapse has not yet occurred, had average moisture contents of 9.7%, 6.7%, 6.5% and 6.3%, respectively, to a depth of 50 feet. Clearly these uncollapsed soils east of the acequia are moisture deficient.

Bull (1964) evaluated moisture deficient alluvial fan soils in the San Joaquin Valley, California, by calculating their moisture equivalents, or moisture field capacities--the amount of water held by capillary action. If the moisture content equals the field capacity the addition of water should cause little or no compaction to the soil. However, if the moisture content is much less than the field capacity the soil can absorb more water. This process produces soil instability. Although no field capacity tests were run on El Llano soils, their

low saturations (see below) indicate that moisture contents are well below field capacity values.

Jennings and Knight (1975, p. 100) empirically derived critical saturations for South African alluvial soils of varying grain size. Critical saturation (S_c) is the saturation below which the soil will collapse if the soil is flooded: for fine gravels $S_c = 6-10\%$, for fine silty sands $S_c = 50-60\%$ and for clayey silts $S_c = 90-95\%$. On Plates 3C-7C are depth profiles of moisture content and saturation for several boreholes across the study area. All collapsible silty sands, poorly graded sands and even some silts and low plasticity clays have saturations well below their critical values. Even west of the acequia the mean saturation for all soils tested was only 39.9% while east of the acequia it averaged 22.3%. According to the above critical saturations, only the high plasticity silts and clays and fully saturated sediments below the water table are non-collapsible.

9.2.3 Atterberg limits and liquid limit vs. dry density criterion

Many of the samples are non-plastic with liquid limits less than 20% indicating their very silty to sandy character with very little clay content. However, the 258 samples tested for liquid limit over the entire study area average 28.1%, while their plasticity indices average 13.4% (Table 2). The silty sands rarely had liquid limits over 30% with very small plasticity indices. The clayey

sands have liquid limits and plasticity indices as high as 40 and 20%, respectively. The low and high plasticity clays and silts (CL, CH, ML, MH) are not as abundant as the silty and clayey sands and non-plastic poorly graded sands.

East of the acequia the liquid limit and plasticity index averaged 27.8% and 12.6%, respectively. West of the acequia these values were only slightly greater (28.8% and 16.6%) as expected because of the more clayey sediments farther down the alluvial fan. If collapsible and non-collapsible soils can be separated by the El Llano acequia then Atterberg limits alone are poor indicators of collapsibility. The T-test showed that the two-tailed probabilities for liquid limit and plasticity index were 0.624 and 0.104. This suggests that both mean values can not be distinguished between the two areas (Table 3).

One example of combining liquid limits with other test data such as dry density to predict collapsibility is shown in Figure 14. This technique, first devised by Gibbs and Bara (1967a), divides collapsible and non-collapsible soils with a line representing the specific limiting density when the soils are 100% saturated. Specific limiting density is the density at which the soil is at its weakest condition when saturated at its liquid limit. Soils plotting above this line, or at dry densities less than their specific limiting density, are considered collapsible. This is illustrated in Case I (Fig. 14) where the void space in the soil is greater than the amount sufficient to hold the liquid limit moisture content. When these soils are

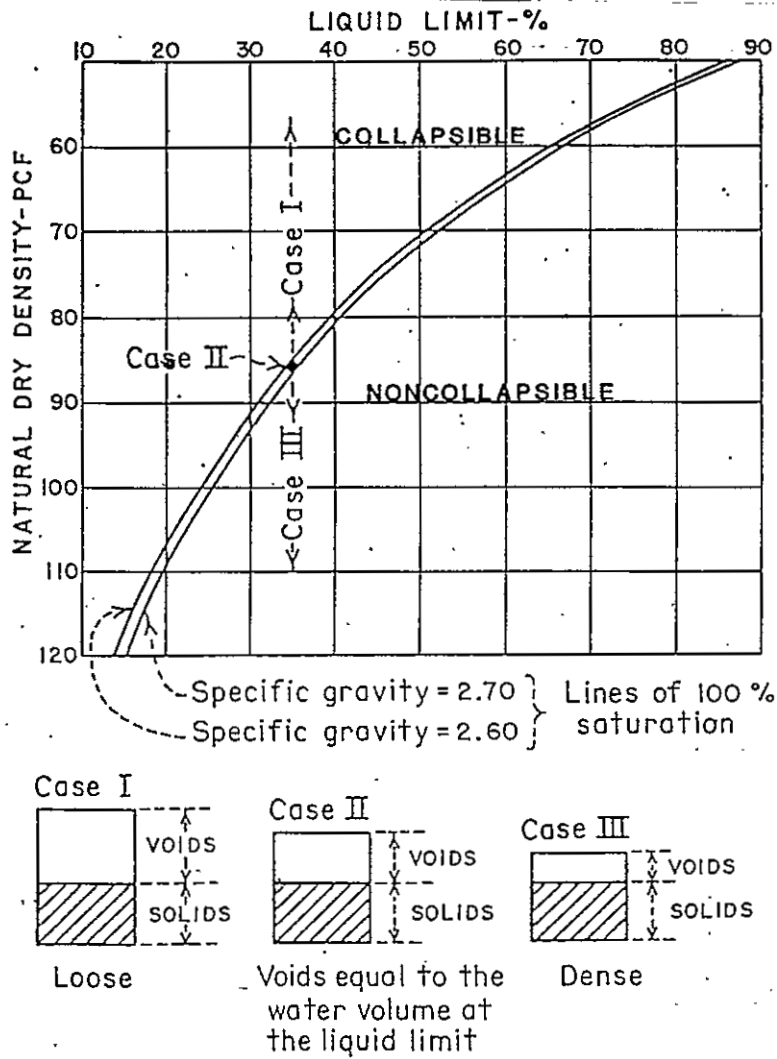
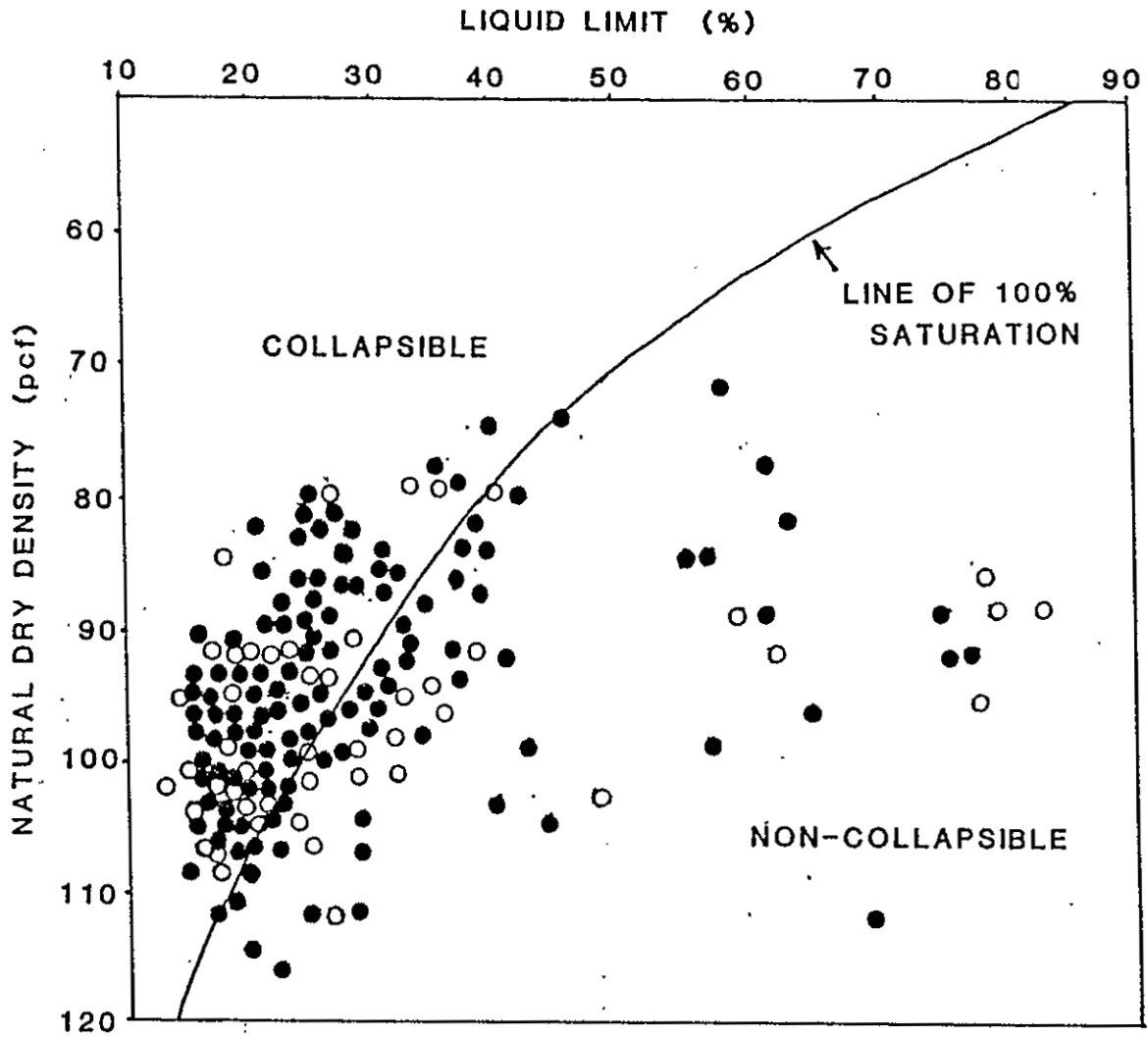


FIGURE 14--Criterion for evaluating soil collapse (modified from Gibbs and Bara, 1967a).

at their liquid limit they still are not saturated. A further increase in moisture content to saturation usually results in the collapse of the soil structure.

In contrast, soils plotting below the line of specific limiting density (having dry densities greater than their liquid limit densities) are non-collapsible as illustrated in Case III (Fig. 14). If the void space is less than the amount necessary to hold the liquid limit moisture content, the soil will already be saturated before it reaches its liquid limit. Therefore the soil will always be in a plastic state and will have greater resistance to particle shifting even when saturated. Both the natural dry density and the density at liquid limit (specific limiting density) are plotted with depth on cross-sections AA' to FF' (Plates 3D-7D). As shown in Figure 15 there are no apparent trends with soils located either east or west of the El Llano acequia when they are plotted on the liquid limit vs. dry density graph.

There are several disadvantages to the liquid limit vs. dry density method; it is only applicable to soils with liquid limits of 20% or greater. Many of the soils in El Llano have very low liquid limits or none at all. Also, this criterion assumes the soils are uncemented and fine-grained without considering soil structure and clay mineralogy. Prokopovich (1984), in a study using this method on alluvial sediments in California, found there was no correlation between collapsible and non-collapsible soils in known unstable and stable areas. This can be



● EAST OF ACEQUIA

○ WEST OF ACEQUIA

FIGURE 15--Liquid limit vs. dry density criterion for soils located east and west of the El Llano acequia (based on 199 observations)..

compared to the results found east and west of the El Llano acequia (Fig. 15). It was generally assumed by Johnpeer and others (1985b) that collapsible and non-collapsible soils were located east and west of the acequia, respectively. Results from Figure 15 refute this assumption.

The poor reliability of the dry density vs. liquid limit criterion lies in the assumption that susceptibility to hydrocompaction requires the soil pore volume to be more than enough to hold the liquid limit moisture content. Much of the collapse in the alluvial soils in El Llano is caused by irrigation and man-induced moisture increases which do not saturate the soil below the root depth. (Even though moisture contents are high in some boreholes down to 50 ft, the soil densities are so low that saturations are still well below 100%.) Therefore, most soil collapse occurs even when the moisture content is well below the liquid limit of the soils. Thus this criterion must be used carefully in conjunction with other soil properties and criteria in order to be effective. In this study, depth profiles of dry density and density at liquid limit are used with moisture content, saturation and blow count profiles and soil lithology to identify collapsible and non-collapsible zones (Section 9.3, Plates 3E-7E).

9.2.4 Grain-size distribution and thin section analyses

The majority of soils tested are silty sands (SM) and poorly graded to slightly silty sands (SP, SP-SM) with minor amounts of clayey sands (SC) and silts and

clays (ML, MH, CL, CH). As shown in Table 2 the mean percentages passing the No. 4, No. 40 and No. 200 sieves for the entire study area were 97.8%, 87.1% and 27.5%, respectively. The poorly graded character of most soils was reflected in their relatively low uniformity coefficient ($C_u < 4$) and their high coefficient of curvature ($C_c > 3$) denoting their generally steep grain-size distribution curve. The effective grain-size diameter (D_{10}) ranged between 0.02mm to 0.09mm for the silty and poorly graded sands.

One unexpected statistic was the low mean percentage (3.3%) of clay-size material ($< 0.002\text{mm}$) in the silty, clayey and poorly graded sands. However, there is a lack of clay-rich rocks in the source area of these alluvial fan sediments so clay percentages should be low.

Visual examination of the coarse sand and gravel fraction of these soils indicated that many of the sedimentary rock fragments from the Tesuque and Chamita Formations were expectedly well rounded. In contrast, the individual quartz grains and other more durable rock fragments were subangular. Although it is beyond the scope of this paper to do detailed point counts of these soils, further examination in thin section revealed similar grain shapes and moderate sorting.

There is little difference in mean grain size percentages between soils located east and west of the acequia (Table 3). The mean percentages passing the No. 4 sieve are virtually the same at 97.8%. Similarly, mean

percentages passing the No. 40 sieve for east and west of the acequia are 86.9% and 87.8%; while those passing the No. 200 sieve are 27.9% and 25.7%, respectively. The clay content of the silty to clayey sands and poorly graded sands is also a little greater east (3.6%) than west of the acequia (2.5%). The T-test showed that all mean grain-size percentages have high two-tailed probabilities (Table 3). This suggests there is little difference between mean values east and those west of the acequia.

Several other workers have attempted, with only limited success, to correlate grain-size distribution with soil collapsibility. Feda (1966, p. 208) found no correlation between collapsible soils of different origin (Fig. 16). The effective grain-size diameter, uniformity coefficient and coefficient of curvature varied greatly.

Holtz and Hilf (1961) plotted grain-size distribution curves for collapsible soils with those of non-collapsible soils and found that they overlapped significantly. Bull (1964, p. A25) plotted average grain-size distributions for mudflow and water-laid deposits. Although there was an obvious difference, with the mudflow sediments being much finer grained and better graded, both soil types were equally collapsible; no concrete grain-size distribution criterion was determined.

In the El Llano area soils with enough fines to have a liquid limit of at least 15 were evaluated for their collapsibility using five collapse index equations derived by previous workers (Section 11.0). One of these criterion,

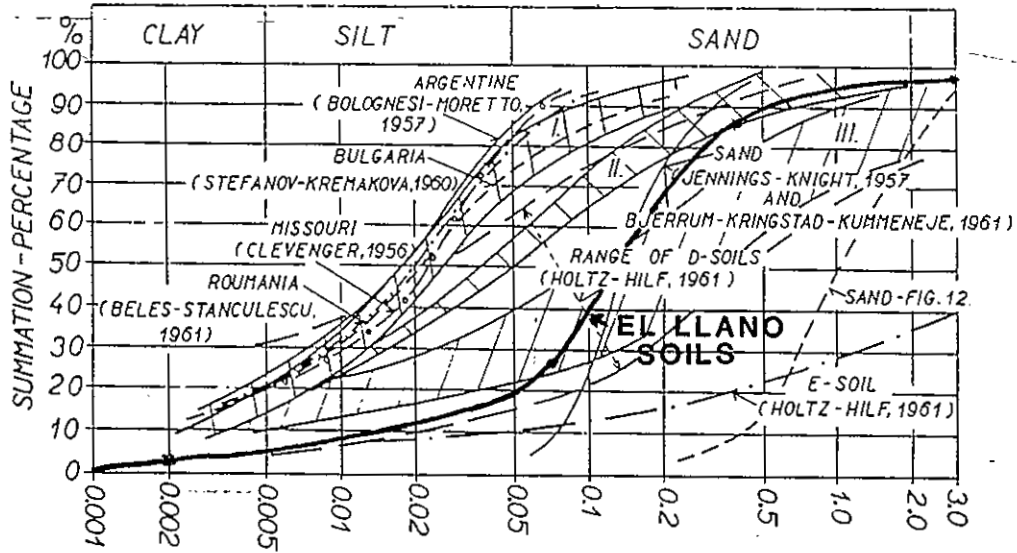


FIGURE 16--Cumulative grain-size distribution curves of collapsible soils of different origin (from Fed1, 1966, p. 208). Note average grain-size distribution of collapsible soils for this study.

the collapse ratio, R , (Gibbs and Bara, 1967a) was chosen to evaluate collapsibility of El Llano soils with grain size distribution (Fig. 17). This ratio is defined by the moisture content at saturation divided by the liquid limit moisture content. No significant differences are noted between collapsible ($R > 1.0$) and non-collapsible ($R < 1.0$) soils on Figure 17. Both exhibit a wide range of grain sizes from gravel to clay. However, El Llano collapsible soils have less clay and have slightly more gravel and coarse to fine sand than the non-collapsible soils. The collapsible soils also tend to exhibit higher uniformity coefficients (C_u) and lower coefficients of curvature (C_c) than non-collapsible soils.

9.2.5 Modified and double consolidation test and collapse potential

The modified consolidation test is a good test to identify collapsible soils because it simulates in situ soil conditions. In the method used for this study an undisturbed sample was incrementally loaded to its overburden stress or to stresses up to 2.2 tsf (depending on the simulated structural load). The sample was then flooded for 24 hrs. Afterwards, each sample was incrementally loaded to the limit of the consolidation machine. Twenty-one samples were loaded to stresses between 0.31 and 2.2 tsf, saturated and then loaded up to 10.12 tsf. Figure 18 shows a typical El Llano collapsible soil consolidation curve plotted on a void

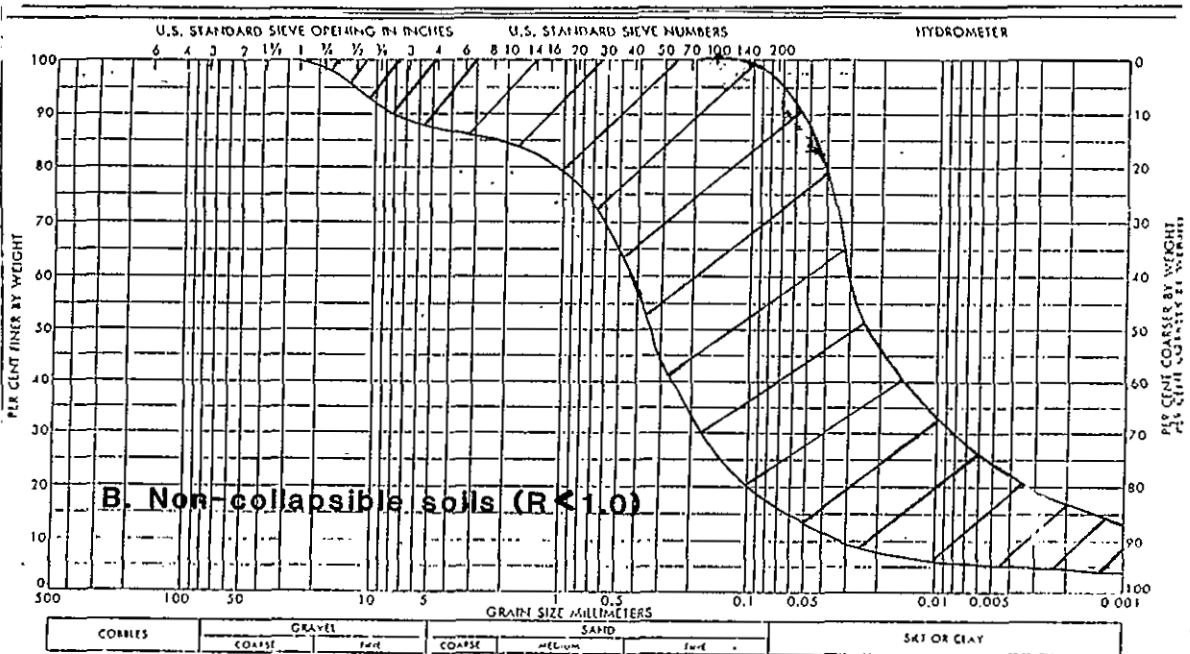
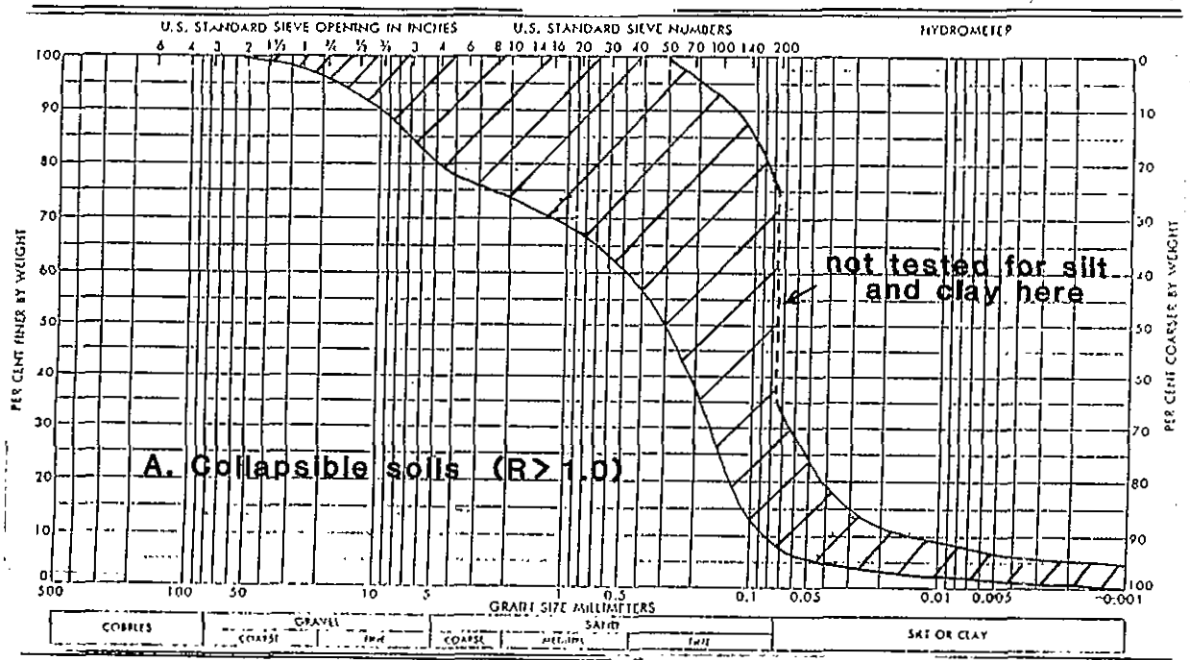
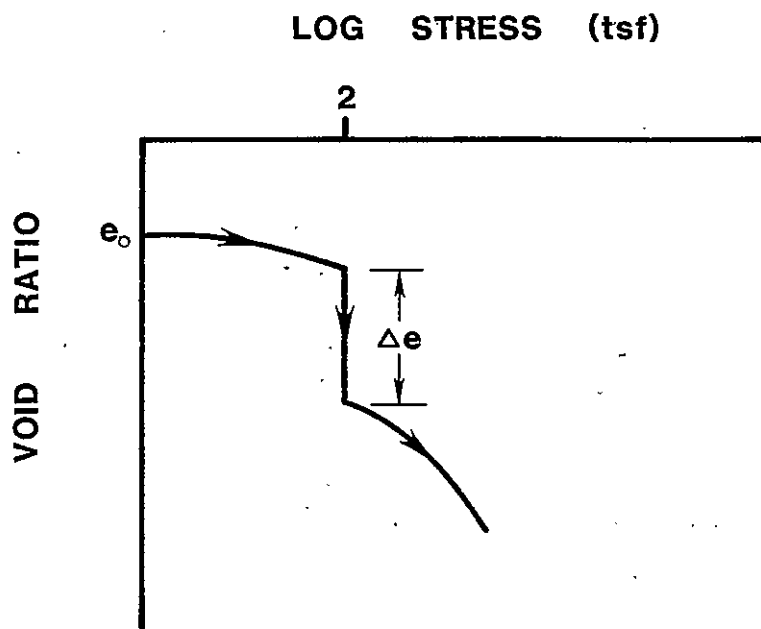


FIGURE 17--Range of grain-size distributions for E1 Llano soils based on the collapse ratio, R (Sec. 11.5).

COLLAPSE POTENTIAL

$$CP = \frac{\Delta e}{1+e_0}$$

CP	SEVERITY OF PROBLEM
0-1%	NO PROBLEM
1%-5%	MODERATE TROUBLE
5%-10%	TROUBLE
10%-20%	SEVERE TROUBLE
> 20 %	VERY SEVERE TROUBLE



**TYPICAL COLLAPSE POTENTIAL
TEST RESULT**

FIGURE 18--Typical El Llano collapsible soil consolidation curve showing its collapse potential.

ratio vs. log stress scale. From these curves a collapse potential can be calculated:

$$CP = \frac{\Delta e}{1 + e_0} \quad (1)$$

where Δe is the change in void ratio during the 24-hr flooding period and e_0 is the initial void ratio of the soil. This criterion only gives a qualitative evaluation of the soil conditions and does not indicate the amount of collapse (Jennings and Knight, 1975).

Collapse potentials for samples tested are presented in Table 4. The average collapse potential for all samples was 4.5%. Samples east and west of the acequia averaged 5.1% and 2.8%, respectively. Thus the data suggest that soils west of the acequia are collapsed but soils on the east side are not collapsed. However, the T-test indicated the data did not provide enough evidence to suggest there was a difference in collapse potential between the two sides of the acequia. There was a high two-tailed probability of 0.218 at a 0.01 level of significance (Table 3).

Double consolidation tests were also run on nine samples both east and west of the acequia. The results are shown in Table 4. For this test two samples from the same borehole and depth interval were loaded incrementally to their overburden stress. Then, one was flooded while the other was left in its natural moisture condition. Each

TABLE 4--Consolidation test data (collapse potential and total per cent consolidation with and without wetting) combined with moisture content, soil type and location east or west of the El Llano acequia.

DRILL HOLE	DEPTH (ft.)	MOISTURE CONTENT (%)	SOIL TYPE	LOCA- TION	CP (%)	(%)	(%)
						TOTAL CONS. W/WET	TOTAL CONS. W/O WET
GGSSI-1	9-11	6.3	SM	East	4.7	10.2	-
GGSSI-2	9-11	2.2	SP-SM	East	2.5	6.5	-
GGSSS-1	9-11	7.3	SM	East	13.1	24.9	-
GGSSS-2	2-4	11.0	SM	East	-	-	3.8
GGSSS-3	19-21	5.2	SM	East	-	9.5	-
GGSSS-4	9-11	7.0	SC	East	-	17.8	12.1
GGSSS-5	9-11	5.6	SM	East	3.8	12.2	-
GGSSS-7	9-11	8.0	SM	East	0.9	16.4	11.4
GGSSS-8	9-11	4.0	SM	West	2.0	11.2	-
GGSSS-12	2-4	11.0	ML	West	7.0	25.9	-
GGSSS-17	4-6	6.0	SM	East	6.0	21.3	-
GGSSS-21	9-11	7.0	SM	East	2.8	11.7	-
ESPDH-5	9-11	4.1	SM	East	8.0	11.0	-
ESPDH-5	19-21	2.7	SP-SM	East	6.0	27.5	14.0
ESPDH-7	10-12	8.8	SM	East	11.5	20.0	-
ESPDH-9	5-7	5.2	SM	East	7.0	22.0	10.0
ESPDH-9	14-16	2.5	SP-SM	East	1.0	4.5	-
ESPDH-9	29-31	2.0	SP-SM	East	2.5	9.0	-
ESPDH-10	14-16	3.8	SM	East	4.0	11.5	4.5
ESPDH-11	5-7	21.2	ML	East	0.5	7.0	-
ESPDH-12	11.5-14	2.9	SM	East	4.5	5.0	-
ESPDH-14	14-16	33.6	ML	East	-	-	7.5
ESPDH-16	9-11	11.4	SM	East	5.0	11.0	-
ESPDH-17	14-16	7.9	SM	West	1.0	5.5	-
ESPDH-17	29-31	23.1	ML	West	-	-	8.5
ESPDH-35	8-10	10.0	SM	East	0.9	17.7	-
ESPDH-38	19-21	34.0	CH	West	0.3	20.3	20.7

sample was then loaded to 10.12 tsf. The mean consolidation without wetting and with wetting was 10.8% and 14.8%, respectively. Samples tested east and west of the acequia had nearly equal mean total consolidation percentages with wetting (14.9% and 14.0%). In contrast, their mean total consolidation percentages without wetting varied from 9.6% east of the acequia to 15.0% west of the acequia. The high standard deviation of 8.5% for the mean value west of the acequia suggests that consolidation percentages here were quite variable. The lower percentage on the east side supports the assumption that most of these soils require both wetting and loading to collapse substantially. The effect of load alone possibly will not suffice to fully collapse some of these soils to the east.

Based on the consolidation data it is concluded that soils east of the acequia are, in general, collapsible where they have moisture contents below 10%, are silty or clayey sands to sandy silts and consolidate more than 10% with wetting. The more poorly graded to slightly silty sands with similar moisture contents located east of the acequia had a wider range of total consolidation percentages with wetting (4.5 to 14.5%) and therefore cannot be classified according to consolidation data alone. Many of the poorly graded sands were too loose and too coarse to place in the consolidometer ring for the consolidation test and therefore were not considered in the statistics. It is suspected that some of these poorly graded sands are also collapsible.

Some soils east of the acequia near damaged structures yielded anomalously low consolidation percentages because they were probably already totally or partially collapsed. These samples were: ESPDH-10, 14-16 ft.; ESPDH-9, 14-16 ft.; and ESPDH-11, 5-7 ft.

9.3 Analysis of cross-sections AA' to FF'--surface and subsurface distribution of collapsible soils

To examine the subsurface conditions around the study area four geologic cross-sections and one fence diagram were drawn (Plates 3A, 4A, 5A, 6A and 7A). Each cross-section has derivative sections showing depth profiles of blow counts, dry density and density at liquid limit, and moisture content and saturation. The ground water table is indicated on the cross-sections with boreholes that penetrated it. Approximate seismic-refraction-velocity boundaries are drawn on each cross-section. The ancestral Rio Grande sandy gravels and the Santa Fe Group rocks, where present, are also shown. Finally, subsidence cracks at GGSS Areas 1 and 4 and at Moya's subsidence pit are drawn on both the fence diagram and the cross-sections. The approximate wetting front from water injection was also shown at GGSS Areas 1 and 4. The cross-sections of collapsible and non-collapsible zones were drawn based on the previously mentioned derivative geologic cross-sections, depth to ground water, seismic velocity and soil type.

9.3.1 Cross-section AA' (Plates 3A-3E)

This section extends in an east-west direction from a few hundred feet east of Airport Road (NM-291) through El Llano, across the acequia, to ESPDH-23 (Plate 1). The cross-section roughly parallels the gentle gradient of the alluvial fan. Observation of Plate 3A reveals the complex interbedding of SP, SP-SM, CL, CH, ML, CH and SC lenses with the dominant SM lithology. Silty sand is interbedded with gravelly, poorly graded sand lenses toward the eastern end of the cross-section. Silty sand is interbedded more with silt and clay lenses at the western end.

The ancestral Rio Grande sandy gravels were encountered in ESPDH-25, 31, 9 and 17. This unit, ranging in thickness from 10 to 20 ft, is the aquifer for the El Llano community. The water table lies between elevations 5615 and 5620 ft. Perched water tables occur at 5625, 5630 and 5635 ft. The sediment below or near the water table is generally not collapsible (Plate 3E). The Chamita and Tesuque Formations were not penetrated by any of the wells. These semi-lithified sediments are not collapsible.

Seismic velocities, although not a key indicator of collapsible soils, can be useful when interpreted along with other soil properties. El Llano soils with seismic velocities less than 1000 ft/sec are considered collapsible (Reynolds, 1985 and McNeill, 1985). However, as shown in Plate 3A, collapsible soils are also present locally even in soils with seismic velocities of 2000 ft/sec. Velocities greater than 5000 ft/sec (as in the Santa Fe Group rocks or in saturated deposits) denote non-collapsible units.

Standard penetration tests (SPT) were conducted at depths ranging from 4 to 125 ft in various boreholes around the study area. The depth profiles of blow counts (or N-values) from standard penetration tests for cross-section AA' indicate the unconfined compressive strength, or bearing capacity, of the subsurface soils. Blow counts averaged only 19.9 while east and west of the acequia their means were 20.8 and 17.9, respectively (Table 3).

Some workers believe N-values below 25 denote a collapsible soil (Beckwith, 1976; Johnpeer and others, 1985a, 1985b). However, Reginatto (1971), in a collapsible soil study in Argentina, showed there was little correlation between blow counts and soil collapsibility. He noted the governing factor for collapsibility was the sensitivity of the intergranular cement in the soil to water dissolution. Thus it could hardly be expected that the standard penetration test relates in any way to collapsibility. In working with N-values moisture content and depth to the water table should be considered because some saturated non-collapsible soils below the water table exhibit very low blow counts. Conversely, some dry collapsible soils will display very high N-values if the standard penetration tester encounters a hard gravelly lense. This fact is further supported by the higher average blow counts east of the acequia as compared with those west of the acequia (Table 3). Surprisingly, the T-test showed a low two-tailed probability of 0.096 which suggests there might be a

difference in mean blow count values between the two areas.

Several SPT test refusals ($N > 50$) were encountered in the ancestral Rio Grande sandy gravels (Plate 3B) indicating this unit's high bearing capacity and non-collapsibility. N-values in the young alluvium ranged between 5 and 55 with the poorly graded sands generally having higher values than the silty and clayey sands, clays and silts.

Depth profiles of the natural dry density and the density at liquid limit for cross-section AA' (Plate 3D) also reveal the variability of collapsible soils. When the density at the liquid limit (specific limiting density, Fig. 14) is greater than the natural dry density, the soil is probably collapsible. These soils were encountered in ESPDH-10, 17 and 31. Non-collapsible soils are more prevalent in ESPDH-21 located west of the acequia.

Moisture content and degree of saturation depth profiles (Plate 3C) show the relatively moisture-deficient soils east of the acequia (ESPDH-3, 10, 25 and 31). In contrast, soils on the west side are much wetter with saturations close to 100% (ESPDH-17, 21 and 23).

Composites of the derivative sections can be used to show the distribution of collapsible and non-collapsible soils (Plate 3E). In general, the collapsible zones partially mimic the complex interbedded alluvial sediments but also quite often cross different soil types. One noticeable trend in cross-section AA' is that the volume of collapsible zones increases toward the east into the El

Llano community. No collapsible soils were encountered below 60 ft in any of the boreholes.

9.3.2 Cross-section BB' (Plates 4A-4E)

This section extends from ESPDH-14 to about 200 feet south of ESPDH-25 (Plate 1). The cross-section shows intertonguing of sediments along the strike of the alluvial fan. A predominance of silty sand is present at the southeastern end of the cross-section near ESPDH-11, 18 and 25. Toward the north-northeast coarser, poorly graded sands and clay and silt lenses are present. This gradual change in sediment type might indicate a variation in depositional processes along the strike of the fan. More stream-channel and overbank deposition may have occurred to the north while sheetflows and mudflows may have been more prevalent to the south during the alluvial fan deposition.

The ancestral Rio Grande sandy gravels were encountered in ESPDH-25 and 39 at elevations of 5614 and 5611 ft, respectively. The water table was encountered at elevations of 5621 ft in ESPDH-39 and 5615 ft in ESPDH-25. Seismic velocity boundaries are also shown with the 1000-ft/sec boundary generally decreasing from 20 ft below the surface at the northern and southern ends of the cross-section to only 5 to 10 ft below the surface near the Moya residence. In this vicinity moisture contents and saturations were abnormally high down to 50 ft. The excess moisture could have elevated the 1000-ft/sec boundary near Moya's. The 2000-ft/sec boundary is

generally horizontal but with a slight downward trend to the north. In contrast, the 5000-ft/sec boundary, nearly coinciding with the water table and the sandy gravel unit, displays a definite downward trend to the south.

Blow counts (Plate 4B) ranged from 1 to 78 with highest values in the ancestral Rio Grande sandy gravels. Sands and clayey sands had a high range in N-values which appear to be related to contrasts in moisture contents (Plate 4C). The sands in ESPDH-14 and 13 have high moisture contents and saturations throughout most of their profile. These are two places where blow counts were correspondingly very low. In contrast, toward the El Llano community to the southeast, moisture contents are generally lower and blow counts are higher for the silty sands. In El Llano most soils are moisture deficient, and, even though blow counts are high, the soils are still collapsible.

This important observation is further supported by the density data (Plate 4D). In boreholes ESPDH-5, 11, 18, 25, 30 and 39 most densities at liquid limit are greater than the corresponding dry densities which denote collapsible soils. To the north the opposite appears to be true with the dry densities greater than the densities at liquid limit.

Plate 4E shows that the area of collapsible zones increases to the southeast. However, a collapsible zone exists along the near-surface of this section and suggests the danger of future subsidence and possible structural damage. The general pattern of the collapsible and

non-collapsible zones is continuous with only minor discontinuous patches. Collapsible zones do not exist below elevations of 5645 ft.

9.3.3 Cross-section CC' (Plates 5A-5E)

Cross-section CC' extends from the south end of the airport runway to about 250 feet west of the El Llano acequia. The section approximately parallels seismic refraction line 2 (Plate 1). The purpose of drawing this section was to study the stratigraphic relationship of soils that had been collapsed due to a ruptured water line near the Moya residence. Even with the good subsurface control along this profile it was still difficult to correlate soils (Plate 5A). Complex interbedding of both fine- and coarse-grained sediments is associated with the predominance of silty sand, especially in the upper 50 ft of the cross-section. Finer grained material interbedded with silty sand is more prevalent at the western end of the profile toward the more distal end of the fan. Thick clay and silt lenses, located underneath the Moya subsidence pit at 10-20 ft, may represent levees or overbank deposits adjacent to buried stream channels. They could also represent mudflow deposits.

The ancestral Rio Grande sandy gravels were encountered in ESPDH-39 and 24 at elevations of 5615 and 5609 ft, respectively. The water table is at elevation 5621 ft in ESPDH-39 and at elevation 5619 ft in ESPDH-24. It dips slightly toward the Rio Grande. Three seismic velocity

boundaries (900, 2000 and 5000 ft/sec) deepen to the west. The 2000-ft/sec boundary is noticeably elevated under the subsidence pit where saturation occurred. Increased moisture contents to a depth of 50 ft could account for the increased seismic velocity there. The 5000-ft/sec boundary approximates the water table and the more dense, saturated, ancient Rio Grande sediments.

Blow counts from SPT tests ranged from 1 to 55 in boreholes along cross-section CC'. The blow counts in ESPDH-1 exhibit fairly low N-values indicative of the low density and saturated character of the subsurface soils. Blow counts greater than 30 commonly correspond to deeper, more consolidated sediments.

The saturation and moisture-content depth profiles (Plate 5C) further demonstrate the large volume of soil that was wetted below the subsidence pit near the Moya residence. Moisture contents as high as 35% with saturations hovering near 100% are not uncommon down to 50 ft as seen in ESPDH-1 and 29. To the east and west of the subsidence pit values are much lower, clearly denoting the moisture-deficient character of the soils. There is still potential for more soil collapse both east and west of the depression should additional soil wetting occur.

Future subsidence is again supported by the density profiles of ESPDH-24, 25, 37 and 39 (Plate 5D). Densities at liquid limit are still greater than natural dry densities beneath Moya residence and the subsidence pit. This indicates a potential for further soil collapse still

remains along some portions of cross-section CC'.

Plate 5E shows the relatively thick and continuous area of collapsible soils that remain. Some zones are labeled non-collapsible because they have already at least partially collapsed. The thick clay and silt lenses beneath the pit were probably non-collapsible, due to their high Atterberg limits, even before the moisture infiltration occurred. The clay and silt units could have limited most of the soil collapse in the upper 20 ft even though deeper sandy soils were saturated. It is unknown whether the collapse of the deeper soils affected the surface subsidence.

9.3.4 Geotechnical Ground Stabilization Study (GGSS)-- fence diagrams of GGSS Area 4 (Plates 6A-6F) and cross-section FF' (Plates 7A-7E)

Both these geologic cross-sections and their derivatives were drawn to examine the soil properties and the nature of the subsidence beneath GGSS Areas 1 and 4. The GGSS demonstrates the possible relationship between soil wetting and subsidence, tests a possible stabilization technique (induced hydrocompaction), and examines the performance of contrasting concrete foundation designs.

GGSS Areas 1, 3 and 4 (Plate 2) are situated approximately 800 feet west of the valley bordering uplands. This area was chosen for the water injection experiment because of its known thickness of collapsible

soils (30-40 ft) above the Santa Fe rocks. All three areas are located east of the El Llano acequia. GGSS Area 2 is located west of the acequia (Plate 2), where the ground has been irrigated for three centuries and where it is suspected that most subsurface soils are either pre-collapsed or non-collapsible. Therefore, this area was used as a control for the water-injection experiment. No subsidence occurred at GGSS Area 2 even after 84 days of water injection (Johnpeer and others, 1985b, p. 12-3).

The fence diagram at GGSS Area 4 was constructed with two cross-sections intersecting at the center of two experimental foundation slabs (Plate 2). Cross-section DD' is oriented N. 68° W. and cross-section EE' is oriented N. 42° E. Compared with the previous cross-sections, which are more regional, this fence diagram displays more homogeneous soil types owing to its very local extent and large scale. The tight well control with ten boreholes surrounding the foundation slabs provided reliable soil correlations.

As shown on Plates 6A and 7A subsurface soils consist mostly of thick silty sand and poorly graded to slightly silty sand units with stringers of well-sorted sand. It is difficult to pinpoint the exact contact between the Holocene alluvium and the older underlying rocks because there is 3 to 5 ft of clayey sands and silty clays (buried soil ?) covering the top of the Santa Fe Group rocks. Borehole samples from this interval have abundant calcium carbonate along ped faces and they are

semi-consolidated. The top surface of the buried Santa Fe Group rocks is not flat but sustains a modestly undulating topography.

Seismic refraction lines 5, 9 and 10 cross GGSS Areas 1, 3 and 4 (Plate 2). The 800-ft/sec velocity boundary deepens to the northwest and ranges from 12 to 25 ft deep. This boundary also deepens from GGSS Area 4 to Area 1 in a southwesterly direction (Plates 6A and 7A). The low velocity boundary deepens toward the El Llano acequia in all the other cross-sections and possibly suggests a thickening wedge of collapsible soils toward the west. The 1750-ft/sec boundary between Areas 1 and 4 approximates the Santa Fe contact at 30 to 35 ft below the surface.

Blow counts with N-values ranging from 6 to 43 (Plates 6B and 7B) reflect the generally soft and loose character of the alluvium. High N-values were encountered in the Santa Fe rocks. However, blow counts were lower directly above the Santa Fe contact which may suggest the presence of a semi-consolidated buried soil.

Density data profiles suggest collapsible soils exist in the top 25 to 30 ft of alluvium (Plates 6D and 7D). Dry densities range from 80 to 100 pcf while densities at liquid limit range from 100 to 115 pcf. Many of these soils had no liquid limit and thus could not be evaluated using this criterion. Moisture contents and saturations are less than 10% and 50%, respectively (Plates 6C and 7C). They both increase in the clayey sands and silty clays near the

Santa Fe contact.

Based on the above criteria, collapsible and non-collapsible zones were drawn (Plates 6F and 7E). Non-collapsible zones represent only a very small volume of soils at depth. A thin gravelly sand stringer (SW) beneath the foundation slabs is probably non-collapsible as is the thicker and more laterally extensive gravelly sand lense beneath GGSS Area 1. The clayey sands, silty clays and silts covering the Santa Fe rocks are also non-collapsible as inferred from their high blow counts, high moisture contents and saturations, and low density values at their liquid limits.

10.0

COLLAPSE MECHANISM

A collapse mechanism experiment was conducted on several undisturbed samples from boreholes GGSSS-17, 4-6 ft and GGSSS-21, 9-11 ft around GGSS Area 4. The purpose of the experiment was twofold: to explain the "macro-mechanism" of subsidence of collapsible soils by studying the cracks and depressions in GGSS Areas 1, 3 and 4; and to describe the "micro-mechanism" of collapse within the soil structure. A series of modified consolidation tests on each sample was also conducted to test the effect that varying load, moisture content and saturation had on the amount of collapse. Detailed

procedures of this experiment are described in Section 9.1.

10.1 GGSS Areas 1-4 water-injection experiments

Controlled water injection was performed at GGSS Areas 1-4. The extent and changes in topography and the growth of subsidence cracks were monitored closely. Appendix IV, Figures 1-7, show the propagation of cracks in GGSS Areas 1-4 during water injection. Table 5 illustrates the amount of water injection and amount of surface subsidence in each area.

At GGSS Area 1 the injection well was 30 ft deep with two shallow 10-ft wells close by. Water injected into the deeper well saturated the deep soils rather than the near-surface soils. As shown on cross-section FF' (Plate 7A), the "bulb" of wetting here is much deeper and less laterally extensive than that at GGSS Area 4 (Plate 6E), where a different method of well construction was used. Because the deeper soils at Area 1 were saturated first, surface subsidence did not occur initially. However, after water was injected into the shallow wells, subsidence did take place. This indicated that the entire 30-foot section of alluvium was collapsible (Johnpeer and others, 1985b, p. 12-3). Figure 2 in Appendix IV shows the very limited surface extent of the concentric cracks produced. The center of the depression was ponded with water from the shallow well injection. Most cracks had scarps 0.5 ft high.

At GGSS Area 2, located 550 ft west of the

GGSS Area	Max. depth of injection wells(s) (ft)	No. days to induce settlement	Water required to induce settlement (gal)	Amount of surface subsidence (ft)	Total water injected (gal)	Duration of experiment (days)
1	30	42	21,294	0.5	42,996	63
2	30	NA	NA	None	24,567	84
3	10	7	~7,000	2.2	16,880	16
4	10	13	19,881	1.4	107,691	28

TABLE 5--Water-injection and settlement data for the GGSS Areas (from Johnpeer and others, 1985b, p. 12-2).

acequia (Plate 2), water was injected into a 30-ft well in an attempt to cause surface subsidence. Moisture and density monitoring with a CPN depthprobe indicated there were no significant increases in moisture content or dry density in the subsurface soils even after 84 days of wetting. In addition, no surface subsidence or cracking occurred. Clearly, the soils at GGSS Area 2 are non-collapsible.

Dramatic subsidence and cracking occurred at GGSS Area 3 where 2.2 ft of collapse took place within 16 days (Fig. 19). Water was injected into a shallow 10-ft well. The near-surface soils absorbed most of the water which led to a rapid soil collapse. This area best models the situation found around the damaged structures in El Llano where a point source of water leakage occurred at fairly shallow depths (less than 15 ft). The volume of water (7000 gal) required to induce subsidence at GGSS Area 3 is approximately equal to the amount used by a family of four in one month (Johnpeer and others, 1985b, p. 12-3).

At GGSS Area 4 water was injected into five 10-ft wells around experimental concrete slabs (Figs. 20 and 21). The purpose of this experiment was to see if soil collapse from water injection could be controlled to induce uniform settlement without foundation cracking. Another objective was to test the performance of the two types of slabs. Both slabs began to subside uniformly without cracking within 13 days after 19,881 gal of water were injected (Fig. 22). A total of 107,691 gal was injected



FIGURE 19--Photograph of GGSS Area 3 showing extensive cracking and surface subsidence. Also note the tilted blocks between each set of cracks. View to south (from Johnpeer and others, 1985b).

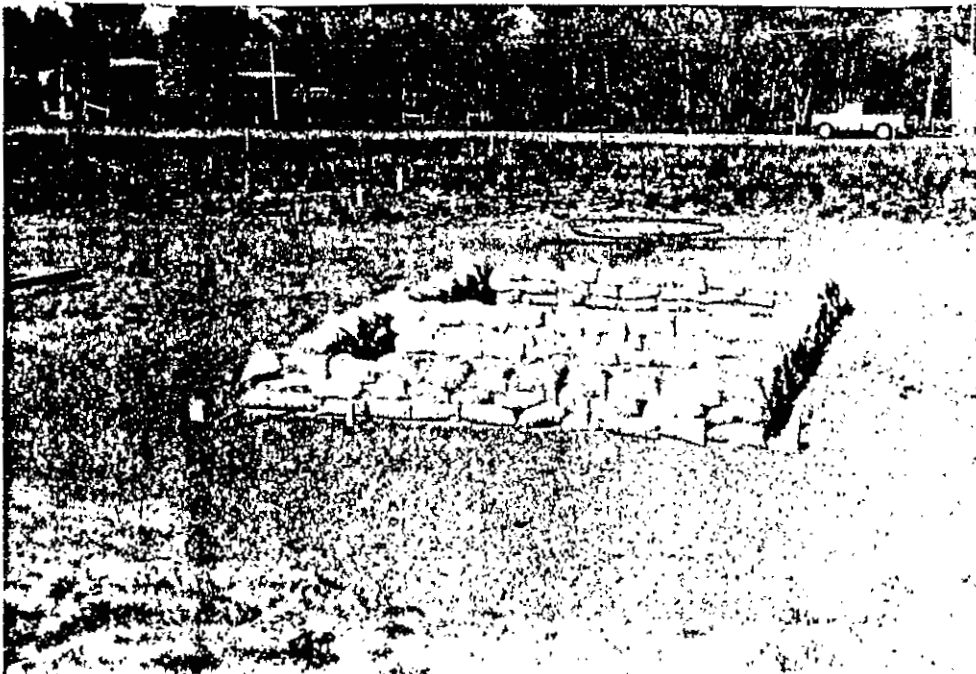


FIGURE 20--Photograph of GGSS Area 4 before collapse occurred. View to west (from Johnpeer and others, 1985b).

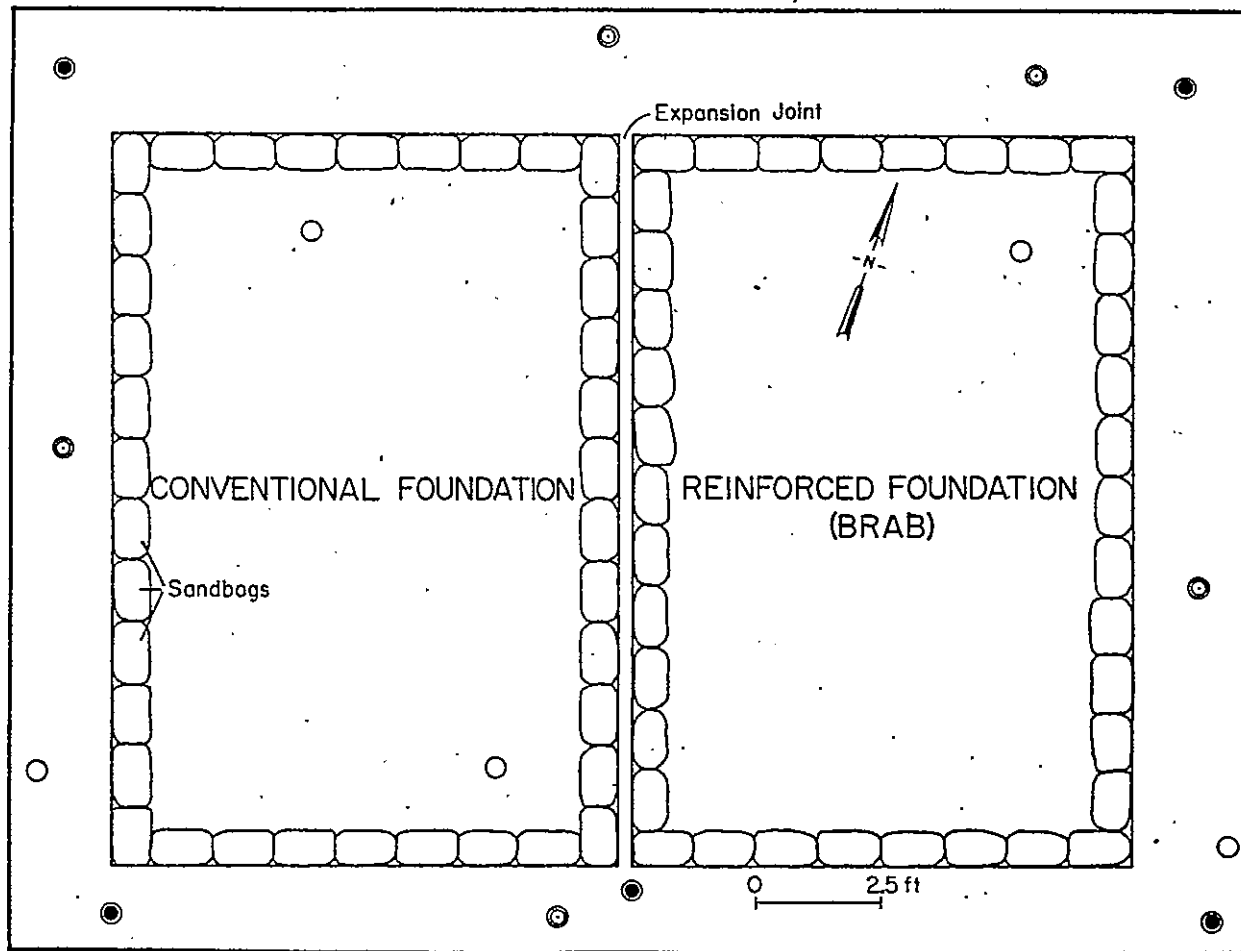


FIGURE 21-- Map of GGSS-Area 4 (concrete foundations) showing well locations.
 (from Johnpeer and others, 1985b).

- Monitoring well symbols:
- water level and injection
 - ⊙ moisture and density
 - settlement

over a three week period and resulted in 1.4 ft of subsidence (Fig. 23). The fence diagram of GGSS Area 4 and cross-section FF' (Plate 6E) shows the wetting front extending down 30 ft to the approximate depth of the non-collapsible clayey sands and silty clays.

Two types of foundation slabs were constructed at GGSS Area 4: a conventional model and a highly reinforced, continuous footing model (BRAB slab). Each foundation measured 10 X 15 feet and was constructed with Type III 3000 psi concrete. The conventional foundation had a footing depth and width of 16 and 8 inches, respectively. Two continuous pieces of 1/2-inch rebar were placed in the footings before the cement was poured. In addition, a 6 X 10-inch wire mesh was laid down in the interior of the foundation. The BRAB slab was constructed with 6 1/2 cubic yards of cement and had a continuous footing depth and width of 24 and 18 inches, respectively. Two sets of two rows of 1/2-inch rebar were placed in the footings. Rebar was also laid down in a one foot square mesh pattern in the interior of the foundation.

In GGSS Areas 1, 3 and 4 CPN depthprobe monitoring indicated a dramatic increase in moisture content and density of the soils down to 30 ft. This simulated the conditions in El Llano where leaking septic tanks, broken water lines and excess runoff soaked the subsurface soils which significantly increased their moisture contents and densities.

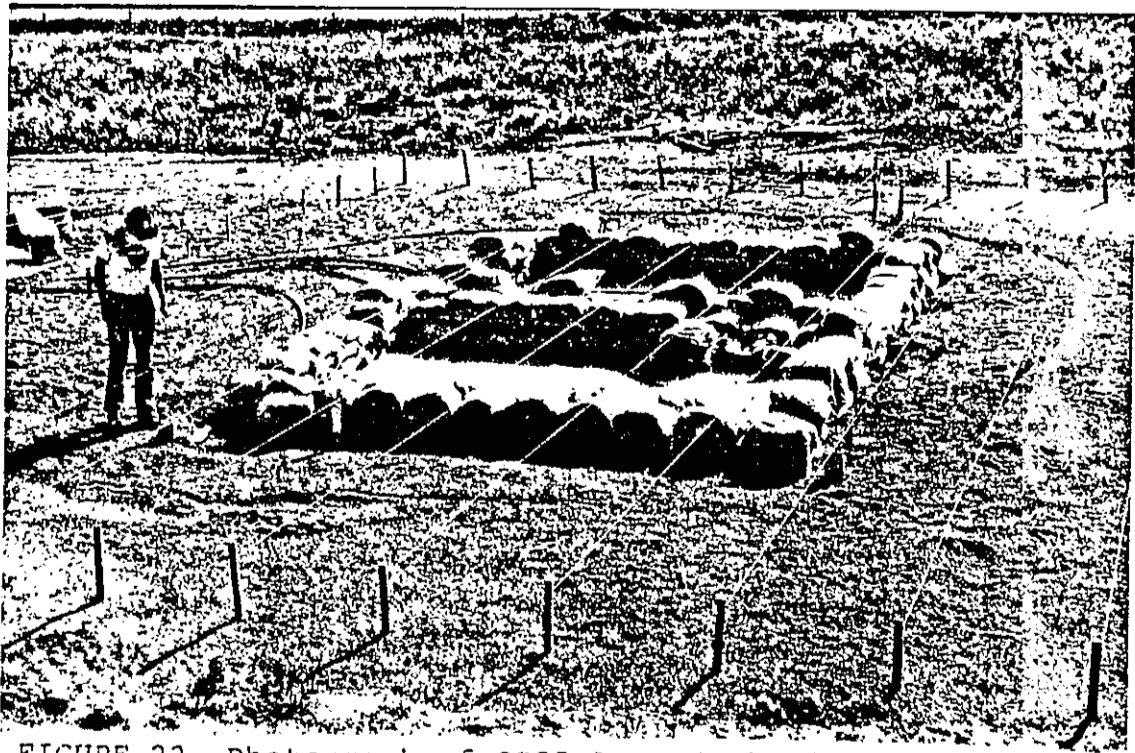


FIGURE 22--Photograph of GGSS Area 4 showing incipient surface subsidence and ground cracks on May 29, 1985. View to west (from Johnpeer and others, 1985b).

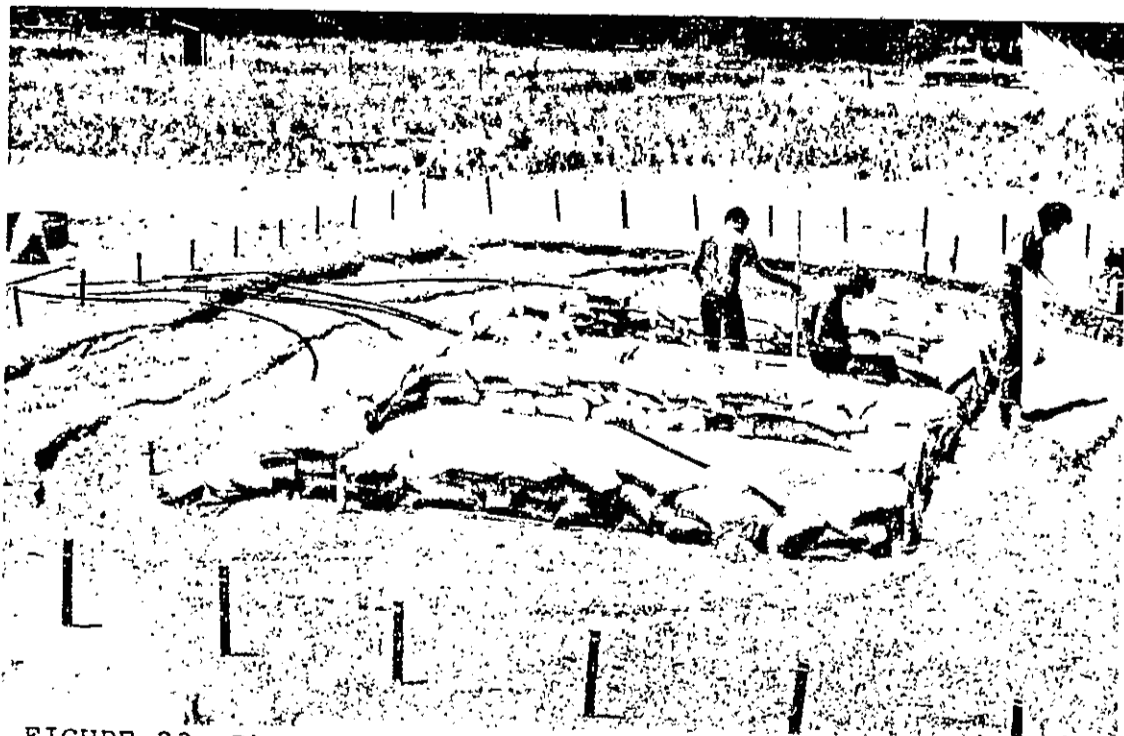


FIGURE 23--Photograph of GGSS Area 4 showing near-to-maximum surface settlement and ground cracks on June 10, 1985. View to west (from Johnpeer and others, 1985b).

10.2 Macro-mechanism

Why do subsidence cracks or large scarps on the surface occur from wetting collapsible soils? Several workers have studied this phenomenon (Bull, 1961, 1954, 1972; Bara, 1972, 1975; Curtin, 1973; Barden and others, 1973; Hall and Carlson; 1965; Lofgren, 1969; and Platt, 1953). As shown in the previous photographs and crack maps (Appendix IV) of GGSS Areas 1, 3 and 4, most of the cracks form around the point source of water injection in a somewhat circular and concentric manner. With continued water injection other sets of cracks create a stepped topography as additional bands of scarps form around the subsidence area. The downthrown side of each crack is nearest the depression. Some scarps at GGSS Area 3 and outside the corners of the foundation slabs at GGSS Area 4 were as high as 15 inches with as much as 6 inches of horizontal separation (Figs. 19, 23 and 24). Other less prominent cracks toward the outside of the depressions had no scarps and only 1- 3 inches of horizontal displacement. Though not abundant, radial cracks were aligned perpendicularly to the main tensional cracks in GGSS Areas 3 and 4. Radial cracks relieve the tensile stresses between the concentric cracks usually at their greatest radius of curvature (Fig. 24).

At the subsidence pit near the Moya residence cracks formed concentric ellipses. Here the area of collapse measures more than 150 ft in diameter with depths ranging up to 5 ft. It includes a subsided volume of



FIGURE 24--Photograph of crack scarps and radial cracks at GGSS Area 4.

approximately 4000 cubic ft (Johnpeer and others, 1985b, p. 6-6). Around the depression there were point sources of water leakage from a septic tank, a broken water line and infiltration from surface runoff and water ponding in the vicinity. This increased the volume of wetted collapsible soils over a much wider area than that modeled at GGSS Areas 1, 3 and 4.

The amount of subsidence and the size and extent of cracks are largely dependent on how deeply water is absorbed and the homogeneity of the soil. Generally, collapse occurs within the upper 15 ft. Deep water injection at GGSS Area 1 collapsed the soils at 30 ft depth but only caused gentle downwarping at the surface. Substantial cracking occurred when water was later injected into the shallower soils.

Based on the preceding observations it appears that the ratio of collapsible soil thickness (T_c) to the depth of water injection (D_w) could control the total amount and character of surface subsidence. At GGSS Area 1 T_c/D_w is 0.5 since the thickness of collapsible soils averages only 15 ft (according to the estimate shown on Plate 7E), while the depth of water injection is 30 ft. In contrast, if the entire wetted column consists of collapsible soils as is the case at GGSS Areas 3 and 4 (Plate 6F), then T_c/D_w approaches unity. This situation is usually characterized by discontinuous subsidence with step cracking. Values of 0.5 or less for this ratio as in Area 1 are characterized by only gentle downwarping and few cracks.

Beneath Moya's subsidence pit the depth of wetting reached 50 ft but also probably extended laterally well beyond the area beneath the depression. As shown on Plate 5E, the collapsible zones represent only about two-thirds of the 50-ft wetted column. Therefore T_c/D_w is 0.67. Although there are large cracks around the depression, they are only slightly stepped with little vertical displacement. The most dramatic feature of this depression is the broad downwarping. Thus it appears Moya's pit has a subsidence character intermediate between GGSS Area 1 and GGSS Areas 3 and 4.

In using the T_c/D_w ratio to predict the character of surface subsidence the relative heterogeneity of the soils should be considered. The fact that El Llano soils are so heterogeneous and complexly interbedded usually makes them homogeneous as a unit down to the depth of wetting (McNeill, pers. comm., 1985).

The formation of subsidence cracks and depressions is related to the decrease in the volume of deposits as the water front moves downward and outward. The amount of collapse is the sum of compaction caused by the weight of the overburden, the weight of the injected water, the soil compaction occurring at the wetted front, and a small amount of true consolidation. Most of the compaction occurs as the water front advances through the soil. The rate of compaction generally decreases after the water has passed through the soil and as equilibrium conditions are met (Bull, 1964, 1972; Curtin, 1973). This was true for GGSS

Area 4 where the rate of settlement was 3 inches per day for the first 7 days. Thereafter it decreased to less than 0.5 inches per day until the end of the experiment (Johnpeer and others, 1985, p. 12-9).

Any process that explains the formation of cracks and depressions, such as those outlined above, must conform to the following:

1) Most cracks are essentially open fissures and are arcuate to vertical in shape. They may extend to depths of 10 ft. Some cracks were detected as anomalously low readings during depthprobe monitoring.

2) Vertical displacement on opposite sides of cracks range from 0 to 15 inches (Figs. 19, 23 and 24).

3) The surface of the blocks between adjacent cracks typically slopes toward the wetted area at less than 10° . This is especially evident at GGSS Area 3 where three or four sets of blocks between cracks slope gently towards the injection well (Figs. 19, 23 and 26).

4) As new cracks farther from the wetted area open, older cracks closer to the center of the depression close (Fig. 25).

Figure 25 presents a possible process for crack formation at GGSS Area 3 and 4. The process is different from the "circular-arc" type of slope failure because vertical instead of lateral support is being removed. In Figure 25A crack 1 has already opened and closed, crack 2 has opened and crack 3 has started to open. The wetted front has intruded past the lower part of crack 2 and has been

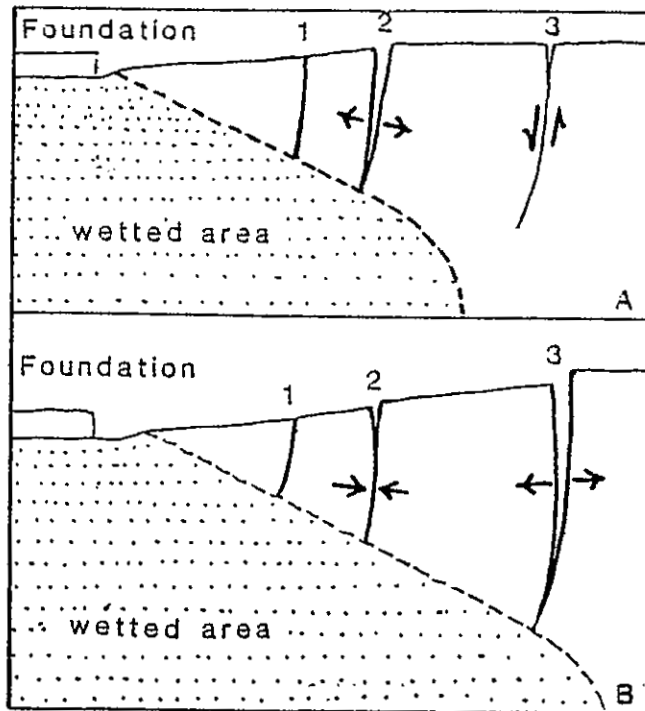


FIGURE 25--Diagrammatic sections showing a possible explanation of subsidence cracks: 1, 2 and 3 are progressively younger cracks (modified from Bull, 1964, p. A22). See text for discussion.

accompanied by soil collapse within the wetted area. The left side of the block between cracks 2 and 3 is not fully supported by the collapsed underlying soils. This causes the block to rotate inwards close crack 2 and further open crack 3 (Fig. 25B).

Vertical displacements between the blocks indicate that the block nearer the wetted area has subsided and rotated more than the outer block due to the loss of support underneath (Bull, 1964, 1972; Curtin, 1973). Vertical offset without block rotation is probably caused by their geometry; the blocks between cracks resist tilting toward the wetted area because of their arcuate shape. In places, blocks nearer the wetted area will rotate inward without slumping as was seen in GGSS Areas 1 and 4. This elevates the outside upper lip of the rotated block slightly above the outside crack. After the blocks have formed other types of failure may occur as material slumps into the open cracks.

Parallel sets of primary cracks open first and roughly parallel the boundary of the wetted area. Secondary cracks, or intercepting and en echelon cracks, form because the blocks between the primary cracks do not have enough strength to withstand rupture (Fig. 26). At GGSS Area 4 these secondary cracks developed within a week after the outermost primary crack started to open.

In GGSS Area 4 the vertical displacement between cracks was the greatest at the corners of the foundation slabs (Figs. 23 and 24) where stress concentrations are



FIGURE 26--Photograph of primary and secondary cracks at GGSS Area 3.

greatest. At GGSS Area 4 the cracks seemed to conform to the general outline of the foundations whereas in GGSS Areas 1 and 3, with no controlling structure, the cracks formed a more circular, concentric pattern.

The mechanics of subsidence and surface cracking sheds light on the reason why the foundation slabs at GGSS Area 4 settled uniformly without any damage. Surface subsidence alone is not damaging to surface structures; it is the differential settlement, or tilt, arising from the shear, tensional and compressional strain around the cracks which causes the most damage. Figure 27 shows the regions of tensile and compressive stresses and strains in the soils around the outer edge of a subsidence pit. Here both horizontal and vertical displacement (tilt) occurs. At the center of the depression there is little strain and only vertical displacement.

The near-surface soils around GGSS Area 4 are mostly silty sand. The structure of the soil in the tensional zone opens horizontally and is reduced in thickness by the amount H1 (Fig. 28) In the compressional zone the soil is compacted. One or more additional layers is formed by grains forced between others, thereby increasing its thickness by the amount H2 (Fig. 28; Kratzch, 1983, p. 338). Each tensional/compressional zone is present in the cracks and subsided blocks around the wetted area.

Because the GGSS foundation slabs were located in the middle of the wetted area where there was only vertical displacement and no strain, no differential

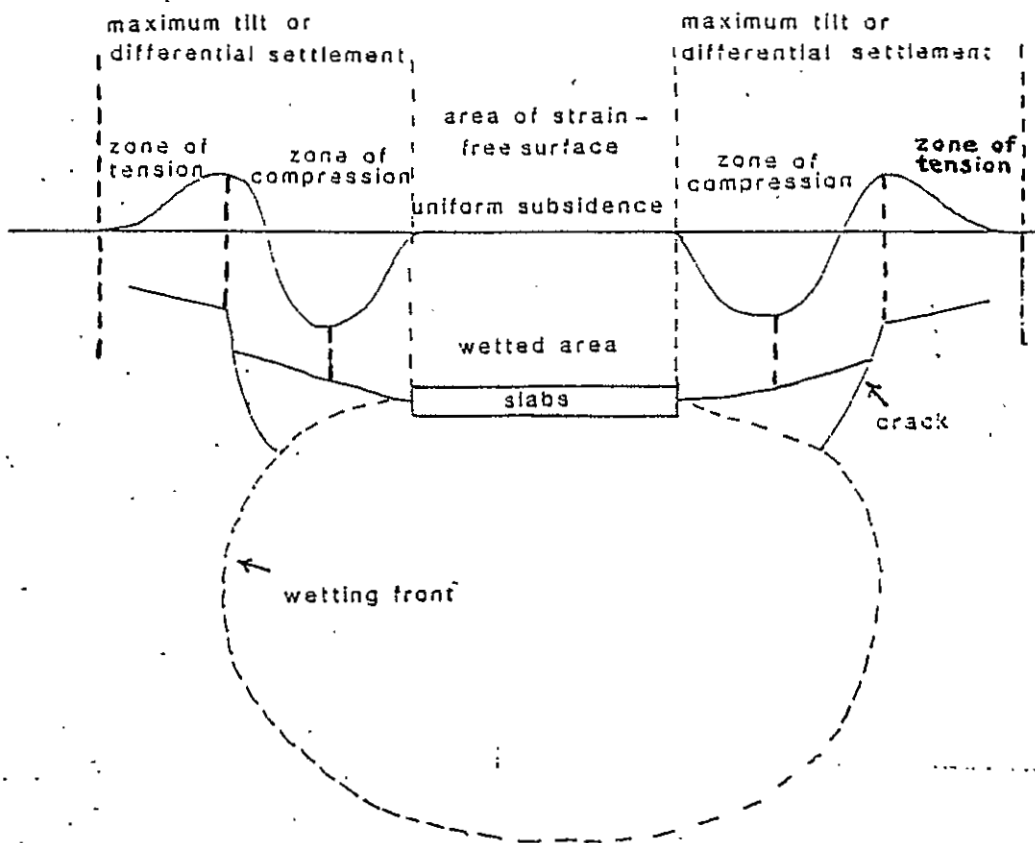


FIGURE 27--Idealized sketch of tensional, compressional and strain-free zones at GGSS Area 4.

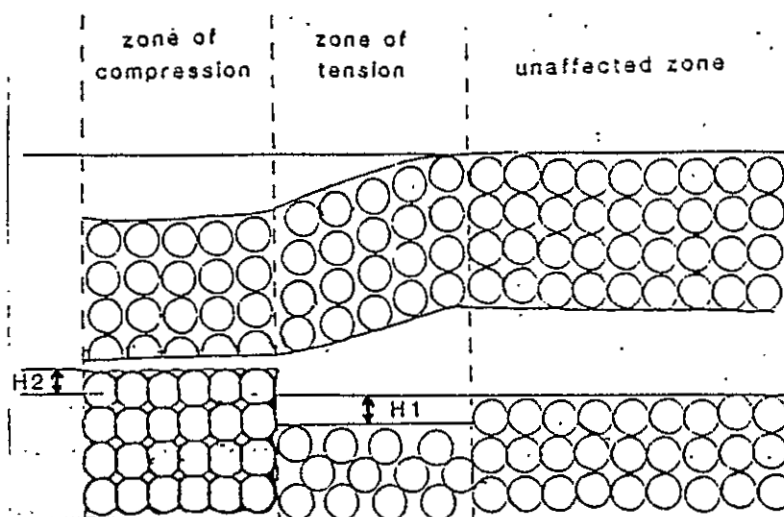


FIGURE 28--Deformation of soil structure in tensional and compressional zones bordering a wetted area (modified from Kratzch, 1983, p. 338).

settlement or concrete cracking occurred. An alternative experiment to demonstrate the destructiveness of the shear, tensional and compressional strains near the cracks would be to inject water in shallow drillholes outside only one edge of a foundation. This would place the edge of the wetting front beneath the edge of the foundation. Surface cracking as well as concrete cracking from differential settlement would likely ensue because the region of maximum strains and horizontal and vertical displacements would be located directly under the foundation.

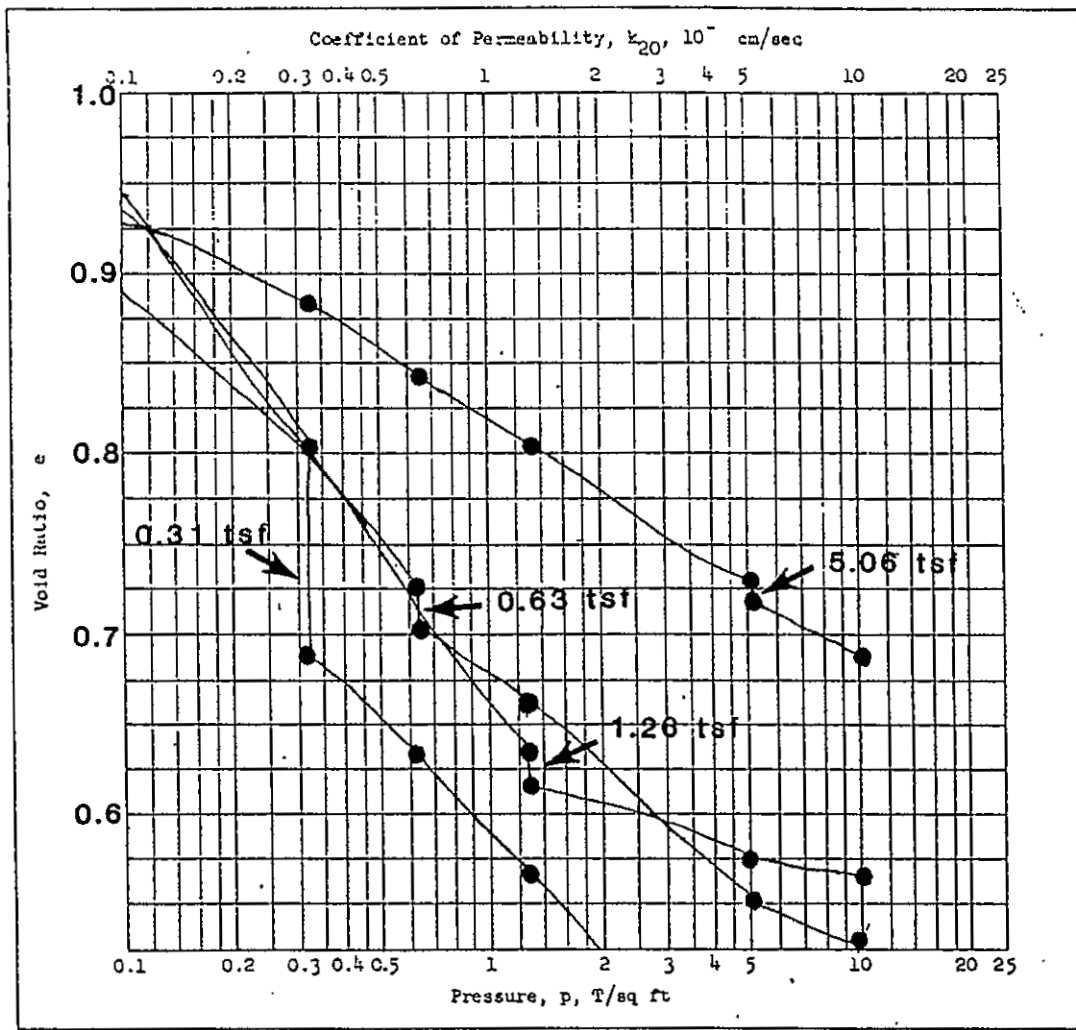
10.3 Micro-mechanism

The processes of collapse in the soil structure are extremely variable and depend mostly on the amount and type of clay, concentration of soluble salts, cementing agents, amount of water and/or load added to the soil, and soil type and structure. These variables must be addressed in any attempt to explain the micro-mechanism of soil collapse. To explain the collapse mechanism in El Llano soils six undisturbed samples from GGSS Area 4 were extensively tested in the laboratory. All six samples were highly collapsible (Table 6).

Four samples from borehole GGSSS-17, 4-6 ft were incrementally loaded in a consolidometer to 0.31, 0.63, 1.26, and 5.06 tsf and then saturated at their respective loads. As shown in Figure 29 the effect of saturation decreases with increasing load. The overburden stress on this soil is approximately equal to 0.31 tsf. At increasing

TABLE 6--Soil properties of the Collapse Mechanism
Experiment samples.

SAMPLE	DRY DENSITY (pcf)	MOISTURE CONTENT (%)	LL (%)	PI (%)	% PASSING			% CLAY
					No.4	No.40	No.200	
GGSSS-17 4-6 ft.	94	6.0	21	1	95	93	24	2.5
GGSSS-21 9-11 ft.	90	7.0	22	1	99	90	21	-



Sample	Collapse Potential
0.31 tsf	5.76%
0.63 tsf	0.31%
1.26 tsf	0.72%
5.06 tsf	0.46%

FIGURE 29--Void ratio vs. log stress consolidation curves and collapse potentials for the Collapse Mechanism Experiment samples.

stresses up to 5.06 tsf most of the compaction occurred without saturating. Water addition caused very little additional collapse at the higher loads.

To observe the effect of moisture intrusion alone and of varying load with saturation on the soil structure, each sample was examined with the SEM and petrographic microscope subsequent to the consolidation tests. Two other samples from GGSSS-17, 4-6 ft were also mounted: one in its natural, undisturbed condition and the other in a saturated, but unloaded condition. The undisturbed sample was used as a control to observe the delicate and porous character of these collapsible soils.

10.3.1 Undisturbed, dry sample

Figure 30 is a scanning electron micrograph showing the sub-rounded to rounded grains with point contacts and the high porosity of this soil. Many of the grains are either coated with clay or have clay flakes attached to them. Most silt and clay particles rest in the interstitial areas and weakly bind larger sands grain together. Thin-section analyses (Fig. 31) also indicate the presence of point contacts with a thin film of clay or calcium cement(?) around most sand grains. This is especially true for the feldspars and rock fragments. The soil consists of approximately 55% quartz, 20% plagioclase and potassic feldspars, 10% granitic and sedimentary rock fragments, 5% clay, 10% calcium cement and a trace of mica and other accessory minerals. The soil is moderately sorted in thin

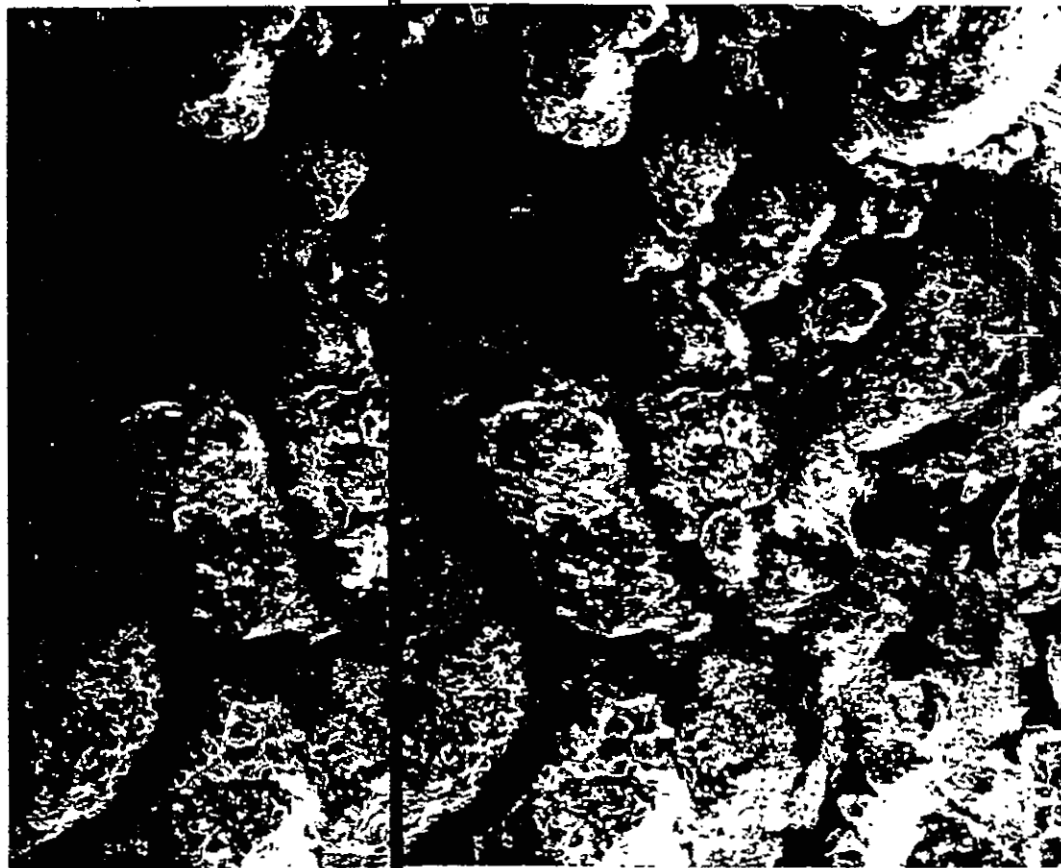


FIGURE 30--Stereo SEM photographs of the undisturbed, dry sample from GGSSS-17, 4-6 ft. (Mag. 200X, 1mm = 5 microns) Note porous structure with point grain contacts.

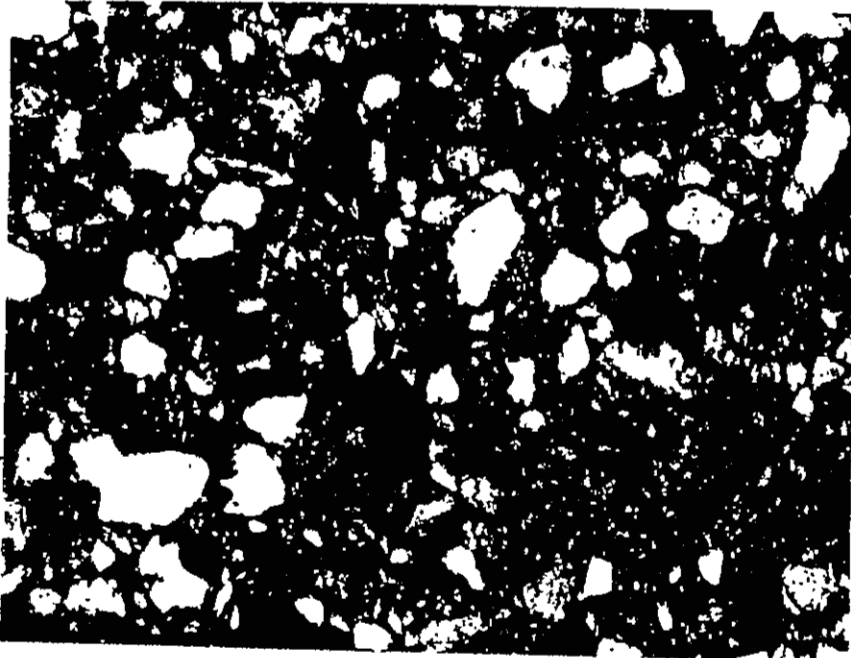


FIGURE-31--Thin-section photograph of same sample as in Figure 30 (Mag. 50X, 1mm = 0.02mm, polarized light).

section with well-rounded feldspars and rock fragments and subangular quartz grains. Porosity is at least 30%.

10.3.2 Undisturbed, saturated sample

The saturated sample exposed to no load experienced significant grain slippage during collapse (Fig. 32) and now exhibits line and overlapping grain contacts. The clay and silt flakes, located on the sand grain surfaces and in the interstitial areas, were reoriented at high angles to the grain surface. Most of the clays and silts in the dry, undisturbed sample are flat. The negative charges from the water repel the negatively charged clays and cause them to become oriented at high angles to the grain surface. Some of the silts and clays are arranged in loosely fit rows. As water enters the soil structure clays and some fine silts are suspended. As the soil dries these particles are possibly redeposited preferentially. As pore water evaporates the remaining water retreats into the narrow passages between sand grains and carries the clays and fine silts with it (Dudley, 1970, p. 936). Grain slippage probably occurs during the time the clays and silts are in suspension.

At grain contacts a normal force (P) and a shear force (T) may be transmitted to the soil grain (Fig. 33). When partially saturated soils are wetted several force changes occur: the friction between the grains decreases; the shear force increases; and the normal capillary force of the grain menisci decreases (Fig. 34; Moore and Millar,

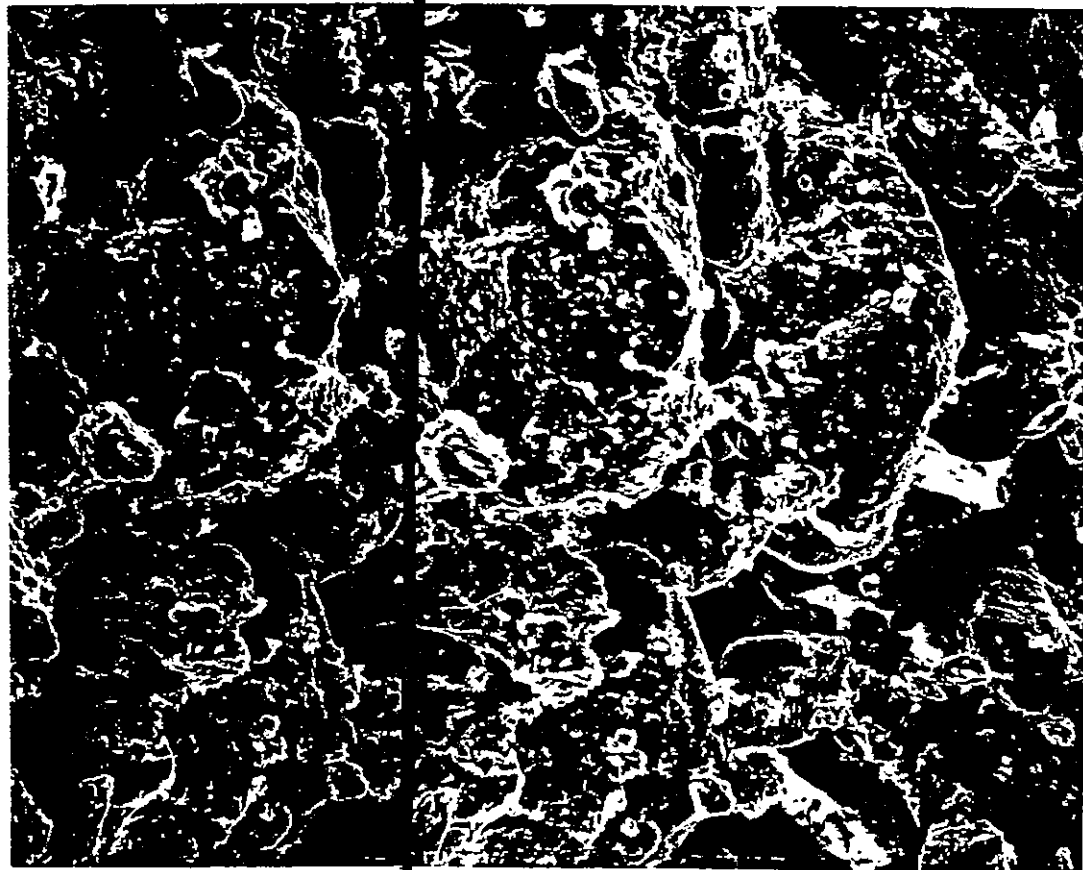


FIGURE 32--Stereo SEM photograph of the undisturbed, saturated sample (GGSSS-17, 4-6 ft). Notice the effect of water has moved the grains into line and overlapping contacts. Also note the clay flakes "standing on end" (Mag. 400X, 1mm = 2.5 microns).

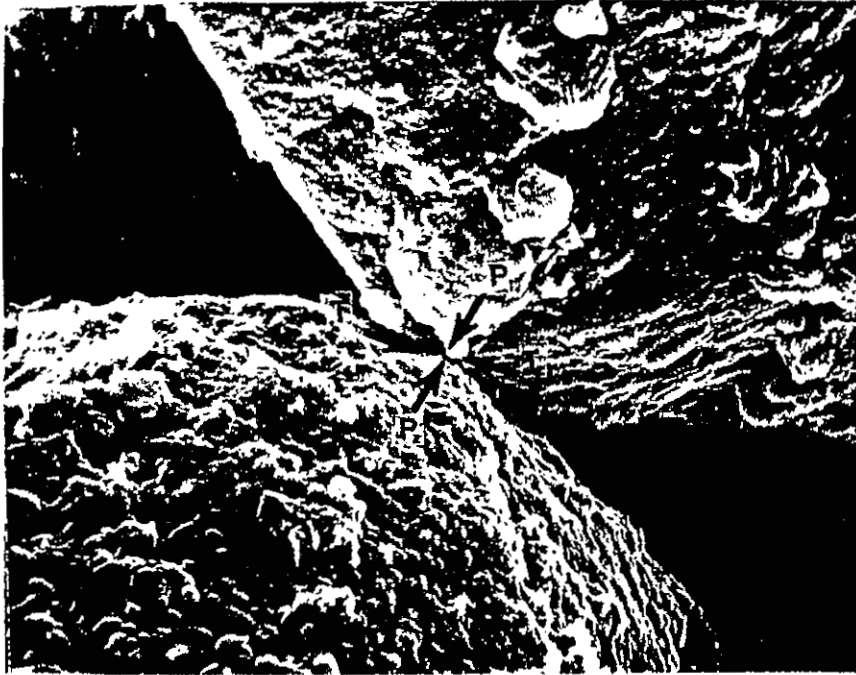


FIGURE 33--SEM photograph of a point contact between two sand grains and the forces transmitted between them (Mag. 2100X, 1mm = 0.47 microns, GGSSS-12, 2-4 ft.). P = normal force, T = shear force. Photograph by M. Hemingway.

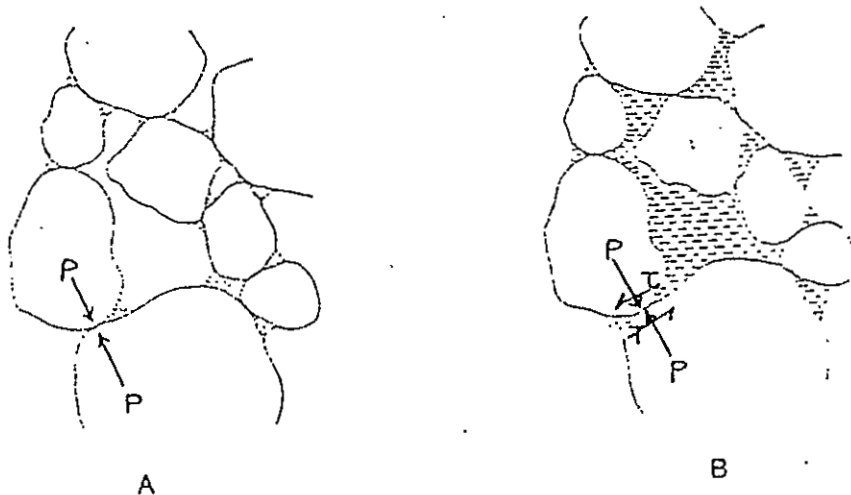


FIGURE 34--Model of a fine silty sand: (A) initially partially saturated soil with grain menisci placing the water under tension to create a stabilizing normal force, P, between the grains; (B) fully saturated soil with increasing shear force, T, and decreasing normal force from the lack of capillary tension between the grains. Grain slippage follows (modified from Burland, 1965, p. 274).

1971; Burland, 1965, p. 272). For stability the ratio T/P must be less than or equal to the friction between the grains, f . With saturation T increases slightly while P and f decrease to make the ratio great enough to overcome the frictional force that inhibits grain slippage. The resultant displacement of the grains is either a rotation, a translation or both.

A safety factor for grain slippage can be computed for partially saturated soils under specific conditions using Mohr Circles and failure envelopes (Eq. 2; Fig. 35). In partially saturated soils the effective stress equation ($\sigma' = \sigma_T - \mu$) no longer applies because all the pores are not filled with water (Blight, 1967; Jennings and Burland, 1962). The pore-water pressure, μ_w , here is the sum of the pore-air pressure, μ_a , and the capillary pressure, μ_c , resulting from the curvature of the grain menisci at the air-water interface.

In the drained consolidation test the air in the pores of unsaturated soils is at atmospheric pressure ($\mu_a=0$). Thus the pressure in the water films around the grains must be negative ($\mu_w = -\mu_c$) and μ_c is actually a tensional stress. Hence the safety factor equation becomes:

$$S.F. = \frac{(\sigma - \mu_c) \tan \phi'}{\frac{1}{2} (\sigma_1 - \sigma_3)} \sin \left(\frac{\pi}{2} + \phi' \right) \quad (2)$$

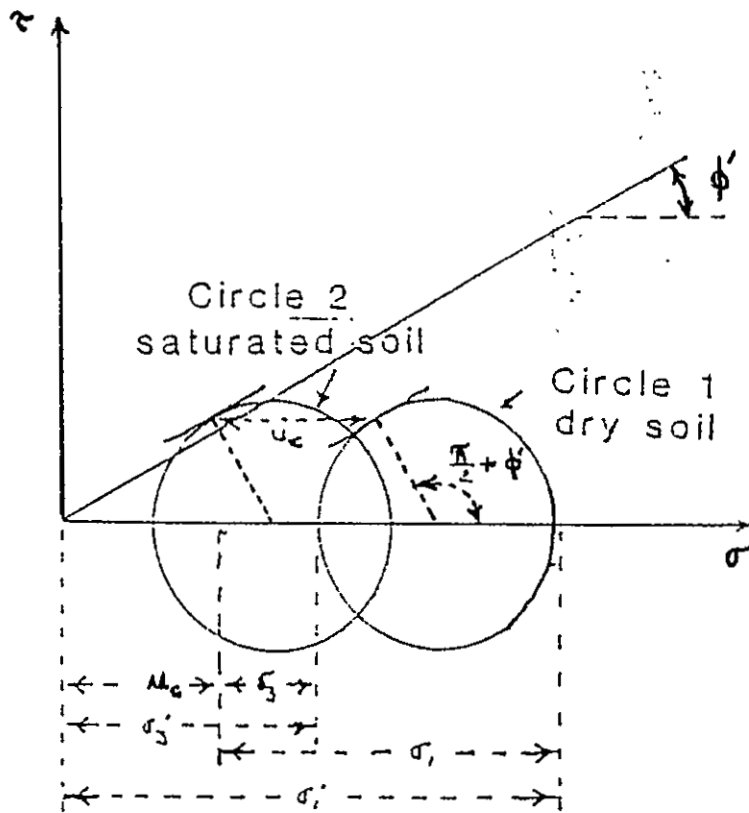
Capillary pressure increases to zero as the

saturation rises to 100%. Thus when a collapsible partially saturated soil is saturated under constant load the capillary pressure vanishes, thereby decreasing the safety factor. This is illustrated by Circle 1 being translated toward the origin by an amount equal to the value of u_c (Circle 2, Fig. 35). Grain instability and soil collapse occur when Circle 2 intersects the Mohr failure envelope (Holtz and Hilf, 1961, p. 678).

The process of collapse by saturation is more related to a shear failure rather than a classic consolidation process in which the air and water are squeezed out of the void spaces. Jennings and Knight (1975, p. 102), concluded after a series of direct shear tests on a partially saturated soil that there was on average 30% reduction of shear strength between sand grains when wetting occurred.

10.3.3 0.31 to 5.06 tsf, saturated samples

With increasing load the sand grains appear to be more and more compacted. This is especially apparent in the samples exposed to the greatest loads where micas are bent around quartz grains. Parallel alignment between elongate grains also occurs perpendicular to the normal stress during consolidation. As the sand grains form line or overlapping contacts a "honeycomb" structure appears (Fig. 36). All the clays and silts are squeezed out of the interstitial areas like tooth paste and are deposited either on the surface of the sand grains or occur as



SYMBOLS:

- σ_1 and σ_3 = major and minor principal normal stresses
 τ = shear stress
 u_c = capillary tension
 ϕ = angle of internal friction

FIGURE 35--Mohr circles and failure envelope for a dry, partially saturated soil (Circle 1) and a saturated, collapsed soil (Circle 2), (modified from Holtz and Hilf, 1961, p. 678).

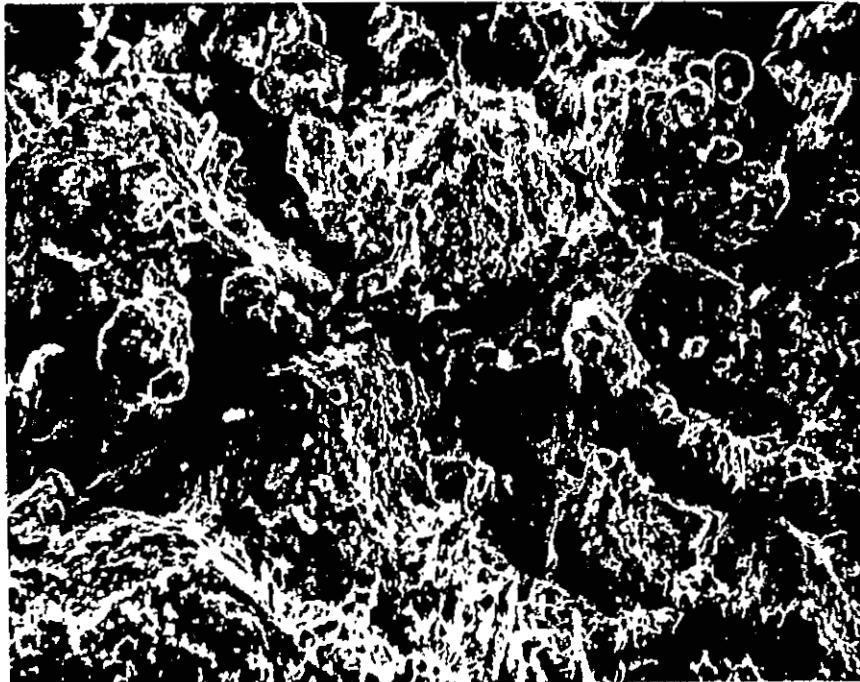


FIGURE 36--SEM photograph of the 5.06 tsf, saturated sample showing a honeycomb structure. Notice clays and silts are squeezed out of interstitial areas like "tooth paste" (Mag. 200X, 1mm = 5 microns, GGSSS-17, 4-6 ft.).

isolated blebs.

The effect of saturation on collapse lessened with increasing load (up to 5.06 tsf). At the higher loads most of the collapse occurred without wetting because there were very few clay and silt aggregates to hold the sand grains together. This is in contrast to collapsible soils studied in California by Bull (1964) and many others who found much greater clay contents (up to 12%). In these soils, clay aggregates hold the sand grains together even under large loads because of their high dry strength. When saturated, however, the clay aggregates lose their strength and grain slippage ensues. El Llano collapsible soils are unusual because of their very low clay content of 1-3%. This allows any appreciable load to compact the sand grains to their densest configuration. Except under very light loads of 0.31 tsf (the approximate overburden stress of this soil), where the collapse potential was 5.96%, the greater loads needed no water to collapse the samples.

10.3.4 Effect of varying moisture content and saturation at constant load:

The second part of the Collapse Mechanism Experiment consisted of three modified consolidation tests with undisturbed samples from borehole GGSSS-21, 9-11 ft (Table 6). Each sample was loaded to 0.31 tsf and then wetted with varying amounts of water in an attempt to correlate collapse potential with the final moisture content and saturation of

each sample. Each sample was uniformly wetted and was allowed to equilibrate for one day. Results are shown in Figure 37. The greatest collapse potential occurred in the sample that was only 70% saturated. Preliminary results from this experiment suggest that El Llano collapsible soils do not have to be 100% saturated to collapse, but can be unstable at much lower moisture contents just above their natural moisture condition. This is true partly because the soils have low dry densities between 80 and 95 pcf. Fully saturating a low density soil requires increasing its moisture content to its liquid limit or greater. Here the dry density vs. liquid limit criterion again applies (Sec. 9.2.3): low density collapsing soils at their liquid limit may still not be fully saturated due to their large void ratios.

The critical saturation, S_c , (the saturation below which collapse will occur) for this particular silty sand (SM) of 70% is close to the values given by Jennings and Knight (1975, p. 100) for the same soil type (Sec. 9.2.2). Booth (1975, p. 61) found a similar relationship between varying moisture content and amount of collapse. Starting with a constant density for all soils, each sample was compacted at moisture contents equivalent to 16.7%, 33.3%, 50.0% and 66.7% saturation. They were then loaded to 440 KN/m (4.5 tsf). Figure 38 shows there was less soil collapse in soils compacted at higher than at lower moisture contents. Particles of fine soil tend to aggregate in clumps at low compaction moisture contents, and

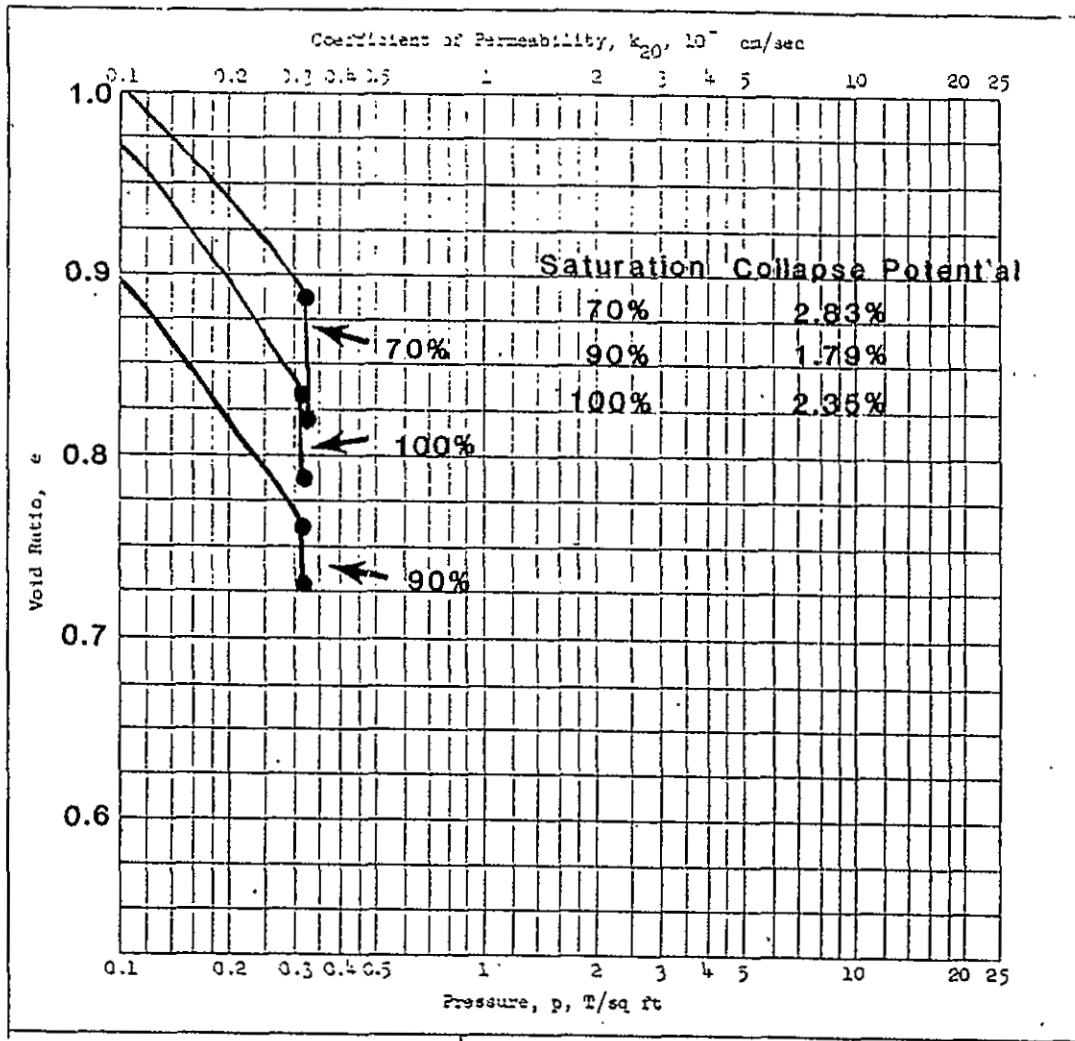


FIGURE 37--Void ratio vs. log stress consolidation curves for varying saturations and collapse potentials of the GGSSS-21, 9-11 ft. samples.

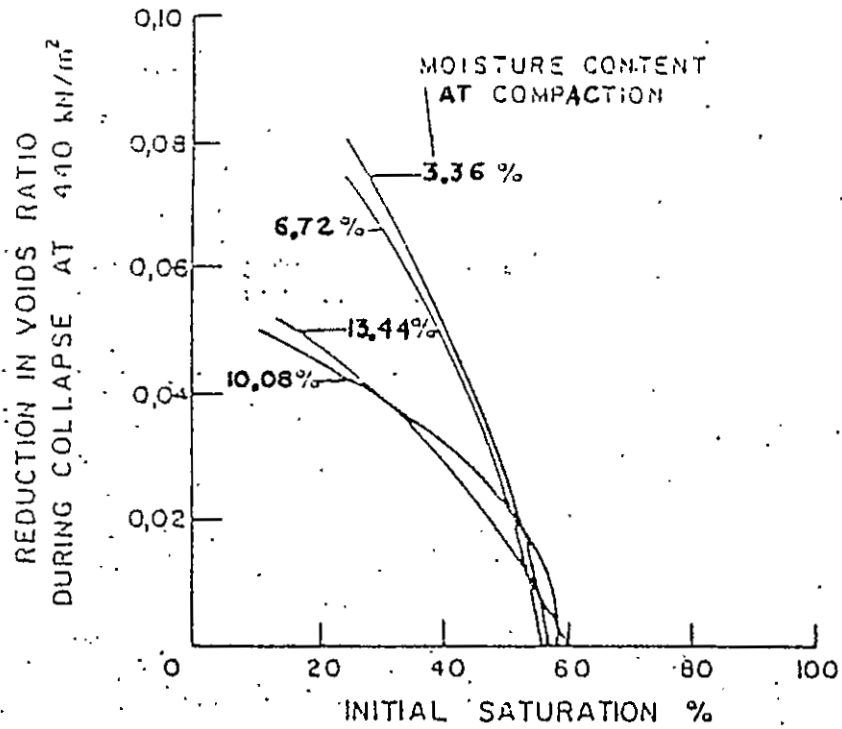


FIGURE 38--Relationship between collapse and saturation for soils compacted at the same dry density at different moisture contents (from Booth, 1975, p. 62).

presumably this gives less resistance to compression.

10.3.5 The role of clay and silt aggregates

Loss of clay-aggregate shear strength between sand grains from wetting has long been regarded as the primary micro-mechanism of collapse (Bull, 1964, 1972; Beckwith, 1976; Dudley, 1970 and Lofgren, 1969). In alluvial sediments near Tucson, Arizona, Barden and others (1973, p. 57) discovered samples compacted above their optimum moisture content (OMC) showed no collapse while samples compacted below their OMC all collapsed. This is due to the open-structured and flocculated nature of the clays in collapsible soils compacted below their OMC. Fine clay platelets flocculate to form bulky peds grouped in a loose "cardhouse" structure between sand grains (Fig. 39). The mechanism governing collapse in clayey to silty sands is not found in the flocculated arrangement of the clays and fine silts at the microscale but rather in the effective granular macrostructure formed by their aggregates (Barden and Sides, 1969, p. 319). These aggregates themselves act as whole grains binding the larger sand grains together.

In El Llano collapsible soils these aggregates consist mostly of silt and a little clay. They do not support the soil structure very well during compaction. Volume reduction seems to be more related to actual grain-to-grain slippage with each grain moving into an adjacent void space, rather than collapse from the loss of

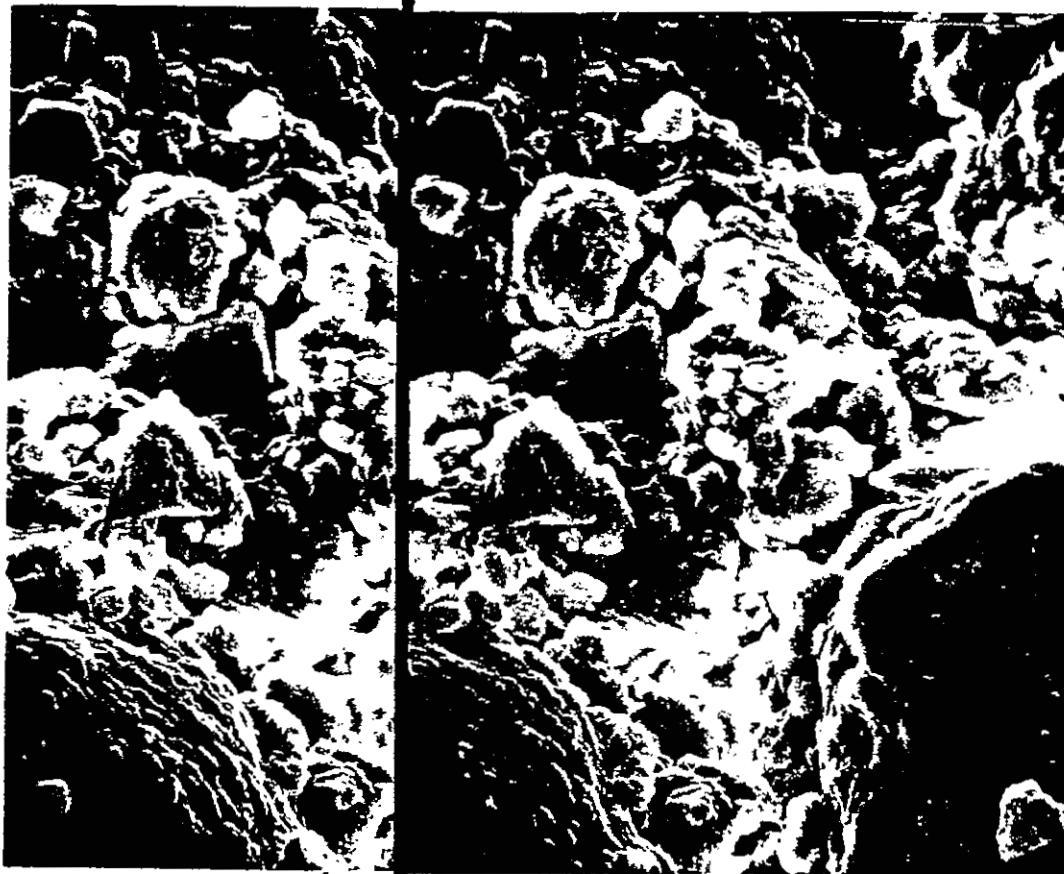


FIGURE 39--Stereo SEM photograph of clay and silt particles in a loose "cardhouse" structure flocculated between two sand grains (Mag. 2000X, 1mm = 0.5 microns, GGSSS-17; 4-6 ft).

clay-aggregate strength. Still the collapse micro-mechanism may be discerned in the internal structure of the silt and clay aggregates. Many of these aggregates are interlaced with air-filled channels and macropores (Fig. 39). Their clay content is so low that even when dry the aggregates can only weakly bind the sand grains together. With applied load alone all the aggregate macropores are reduced because there are few clays to resist the normal force. Subsequent wetting then disperses the fines and the sand grains slip by one another into vacant void spaces. Overall, the cause of collapse is not only the result of a change from a flocculated to a dispersed structure, but also to a reduction of interpedal channels and pore volume within the clay and silt aggregates.

10.3.6 The role of clay mineralogy

Even though El Llano collapsible soils have a low clay content it is still relevant to discuss how clay mineralogy and content affect the collapse mechanism. X-ray diffraction analyses on the GGSSS-17 samples were semi-quantitative (parts in 10) for the contained clay mineral groups (Austin, written comm., 1985). The clays in the samples contained an average of 4 parts kaolinite, 2 parts smectite, 2 parts illite and 2 parts mixed-layer clays.

It was thought originally there were more expansive clays (smectite and mixed-layer clays) in these soils and that they partially controlled the strength

behavior of the clay and silt aggregates. Because expansive clays have such high surface area per unit volume, it gives them a greater ability to hold water (Borchardt, 1977, p. 319). Montmorillinite holds water more tightly and is thus appreciably stronger at low moisture contents. The dry soils in El Llano probably have some of their pore water absorbed in these clays. As water is evaporated from the pores a pressure difference develops across the air-water interfaces which occur where water bridges the particles. These interfaces, or menisci, become more concave with evaporation and hold the sand grains tightly together.

At low moisture contents of 1-8%, as in El Llano soils, smectite clays have the greatest shear strength followed by illite and then kaolinite (Brown, 1977, p. 696). At high moisture contents near saturation smectites have the lowest shear strength. Bull (1964; p. A54) found that for a given decrease in clay content there was a corresponding decrease in shear strength of the clays in collapsible soils in California. Hence, upon saturation, El Llano collapsible soils should exhibit little shear resistance to the forces exerted by the excess water and applied load.

The role of expansive clay minerals in swelling the aggregates may be one of a "ball-bearing" effect between sand grains that enhances grain slippage and volume reduction. With wetting under light loads, the aggregate initially expands and loses its binding capacity;

slippage then follows. However, according to Burland (1965, p. 275) it is also quite possible that soaking under light loads will first result in a rapid reduction in soil volume from the removal of intergranular bonds. A slow volume increase may occur later after collapse due to the absorption of water in the expandable clay lattices. Surface subsidence followed by soil expansion has been reported around Tucson, Arizona (Sultan, 1969). It is not clear whether the expansive clay minerals in El Llano collapsible soils occur in amount sufficient to play a significant role in the collapse mechanism.

The micro-structural arrangement of clay and silt aggregates is characterized by a network of small clusters connected by links of particles, or domains (Fig. 40). Domains partially break down upon consolidation and congeal to form groups of cluster-oriented particles. This process is inversely related to the amount of expansive clay minerals present because, when dry, these clays will resist movement. The Collapse Mechanism Experiment showed that most of the soil collapse occurred without water addition even with high consolidation stresses up to 5.06 tsf. Presumably the small amount of expansive clays in these consolidation samples was insufficient to resist this load.

The mechanism of collapse within the clay and silt aggregates is a shearing process that involves the movement of the aggregate as a unit. This occurs in conjunction with deformation of domains and clusters (Rieke and Chilingarian, 1974, p. 214). Under small loads, domains and

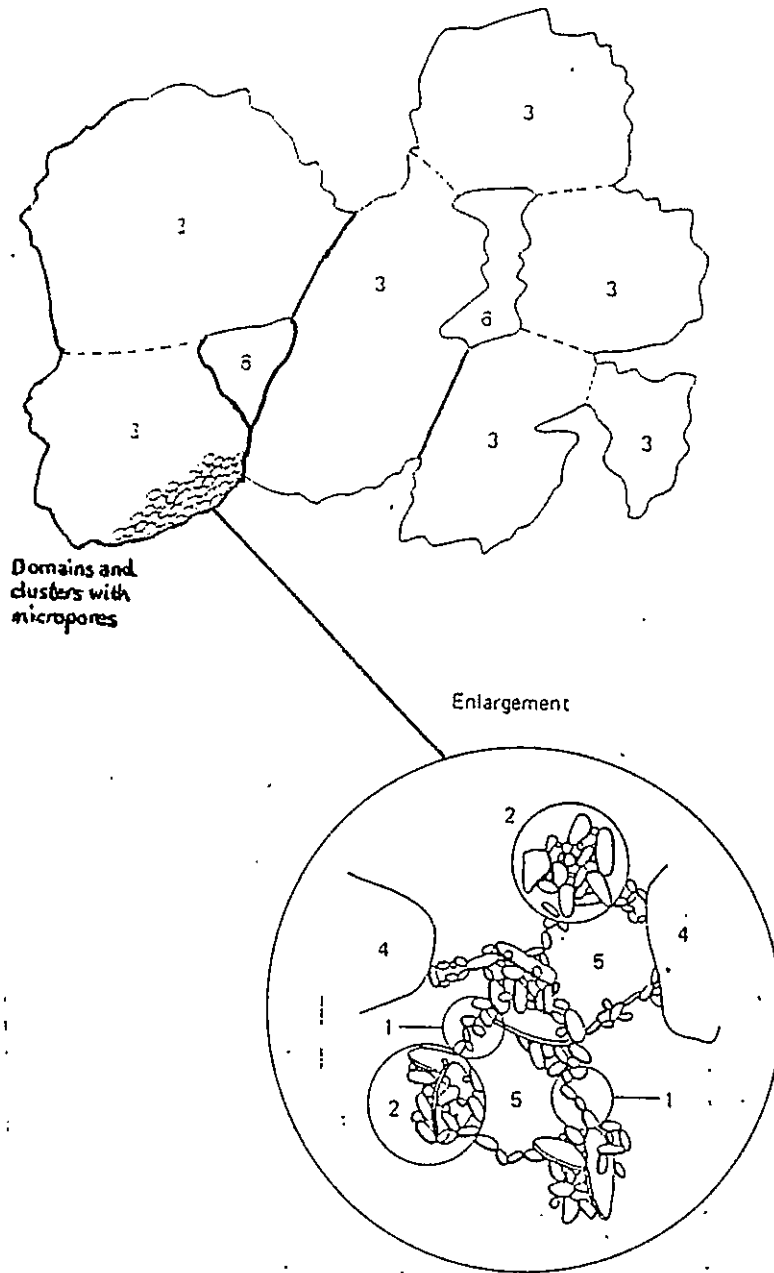


FIGURE 40--Schematic diagram of a soil microfabric and macrofabric: 1=domain; 2=cluster; 3=ped; 4=silt grain; 5=micropores; and 6=macropore (from Holtz and Kovacs, 1981, p. 98).

clusters become oriented parallel to each other. Initial collapse is represented by micro-fissures through the entire clay aggregate. With increased load and/or moisture, the clay aggregates tend to orient themselves in a preferred failure plane, or micro-shear plane (Barden, 1971, p. 162). This is illustrated in Figure 41 where the clays are oriented in aligned groups after having been loaded, saturated and then sheared.

The degree of clay aggregate orientation in the failure plane becomes high only after large shear displacements occur and after the formation of a Coulomb slip plane. This evidence suggests that the reorientation of the failure zone is a result rather than a cause of collapse. The governing factor for failure is proportional to the defect density in the aggregate--the ratio of the area of defects such as micropores, channels and fissures to the total cross-sectional area (Barden, 1971, p. 162). Apparently a high defect density within the clay and silt aggregates encourages the development of these micro-shear failure zones. Clays and clay aggregates should be viewed with the scanning electron microscope at different stages of deformation in the consolidometer to monitor and better describe this collapse mechanism.

10.3.7 The influence of soluble salts and cements

Soluble salts, oxides, silicates and calcium carbonate also have a significant effect on the wet and dry

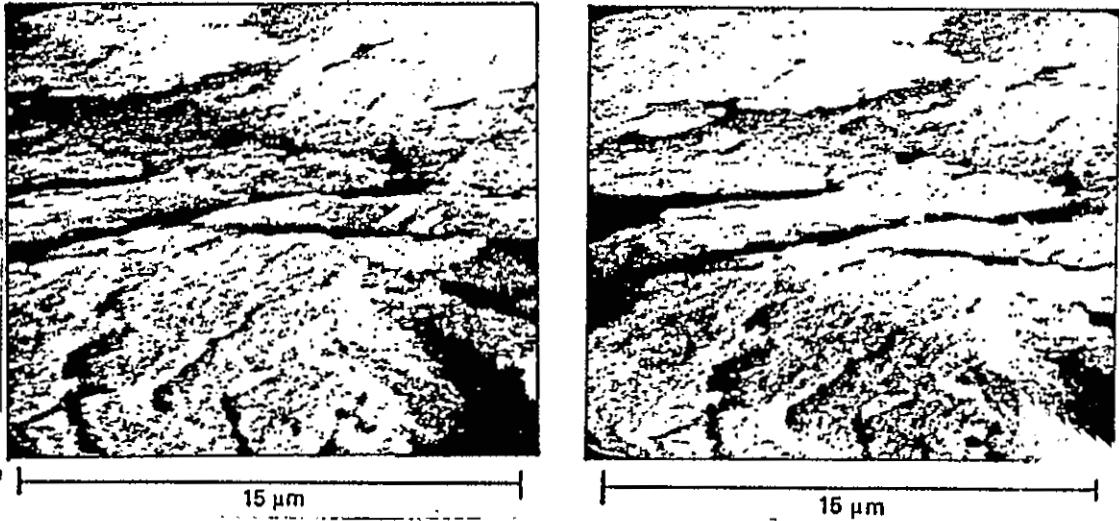


FIGURE 41--Dynamic study of the failure of a clay aggregate. Note failure plane where slippage occurs with increasing load and moisture content (from Smart and Tovey, 1982, p. 32).

strength of collapsible soils. Although no soil chemical analyses were done, it is known that most near-surface soils are alkaline and commonly exhibit calcium carbonate filaments and nodules. Soils containing natural soluble salts and calcium carbonate, which are in equilibrium with their climatic and hydrologic environment, persist throughout cycles of wetting and drying and cement soil grains. If environmental conditions change such that these salts and cements are eluted from the soil, or are dissolved far beyond their normal seasonal dilution, then a lessening of the soil bonds occurs (Ingles and Aitchison, 1969, p. 345). This enhances collapse.

The dissolution of salts and cement from irrigation in El Llano is probably very low because the water is already charged with salts. Soils in the study area, at least in the upper 10 ft, have some gypsum fibers present. However, dissolution of gypsum is probably not a cause of collapse since it does not support the grains within the soil structure. Bull (1964, p. A61) also suspects that gypsum has no effect on soil subsidence.

Replacement of cations in the clays from percolating waters may weaken particle bonds. Sodium in irrigation waters can replace the calcium in montmorillinite and thus lower its strength and increase swelling. Alkaline soils are the most vulnerable to dispersion. If the soils' acidity increases, either by saturation from leaking septic tanks or from rainwater runoff, the total exchangeable cations for the clays are reduced but the percentage of

exchangeable sodium is increased (Weaver and Pollard, 1973).

An interesting test would be to compare the amount and rate of consolidation in El Llano soil samples soaked with regular distilled water and with sodium-charged water. Bull (1964, p. A62) performed a similar test and found a doubled rate of consolidation with soils soaked in sodium saturated solution.

10.3.8 The hydrodynamic effect

The disturbing force which destroys the metastable equilibrium in a collapsible soil may also be a hydrodynamic force from the intruding water (Ingles, 1964). This is especially true for silty to clayey sands in semi-arid to arid environments which have not been previously wetted. The hydrodynamic effect of the water front moving through the soils causes collapse without any applied load (e.g. GGSS Areas 1 and 3 and Moya's subsidence pit). In this situation the perturbation arising from the gross dissolution of salts in the electrolytes at points of particle contact may also be sufficient to cause soil collapse.

11.0 EXISTING COLLAPSE PREDICTION CRITERIA

The purpose of this section is to outline five

collapse index criteria of previous workers and use them to predict collapse for soils in the study area. Because every criterion requires at least moisture content, dry density and liquid limit values for the soils, not all samples could be evaluated. Approximately 200 samples located around the study area at various depths were used. The average values of all five criteria for soils in the entire study area and for soils east and west of the acequia are given in Tables 8 and 9.

A considerable amount of work has been done in the past toward quantifying parameters that describe settlements associated with collapsible soils, particularly those concerned with an increase in moisture content. These include laboratory tests such as the double oedometer method (Jennings and Knight, 1957), triaxial and shear tests (Grigorian, 1967), and in situ field tests like the "sausage test" (Jennings and Knight, 1975; Clemence and Finbarr, 1981), the "coke bottle test" (McNeill, pers. comm., 1985) and the soil dispersion test (Sultan, 1971). The main disadvantage with these types of collapse prediction in the laboratory is that they are specialized and time-consuming, and may not be time or cost effective in a large geotechnical investigation. The field tests are quick and simple but do not quantify collapsibility. Methods of predicting soil collapse from simple, readily available index parameters are therefore more appropriate.

TABLE 7--Means, standard deviations and ranges of other workers' collapse criteria applied to El Llano soils.

CRITERIA	MEAN	S.D.	MIN.	MAX.	CASES
Coefficient of Subsidence, K (Denisov, 1951)	1.008	0.497	0.495	4.011	199
Coefficient of Collapse, τ (Beles and Stanculescu, 1961)	-0.004	0.220	-0.932	0.977	199
Collapse Criteria, Kd (Prinklonskij, 1952)	2.802	2.297	0.000	9.500	91
Subsidence Index, K1 (Fedá, 1966)	1.353	2.131	-2.560	9.081	91
Collapse Ratio, R (Gibbs and Bara, 1967a)	1.141	0.357	0.250	2.537	199

TABLE 8--Means, standard deviations and two-tailed probabilities at a 0.01 level of significance of other workers' collapse criteria applied to soils east and west of the El Llano acequia.

CRITERIA	LOCATION	MEAN	S.D.	2-TAILED PROBABILITY	CASES
Coefficient of Subsidence, K	East	0.9928	0.471	0.455	149
	West	1.0537	0.573		50
Coefficient of Collapse, τ	East	0.0054	0.212	0.282	149
	West	-0.0334	0.243		50
Collapse Criterion, Kd	East	2.7538	2.266	0.700	72
	West	2.9837	2.470		19
Subsidence Index, K1	East	1.4032	2.083	0.667	72
	West	1.1645	2.356		19
Collapse Ratio, R	East	1.1455	0.340	0.779	149
	West	1.1290	0.408		50

11.1 Denisov's (1951) coefficient of subsidence, K

Denisov (1951) was among the first to suggest that the potential subsidence of soils is controlled by their natural porosity. He based his criterion on the ratio of the void ratio at the liquid limit (e_L) to the natural void ratio (e_0). He called this ratio the coefficient of subsidence, K .

This criterion was developed for loessical soils in Russia and Eastern Europe. It does not account for the applied stress level on the soil structure but only considers whether a soil is capable of absorbing enough water to elevate it to or past its liquid limit. Denisov therefore suggested that a soil may be collapsible if $K < 1.0$. The mean value of K for El Llano was 1.008 with a standard deviation of 0.497 (Table 8). East of the acequia, K averaged 0.9928 and west of the acequia it averaged 1.0537. Both means had fairly high standard deviations indicating a considerable variability in K values. Also, the T-test showed that there was a high two-tailed probability of 0.455 at a 0.01 level of significance. Thus there was not a significant difference between K values east and west of the acequia (Table 9).

11.2 Beles and Stanculescu's (1961) coefficient of collapse, τ

The coefficient of collapse predicts instability in soils that are less than 60% saturated. Thus it should work well with the partially saturated soils in El Llano. It is similar to Denisov's criterion in that the coefficient of

collapse only compares parameters related to the porosity (or void ratio) of a soil. Soil collapse will occur if:

$$\tau = \frac{e_0 - e_1}{1 + e_0} > -0.1 \quad (3)$$

The mean value for the entire study area was -0.004. East and west of the acequia the averages were 0.0054 and -0.0334, respectively, indicating that both areas are collapsible according to this criterion (Tables 8 and 9). However, the relatively high standard deviation for both areas again suggests high variability. The T-test did not provide enough evidence to suggest a significant difference in values east and west of the acequia. The 0.282 two-tailed probability carries only a 0.01 level of significance.

11.3 Prinklonskij's (1952) collapse criterion, K_d , for saturated soils

Prinklonskij (1952) was the first to suggest a criterion including parameters related to the strength of a soil. His criterion, K_d , is limited to collapse of soils upon saturation. For subsidence:

$$K_d = (W_l - W_o) / I_p < +0.5 \quad (4)$$

where W_l = the liquid limit moisture content;

W_o = the natural moisture content;

I_p = the plasticity index.

The mean K_d value for the entire study area is 2.802 (Table 8), too high to render a realistic prediction of soil collapse. Similarly, east and west of the acequia K_d is equally as high (Table 9). Because natural moisture contents and plasticity indices are so low for most unsaturated El Llano soils and because collapse generally occurs at saturations well below 100%, the K_d values are always too high and far too conservative (predicts collapse the least).

11.4 Fedá's (1966) subsidence index, K_1

Fedá (1966) invented probably the most comprehensive criterion and based his research on evolving a parameter related to the sensitivity of a soil. The sensitivity is defined as the ratio of undisturbed and remolded soil strengths under similar conditions so that a highly sensitive soil would therefore be structurally unstable (Darwell and Denness, 1976, p. 546). Fedá used the liquidity index, I_L [$I_L = (W_o - W_p)/I_p$], which predicts instability for saturated soils, to invent a new criterion for unsaturated soils. With increasing porosity of a saturated soil the liquidity index increases and so does its sensitivity. For unsaturated soils one can use the relation:

$$S_o \cdot e_o = W_o \cdot G_s \quad (5)$$

where S_o , e_o , W_o and G_s are the natural degree of saturation,

void ratio, moisture content and specific gravity of the grains, respectively.

Then, based on equation (5) a subsidence index, K_1 , for unsaturated soils may be defined:

$$K_1 = (W_o/S_o) - W_p/I_p \quad (6)$$

Based on correlations between liquidity index and this subsidence index it was determined that any soils with values of K_1 greater than 0.85 were collapsible. Fedá imposed two constraints on his criterion: the soil should have a natural porosity of 40% or greater and the soil should be subjected to a high enough external load for structural collapse to occur upon wetting.

The mean subsidence index, K_1 , for the entire study area was 1.353 with a very high standard deviation of 2.131 indicating the high variability of the values (Table 8). East and west of the acequia K_1 values are 1.4032 and 1.1645, respectively (Table 9). According to this criterion even the average K_1 value west of the acequia is collapsible (> 0.85), which suggests that K_1 renders a fairly liberal evaluation of collapsibility in El Llano. The T-test showed a high two-tailed probability of 0.667 indicating there is no substantial difference between mean K_1 values east and west of the acequia.

Darwell and Denness (1976) modified Fedá's subsidence index to include dry density and specific gravity of the grains in the equation.

Since

$$W_o/S_o = p_w/p_d - 1/G_s \quad (7)$$

then

$$p_w/p_d - 1/G_s - w_p > 0.85(w_l - w_p) \quad (8)$$

or

$$w_l + 3/17w_p < 1/0.85(p_w/p_d - 1/G_s) \quad (9)$$

where p_w = density of water

p_d = dry density of the soil.

This expression can be represented as a series of parallel lines on a graph of liquid limit against plastic limit; each line is given a unique combination of dry density and specific gravity (Fig. 42) and runs from a point where $w_l = w_p$ (i.e. $I_p = 0$) to the horizontal (liquid limit) axis where $w_p = 0$. A collapsible soil with K_l values greater than 0.85 plots to the left of the line given by its dry density and specific gravity. A specific gravity of the grains of 2.60 was assumed for all soils in the study area. A stable soil with a K_l value less than 0.85 plots to the right of its dry density and specific gravity line.

11.5 Gibbs and Bara's (1967a) collapse ratio, R

The collapse ratio, R, is defined by the moisture content at saturation divided by the liquid limit moisture content. Presumably, if a soil is at its liquid limit and it is still not saturated the soil probably has a high void ratio and is very unstable. Any increase in moisture content past the liquid limit would lead to collapse. Thus

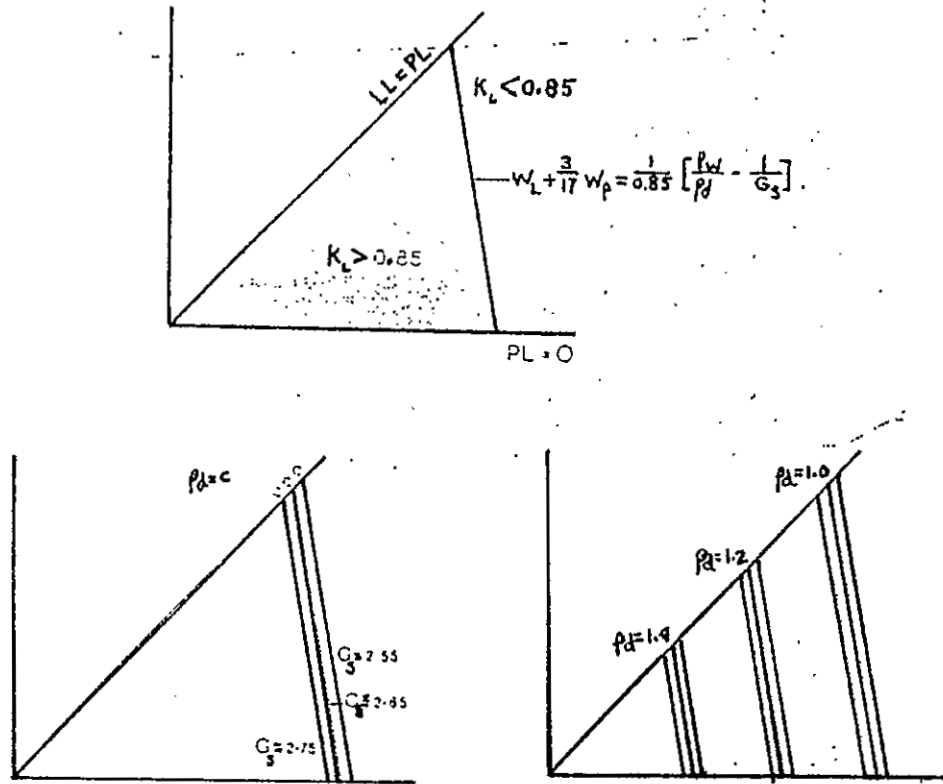


FIGURE 42--Metastability evaluation graph (from Darwell and Denness, 1976, p. 548-549).

collapsible soils generally have R values greater than 1.0.

Since

$$R = w_{sat}/w_l \quad (10)$$

where w_{sat} = the moisture content at saturation;

w_l = the liquid limit

and

$$w_{sat} = (p_w/p_d) - (1/G_s) \quad (11)$$

then

$$R = (p_w/p_d) - (1/G_s)/w_l \quad (12)$$

This collapse index does not account for the type and nature of the bonds between the grains, nor does it account for the applied load on the soil. The mean R value over the entire study area is 1.141 with a standard deviation of 0.357 (Table 8). East and west of the acequia R values are 1.1455 and 1.1290, respectively, indicating this criterion is somewhat liberal in its evaluation El Llano soils. The data do not show significant differences between the mean R values in soils east and west of the acequia since the two-tailed probability is 0.779 at a 0.01 level of significance. However, because the collapse ratio only requires dry density and liquid limit, it was calculated for the greatest number of samples in the study area (199). Therefore this collapse index will be used in the following regression analysis as the dependent variable to predict collapsibility.

11.6 Comparison of criteria

Excluding Prinklonskij's (1952) collapse criterion because it only applies to saturated soils, Denisov's (1951) coefficient of subsidence appears to be the most conservative, or predicts collapse the least, of all the criteria. It can also be shown from Table 8 that Fedor's, (1966) subsidence index is the most liberal, or predicts collapse the most. Beles and Stanculescu's (1961) coefficient of collapse and Gibbs and Bara's (1966) collapse ratio appear to be equally biased and fall between the other more conservative and liberal criteria.

12.0 REGRESSION AND DISCRIMINANT FUNCTION ANALYSIS--

SUGGESTED CRITERION FOR COLLAPSIBLE SOILS IN EL LLANO

One of the ultimate goals of this study is to generate linear and logarithmic regression equations to predict soil collapsibility in El Llano. Using the collapse ratio, R , as the dependent variable and dry density, moisture content, Atterberg limits, and per cent passing the No. 4, No. 40, and No. 200 sieves as the independent variables, a stepwise multiple regression analysis was conducted. Other variables such as per cent consolidation with and without wetting, collapse potential, per cent clay and blow counts were not used in the

regression analysis because they had too many missing values in the data file.

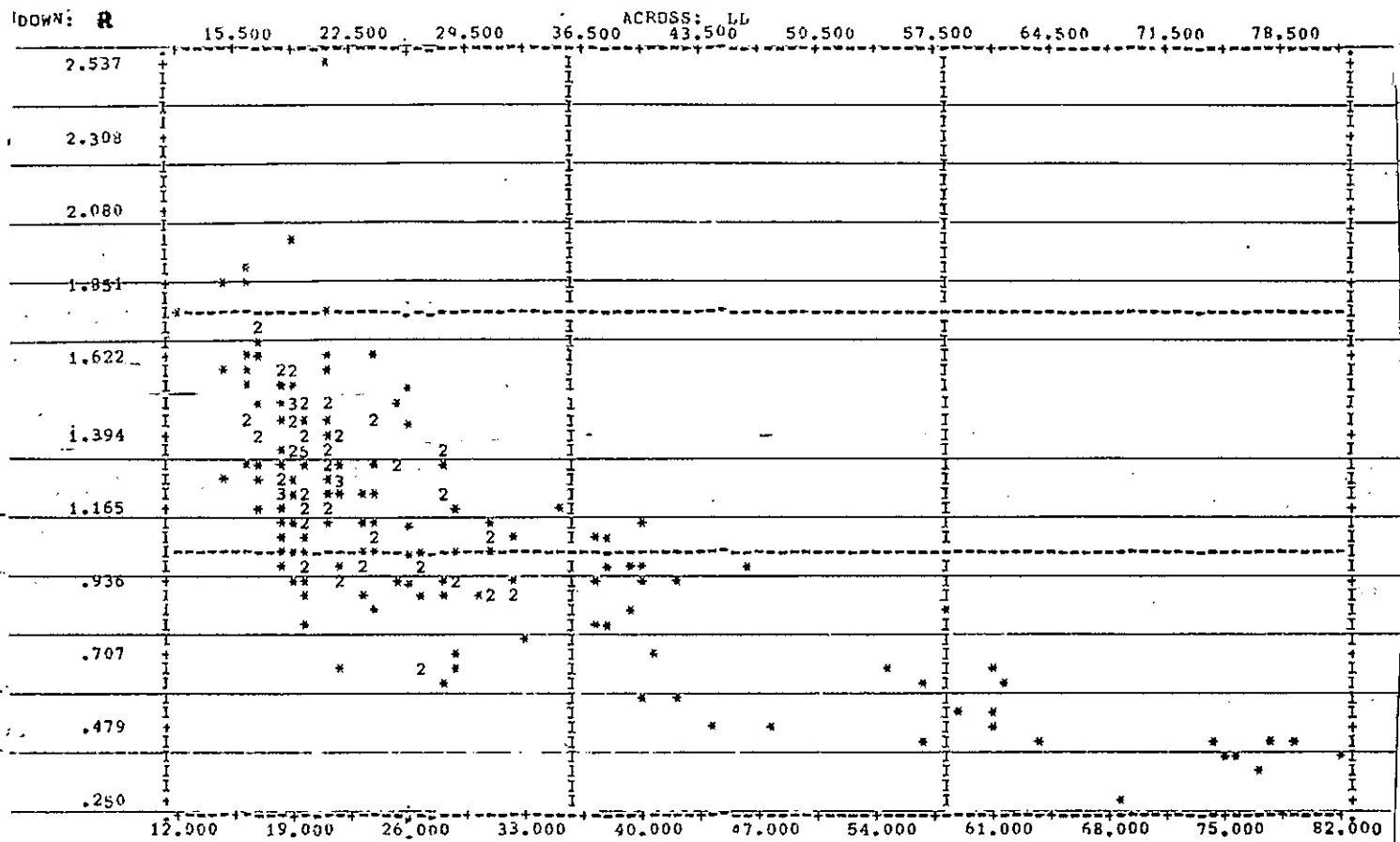
12.1 Pearson Correlations

A table of Pearson correlation coefficients, number of cases analyzed and the two-tailed probabilities at a 0.01 level of significance among all variables including the collapse ratio, R , is presented in Appendix V (Table 1). The natural log of R ($\ln R$) was calculated and was similarly correlated with all the other independent variables (Appendix VI, Table 2). Both R and $\ln R$ have strong negative correlations (< -0.5) with liquid limit, plasticity index, per cent fines (silt and clay), per cent clay and total per cent consolidation without wetting. The Pearson correlation coefficients between $\ln R$ and these variables are slightly better than those with R and suggest that R varies logarithmically instead of linearly with the independent variables. This is illustrated in the scatterplot of R vs. liquid limit (Fig. 43).

Dry density, per cent passing the No. 4 (gravel) and No. 40 (fine sand) sieves, total per cent consolidation with wetting and collapse potential all have poor correlations (between -0.5 and 0.5) with both R and $\ln R$.

12.2 Stepwise Regression Analysis

This stepwise regression analysis is based on the Pearson correlations with R and $\ln R$ and the independent variables. In stepwise regression the strongest single



10 Nov 85 SPSS-X RELEASE 1.0 FOR TEC-20 May 21, 1984
 N.H.I.M.T Computer Center DECSYSTEM - 2060 Tops-20

STATISTICS							
CORRELATION (R) =	-.74519	R SQUARED	=	.55522	SIGNIFICANCE	=	.00000
STD ERR OF EST =	.23852	INTERCEPT (A) =	1.65404	SLOPE (B) =	-.01855		
PLOTTED VALUES =	201	EXCLUDED VALUES =	0	MISSING VALUES =	431		

FIGURE 43--Scatterplot of collapse ratio, R, vs. liquid limit for El Llano soils showing their relation to $\ln R = 0.61114 - 0.02039LL$.

independent variable, or one with the greatest Pearson correlation coefficient, is first obtained; this is then "held constant" statistically to identify the second strongest variable. This process continues until no variables in the regression equation need to be removed and no variables not in the equation are eligible for entry (Krumbein and Graybill, 1965; SPSS Inc., 1983).

Redundant independent variables, or those that in large part restate what some other variables have already measured, are commonly excluded from the regression equation. For example, because liquid limit and plasticity index have a high correlation of 0.9643 (Appendix VI Table 1), they both are varying equally with changes in R or $\ln R$. Thus, in the linear regression equation, plasticity index is excluded while in the logarithmic regression equation PI is included but has a very small coefficient (Eq. 14). Other variables having a poor correlation with R and $\ln R$, noted earlier, are also omitted from the regression equations because they have relatively little effect in varying the dependent variable.

The coefficient of determination, R squared, for the linear regression equation is 0.873. This indicates that 87% of the variance in the collapse ratio is accounted for by the independent variables: liquid limit, dry density and per cent fines (Roscoe, 1969). The logarithmic regression analysis has an even better R squared value of 0.959 suggesting that almost 96% of the variance in $\ln R$ is accounted for by liquid limit,

dry density, per cent fines and the plasticity index.

The linear regression equation for El Llano soils is:

$$R = 3.47131 - 0.01416LL - 0.02035DEN - 0.00308517FINES \quad (13)$$

and the logarithmic regression equation is:

$$\ln R = 2.8235 - 0.01438LL - 0.02405DEN - 0.0025958FINES - 0.00812944PI \quad (14)$$

where R = collapse ratio (wsat/wl);

lnR = natural log of the collapse ratio;

LL = liquid limit (%);

DEN = natural dry density (pcf);

FINES = per cent fines (silt and clay);

PI = plasticity index (%).

These regression equations apply specifically to soils in the study area. Using this criterion in other areas is not advised unless it is used with caution and with other criteria.

Anderson (1968) performed a similar stepwise logarithmic regression analysis for collapsible soils in Tucson, Arizona using collapse ratio, R, as the dependent variable. His equation follows:

$$R = 5.5 - 3.82 \log(wl/wp) - 1.63 \log(wp) - 1.24 \log(Cu) - 0.918(P10) + 0.465(D60/D40) - 0.45(D99/D50) - 0.303(P200) \quad (15)$$

where w_l = liquid limit (%);

w_p = plastic limit (%);

C_u = uniformity coefficient;

P_{10} = fraction passing the No. 10 sieve;

P_{200} = fraction passing the No. 200 sieve;

D_{99} , D_{60} , D_{50} , D_{40} = soil grain diameters at 99%, 60%,
50% and 40% finer by weight (mm).

Anderson's work indicated that the plastic limit and the uniformity coefficient are apparently related to the collapse ratio.

12.3 Discriminant function analysis

The final objective of this study is to ultimately determine if there is a difference in soil properties and collapsibility east and west of the El Llano acequia. To do this a discriminant function analysis was conducted using a SPSS, Inc. (1983) computer program. The unstandardized canonical discriminant function coefficients are listed in Table 9.

TABLE 9--Unstandardized canonical discriminant function coefficients for soils located east and west of the acequia.

DISCRIMINATING VARIABLE	COEFFICIENT
Dry density	-0.036
Moisture content	-0.043
Liquid limit	-0.006
Plasticity Index	+0.039
% passing No. 4 sieve (gravel)	+0.224
% passing No. 40 sieve (fine sand)	-0.201
% passing No. 200 sieve (silt and clay)	+0.046
Collapse ratio, R	+4.072
Constant	-12.30

Two-tailed probability: 0.087

The above canonical discriminant function evaluated with the discriminating variable means yielded the following discriminant scores for soils east and west of the acequia:

East of acequia 0.207

West of acequia -0.809

There is a slight difference between the two soils. However, if the the level of significance is 0.01 then the two-tailed probability of 0.087 (Table 9), calculated in the discriminant function analysis, indicates that there is not much difference in the soil properties and collapsibility bewteen the two areas. One could say there is a difference only if the tolerance is increased to 0.10.

Nevertheless, according to Table 10, 29.7% of the samples located east of the acequia were misclassified (according to the discriminant function analysis) to be located, based on their soil properties, west of the acequia. Conversely, 21.1% of the soils on the west side were misclassified as being located on east of the acequia.

TABLE 10--Classification results of soils located both east and west of the El Llano acequia showing percentages of correctly classified and misclassified cases.

ACTUAL LOCATION	NO. OF CASES	PREDICTED LOCATION MEMBERSHIP	
		EAST	WEST
East of acequia	74	52 70.3%	22 29.7%
West of acequia	19	4 21.1%	15 78.9%

Per cent of "grouped" cases classified correctly: 72.04%

These very high misclassified group percentages suggest the relative difficulty in separating these soils by their soil properties and collapsibility. For this reason caution should be exercised when delineating collapsible and non-collapsible soil areas in El Llano; the acequia may not represent the actual dividing line.

13.0

CONCLUSIONS

Collapsible soils still are somewhat enigmatic and cannot be consistently identified all the time in the study area. Their extreme variability in soil properties, sedimentological origin, areal and subsurface distribution, and their collapse mechanism makes collapsible soils difficult to locate. The safest stabilization method for structures in the study area would assume all surrounding soils are collapsible and proceed to pre-collapse them by water injection as was done in the GGSS Areas. This process should be continued before, during and after construction. It should be done in conjunction with soil compaction techniques to ensure all soils have lost their collapsible soil structure. Although stabilization and preventive methods for collapsible soils are beyond the scope of this study, they have been thoroughly researched in other works, by Aitchison (1973), Bally and others (1984), Bhatia and Quast (1984), Bara (1972, 1975), Clemence and Finbarr

(1981), Crossley (1968), Gibbs and Bara (1967b), Hall and Carlson (1965), Jennings and Knight (1975), Johnpeer and others (1985a, 1985b), Litvinov (1961), Lovelace and others (1982), and Williams and Marais (1971).

The following conclusions are based on the preceding field and laboratory tests and statistical analyses on El Llano soils:

1) El Llano is located on a low-gradient (1-2%) coalescing alluvial fan surface consisting of complex interbedded tongues of mostly unconsolidated, Holocene, silty to clayey sands and poorly graded sands with minor lenses of clay, silt and gravel. These sediments were probably deposited by mudflows, sheetflows and water-laid processes consisting of braided stream and arroyo channel deposition. This is based upon grain-size distributions, stratigraphic and lithologic relationships and sedimentary structures.

2) Averages of soil dry density, moisture content, Atterberg limits, grain-size distribution, per cent consolidation and blow counts reveal that most suspected collapsible soils in El Llano are loose, moisture deficient, non-plastic to slightly plastic, silty to clayey sands and poorly graded sands. Most of the gravelly sands and low to high plasticity clays exhibit little collapsibility.

3) Analyses of cross-sections in the study area demonstrate the complex subsurface distribution of collapsible soils. Collapsible and non-collapsible zones may be delineated by using a combination of field and laboratory data and collapse criteria such as depth profiles

of blow counts, moisture content and saturation, and natural dry density and density at liquid limit. Seismic velocity boundaries and location of wetting fronts can be used in conjunction with the above criteria. Collapsible zones tend to follow soil type boundaries but may also display a more random and "patchy" distribution.

4) Surface subsidence and cracks from wetting collapsible soils are produced by the loss of underlying support caused by soil hydrocompaction. Cracks form on the surface and exhibit vertical displacements of 0 to 15 inches with horizontal separations of 0 to 6 inches. Cracks are generally linear to arcuate in shape and are generated outward in sets from the wetted area in a concentric pattern. The zones of tensional and compressional strain around the cracks produce the differential settlement and structural damage to buildings.

The micro-mechanism of soil collapse in El Llano is best described by the decrease in friction between sand grains, the decrease in normal force between the grain menisci, and the increase in shear strength across the grain contacts which all result from wetting the soil. The micro-shearing within the clay and silt aggregates, which loosely bond the sand grains together, is caused by loading and wetting the soil. Thus sand grains lose their intergranular support and slip by one another into vacant void space.

Expansive clays probably enhance the failure of clay and silt aggregates by swelling them and thus lifting

the once supported sand grains into unstable slip positions. Soluble salts and cements also bond the larger sand grains together. When they are dissolved a collapsing soil structure results.

5) After evaluating five collapse criteria of previous workers it was found that the collapse ratio, R (Gibbs and Bara, 1967a), best represented El Llano soil conditions. All five criteria failed to show a significant difference in collapsibility values east and west of the El Llano acequia. It was originally thought by Johnpeer and others (1985b) that the acequia was the dividing line between collapsible and non-collapsible soils. This was further supported by the lack of subsidence at GGSS Area 2 after water injection and by the dramatic subsidence and cracking at GGSS Areas 1, 3 and 4. However, only one water injection study was conducted west of the acequia. Water injection should be performed at several different areas west of the acequia to better outline any differences.

Except for dry density, moisture content and blow counts there were no obvious mean soil property differences between the two sides of the acequia. Because soils on the west side have been irrigated for over 300 years it was thought they were non-collapsible soils that had already compacted. The extreme variability of these collapsible soils makes it almost impossible to say without question whether they will not occur in one area as opposed to another.

Discriminant analysis showed there was little

difference in soil properties and collapsibility between soils located east and west of the acequia unless the tolerance level of significance was increased to 0.10. Still, a high percentage of soils were misclassified into the wrong area based on their discriminant scores from the canonical discriminant function. Overall, it should be assumed collapsible and non-collapsible soils exist on both sides of the acequia.

6) The collapse ratio, R, was used as a dependent variable in linear and logarithmic stepwise regression analysis. The logarithmic regression equation models El Llano soils the best and indicates that 96% of the variance in lnR is accounted for by the independent variables (dry density, liquid limit, per cent fines, and plasticity index). The linear and logarithmic regression equations are:

$$R = 3.47131 - 0.01416LL - 0.02035DEN - 0.00308517FINES$$

$$\ln R = 2.8235 - 0.01438LL - 0.02405DEN - 0.0025958FINES - 0.00812944PI.$$

These equations strictly apply to El Llano soil conditions. If used elsewhere they should be complemented with other criteria and used with caution.

The complex mechanism of collapse in these problem soils necessitates more research on the role of clay, soluble salts and cement, and water chemistry in creating instability. Different stages of collapse should be observed under the scanning electron microscope and in thin section to study the micro-fissures in the clay and silt

aggregates. More consolidation testing is required on identical soil samples with varying final moisture contents and saturations to better examine their effect on collapse. Finally, and most important, by more thoroughly understanding the "macro-mechanism" of surface subsidence, cracking and the strain distribution that causes structural damage, homeowners and developers should be able to effectively stabilize buildings and retard soil collapse.

ACKNOWLEDGEMENTS

I am grateful to the New Mexico Bureau of Mines and Mineral Resources for providing me a research assistantship and the laboratory facilities to do this study. The New Mexico Tech Geoscience Department funded part of the scanning electron microscope work. I would like to thank Gary Johnpeer, my technical advisor, for his endless support, advice and encouragement; John Hawley; Dave Love; Danny Bobrow and Mark Hemingway for all the work they did in the field and for their valuable assistance in the laboratory and in reviewing this thesis. Special thanks go to Drs. J.R. MacMillan, Cathy Aimone, Anita Singh, Robert McNeill, Kalman Oravec and George Austin for their expert advice. The New Mexico State Highway Department provided funding to do the drilling at the GGSS Areas. I am grateful to Molly Miller and Carol Hjellming for editing the final draft.

REFERENCES

- Aitchison, G. D., 1973, Problems of soil mechanics and construction on structurally unstable soils (collapsible, expansive and others): Journal of Soil Mechanics and Foundation Engineering, Proceedings, 8th International Conference on Soil Mechanics and Foundation Engineering, Moscow, USSR, v. III, pp. 161-190.
- Alfi, A. A. S., 1984, Electron optical properties of a stabilized collapsible soil in the Tucson, Arizona area: unpublished Ph.D. dissertation, University of Arizona, 331 pp.
- American Society for Testing and Materials, 1984, Annual book of ASTM Standards; soil and rock; building stones: American Society for Testing and Materials, sec. 4, v. 04.08.
- Anderson, F. J., 1968, Collapsing soils and their basic parameters in an area in the Tucson, Arizona vicinity: unpublished M.S. thesis, University of Arizona, 156 pp.
- Arman, A., and Thornton, S., 1973, Identification of collapsible soils in Louisiana: Highway Research Record 426, pp. 14-22.
- Army Engineering and Design Laboratory, 1965, Army Engineering and Design Laboratory soils testing manual: Army Engineering and Design Laboratory, Manual, EM 1110-2-1906, Appendix VIII.
- Bally, R. J., Antoescu, I. P., Andrei, S. V., Dron, A., and Popescu, D., 1972, Hydrotechnical structures on collapsing soils: Journal of Soil Mechanics and Foundation Engineering, Proceedings, 8th International Conference on Soil Mechanics and Foundation Engineering, v. 4, p. 4.
- Bara, J. P., 1972, Wetting requirements for collapsing foundation soils: Paper presented to the American Society of Civil Engineers, Houston, Texas, Oct. 16-20, 1972; U.S. Bureau of Reclamation, 23 pp.
- Bara, J. P., 1975, Precollapsing foundation soils by wetting: Journal of Soil Mechanics and Foundation Engineering, Proceedings, 5th Pan-American Conference on Soil Mechanics and Foundation Engineering, 20 pp.
- Barden, L., 1971, The influence of structure on deformation

- and failure in clay soil: *Geotechnique*, v. 22, no. 1, pp. 159-163.
- Barden, L., McGown, A., and Collins, K., 1973, The collapse mechanism in partly saturated soil: *Engineering Geology*, v. 7, pp. 49-60.
- Barden, L., and Sides, G. R., 1969, The influence of structure on the collapse of compacted clay: Texas A&M University, Proceedings, 2nd International Research and Engineering Conference on Expansive Clay Soils, pp. 318-326.
- Bates, R. L., and Jackson, J. A., 1980, Glossary of Geology, 2nd edition: American Geological Institute, Falls Church, Virginia, 749 pp.
- Beckwith, G. H., 1976, Experiences with collapsing soils in the Rio Grande valley: Paper presented to the American Society of Civil Engineers, New Mexico Section, Fall 1976 Meeting, Oct. 15, 1976.
- Beles, A. A., and Stanculescu, I. I., 1961, Settlements of structures founded on highly porous soils: *Journal of Soil Mechanics and Foundation Engineering, Proceedings*, 5th International Conference on Soil Mechanics and Foundation Engineering, v. 1, pp. 587-594.
- Bhatia, S. K., and Quast, D., 1984, The behavior of collapsible soil under cyclic loading: *Journal of Soil Mechanics and Foundation Engineering, Proceedings*, 4th Australian Conference on Geomechanics, v. 84, no. 2, pp. 73-77.
- Bishop, A. W., and Blight, G. E., 1963, Some aspects of effective stress in saturated and partly saturated soils: *Geotechnique*, v. 13, no. 3, pp. 177-197.
- Blackwelder, E., 1928, Mudflows as a geologic agent in semi-arid mountains: *Bulletin, Geological Society of America*, v. 39, pp. 465-484.
- Blight, G. E., 1967, Effective stress evaluation for unsaturated soils: *Journal of Soil Mechanics and Foundation Engineering, SM-2*, v. 93, pp. 125-148.
- Booth, A. R., 1975, The factors influencing collapse settlement in compacted soils: *Journal of Soil Mechanics and Foundation Engineering, Proceedings*, 6th Regional Conference for Africa on Soil Mechanics and Foundation Engineering, Durban, South Africa, pp. 57-63
- Borchardt, G. A., 1977, Montmorillinite and other smectite minerals; *in* Dixon, J. B. (ed.), *Minerals in Soil Environments*: Soil Science of America, Madison, Wisconsin, pp. 293-330.

- Brink, A. B. A., and Kantey, B. A., 1961, Collapsible grain structure in residual granite soil in southern Africa: *Journal of Soil Mechanics and Foundation Engineering, Proceedings, 5th International Conference on Soil Mechanics and Foundation Engineering, v. 1, Division 1-3A*, pp. 611-614.
- Brown, K. W., 1977, Shrinking and swelling of clay, clay strength and other properties of clay soils and clay; *in* Dixon, J. B., (ed.), *Minerals in Soil Environments: Soil Science of America*, Madison, Wisconsin, pp. 689-707.
- Bull, W. B., 1961, Causes and mechanics of near-surface subsidence in western Fresno County, California: U.S. Geological Survey Professional Paper 424B, pp. B187-B189.
- Bull, W. B., 1964, Alluvial fans and near-surface subsidence in western Fresno County, California: U.S. Geological Survey Professional Paper 437A, 71 pp.
- Bull, W. B., 1972, Prehistoric near-surface subsidence cracks in western Fresno County, California: U.S. Geological Professional Paper 437C, 85 pp.
- Burland, J. B., 1965, Some aspects of the mechanical behavior of partly saturated soils: *Journal of Soil Mechanics and Foundation Engineering, Proceedings, Symposium on Moisture Equilibria and Moisture Changes in Soils Beneath Covered Areas, Sydney, Australia*, pp. 270-278.
- Carrillo, C. M. and Mirabal, F. R., 1985, Acequia systems of El Llano, New Mexico; El Llano and vicinity geotechnical study: New Mexico Bureau of Mines and Mineral Resources, Open-file Report 226, v. 4, 24 pp.
- Chapin, C. E., 1971, The Rio Grande rift, Part I--modifications and additions: *New Mexico Geological Society, Guidebook to 22nd Field Conference*, pp. 191-201.
- Clary, J. H., 1980, Collapsing soils of the Albuquerque area: *Association of Engineering Geologists, Programs and Abstracts, Annual Meeting, Dallas, Texas*, pp. 29-30.
- Clary, J. H., Korecki, N. T., and Mondragon, R. R., 1984, *Geology of Albuquerque, New Mexico: Association of Engineering Geologists, Bulletin, v. XXI, no. 2*, pp. 127-156.
- Clary, J. H., and Korecki, N. T., 1985, Geotechnical investigation of Units 2 and 3, La Vista del Rio subdivision, Española, New Mexico: Albuquerque Testing Laboratory, Inc., unpublished report, pp. 1-11.
- Clemence, S. P., and Finbarr, A. O., 1981, Design considerations for collapsing soils: *Journal of Soil*

- Mechanics and Foundation Engineering, GT3, v. 107, pp. 305-317.
- Collinson, J. D., 1978, Alluvial sediments; in Reading, H. G. (ed.), Sedimentary Environments and Facies: Elsevier Publishing Co., New York, pp. 15-59.
- Crossley, R. W., 1968, A geologic investigation of foundation failures in small buildings in Tucson, Arizona: unpublished M.S. thesis, University of Arizona, 94 pp.
- Curtin, G., 1973, Collapsing soil and subsidence; in Geology, Seismicity, and Environmental Impact: Association of Engineering Geologists Special Publication, pp. 89-100.
- Darwell, J. L., and Denness, B., 1976, Prediction of metastable soil collapse: International Association of Hydrological Sciences, Publication No. 121, pp. 544-552.
- Denisov, N. Y., 1946, Settlement properties of loessical soils: Soviet Science, U.S.S.R. Government Publishing Office, Moscow, pp. 34-64.
- Denisov, N. Y., 1951, The engineering properties of loess and loess-like soils: Gosstroizdat, Moscow, 133 pp. (in Russian).
- Dudley, J. H., 1970, Review of collapsing soils: Journal of Soil Mechanics and Foundation Engineering, SM-3, v. 96, pp. 925-947.
- Feda, J., 1966, Structural stability of subsident loess from Praha-Dejvice: Engineering Geology, v. 1, no. 3, pp. 201-219.
- Folk, R. L., 1980, Petrology of sedimentary rocks: Femp Hill Publishing Company, Austin, Texas, pp. 33-37.
- Fuqua, W. D., and Richter, R. C., 1960, Photographic interpretation as an aid in delimiting areas of shallow land subsidence in California; in Manual of Photographic Interpretation: American Society of Photogrammetry, pp. 442-456.
- Gabin, V. L., and Lesperance, L. E., 1977, New Mexico climatological data--precipitation, temperature, evaporation and wind; monthly and annual means 1850-1975: W. K. Summers and Associates, Socorro, New Mexico, 436 pp.
- Galusha, T., and Blick, J. C., 1971, Stratigraphy of the Santa Fe Group, New Mexico: American Museum of Natural History Bulletin, v. 144, Art. 1, 127 pp.

- Gibbs, H. J., and Bara, J. P., 1967a, Predicting surface subsidence from basic soil tests, Soils Engineering Report EM-658, paper presented to the American Society for Testing and Materials, 4th Pacific Area National Meeting, Los Angeles, California; U.S. Bureau of Reclamation, 21 pp.
- Gibbs, H. J., and Bara, J. P., 1967b, Stability problems of collapsing soils: Journal of Soil Mechanics and Foundation Engineering, SM-4, v. 93, pp. 577-594.
- Gile, L. H., Hawley, J. W., and Grossman, R. B., 1981, Soils and geomorphology in the Basin and Range area of southern New Mexico--guidebook to the Desert Soil Project: New Mexico Bureau of Mines and Mineral Resources, Memoir 39, 222 pp.
- Gipson, M., 1966, Preparation of oriented slides for X-ray analysis of clay minerals: Journal of Sedimentary Petrology, v. 36, No. 4, pp. 1143-1162.
- Grigorian, A. A., 1967, Prediction of deformation of loess soils under building and structure foundations: Journal of Soil Mechanics and Foundation Engineering, Proceedings, 3rd Asian Regional Conference, v. 1, no. 3, pp. 9-12.
- Hall, C. E., and Carlson, J. W., 1965, Stabilization of soils subject to hydrocompaction: Engineering Geology, v. 2, pp. 47-58.
- Hawley, J. W., compiler, 1978, Guidebook to the Rio Grande rift in New Mexico and Colorado: New Mexico Bureau of Mines and Mineral Resources, Circular 163, 241 pp.
- Haq, I., 1976, Collapsible soils along the Chashma Fight Bank Canal: Collapsing Soils Case History Conference, University of Missouri (Rolla), pp. 665-669.
- Holtz, R. D., and Kovacs, W. D., 1981, Introduction to Geotechnical Engineering: Prentice-Hall Publishing Company, Civil Engineering and Engineering Mechanics Series, Englewood Cliffs, New Jersey, 733 pp.
- Holtz, W. G., and Hilf, J. W., 1961, Settlement of soil foundations due to saturation: Journal of Soil Mechanics and Foundation Engineering, Proceedings, 5th International Conference on Soil Mechanics and Foundation Engineering, v. 1, Divisions 1-3A, pp. 673-679.
- Ingles, O. G., 1964, The water-soil regime in three dams sampled during failure: CSIRO, Division of Soil Mechanics, Colloquium on Failure of Small Earth Dams, Paper 31, pp. 34-45.

- Ingles, O. G., and Aitchison, G. D., 1969, Soil-water disequilibrium as a cause of subsidence in natural soils and earth embankments: Association of Scientific Hydrology--United Nations Economic, Social and Cultural Organization, Tokyo, Japan, Colloquium on Land Subsidence, v. 11, pp. 342-352.
- Jennings, J. E., and Burland, J. B., 1962, Limitations to the use of effective stress in partly saturated soils: *Geotechnique*, v. 12, No. 2, pp. 125-144.
- Jennings, J. E., and Knight, K., 1956, Recent experiences with the consolidation test as a means of identifying conditions of heaving or collapse of foundations on partially saturated soils: *South African Institute Civil Engineers Transactions*, v. 6, No. 8, pp. 1-13.
- Jennings, J. E., and Knight, K., 1957, The additional settlement of foundations due to a collapse of structure of sandy sub-soils on wetting: *Journal of Soil Mechanics and Foundation Engineering, Proceedings, 4th International Conference on Soil Mechanics and Foundation Engineering*, pp. 316-319.
- Jennings, J. E., and Knight, K., 1975, A guide to construction on or with materials exhibiting additional settlement due to collapse of grain structure: *Journal of Soil Mechanics and Foundation Engineering, 6th Regional Conference for Africa on Soil Mechanics and Foundation Engineering, Durban, South Africa*, pp. 99-105
- Johnpeer, G. W., Love, D. W., Hawley, J. W., Bobrow, D. J., Hemingway, M., and Reimers, R. F., 1985a, El Llano and vicinity geotechnical study--interim report: *New Mexico Bureau of Mines and Mineral Resources, Open-file Report 225, 4 v., 850 pp., 21 appendices.*
- Johnpeer, G. W., Love, D. W., Hawley, J. W., Bobrow, D. J., Hemingway, M., and Reimers, R. F., 1985b, El Llano and vicinity geotechnical study--final report: *New Mexico Bureau of Mines and Mineral Resources, Open-file Report 226, 4 v., 578 pp., 23 appendices.*
- Johnson, A. I., Moston, R. P., and Morris, D. A., 1968, Physical and hydrologic properties of water-bearing deposits in subsiding areas in central California: *U.S. Geological Survey Prof. Paper 497A, 71 pp., 14 plates.*
- Knight, K., 1959, The microscopic study of the structure of collapsing sands: *Journal of Soil Mechanics and Foundation Engineering, Proceedings, 2nd South African Regional Conference on Soil Mechanics and Foundation Engineering*, pp. 1-11.
- Knight, K., 1961, The collapse of sandy subsoils on wetting:

- unpublished M.S. thesis, University of Witwaterstand, South Africa, 143 pp.
- Knight, K., 1963, The origin and occurrence of collapsing soils: *Journal of Soil Mechanics and Foundation Engineering, Proceedings, 3rd Regional Conference for Africa on Soil Mechanics and Foundation Engineering*, v. 1, pp. 127-130.
- Knight, K., and Dehlen, G. L., 1963, The failure of a road constructed on a collapsing soil: *Journal of Soil Mechanics and Foundation Engineering, Proceedings, 3rd African Conference on Soil Mechanics and Foundation Engineering*, v. 1, pp. 31-34.
- Kratzsch, H., 1983, *Mining subsidence engineering*: Springer-Verlag Publishing Company, New York, pp. 336-339.
- Krumbein, W. C., and Graybill, F. A., 1965, *An introduction to statistical models in geology*: McGraw-Hill Book Company, New York, 475 pp.
- Krutov, V. I., Rabinovich, I. G., Kogai, V. K., Naumov, V., and Skakhov, O. A., 1984, Experience with collapsible soil consolidation by preliminary wetting in rural construction in foothill regions in Uzbekistan: *Scientific Research Institute of Bases and Underground Structures, USSR; Journal of Soil Mechanics and Foundation Engineering*, v. 21, no. 4, pp. 139-144 (English translation by F. Osnovaniya).
- Lambe, T. W., 1951, *Soil testing for engineers*: John Wiley and Sons Publishing Company, New York, 165 pp.
- Lin, Z., and Liang, W., 1979, Distribution and engineering properties of loess and loess-like soils in China-- Schematic map of engineering geologic zoning: *International Association of Engineering Geologists Bulletin*, no. 21, pp. 112-117.
- Litvinov, I. M., 1961, Stabilization of settling and weak clayey soils by thermal treatment: *Highway Research Board Special Report 60*, pp. 94-111.
- Lobdell, G. T., 1981, Hydroconsolidation potential of Palouse loess: *Journal of Soil Mechanics and Foundation Engineering, GT-6*, v. 107, pp. 733-742.
- Lofgren, B. E., 1969, Land subsidence due to the application of water, *in* *Review in engineering geology*: *Geological Society of America*, v. 2, pp. 271-303.
- Lovelace, A. D., Bennett, W. T., and Lueck, R. D., 1982, Test section for the stabilization of collapsible soils on Interstate 25, Project 1-025-4 (58) 243, Algodones, New

- Mexico: New Mexico State Highway Department, Geotechnical Section, Materials Laboratory Bureau, 37 pp.
- Maker, H. J., Dregne, H. E., Link, V. G., and Anderson, J. V., 1974, Soils of New Mexico: New Mexico State University, Agricultural Experiment Station, Research Report 285, 132 pp.
- Manley, K., 1978a, Structure and stratigraphy of the Española Basin, Rio Grande rift, New Mexico: U.S. Geological Survey, Open-file Report 78-667, 24 pp.
- Manley, K., 1978b, Cenozoic geology of Española Basin, in Hawley, J. W. (compiler), Guidebook to the Rio Grande rift in New Mexico and Colorado: New Mexico Bureau of Mines and Mineral Resources, Circular 163, pp. 201-204.
- McNeill, R. L., 1985, Consulting reports, in El Llano and vicinity geotechnical study--final report: New Mexico Bureau of Mines and Mineral Resources, Open-file Report 226, v. 2, appendix VIII.
- Minkoy, M., 1984, Quantitative prediction of collapsible loess soils: Engineering Geology, Proceedings, 27th International Geological Congress, v. 17, pp. 145-169.
- Moore, P. J., and Millar, D. V., 1971, The collapse of sands upon saturation: Journal of Soil Mechanics and Foundation Engineering, Proceedings, 1st Australia-New Zealand Conference on Geomechanics, pp. 54-60.
- Platt, W. S., 1963, Land surface subsidence in the Tucson area: unpublished M.S. thesis, University of Arizona, 94 pp.
- Prinklonskij, V. A., 1952, Gruntovedenie, Vtoriaia Chast, (Soil Science II): Gosgeolizdat, Moscow, p. 371 (in Russian).
- Prokopovich, N. P., 1963, Hydrocompaction of soils along the San Luis Canal alignment, western Fresno Courty, California (abs): Geological Society of America, Special Paper 73, p. 60.
- Prokopovich, N. P., 1975, Past and future subsidence along San Luis drain, San Joaquin Valley, California: Association of Engineering Geologists Bulletin, v. XII, no. 1, pp. 1-22.
- Prokopovich, N. P., 1984, Validity of density-liquid limit predictions of hydrocompaction: Association of Engineering Geologists Bulletin, v. XXI, no. 2, pp. 191-205.
- Reginatto, A. R., 1971, Standard penetration tests in

- collapsible soils: Journal of Soil Mechanics and Foundation Engineering, Proceedings, 4th Pan-American Conference on Soil Mechanics and Foundation Engineering, pp. 77-84.
- Reynolds, C. B., 1985, Shallow seismic report, in El Llano and vicinity geotechnical study--final report: New Mexico Bureau of Mines and Mineral Resources, Open-file Report 226, v. 2, Appendix VII.
- Rieke, H. H., and Chilingarian, G. V., 1974, Compaction of argillaceous sediments: Elsevier Scientific Publishing Company, New York, 424 pp.
- Roscoe, J. T., Fundamental research statistics for the behavioral sciences: Holt, Reinhart and Winston, Incorporated, New York, 336 pp.
- Shelton, D. C., Barrett, R. K., and Ruckman, A. C., 1975, Hydrocompacting soils on the Interstate 70 route near Grand Valley, Colorado: 26th Annual Highway Geology Symposium, Coeur d'Alene, Idaho, pp. 257-271.
- Smart, P., and Tovey, N. K., 1982, Electron microscopy of soils and sediments--techniques: Clarendon Press, Oxford, England, 264 pp.
- Soil Conservation Service, 1975, Soil taxonomy--a basic system of soil classification for making and interpreting surveys: U.S. Department of Agriculture, Soil Conservation Service, Handbook No. 436, 753 pp.
- SPSS, Inc., 1983, SPSS-X, Statistical package for the social sciences: McGraw-Hill Book Company, New York, 806 pp.
- Stephens, D. B., and Knowlton, R. G., 1985, Laboratory, field and numerical studies to predict soil collapse for the El Llano geotechnical investigation near Española, New Mexico; El Llano and vicinity geotechnical study--final report: New Mexico Bureau of Mines and Mineral Resources, Open-file Report 226, v. 4, 53 pp.
- Sultan, H. A., 1969, Foundation failures on collapsing soils in the Tucson, Arizona area: Texas A&M University, Proceedings, 2nd International Research and Engineering Conference on Expansive Clay Soils, pp. 394-403.
- Sultan, H. A., 1971, Some engineering aspects of collapsing soils: Highway Research Board, Paper presented at the Highway Research Board Meeting, January, 1971, 25 p.
- Thornton, S. I., and Arulanadan, K., 1975, Collapsible soils--state-of-the-art: Idaho Transportation Dept., Division of Highways, 26th Annual Highway Geology Symposium,

Boise, Idaho, pp. 205-219.

U.S. Bureau of Reclamation, 1980, Subsidence characteristics of low density silty soils in areas of upper Meeker Canal, Missouri River Basin Project PE41.2: U.S. Bureau of Reclamation, Division of Engineering Laboratories, Earth Laboratory Report No. Em-545.

Valdez, L. J., 1979, La Vista del Rio subdivision engineering report, Espanola, New Mexico: Valdez Engineering and Testing, unpublished geotechnical report, pp. 1-6.

Weaver, C. E., and Pollard, L. D., 1973, The chemistry of clay minerals: Elsevier Scientific Publishing Company, New York, 213 pp.

Williams, A. A. B., and Marais, G. P., 1971, The use of an impact roller in compacting a collapsing sand subgrade for a freeway: Highway Research Board, Record 374, pp. 43-56.

Woodward-Clevenger & Associates Inc., 1973, Geotechnical report on the Montessa Park Police Detention Compound, Albuquerque, New Mexico: Woodward-Clevenger and Associates Incorporated, unpublished geotechnical report, 20 pp.

APPENDIX I

Plates 1-7

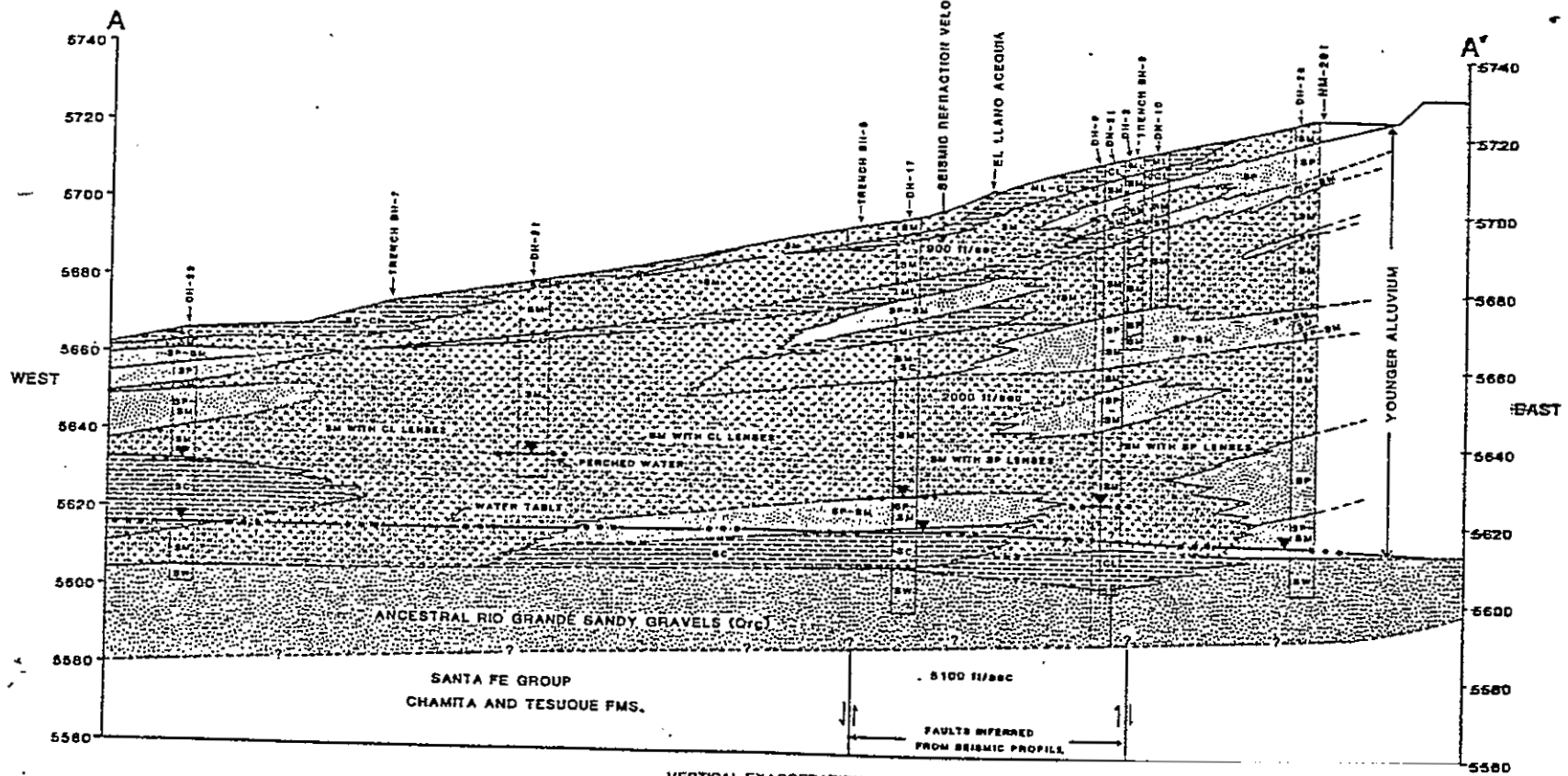


PLATE 3A: EAST-WEST GEOLOGIC CROSS-SECTION THROUGH EL LLANO SEE APPENDIX I PLATE 1

VERTICAL EXAGGERATION=10X
HORIZONTAL SCALE 1"=200'

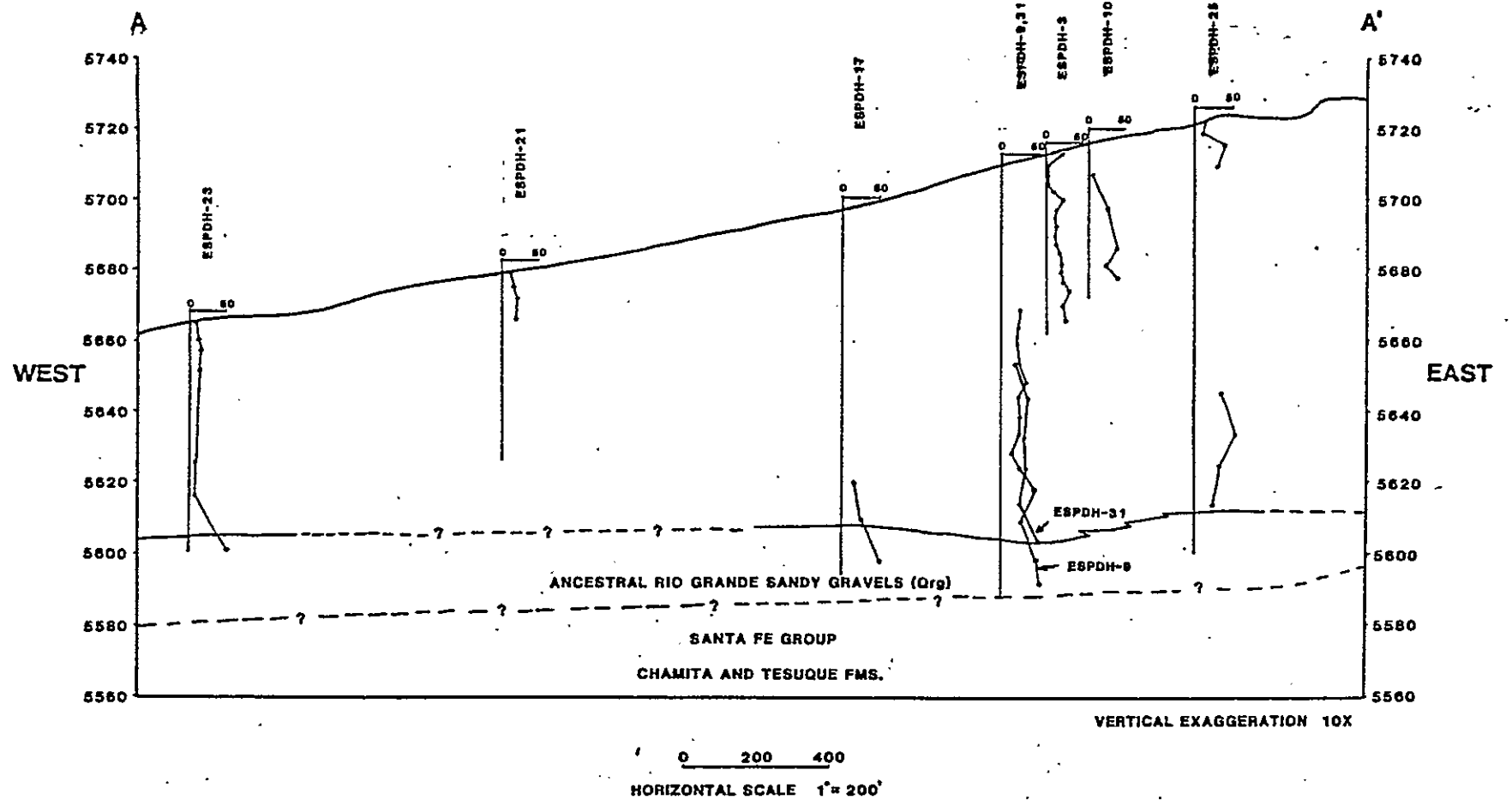


PLATE 3B: CROSS-SECTION AA' SHOWING DEPTH PROFILES OF BLOW COUNTS

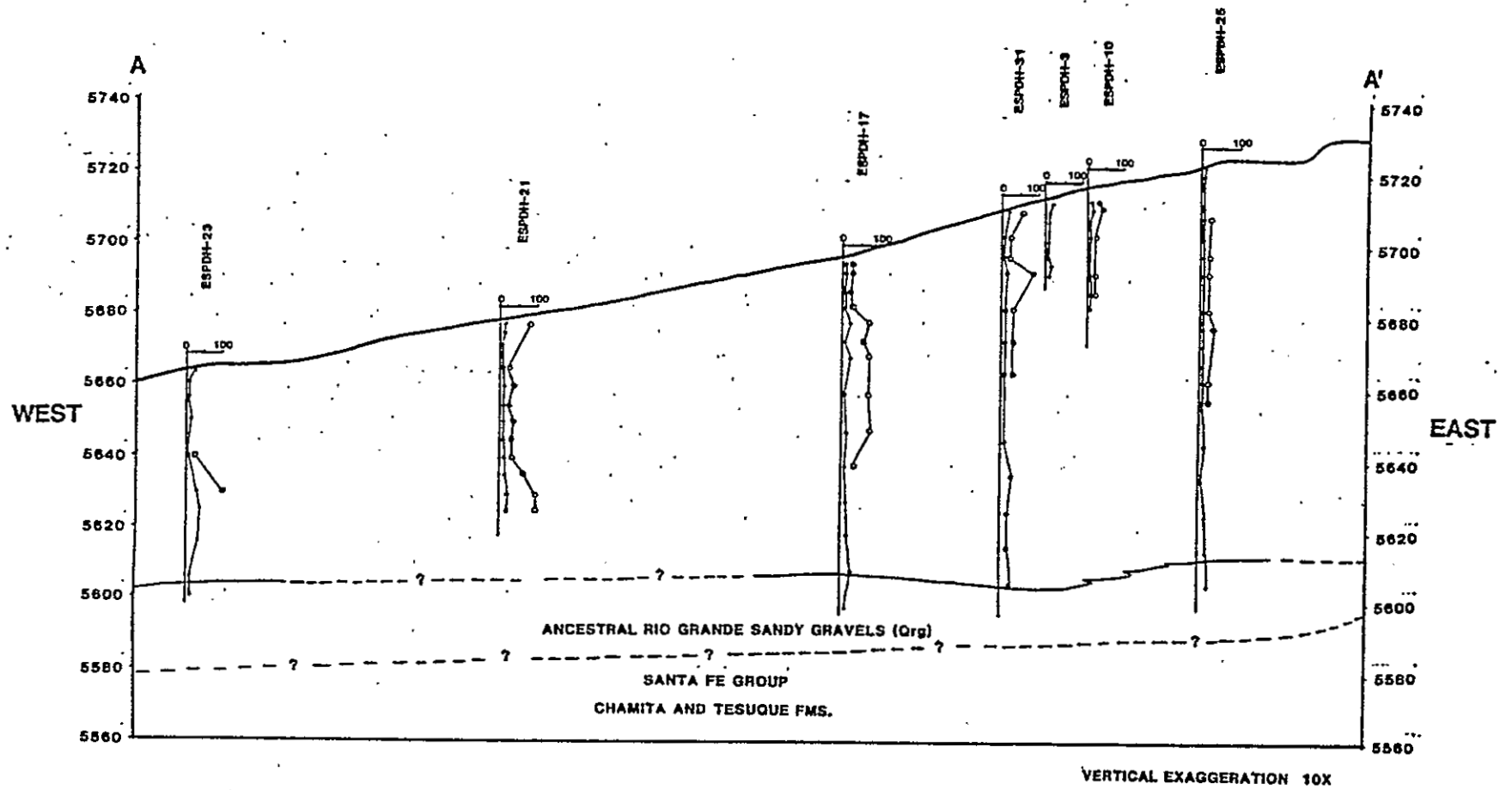


PLATE 3C: CROSS-SECTION AA' SHOWING DEPTH PROFILES OF MOISTURE CONTENT AND SATURATION

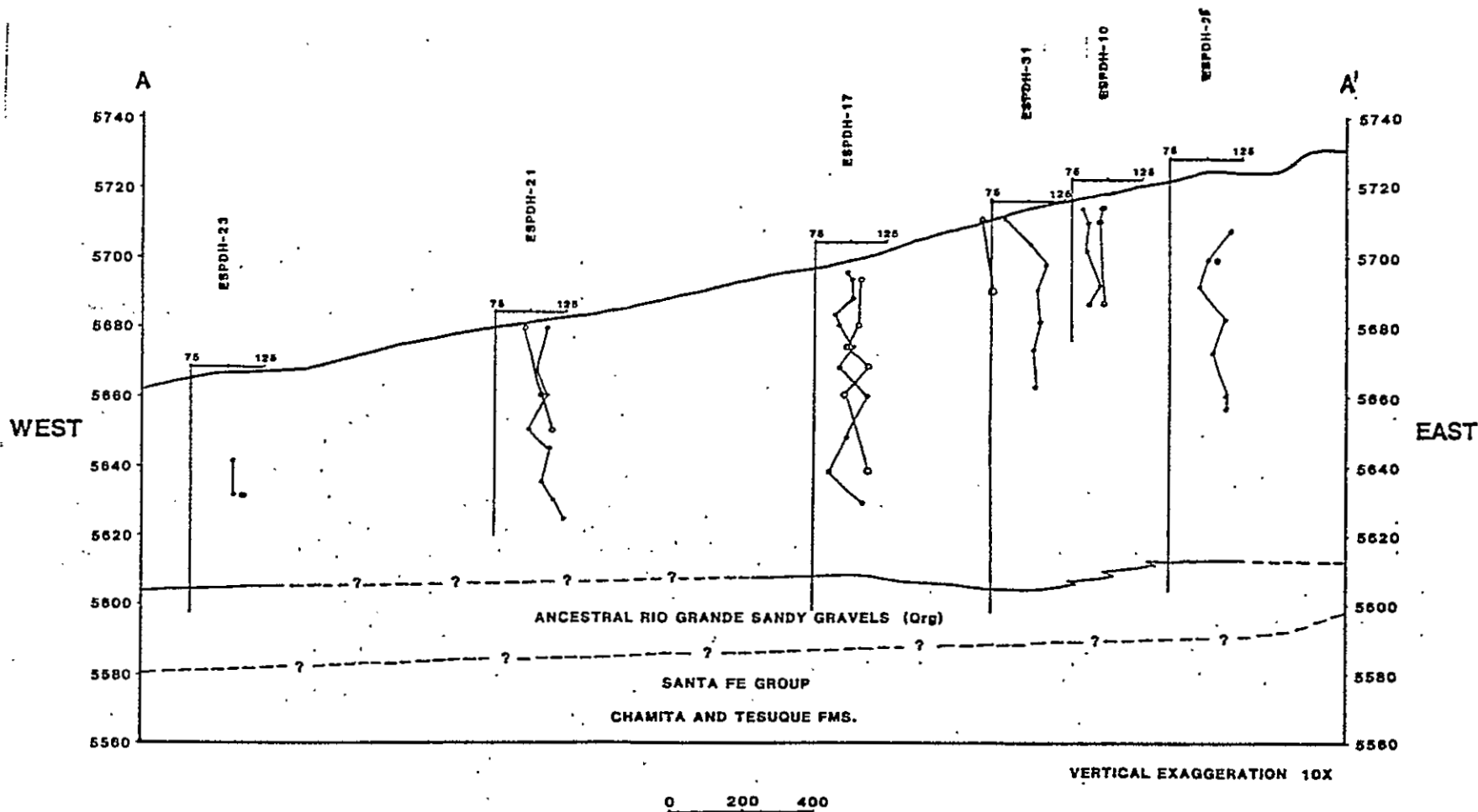
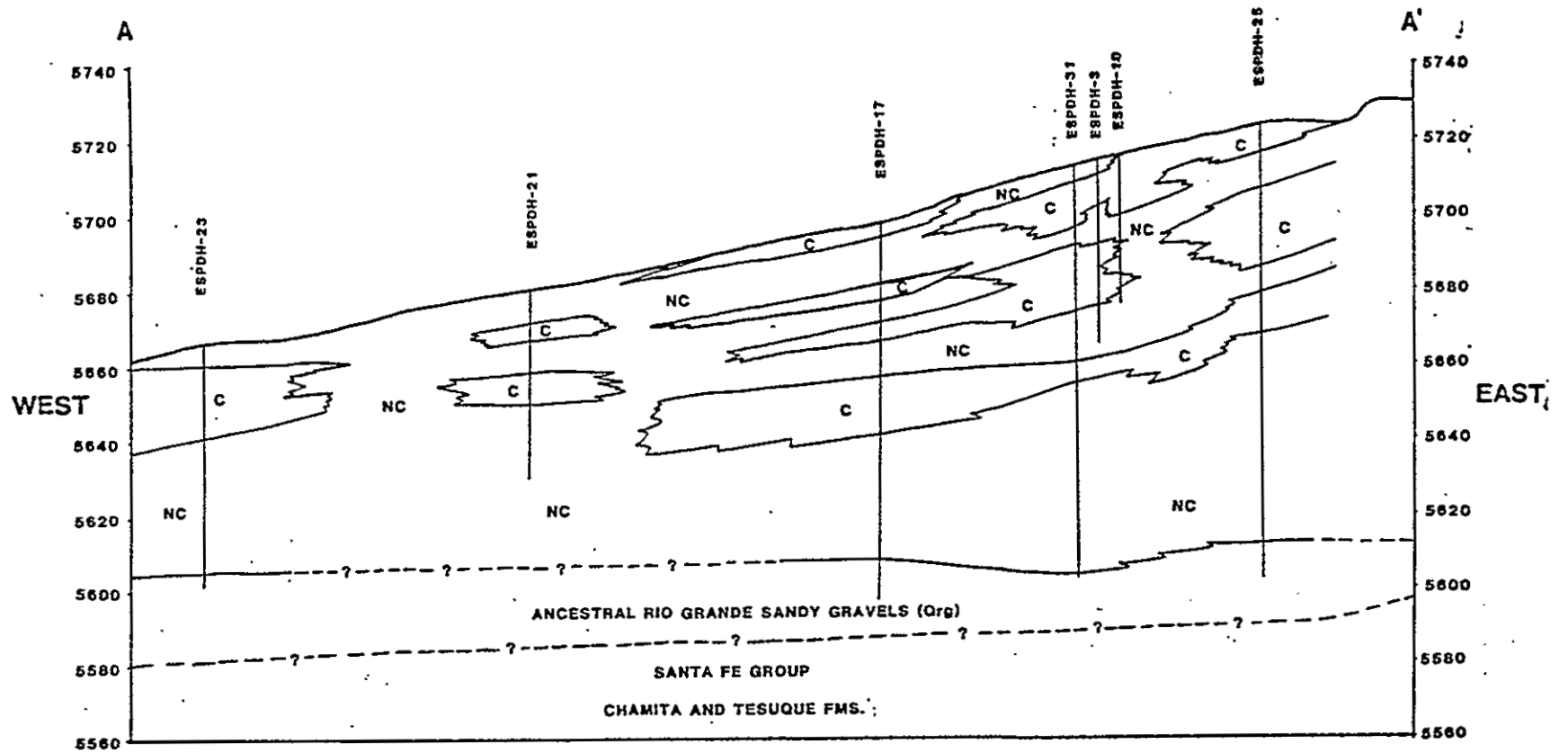


PLATE 3D:

CROSS-SECTION AA' SHOWING DEPTH PROFILES OF
NATURAL DRY DENSITY AND DENSITY AT LIQUID LIMIT

- KEY:
- NATURAL DRY DENSITY (pcf)
 - DENSITY AT LIQUID LIMIT (pcf)



VERTICAL EXAGGERATION 10X

0 200 400

HORIZONTAL SCALE 1" = 200'

KEY:

COLLAPSIBLE (C)

NON-COLLAPSIBLE (NC)

PLATE 3E:

CROSS-SECTION AA' SHOWING COLLAPSIBLE
AND NON-COLLAPSIBLE ZONES

BASED ON PLATES 3A-3D

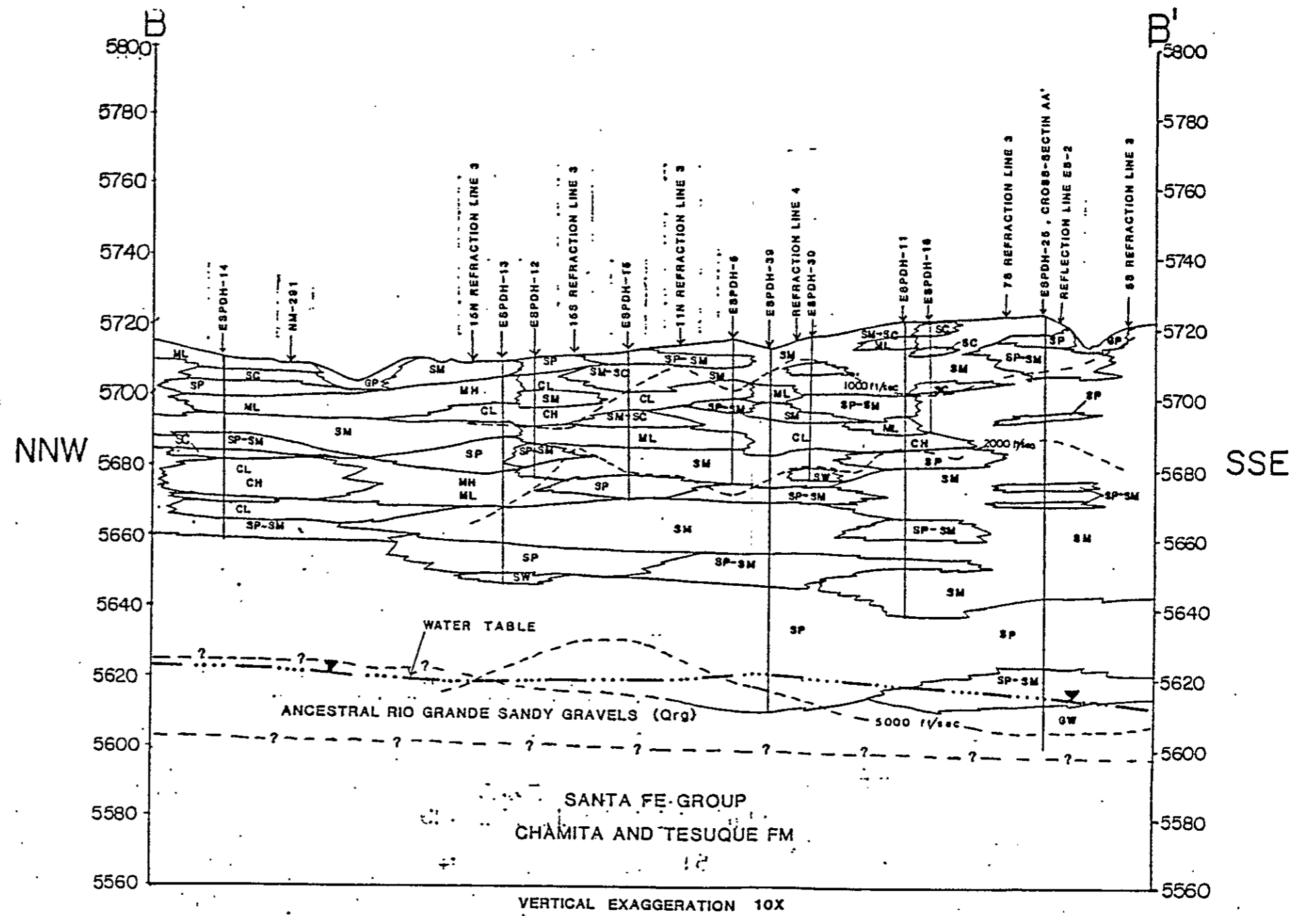


PLATE 4A: NNW-SSE GEOLOGIC CROSS-SECTION THROUGH EL LLANO
 SEE PLATE

SEE APPENDIX I PLATE 1

KEY: SM, SM-SC []
 SC []
 SP, SP-SM []
 GP, GW, SW []

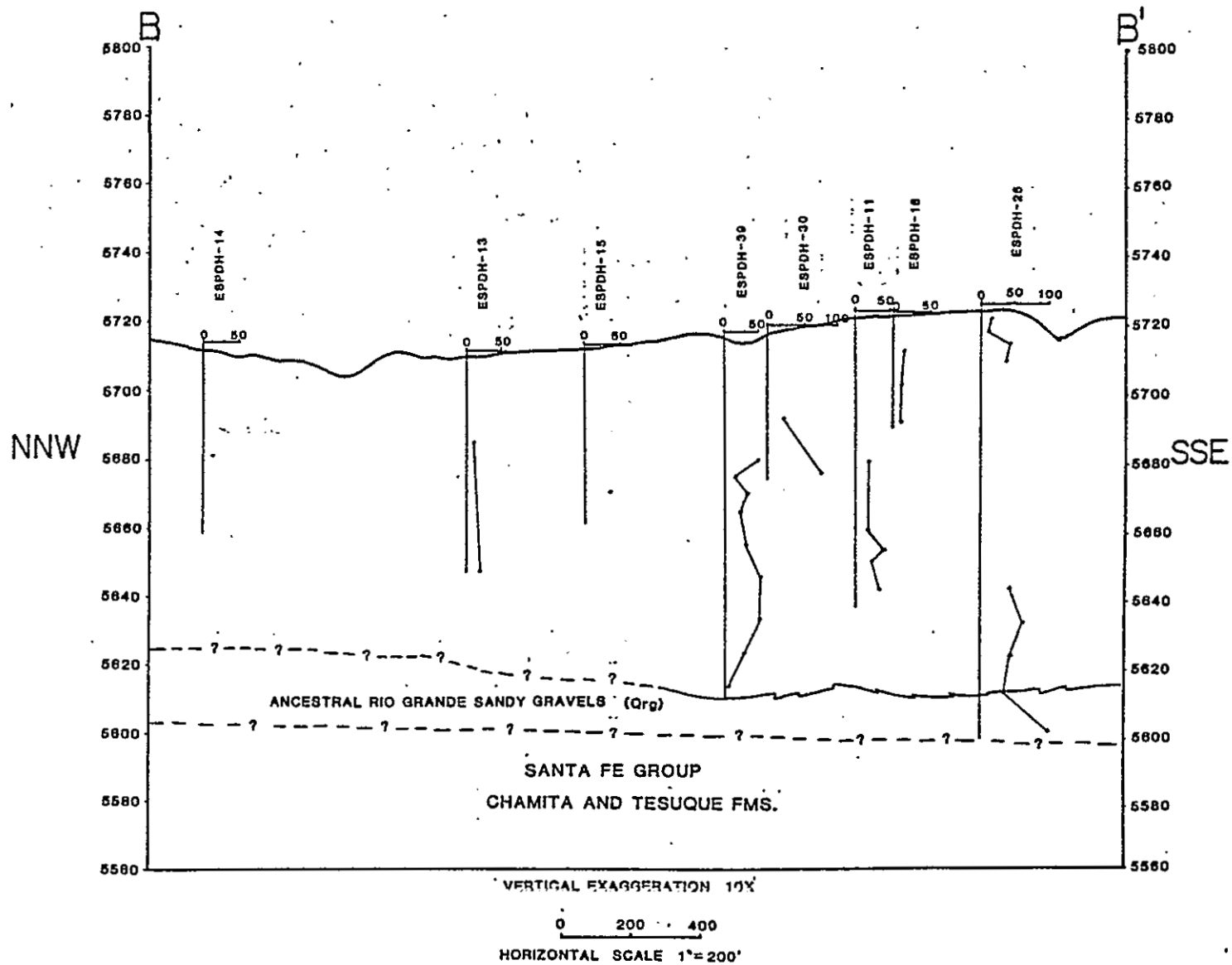


PLATE 4B: CROSS-SECTION BB' SHOWING DEPTH PROFILES OF BLOW COUNTS

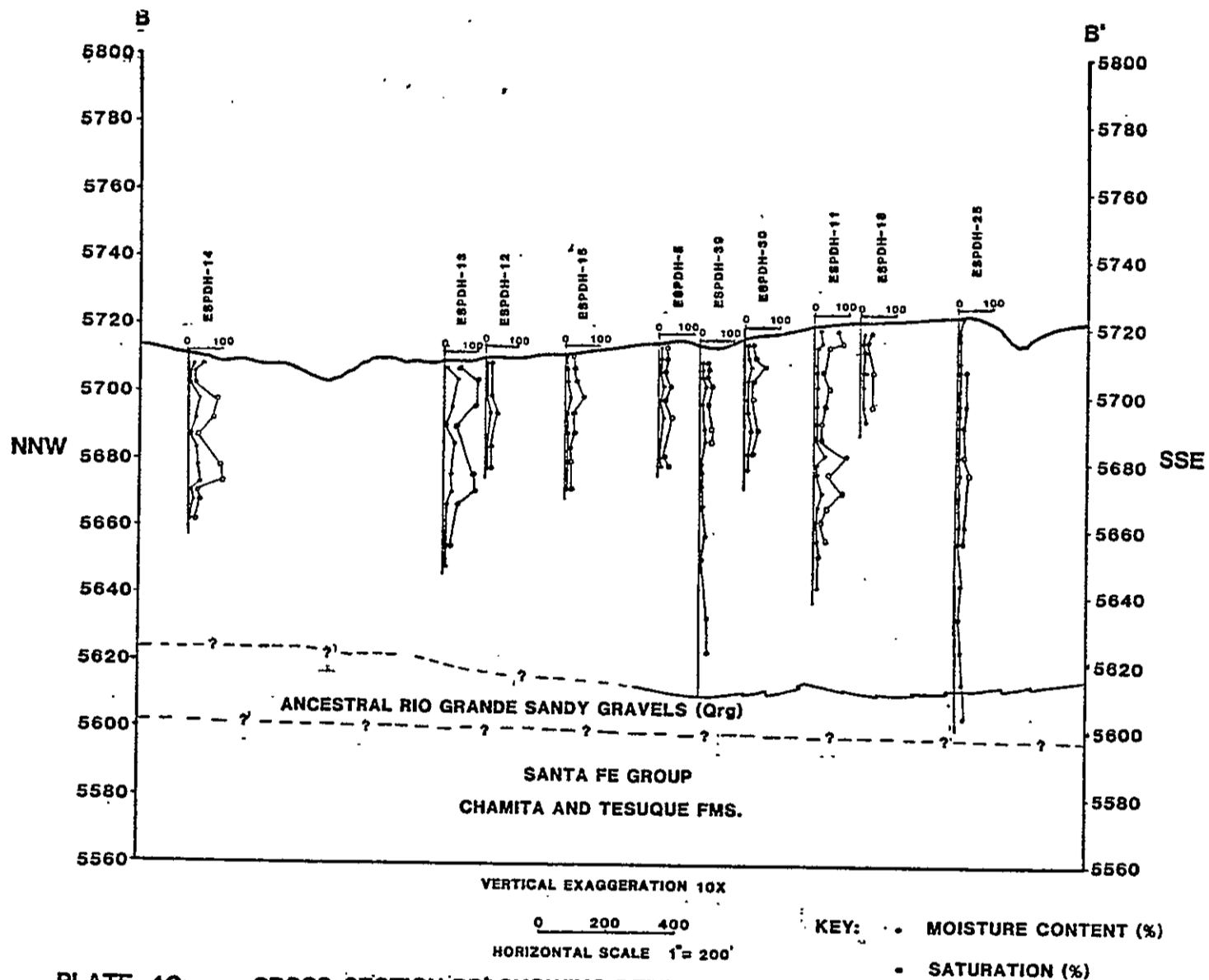


PLATE 4C: CROSS-SECTION BB' SHOWING DEPTH PROFILES OF MOISTURE CONTENT AND SATURATION

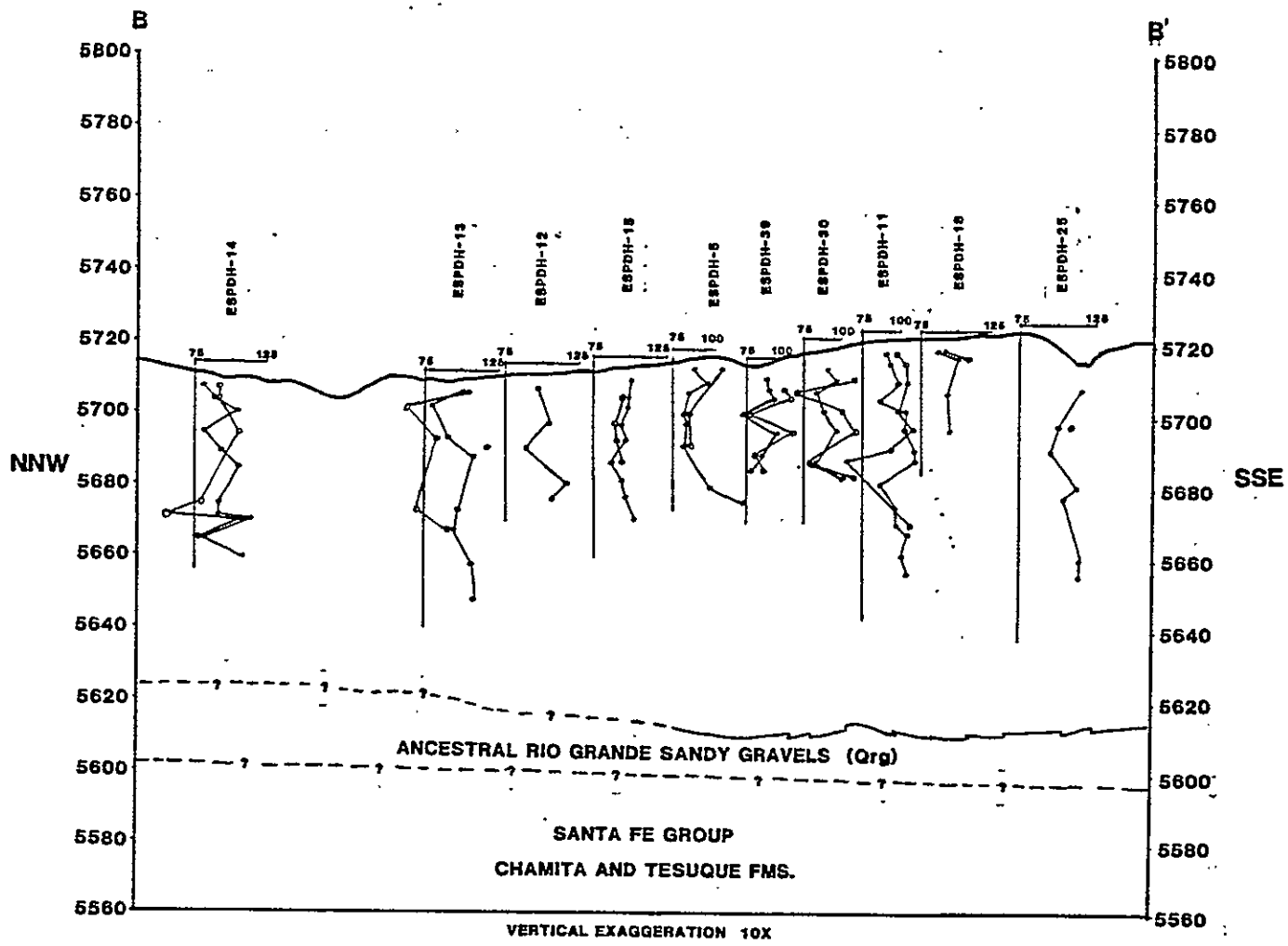


PLATE 4D: CROSS-SECTION BB' SHOWING DEPTH PROFILES OF NATURAL DRY DENSITY AND DENSITY AT LIQUID LIMIT

KEY: ● NATURAL DRY DENSITY (pcf)
○ DENSITY AT LIQUID LIMIT (pcf)

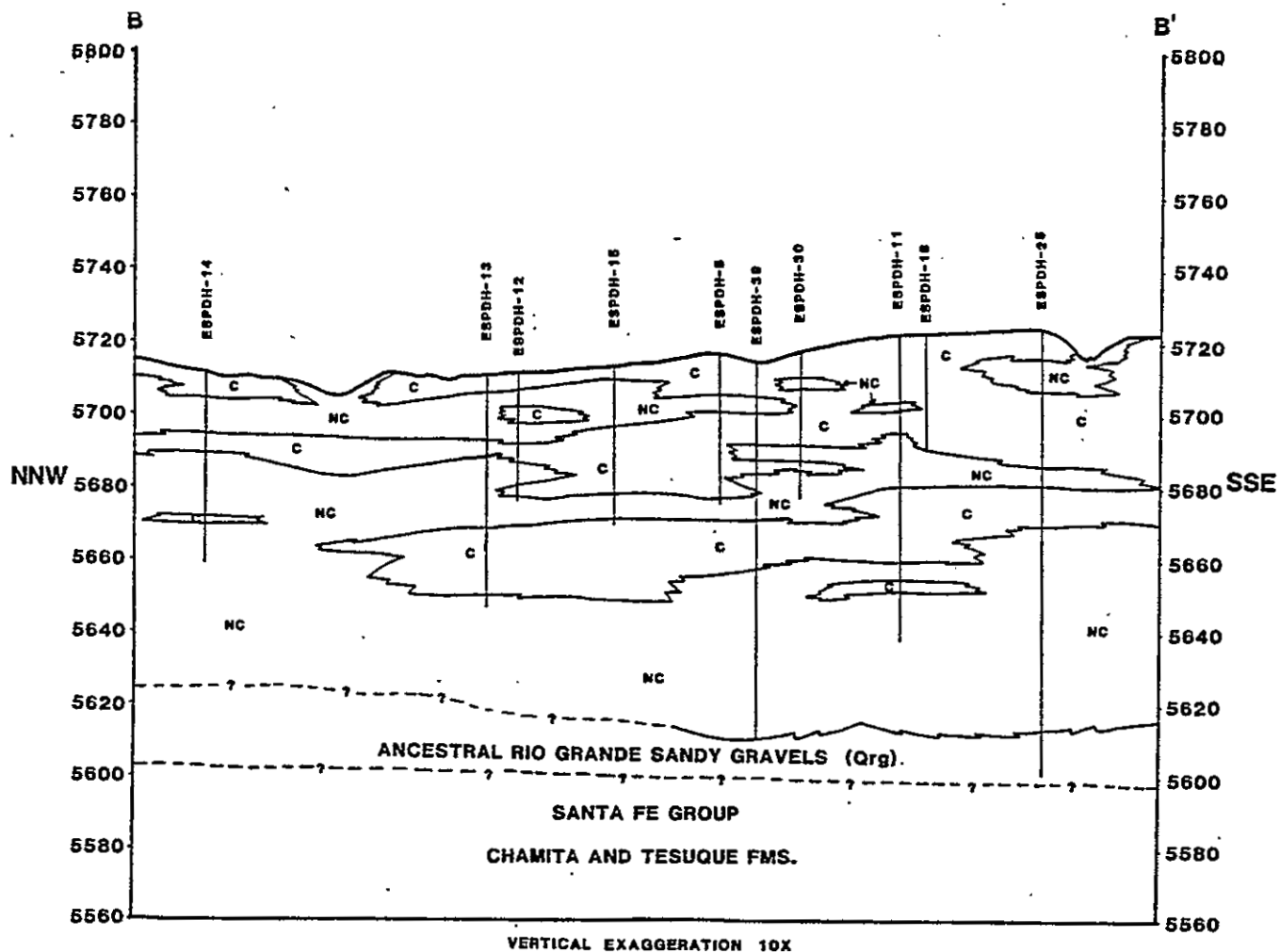
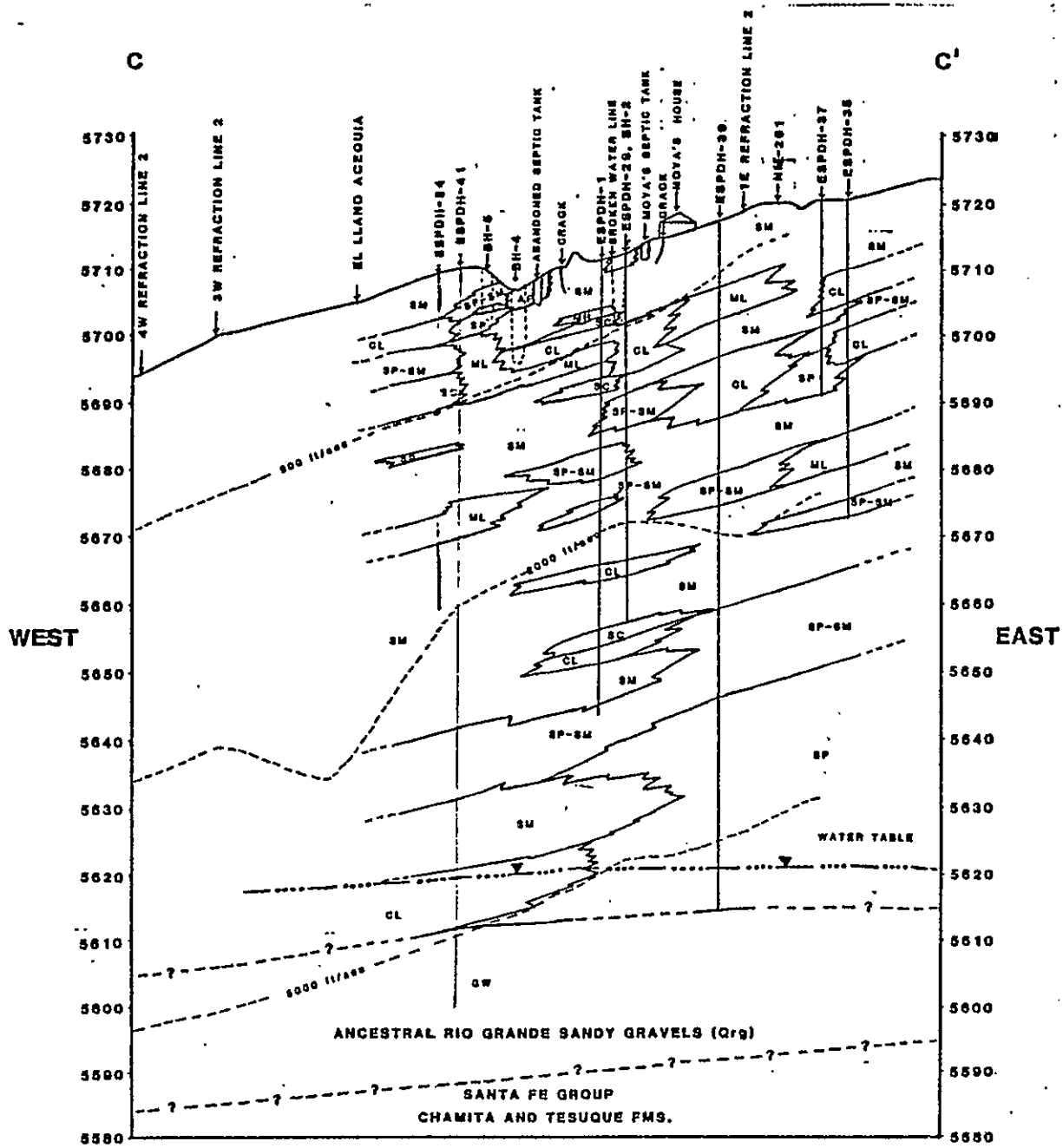


PLATE 4E: CROSS-SECTION BB' SHOWING COLLAPSIBLE AND NON-COLLAPSIBLE ZONES

BASED ON PLATES 4A-4D



VERTICAL EXAGGERATION 10X.

0 100 200

HORIZONTAL SCALE 1"=100'

PLATE 5A: EAST-WEST GEOLOGIC CROSS-SECTION THROUGH MOYA'S SUBSIDENCE PIT IN EL LLANO

SEE APPENDIX I PLATE 1

- KEY:**
- SM, SM-SC.
 - SC
 - SP, SP-SM
 - GP, GW, SW
 - ML, MH
 - CL, CH
 - ARTIFICIAL FILL

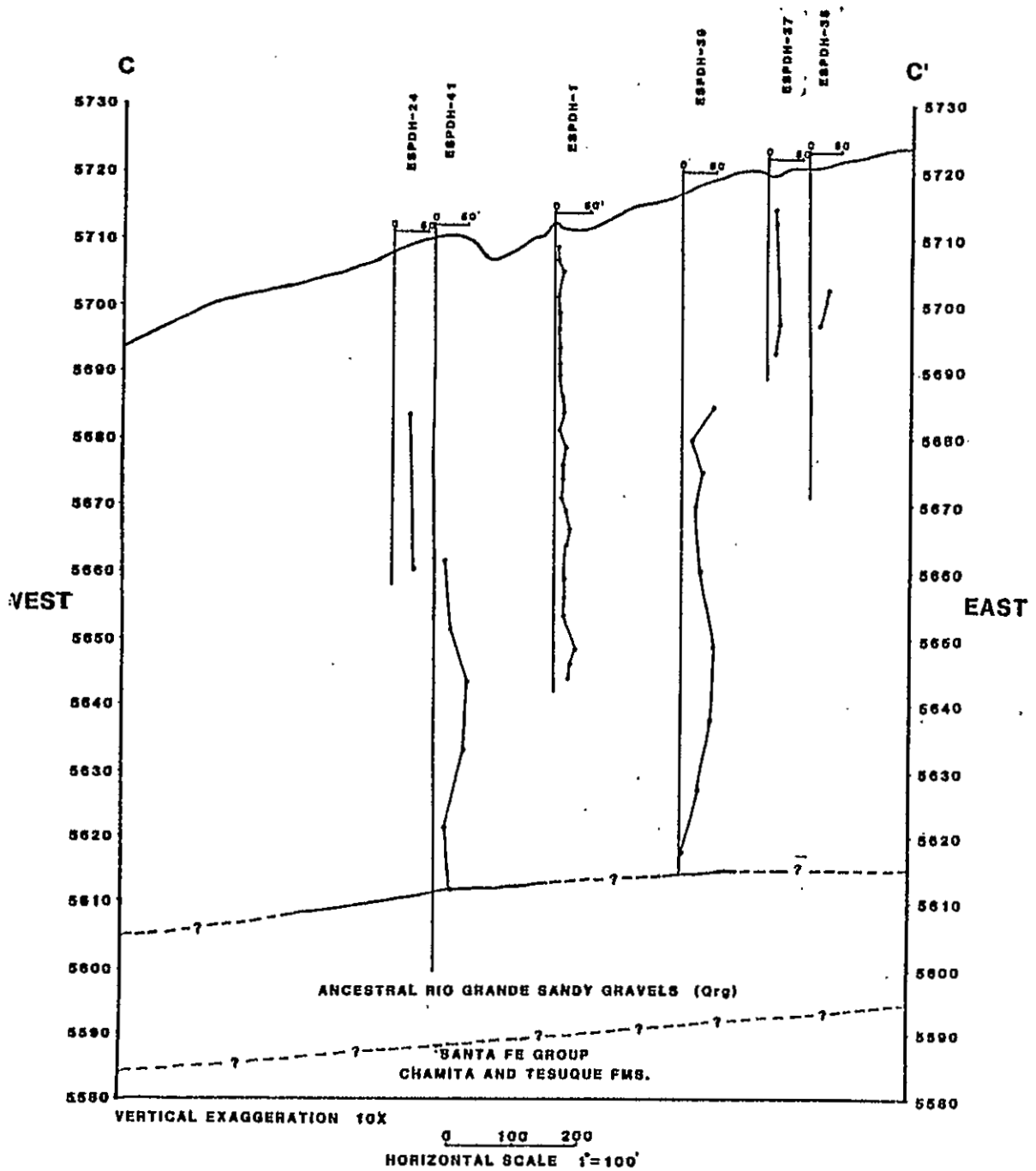


PLATE 5B: CROSS-SECTION CC' SHOWING DEPTH PROFILES OF BLOW COUNTS

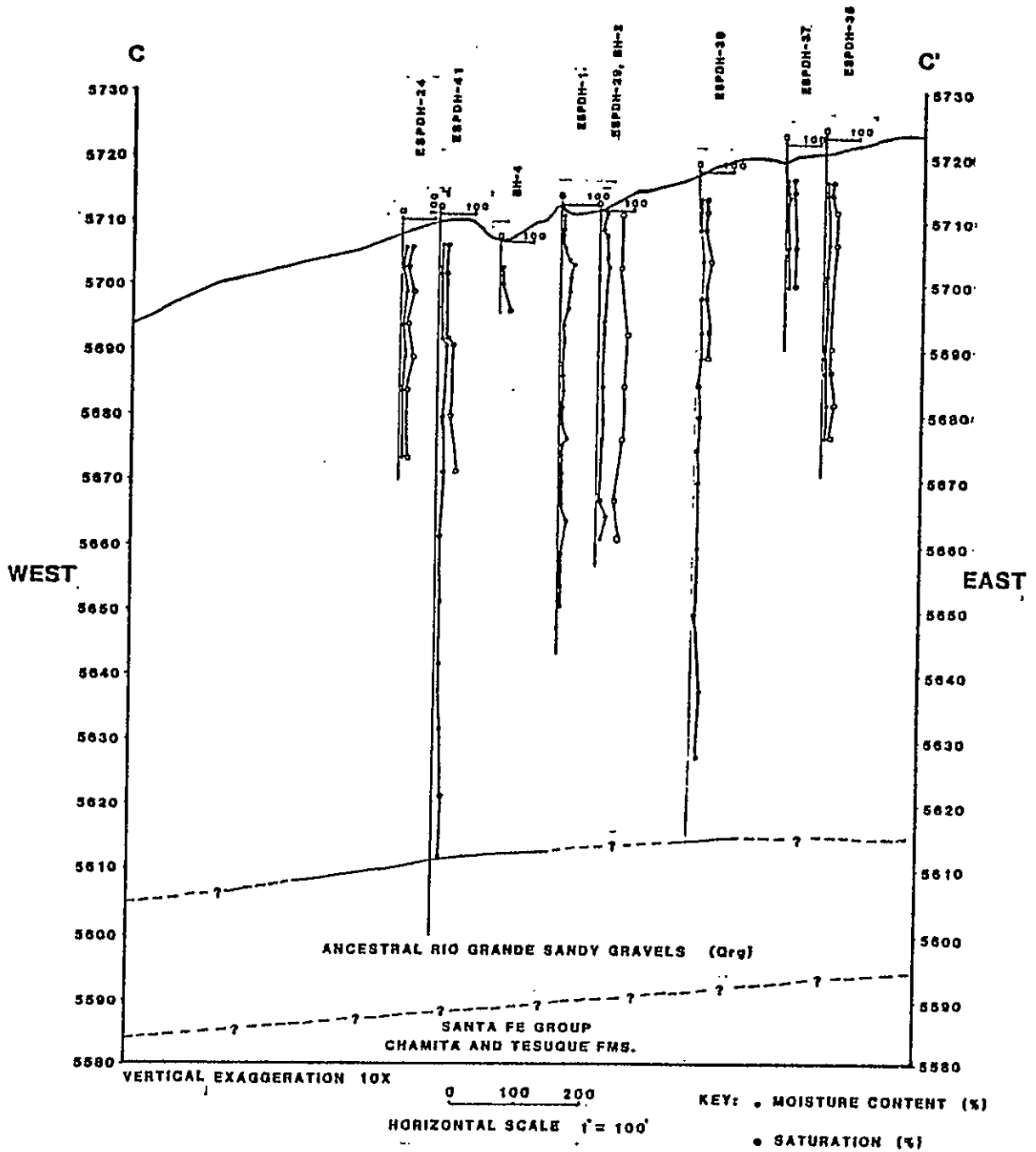


PLATE 5C: CROSS-SECTION CC' SHOWING DEPTH PROFILES OF MOISTURE CONTENT AND SATURATION

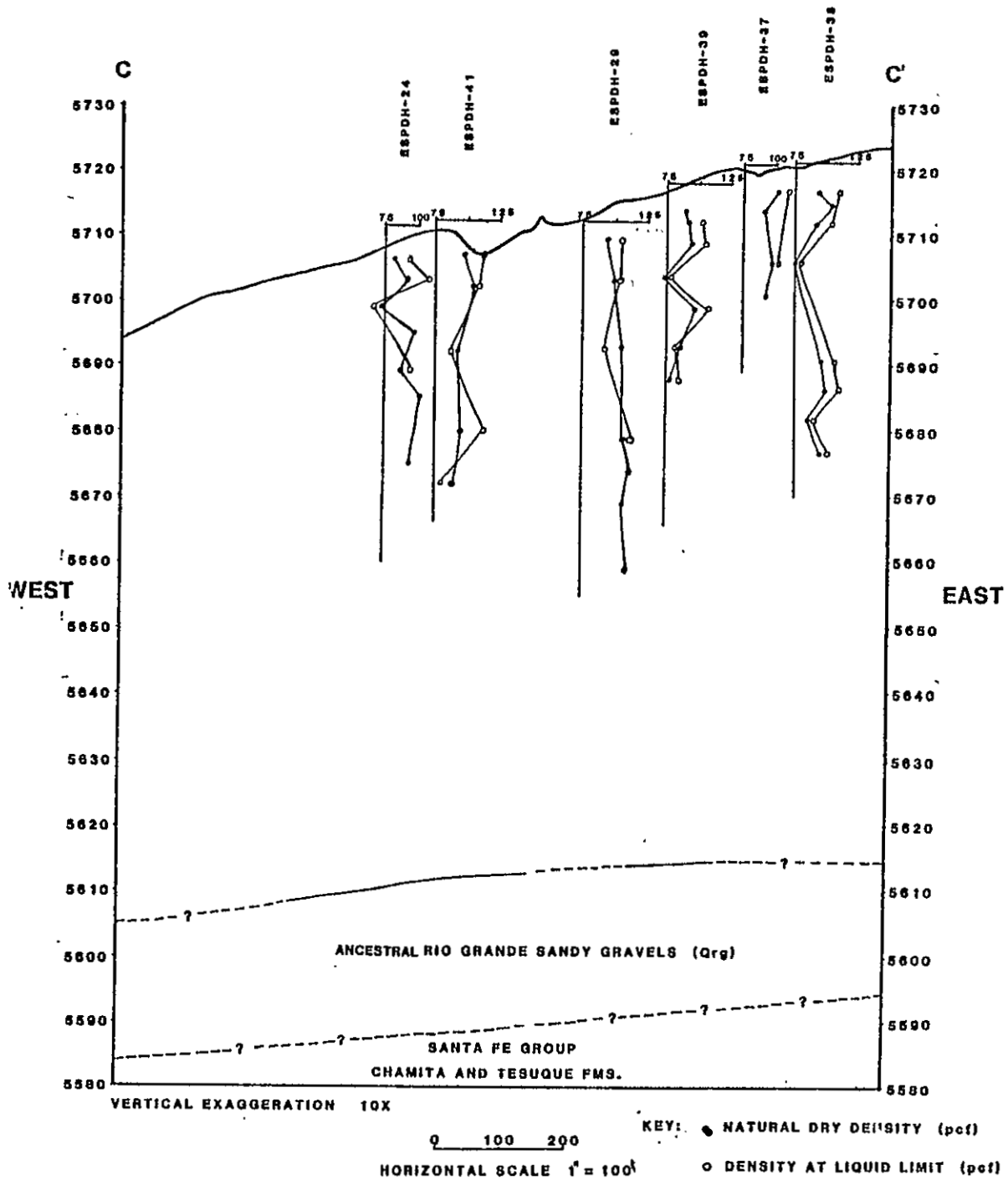


PLATE 5D: CROSS-SECTION CC' SHOWING DEPTH PROFILES OF NATURAL DRY DENSITY AND DENSITY AT LIQUID LIMIT

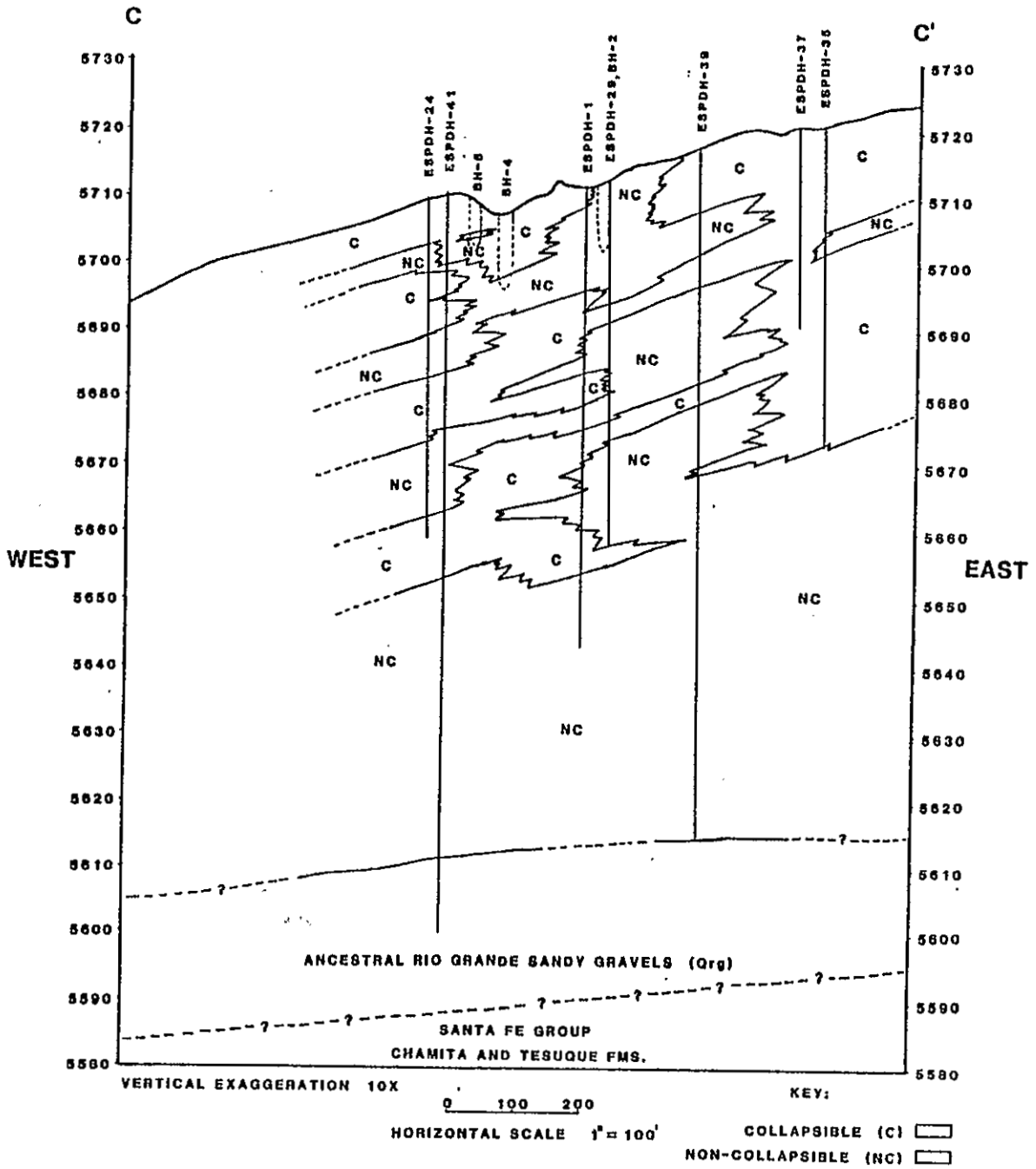
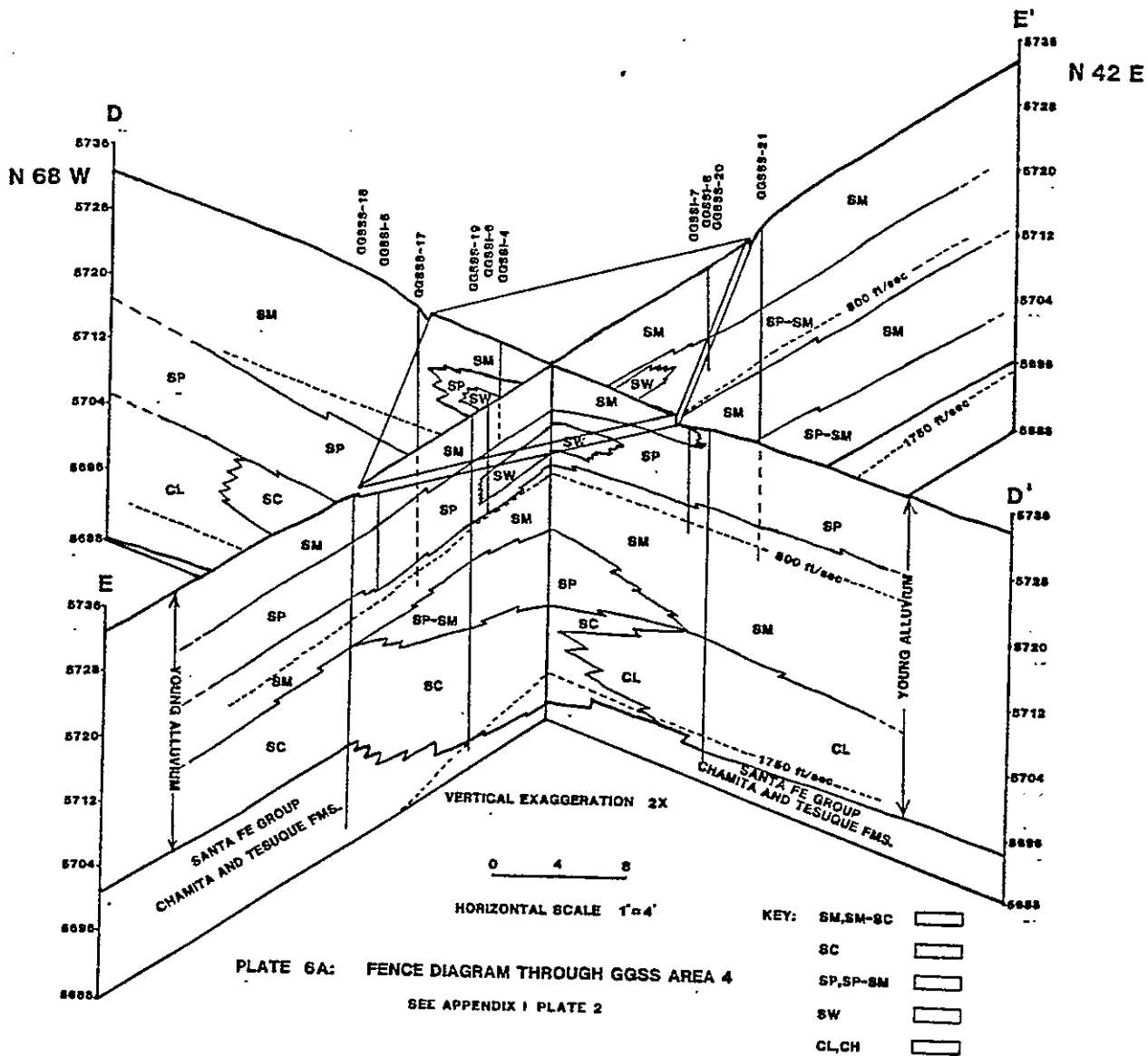


PLATE 5E: CROSS-SECTION CC' SHOWING COLLAPSIBLE AND NON-COLLAPSIBLE ZONES

BASED ON PLATES 5A-5D



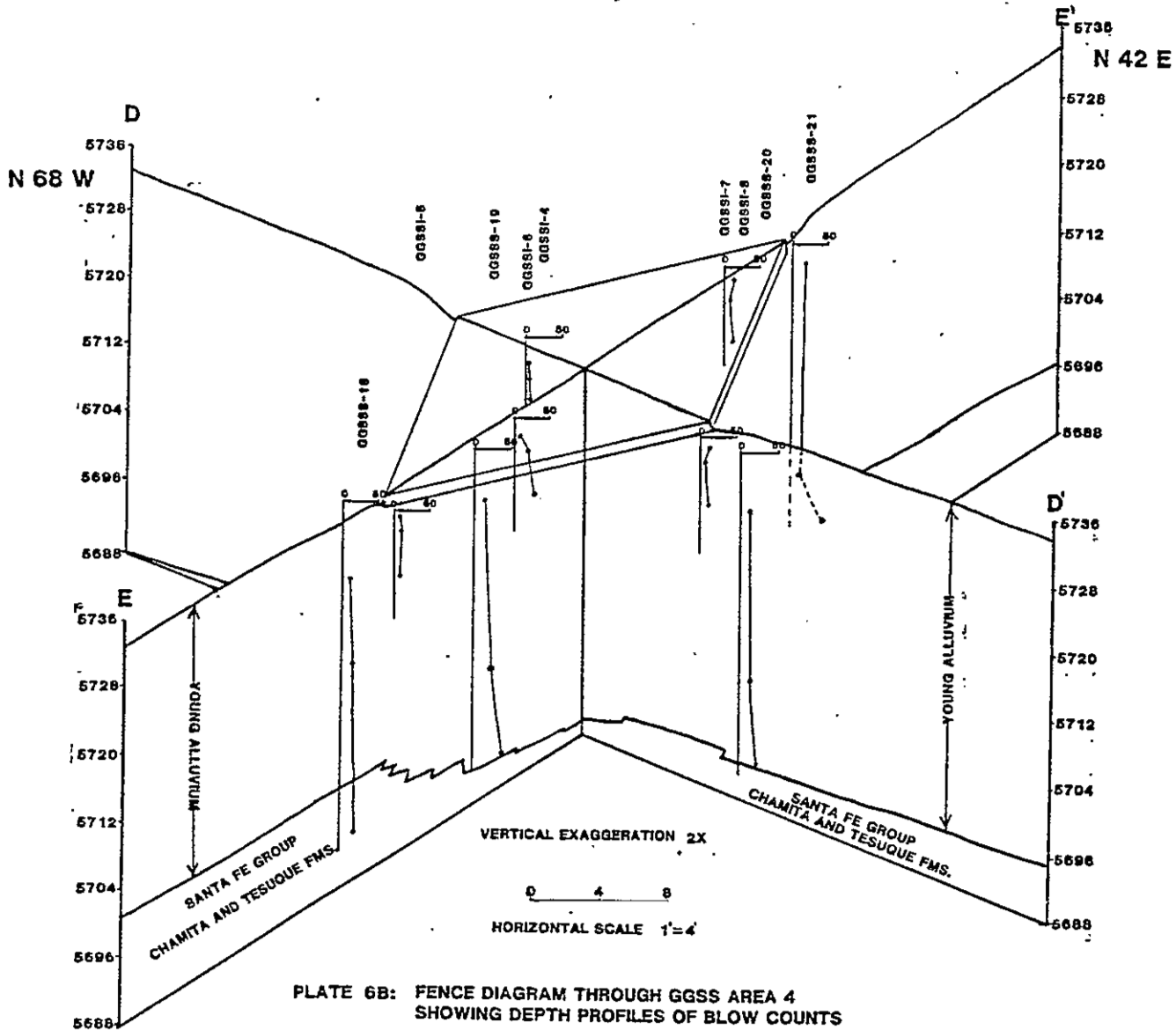
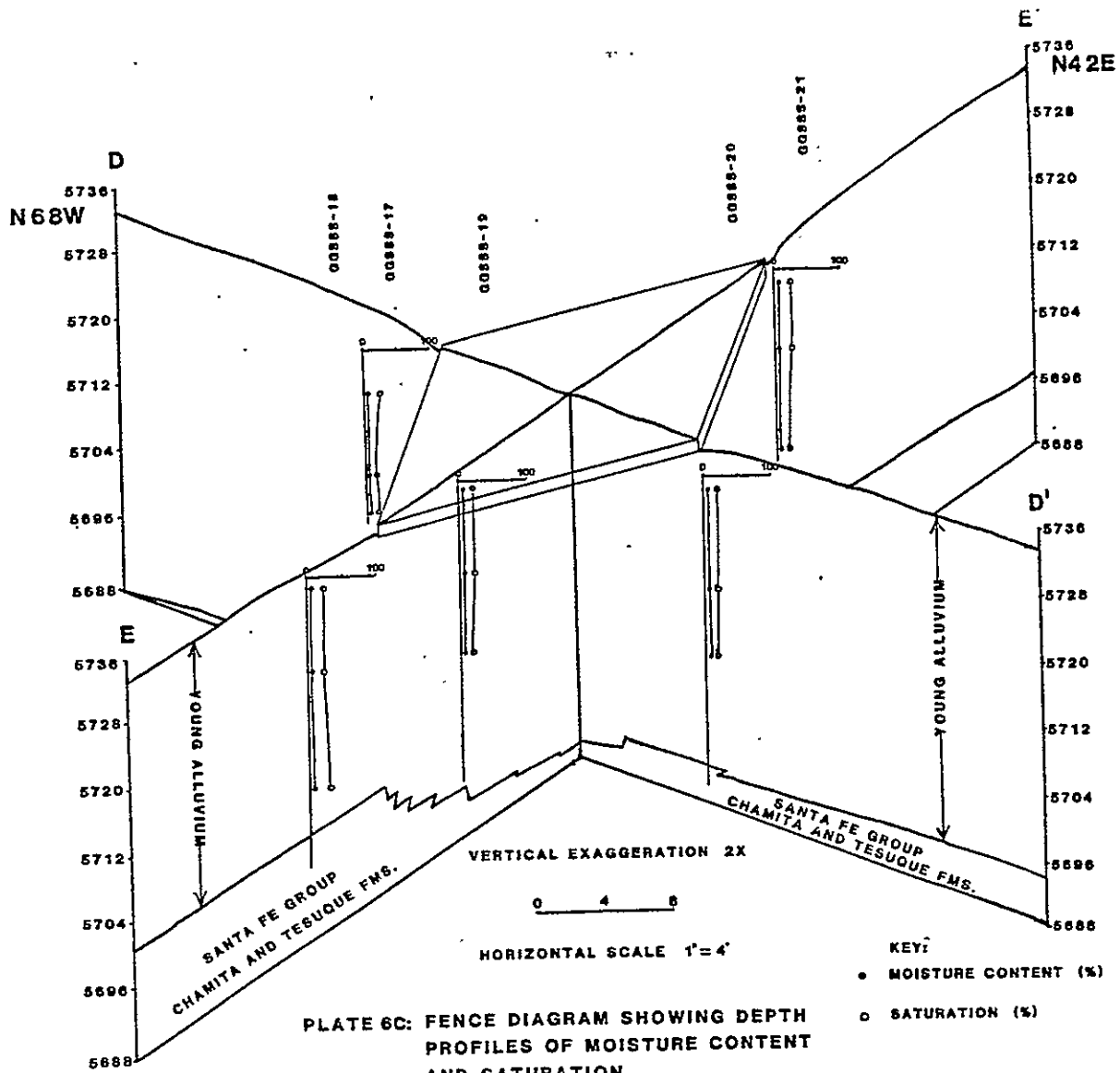
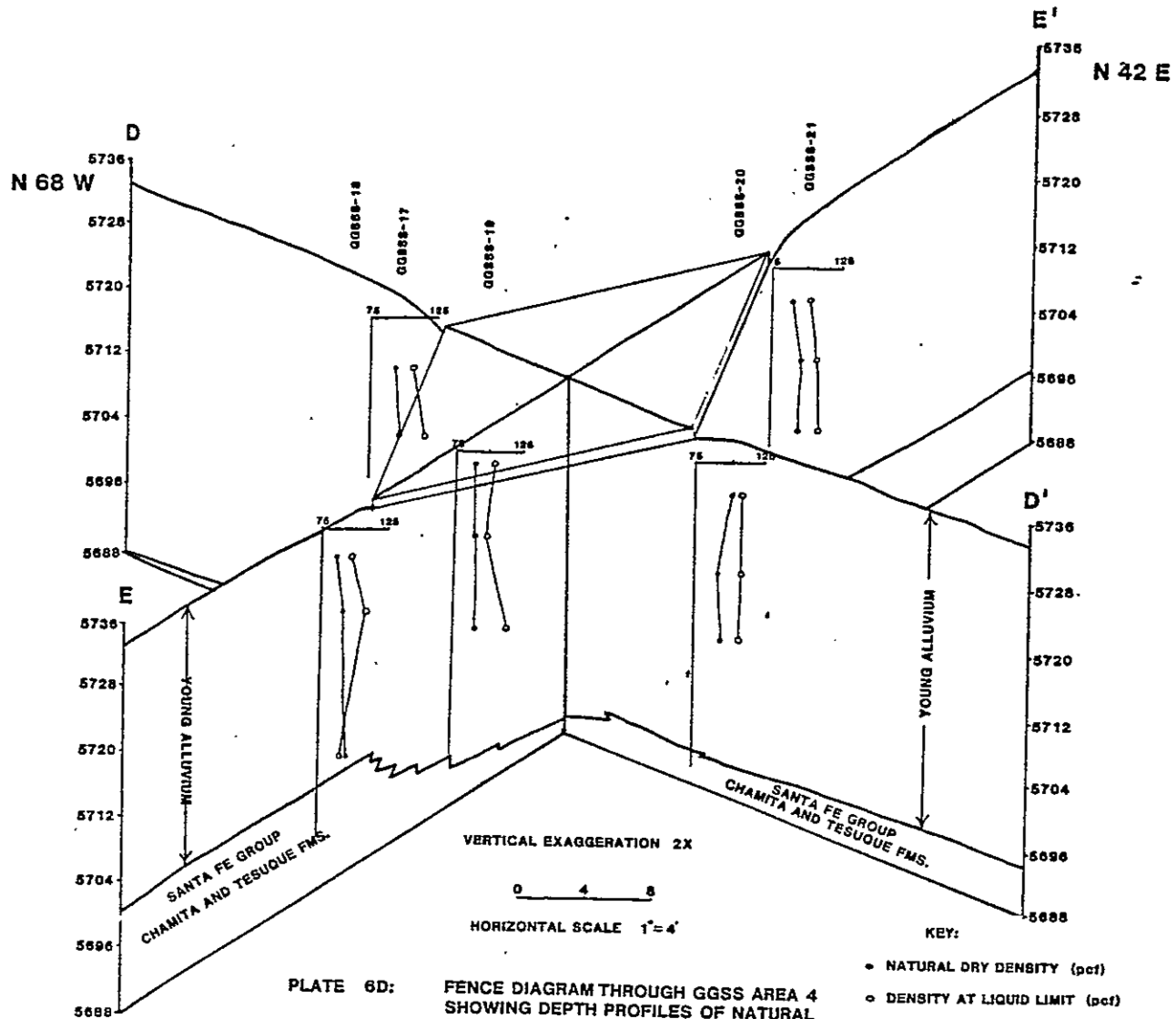
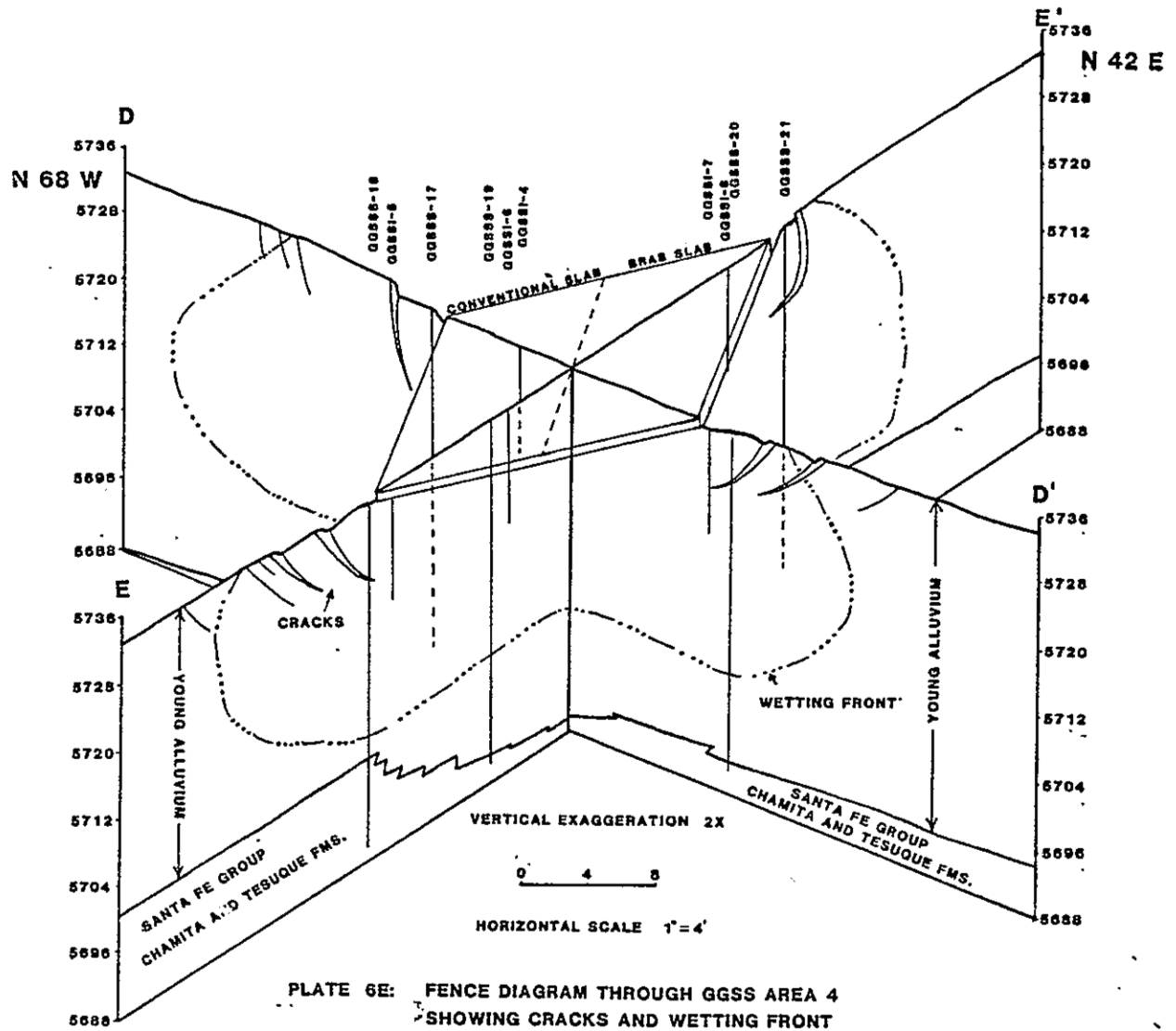


PLATE 6B: FENCE DIAGRAM THROUGH GGSS AREA 4
SHOWING DEPTH PROFILES OF BLOW COUNTS







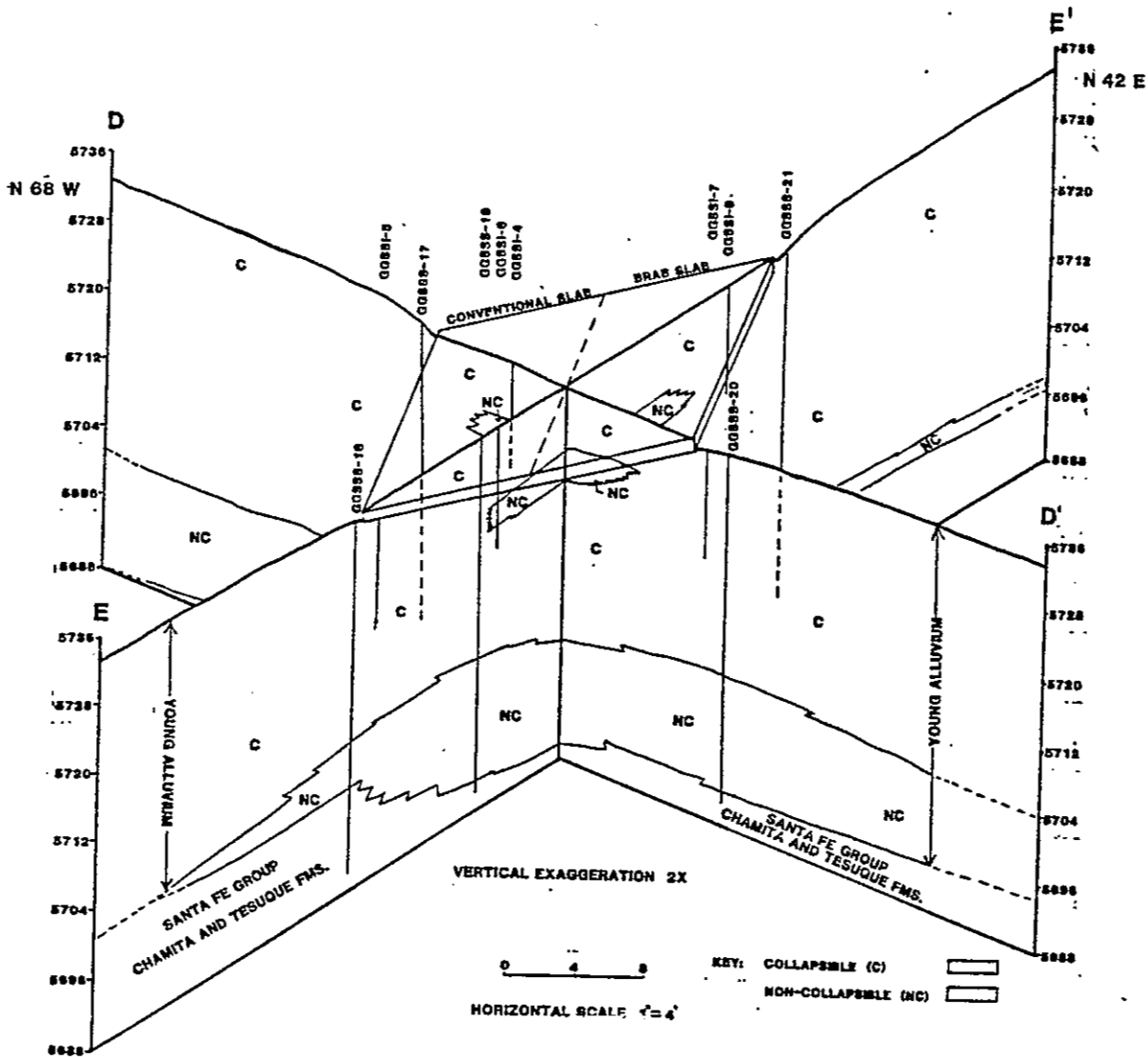


PLATE 6F: FENCE DIAGRAM THROUGH GGSS AREA 4 SHOWING COLLAPSIBLE AND NON-COLLAPSIBLE ZONES BASED ON PLATES 6A-6E

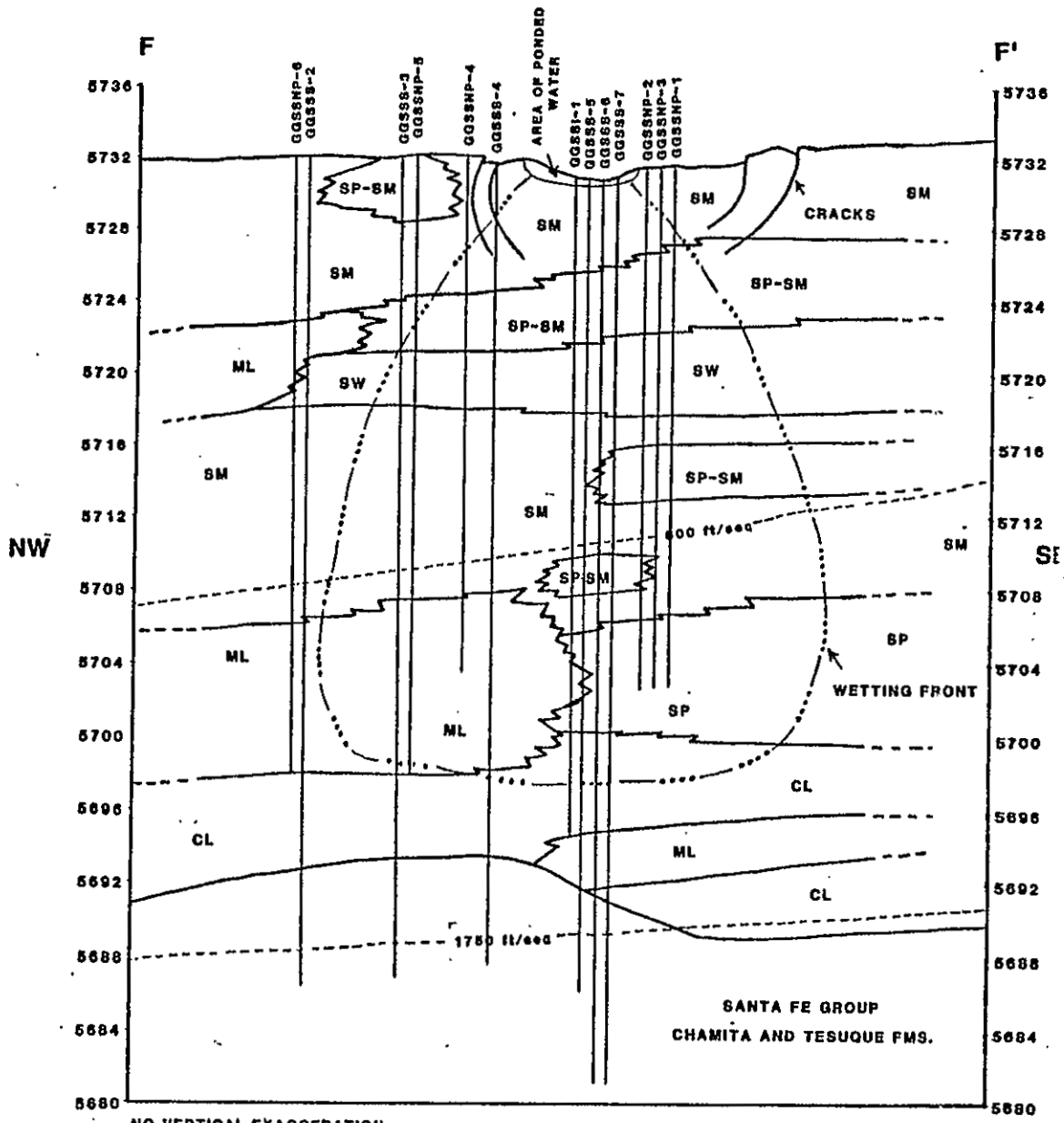


PLATE 7A: NW-SE GEOLOGIC CROSS-SECTION THROUGH GGSS AREA 1

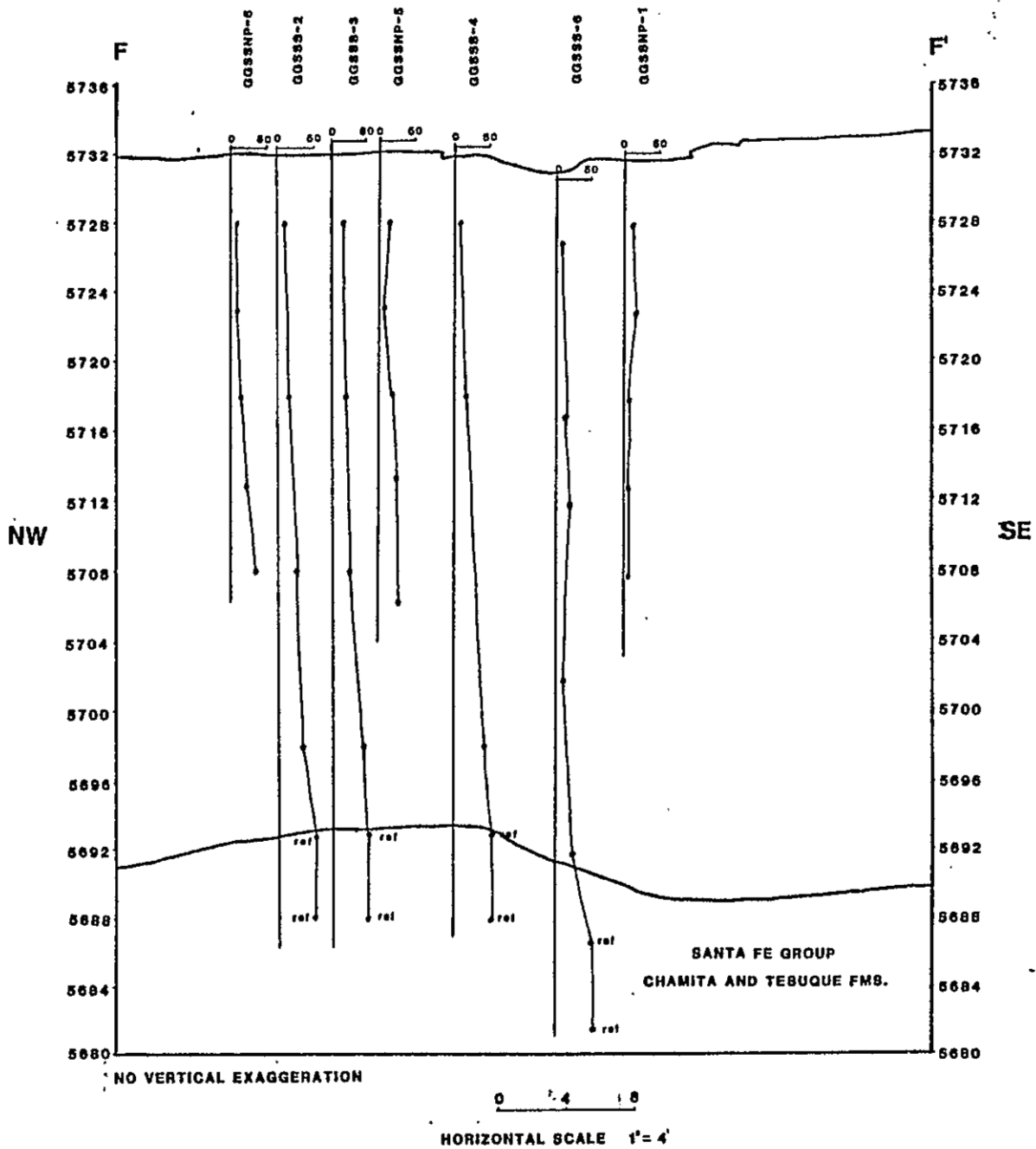


PLATE 7B: CROSS-SECTION FF' SHOWING DEPTH PROFILES OF BLOW COUNTS THROUGH GGSS AREA 1

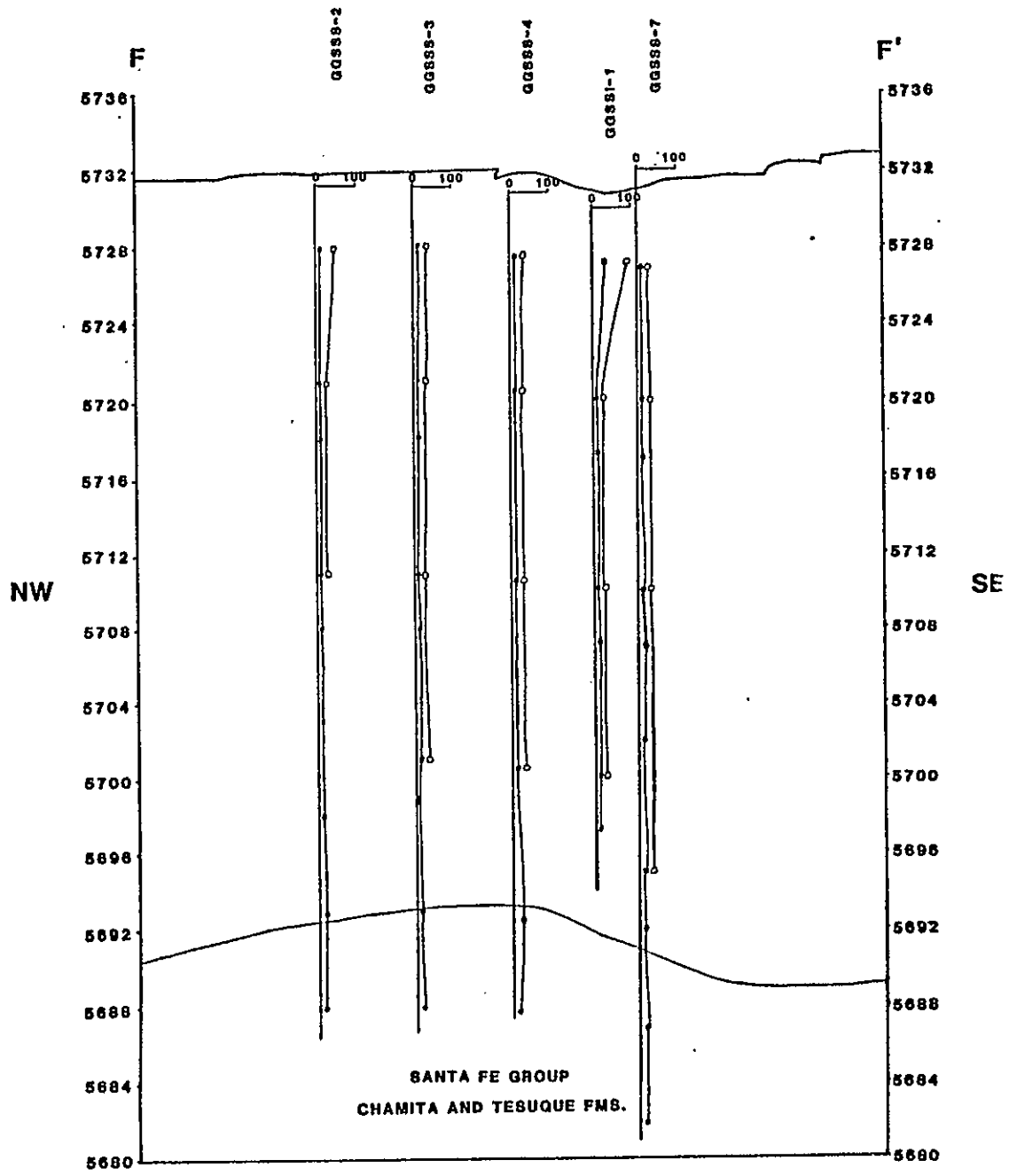
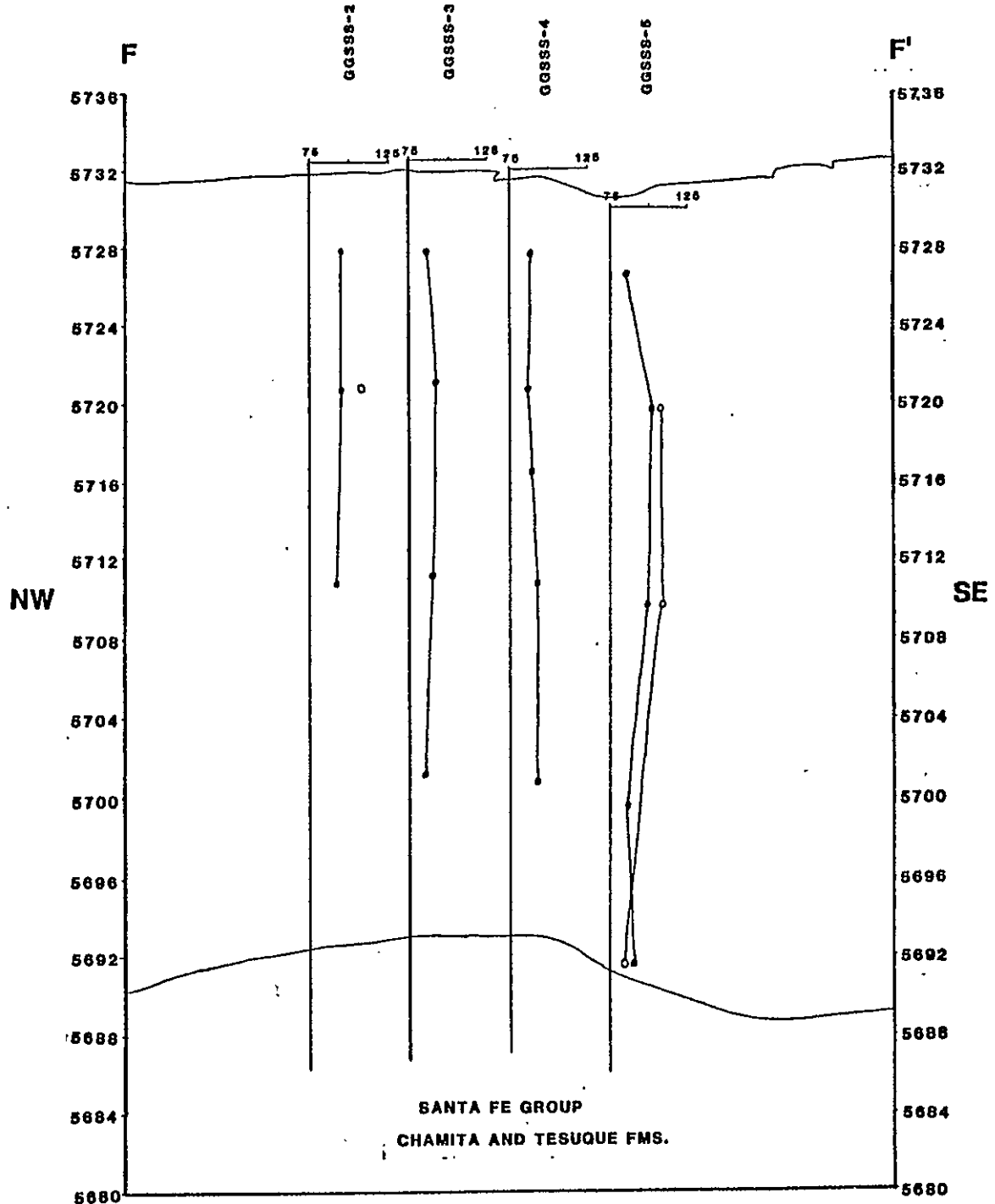
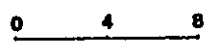


PLATE 7C: CROSS-SECTION FF' SHOWING DEPTH PROFILES OF MOISTURE CONTENT AND SATURATION THROUGH GGSS AREA 1



NO VERTICAL EXAGGERATION

KEY:



HORIZONTAL SCALE 1" = 4'

- NATURAL DRY DENSITY (pcf)
- DENSITY AT LIQUID LIMIT (pcf)

PLATE 7D: CROSS-SECTION FF' SHOWING DEPTH PROFILES OF NATURAL DRY DENSITY AND DENSITY AT LIQUID LIMIT THROUGH GGSS AREA 1

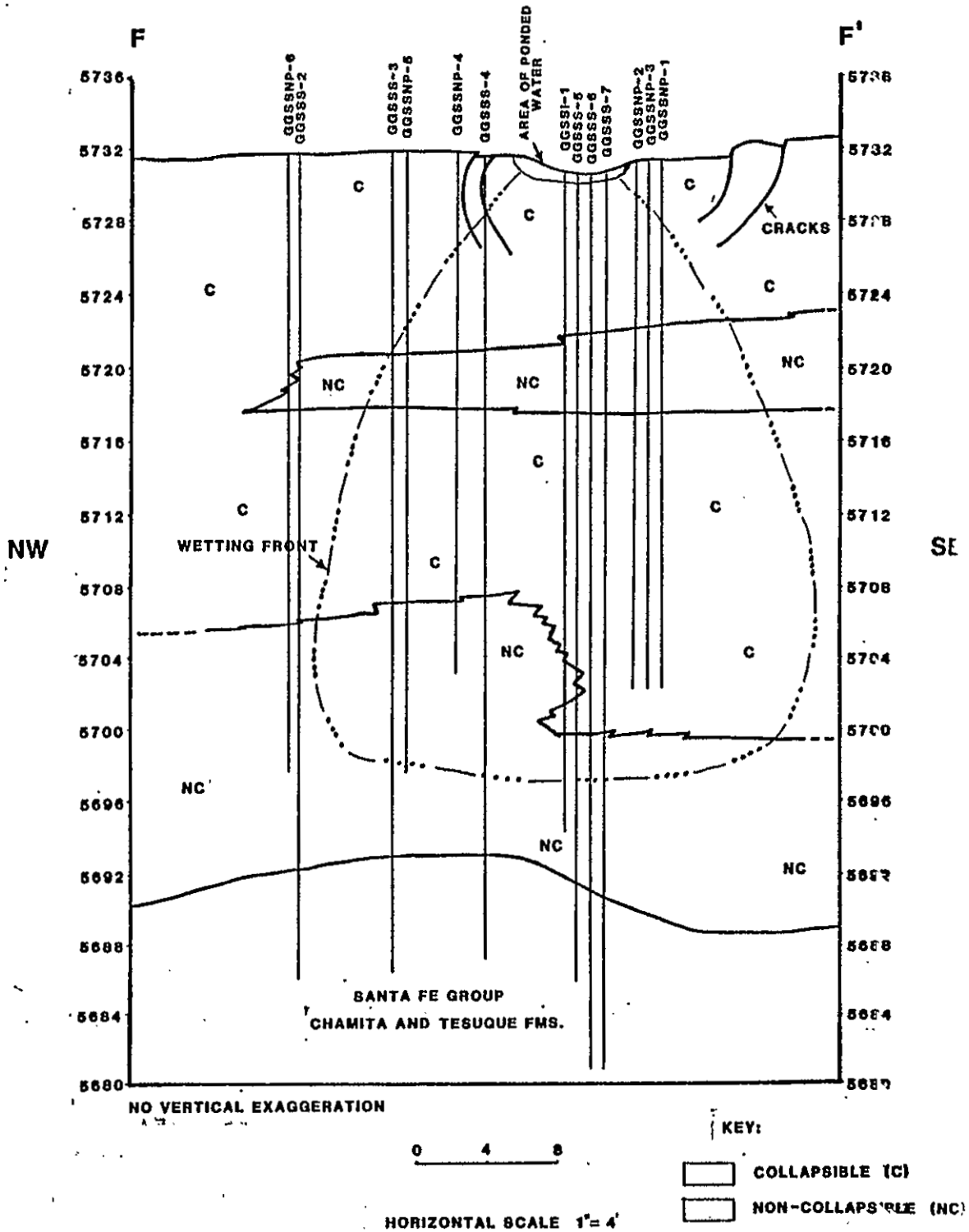


PLATE 7E: CROSS-SECTION FF' SHOWING COLLAPSIBLE AND NON-COLLAPSIBLE ZONES THROUGH GGSS AREA 1 BASED ON PLATES 7A-7D.

APPENDIX II

Climatic precipitation data

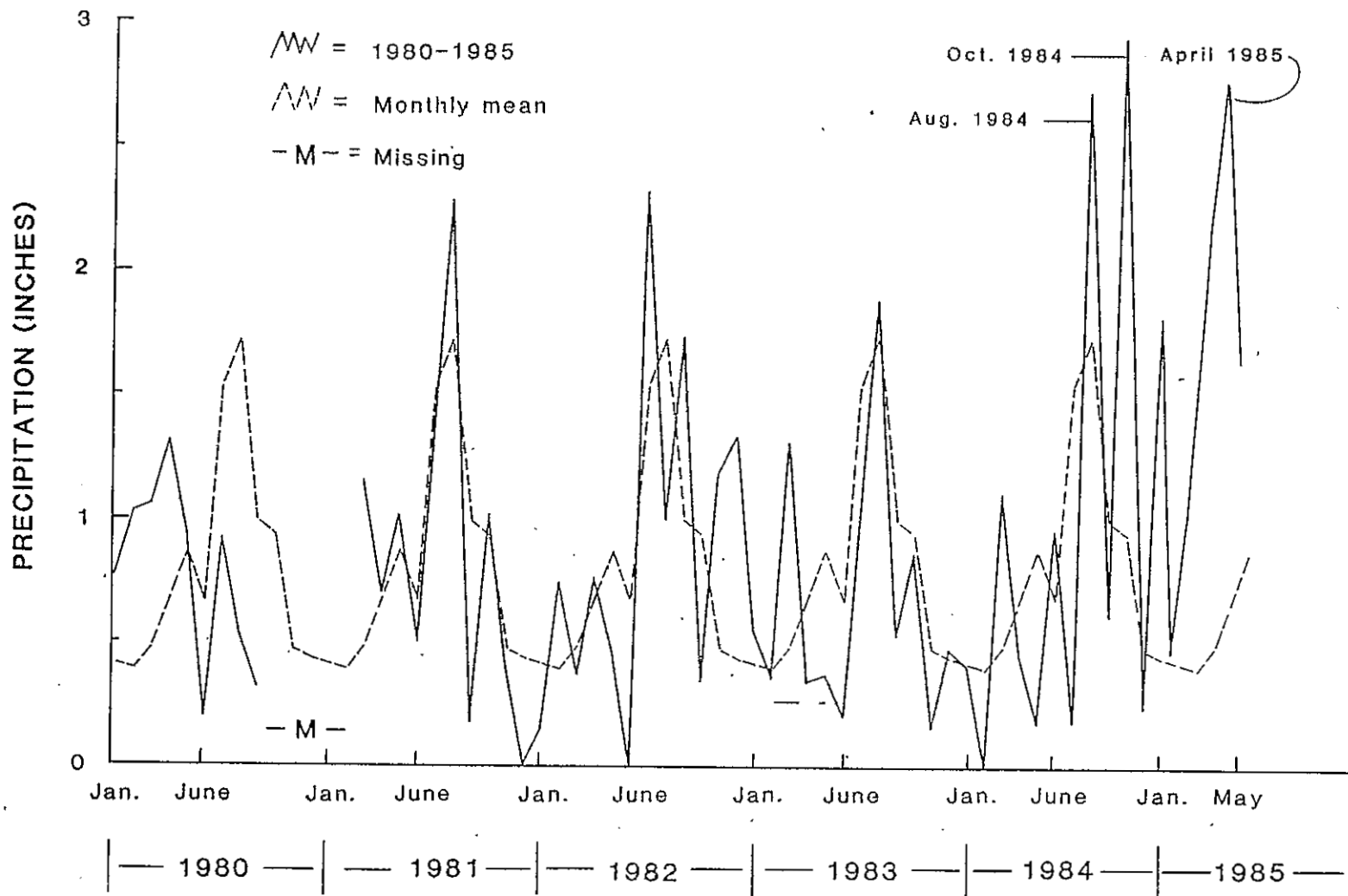


FIGURE 1 — Monthly precipitation 1980-1985, the dashed line represents the mean monthly precipitation 1895-1976 (Gabin and Lesperance, 1977). 28 JUNE 1985

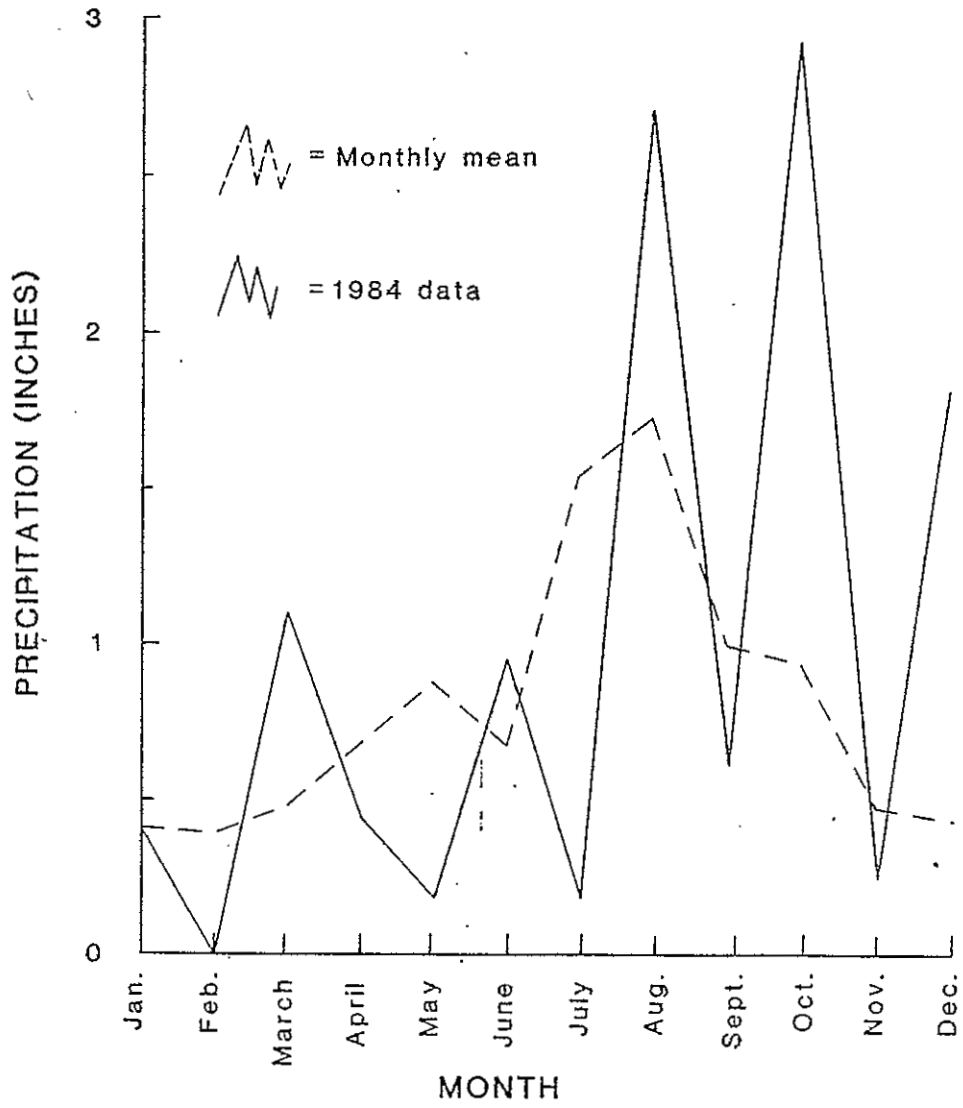
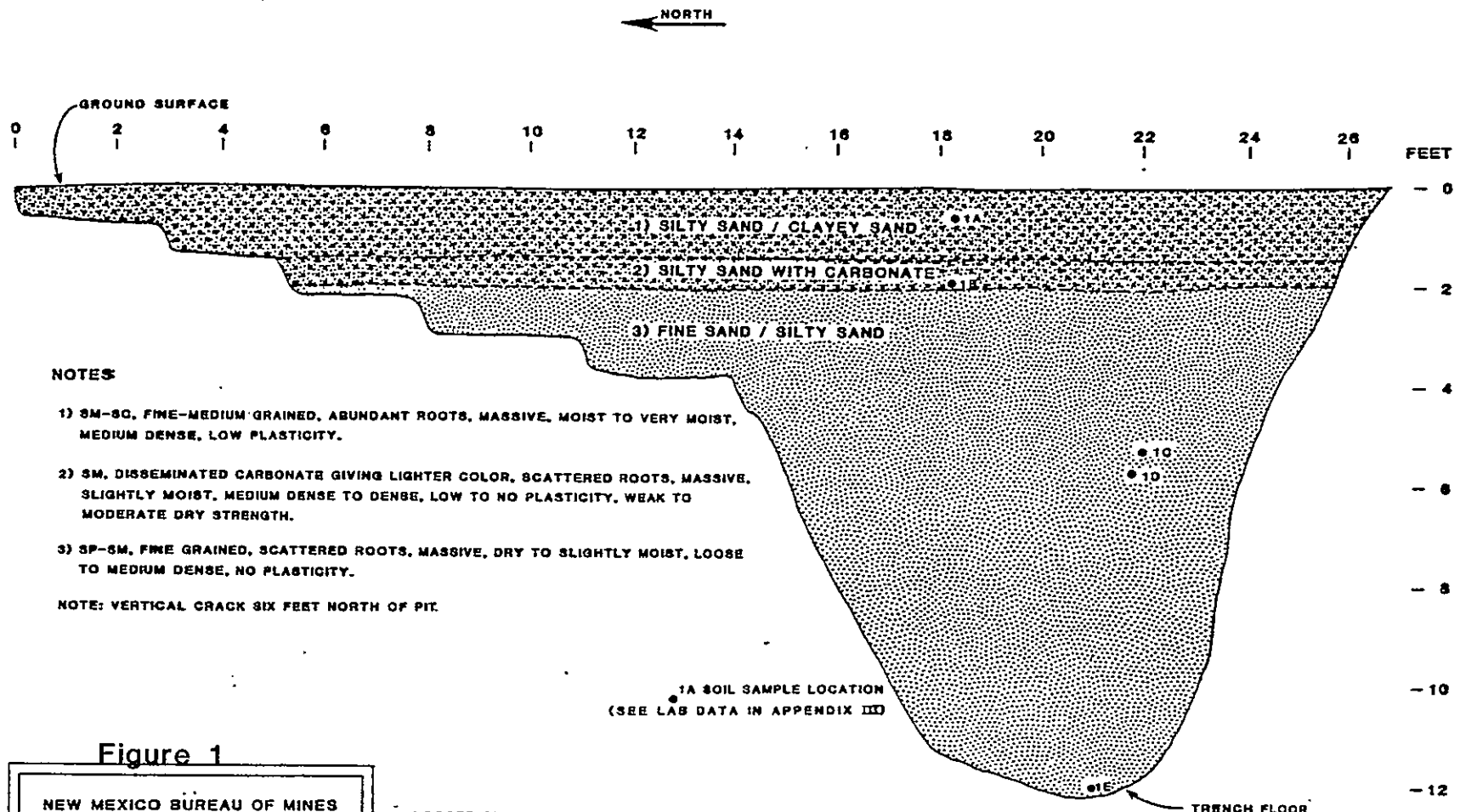


FIGURE 2—Monthly precipitation for 1984, the dashed line represents the mean monthly precipitation 1895–1976 (Gabin and Lesperance, 1977). 28 JUNE 1985

APPENDIX III

Trench logs



NOTES

- 1) SM-SC, FINE-MEDIUM GRAINED, ABUNDANT ROOTS, MASSIVE, MOIST TO VERY MOIST, MEDIUM DENSE, LOW PLASTICITY.
- 2) SM, DISSEMINATED CARBONATE GIVING LIGHTER COLOR, SCATTERED ROOTS, MASSIVE, SLIGHTLY MOIST, MEDIUM DENSE TO DENSE, LOW TO NO PLASTICITY, WEAK TO MODERATE DRY STRENGTH.
- 3) SP-SM, FINE GRAINED, SCATTERED ROOTS, MASSIVE, DRY TO SLIGHTLY MOIST, LOOSE TO MEDIUM DENSE, NO PLASTICITY.

NOTE: VERTICAL CRACK SIX FEET NORTH OF PIT.

1A SOIL SAMPLE LOCATION
(SEE LAB DATA IN APPENDIX III)

Figure 1

NEW MEXICO BUREAU OF MINES
AND MINERAL RESOURCES
EL LLANO SUBSIDENCE PROJECT
LOG OF TRENCH ESBH-1
FINAL 28 JUNE 1985

LOGGED BY G. JOHNPEER
12-4-84
SEE ACTIVITY LOCATION MAP FOR TRENCH LOCATION

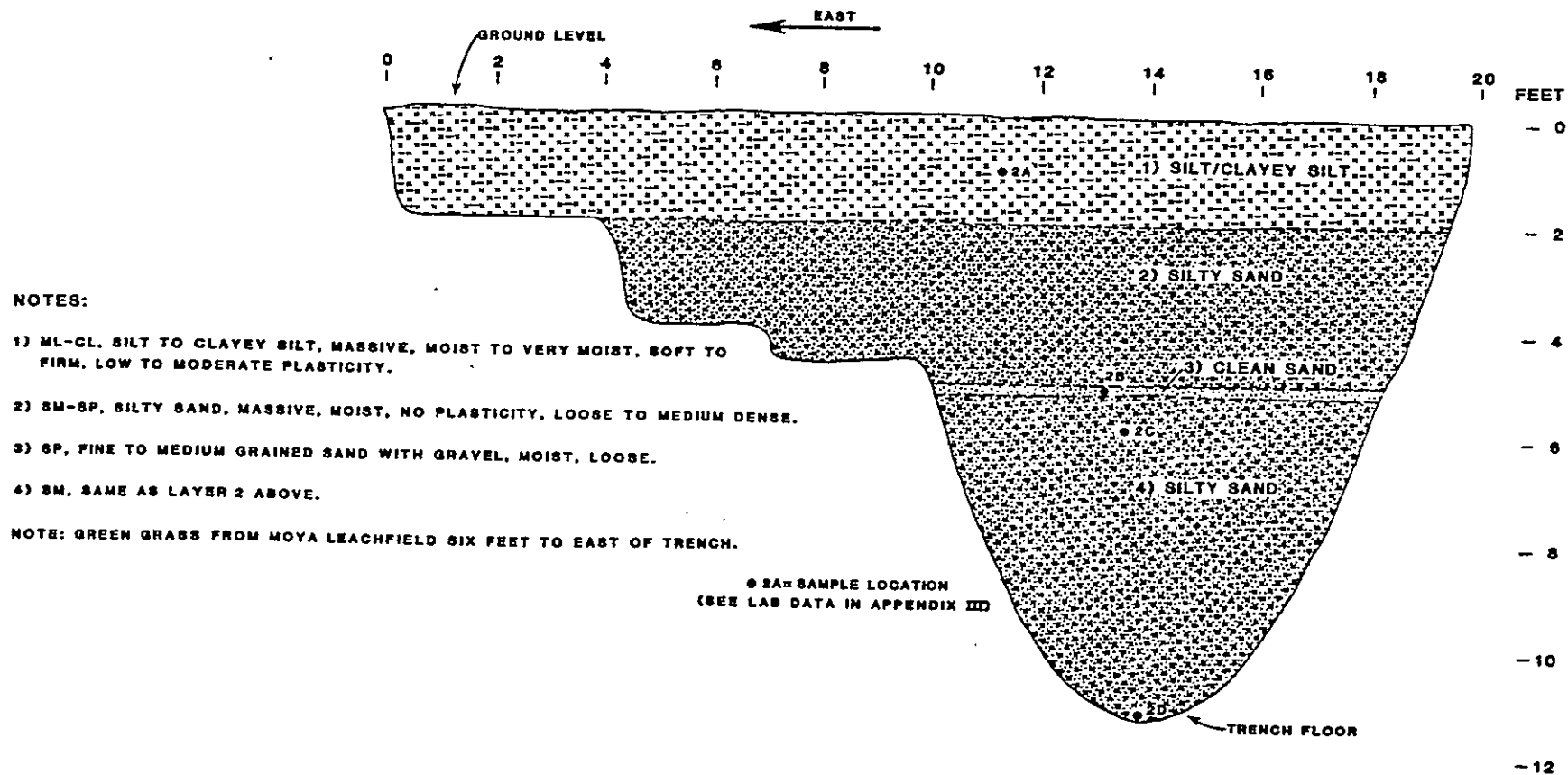
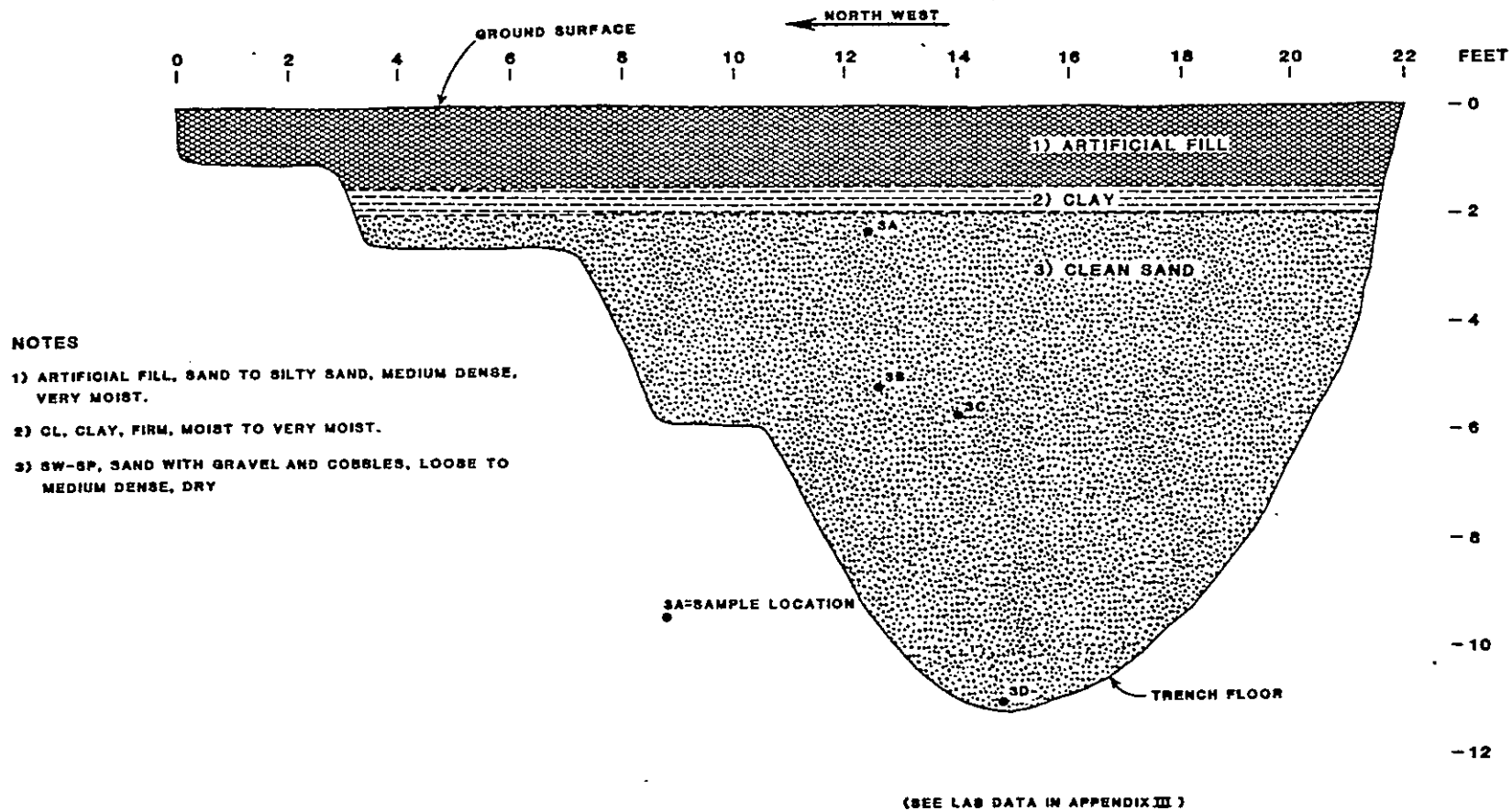


Figure 2

NEW MEXICO BUREAU OF MINES
AND MINERAL RESOURCES
EL LLANO SUBSIDENCE PROJECT
LOG OF TRENCH ESBH-2
FINAL 28 JUNE 1986

LOGGED BY: G. JOHNPEER
12-4-84
SEE ACTIVITY LOCATION MAP FOR TRENCH LOCATION



NOTES

- 1) ARTIFICIAL FILL, SAND TO SILTY SAND, MEDIUM DENSE, VERY MOIST.
- 2) CL. CLAY, FIRM, MOIST TO VERY MOIST.
- 3) SW-SP, SAND WITH GRAVEL AND COBBLES, LOOSE TO MEDIUM DENSE, DRY

LOGGED BY G. JOHNPEER
12-4-64

SEE ACTIVITY LOCATION MAP FOR TRENCH LOCATION

Figure 3

NEW MEXICO BUREAU OF MINES
AND MINERAL RESOURCES
EL LLANO SUBSIDENCE PROJECT
LOG OF TRENCH ESBH-3
FINAL 28 JUNE 1965

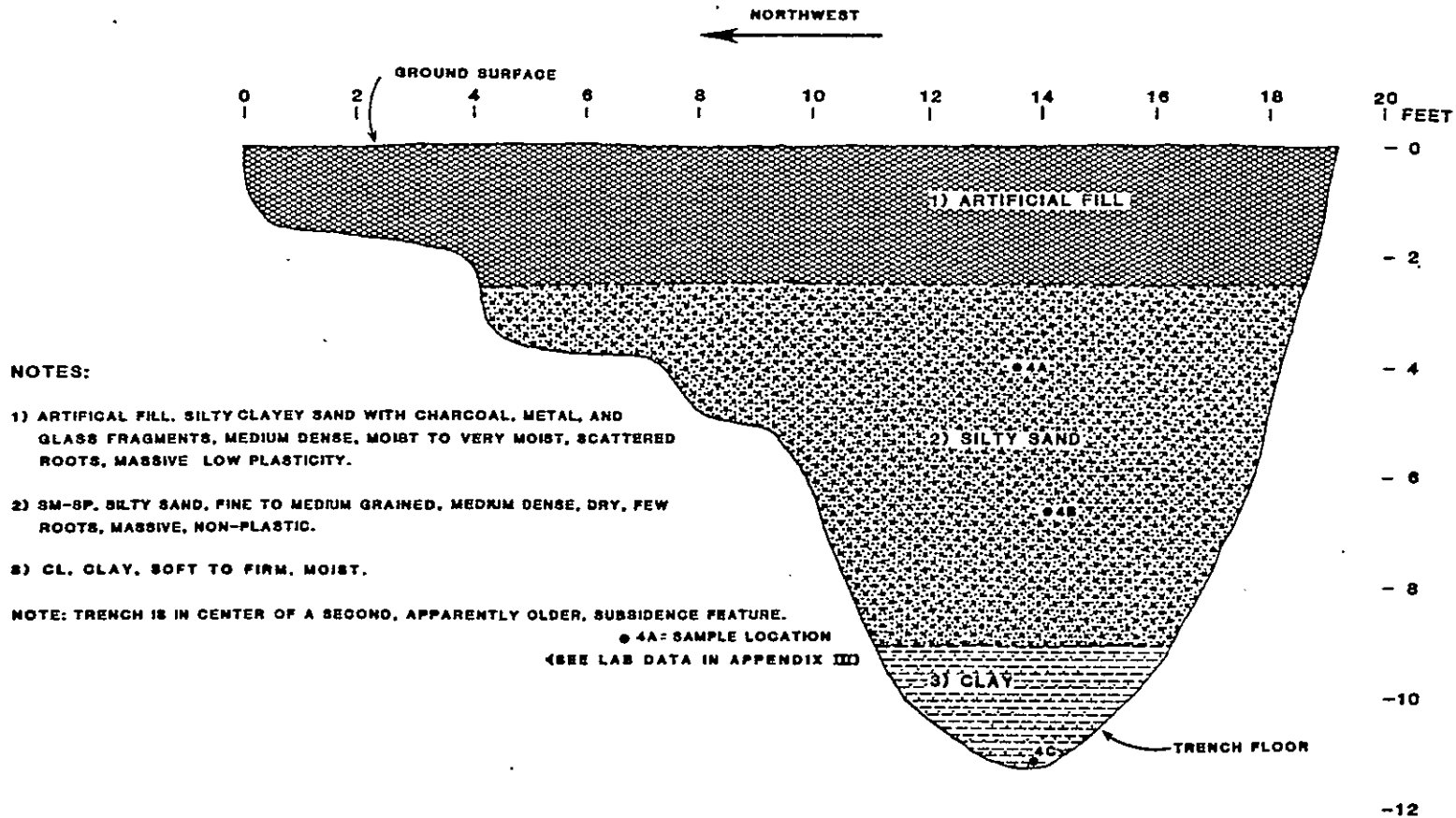


Figure 4

NEW MEXICO BUREAU OF MINES
AND MINERAL RESOURCES
EL LLANO SUBSIDENCE PROJECT
LOG OF TRENCH ESBH-4
FINAL 28 JUNE 1985

LOGGED BY G. JOHNPEER
12-4-84
SEE ACTIVITY LOCATION MAP FOR TRENCH LOCATION

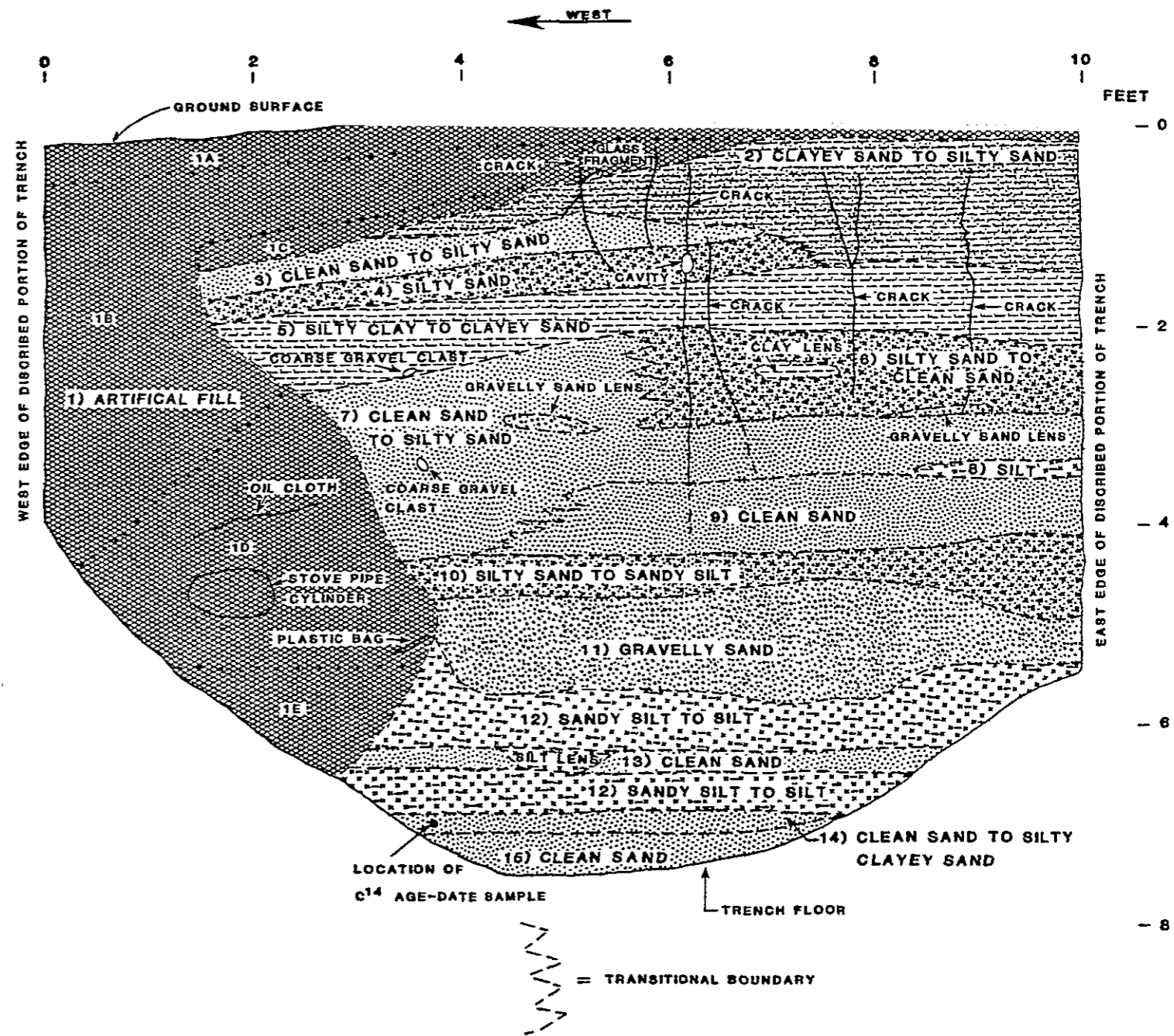
NOTES:

- 1) ARTIFICIAL FILL, SLIGHTLY MOIST TO MEDIUM MOIST, LOOSE, SCATTERED CRACKS, SUBDIVIDED AS FOLLOWS:
- A) SM-ML, SILTY SAND TO SANDY SILT, SURFICIAL DISTURBED LAYER, GLASS FRAGMENTS.
 - B) SM-SC, SILTY TO CLAYEY SAND.
 - C) TRASH WITH GLASS FRAGMENTS.
 - D) TRASH, INCLUDING GLASS FRAGMENTS, CLOTH, STOVE PIPE, AND A PLASTIC BAG CIRCA DECEMBER, 1959.
 - E) SM, SILTY SAND.
- 2) SC-SM, CLAYEY TO SILTY SAND, SLIGHTLY MOIST, LOOSE, SCATTERED CRACKS.
- 3) SP-SM, VERY FINE-GRAINED CLEAN TO SILTY SAND, SLIGHTLY MOIST TO MEDIUM MOIST, SCATTERED CRACKS.
- 4) SM, SILTY SAND, SLIGHTLY MOIST TO MEDIUM MOIST, LOOSE, SCATTERED CRACKS, NOTE SINGLE 3 INCH CAVITY ALONG CRACK.
- 5) CL-SC, SILTY CLAY TO CLAYEY SAND, VERY MOIST, SCATTERED CRACKS, NOTE SINGLE 1.5 INCH GRAVEL CLAST AT BASE.
- 6) SM-SP, SILTY TO CLEAN SAND, MEDIUM MOIST, LOOSE, SCATTERED CRACKS, NOTE SINGLE GRAVELLY SAND LENS AT BASE AND SINGLE CLAY LENS.
- 7) SP-SM, VERY FINE-GRAINED CLEAN TO SILTY SILTY SAND, MEDIUM MOIST, LOOSE, SCATTERED CRACKS AND LENSES OF GRAVELLY SAND, NOTE SINGLE 2 INCH GRAVEL CLAST.
- 8) ML, SILT, MEDIUM MOIST, FIRM, LOW PLASTICITY.
- 9) SP, VERY FINE-GRAINED CLEAN SAND, MEDIUM MOIST, LOOSE, SCATTERED CRACKS AND LENSES OF GRAVELLY SAND.
- 10) SM-ML, SILTY SAND TO SANDY SILT, VERY MOIST.
- 11) SW, GRAVELLY SAND, MEDIUM MOIST, LOOSE.
- 12) ML, SANDY SILT TO SILT, MEDIUM MOIST, FIRM, LOW PLASTICITY.
- 13) SP, VERY FINE-GRAINED CLEAN SAND, MEDIUM MOIST, LOOSE, NOTE SINGLE SILT LENS.
- 14) SP-SM, VERY FINE-GRAINED CLEAN TO SILTY CLAYEY SAND, MEDIUM MOIST, LOOSE, SCATTERED FIRE-CRACKED GRAVEL AND CHARCOAL (CHARCOAL C¹⁴ AGE 2330 ± 70 YEARS).
- 15) SP, VERY FINE-GRAINED CLEAN SAND, MEDIUM MOIST, LOOSE.

Figure 5

NEW MEXICO BUREAU OF MINES
AND MINERAL RESOURCES
EL LLANO SUBSIDENCE PROJECT
LOG OF TRENCH ESBH- 5
FINAL 28 JUNE 1985

LOGGED BY: J. HAWLEY
1-24-85
SEE ACTIVITY LOCATION
MAP FOR LOCATION.



- 1) ARTIFICIAL FILL, MOIST (FROZEN), LOOSE, ABUNDANT ROOTS, SCATTERED PORCELAIN, GLASS, AND METAL FRAGMENTS, SCATTERED CRACKS.
- 2) SP-SM, SLIGHTLY SILTY SAND, MOIST, LOOSE TO MEDIUM DENSE, POORLY LAMINATED, SCATTERED CRACKS, FINE- TO COARSE-GRAINED GRAVEL AND FINE-GRAINED COBBLES, AND LENSES OF SANDY GRAVEL AND GRAVELLY SAND.
- 3) SP, CLEAN SAND, MEDIUM MOIST, MEDIUM DENSE, NOTE SINGLE FLATTENED CLAY LENS AND SCATTERED CRACKS.
- 4) CH, CLAY, MOIST, FHM, HIGH PLASTICITY, 2 INCHES THICK.
- 5) SM-ML, SILTY SAND TO SILT, MEDIUM MOIST TO DRY (NOTE MOISTURE BOUNDARY), MEDIUM DENSE SLIGHTLY PLATTY AND POORLY LAMINATED SCATTERED FINE-GRAINED GRAVEL, CRACKS, DEFORMED CLAY STRINGERS, NOTE SINGLE LENS OF MOIST SILTY SAND WITH AN UNDULATORY UPPER SURFACE.
- 6) SP-SM, SLIGHTLY SILTY SAND, MEDIUM MOIST TO DRY (NOTE MOISTURE BOUNDARY), MEDIUM DENSE, FAINTLY LAMINATED, SCATTERED CRACKS AND CLAY STRINGERS.
- 7) SC, CLAYEY SAND, DRY, MEDIUM DENSE, LAMINATED, SCATTERED CRACKS.
- 8) SP-SM, SLIGHTLY SILTY SAND, DRY, MEDIUM DENSE, CROSS-LAMINATED, SCATTERED CRACKS.
- 9) SP, CLEAN SAND, DRY, MEDIUM DENSE, DISCONTINUOUS, SCATTERED CRACKS AND FINE-GRAINED GRAVEL.
- 10) ML, SILT, DRY, FHM, LOW PLASTICITY, WELL-LAMINATED, SCATTERED CRACKS AND 1 INCH THICK INTERBEDS OF CLEAN SAND.
- 11) SP, CLEAN SAND, DRY, MEDIUM DENSE, SCATTERED CRACKS.
- 12) SP-SM, SLIGHTLY SILTY SAND, DRY, MEDIUM DENSE, SCATTERED CRACKS, GRAVELLY SAND LENSES, AND CLAY STRINGERS, NOTE SINGLE 3 INCH DIAMETER CLAY-FILLED KROTOVINA.
- 13) SP, CLEAN SAND, DRY, MEDIUM DENSE, WELL-LAMINATED, ABUNDANT CLAY STRINGERS, SCATTERED CRACKS AND GRAVELLY SAND LENSES, NOTE SINGLE 5 INCH DIAMETER CLAY-FILLED KROTOVINA.
- 14) CL-ML, CLAY, DRY, FHM, LOW PLASTICITY, MASSIVE, SCATTERED CRACKS.

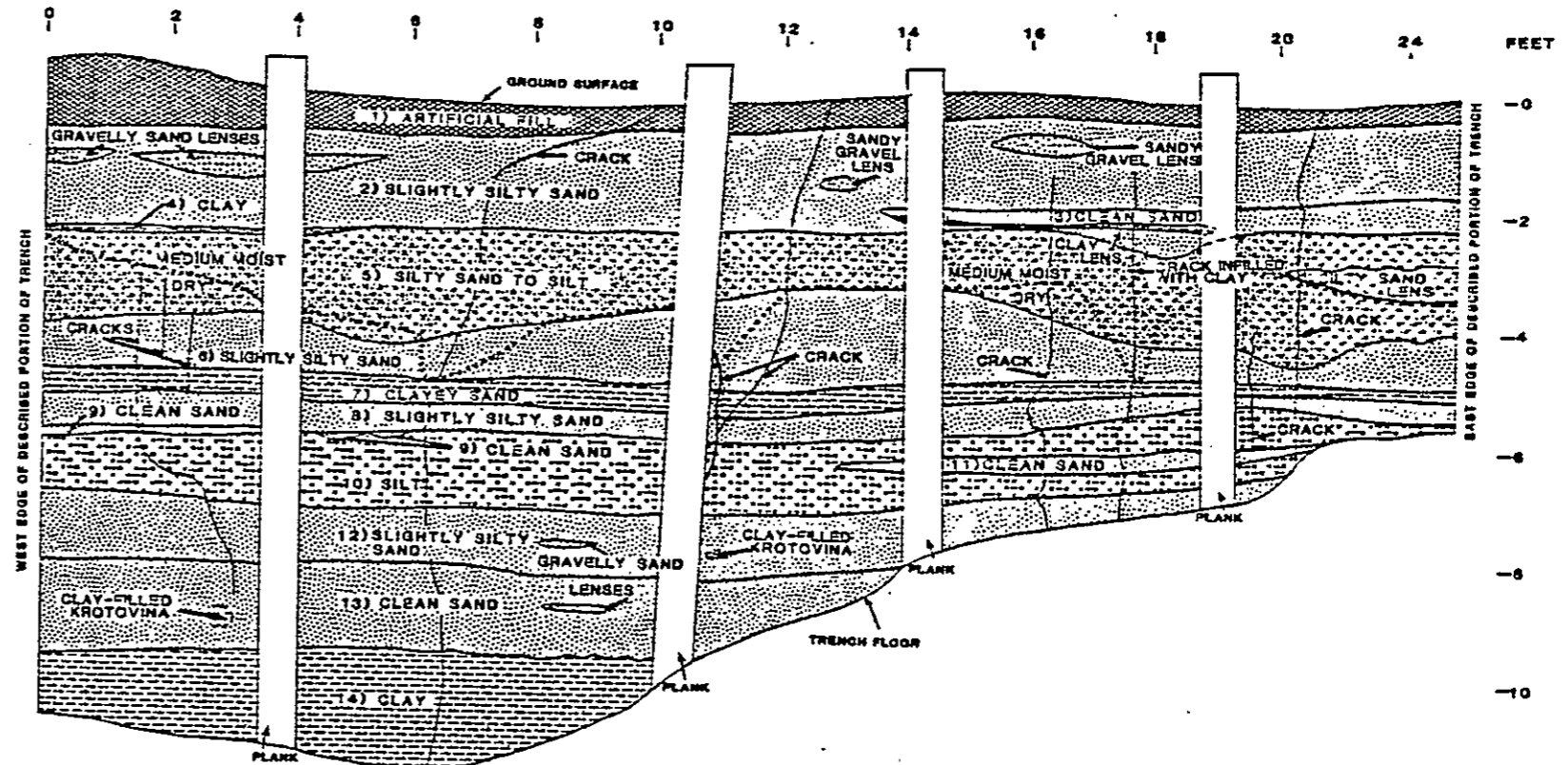


Figure 6

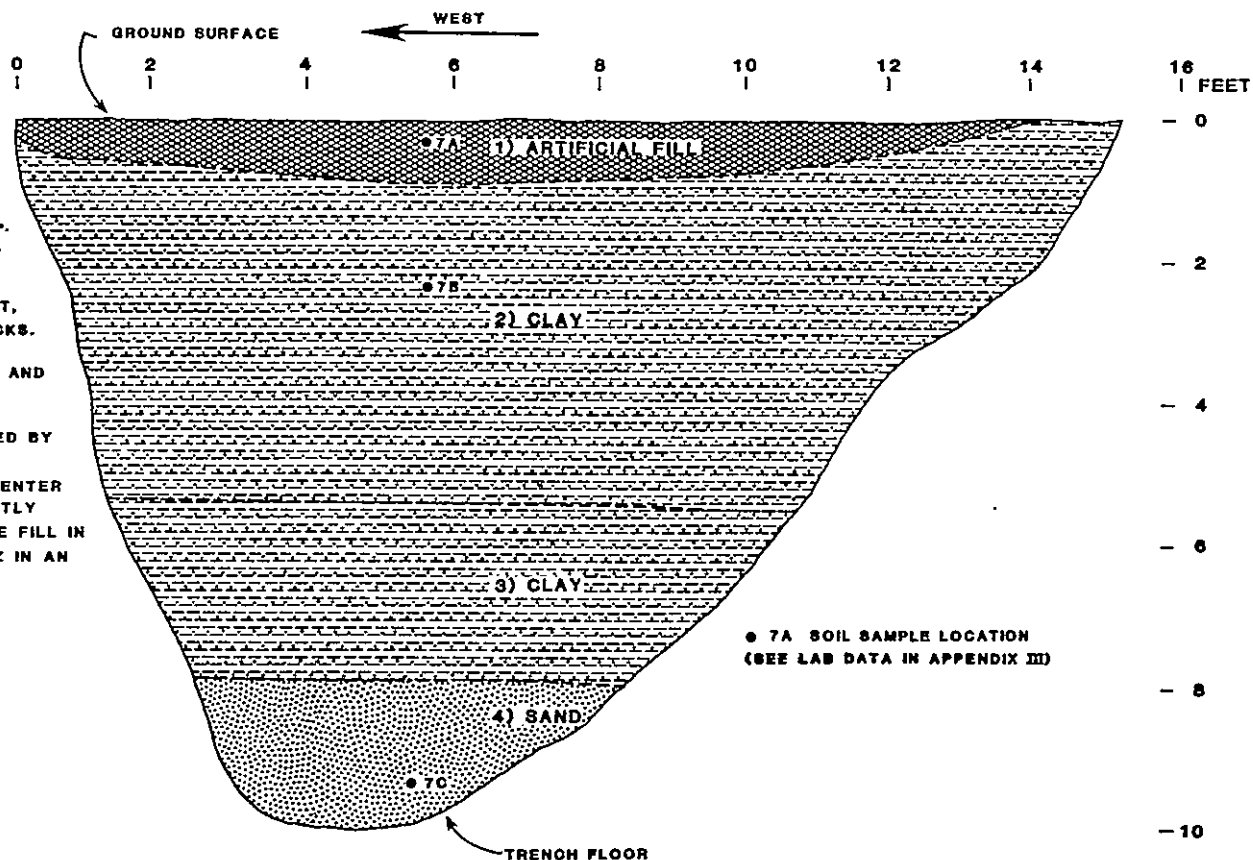
NEW MEXICO BUREAU OF MINES
AND MINERAL RESOURCES
EL LLANO SUBSIDENCE PROJECT
LOG OF TRENCH ESBH-6
FINAL 28 JUNE 1966

LOGGED BY M. HEMINGWAY
1-24, 28-66
SEE ACTIVITY LOCATION MAP
FOR TRENCH LOCATION

NOTES:

- 1) ARTIFICIAL FILL, WET TO VERY MOIST, MEDIUM DENSE, SCATTERED METAL FRAGMENTS.
- 2) CL-CH, CLAY, SATURATED TO VERY MOIST, SOFT, LOW TO MODERATE PLASTICITY, SCATTERED LIVE ROOTS.
- 3) CL-ML, CLAY TO SILT, MEDIUM TO SLIGHTLY MOIST, FIRM TO HARD, LOW PLASTICITY, ABUNDANT CRACKS.
- 4) SP, CLEAN MEDIUM-GRAINED SAND WITH GRAVEL AND COBBLES, DRY, LOOSE TO MEDIUM DENSE.

NOTE: TRENCH DUG OVER "BOTANO" REPORTED BY F. VALDEZ AT WESTERN END OF HIS PROPERTY. IRRIGATION WATER WOULD ENTER THE BOTANO AND DRAIN OFF, APPARENTLY THROUGH THE CRACKS IN LAYER 3. THE FILL IN LAYER 1 WAS REPLACED BY F. VALDEZ IN AN ATTEMPT TO PLUG THE BOTANO.



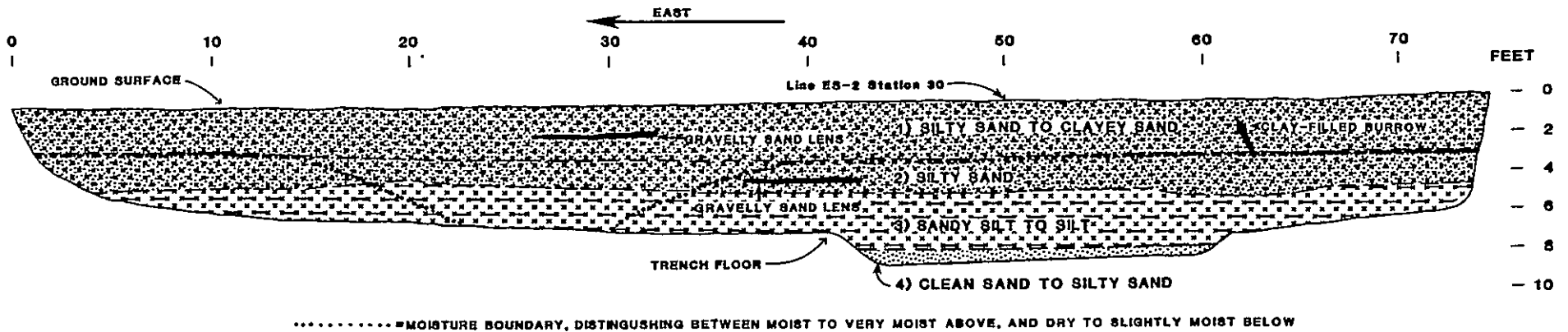
● 7A SOIL SAMPLE LOCATION
(SEE LAB DATA IN APPENDIX III)

Figure 7

NEW MEXICO BUREAU OF MINES
AND MINERAL RESOURCES
EL LLANO SUBSIDENCE PROJECT
LOG OF TRENCH ESBH-7
FINAL 28 JUNE 1985

LOGGED BY G. JOHNPERR
1-28-85

SEE ACTIVITY LOCATION MAP FOR TRENCH LOCATION



NOTES:

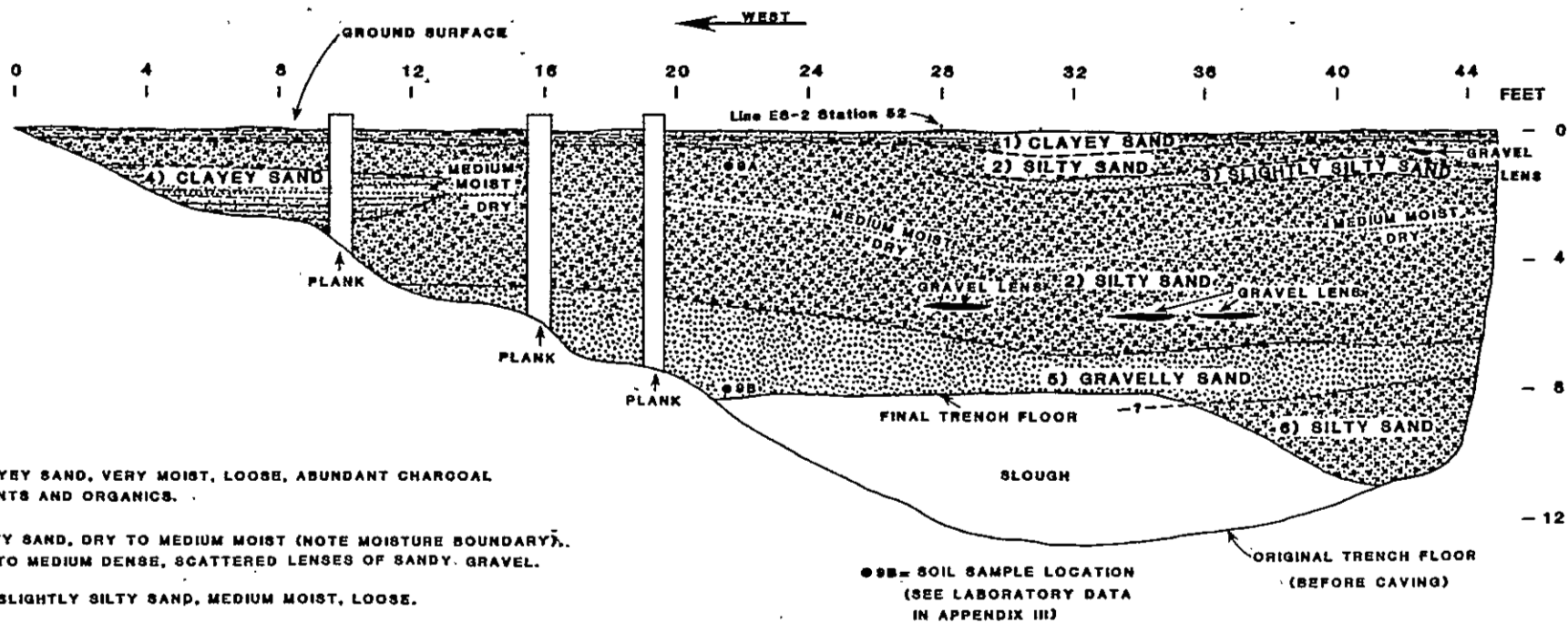
- 1) SM-SC, SILTY SAND TO CLAYEY SAND, MOIST TO VERY MOIST, LOOSE TO MEDIUM DENSE, SCATTERED SILTY CLAY TO SANDY SILT ZONES, GRAVEL, GRAVELLY SAND LENSES, NOTE SINGLE BURROW INFILLED WITH CLAY.
- 2) SM, SILTY SAND, DRY TO VERY MOIST(NOTE MOISTURE BOUNDARY), LOOSE TO MEDIUM DENSE, POORLY STRATIFIED TO MASSIVE, SCATTERED FINE-GRAINED GRAVEL AND GRAVELLY SAND LENSES.
- 3) ML, VERY FINE-GRAINED SANDY SILT TO SILT, DRY TO VERY MOIST(NOTE MOISTURE BOUNDARY), LOOSE TO MEDIUM DENSE, LOCALLY LAMINATED AND PLATY, SCATTERED SILTY SAND LENSES.
- 4) SP-SM, FINE-GRAINED CLEAN SAND TO SILTY SAND, DRY TO SLIGHTLY MOIST, LOOSE TO MEDIUM DENSE.

NOTE: TRENCH EXCAVATED OVER TRACE OF GEOPHYSICALLY INTERPRETED FAULT.

Figure 8

NEW MEXICO BUREAU OF MINES
AND MINERAL RESOURCES
EL LLANO SUBSIDENCE PROJECT
LOG OF TRENCH ESBH-8
FINAL 28 JUNE 1985

LOGGED BY J. HAWLEY
1-25-85
SEE ACTIVITY LOCATION MAP FOR TRENCH LOCATION.



NOTES:

- 1) SC, CLAYEY SAND, VERY MOIST, LOOSE, ABUNDANT CHARCOAL FRAGMENTS AND ORGANICS.
- 2) SM, SILTY SAND, DRY TO MEDIUM MOIST (NOTE MOISTURE BOUNDARY). LOOSE TO MEDIUM DENSE, SCATTERED LENSES OF SANDY GRAVEL.
- 3) SP-SM, SLIGHTLY SILTY SAND, MEDIUM MOIST, LOOSE.
- 4) SC-CL, CLAYEY SAND, DRY TO MEDIUM MOIST (NOTE MOISTURE BOUNDARY), MEDIUM DENSE.
- 5) SW-GW, GRAVELLY SAND, GRAVEL FRACTION FINE-TO MEDIUM-GRAINED, ROUNDED TO SUBROUNDED, DRY, MEDIUM DENSE.
- 6) SM, SILTY SAND, DRY, MEDIUM DENSE.

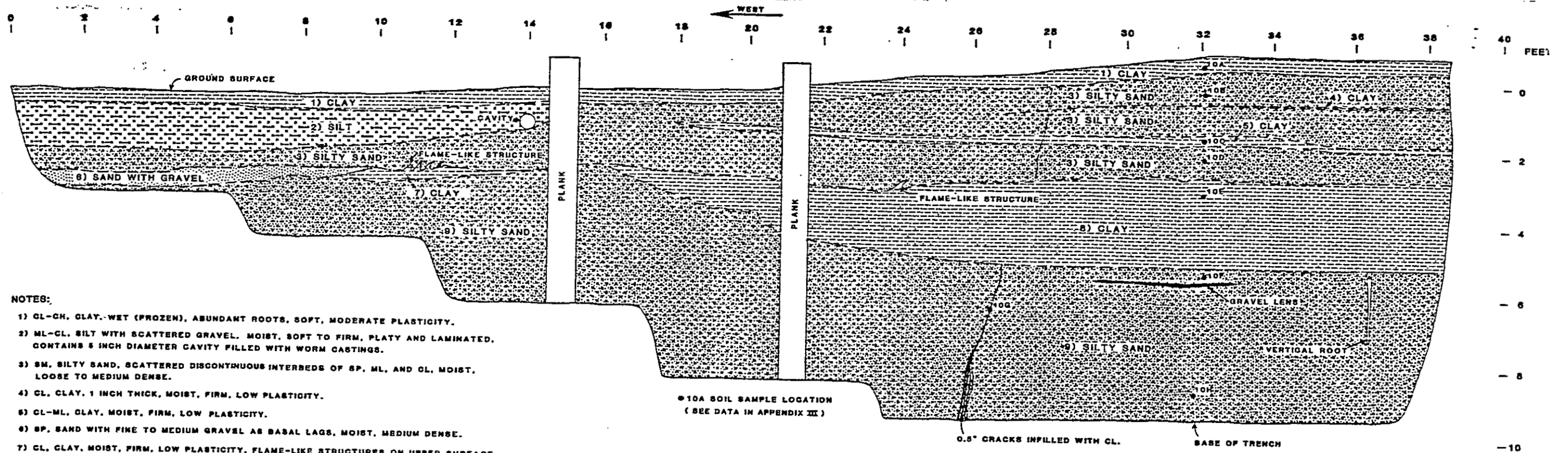
NOTE: DUE TO INSTABILITY OF TRENCH WALLS, TRENCH EAST OF PLANKS WAS LOGGED FROM THE SURFACE. TRENCH EXCAVATED ACROSS TRACE OF GEOPHYSICALLY INTERPRETED FAULT.

Figure 9

NEW MEXICO BUREAU OF MINES
AND MINERAL RESOURCES
EL LLANO SUBSIDENCE PROJECT
LOG OF TRENCH E6H-9
FINAL 28 JUNE 1985

LOGGED BY: G. JOHNPEER, M. HEMINGWAY,
AND D. SOBROW
1-80-85

SEE ACTIVITY LOCATION MAP
FOR TRENCH LOCATION.



NOTES:

- 1) CL-CH, CLAY-WET (PROZEN), ABUNDANT ROOTS, SOFT, MODERATE PLASTICITY.
- 2) ML-CL, SILT WITH SCATTERED GRAVEL, MOIST, SOFT TO FIRM, PLATY AND LAMINATED, CONTAINS 5 INCH DIAMETER CAVITY FILLED WITH WORM CASTINGS.
- 3) SM, SILTY SAND, SCATTERED DISCONTINUOUS INTERBEDS OF SP, ML, AND CL, MOIST, LOOSE TO MEDIUM DENSE.
- 4) CL, CLAY, 1 INCH THICK, MOIST, FIRM, LOW PLASTICITY.
- 5) CL-ML, CLAY, MOIST, FIRM, LOW PLASTICITY.
- 6) SP, SAND WITH FINE TO MEDIUM GRAVEL AS BASAL LAGS, MOIST, MEDIUM DENSE.
- 7) CL, CLAY, MOIST, FIRM, LOW PLASTICITY, FLAME-LIKE STRUCTURES ON UPPER SURFACE.
- 8) CL-ML, CLAY, MOIST, FIRM, LOW PLASTICITY, SCATTERED ZONES OF REDDISH-BROWN MOTTLING, FLAME-LIKE STRUCTURES ON UNDULATORY UPPER SURFACE, PORTIONS OF LOWER SURFACE ALSO UNDULATORY.
- 9) SM-SC, SILTY SAND, MEDIUM MOIST, MEDIUM DENSE, MASSIVE WITH SCATTERED LENSES OF SP, FINE TO MEDIUM GRAVEL, AND CL, 21 INCH VERTICAL ROOT AT EAST END OF TRENCH.

NEW MEXICO BUREAU OF MINES
 AND MINERAL RESOURCES
 EL LLANO SUBSIDENCE PROJECT
 LOG OF TRENCH ESBH-10
 FINAL 28 JUNE 1965

● 10A SOIL SAMPLE LOCATION
 (SEE DATA IN APPENDIX III)

LOGGED BY G. JOHNPEER, M. HEMINGWAY AND D. LOVE
 1-24-65
 SEE ACTIVITY LOCATION MAP FOR TRENCH LOCATION

Figure 10

NOTES:

- 1) ARTIFICIAL FILL, MOIST (FROZEN), LOOSE, SCATTERED LIVE TREE ROOTS, WOOD, AND FRAGMENTS OF ORGANICS, CHARCOAL, METAL, PORCELAIN, AND GLASS.
- 2) SM, SILTY SAND, SLIGHTLY MOIST TO DRY (NOTE MOISTURE BOUNDARY), MEDIUM DENSE, ABUNDANT CRACKS AND CLAY-FILLED KROTOVINAS, SCATTERED LENSES OF CLAY, CLAYEY SILT, COARSE-GRAINED SILTY SAND, AND SANDY GRAVEL WITH COBBLES, SCATTERED CLAY STRINGERS, FINE-GRAINED GRAVEL, WOOD FRAGMENTS (POSSIBLY ROOTS), NOTE SINGLE CIRCULAR HOLE INFILLED WITH CLEAN SAND.
- 3) SP, CLEAN SAND, DRY, MEDIUM DENSE, ABUNDANT FINE LAMINATIONS OF SILT, SCATTERED CRACKS.
- 4) SM-SP, SILTY SAND, DRY, MEDIUM DENSE, DISCONTINUOUS, SCATTERED 1 TO 2 INCH INTERBEDS OF SLIGHTLY SILTY SAND, SCATTERED CRACKS.
- 5) SP, CLEAN SAND, DRY, MEDIUM DENSE, DISCONTINUOUS, WELL-LAMINATED, SCATTERED CRACKS.
- 6) CL-ML, CLAY, DRY, FIRM, LOW PLASTICITY, DISCONTINUOUS.
- 7) SM, SILTY SAND, DRY, MEDIUM DENSE, MASSIVE, SCATTERED CRACKS AND CLAY-FILLED KROTOVINAS.
- 8) SP, CLEAN SAND, DRY, MEDIUM DENSE, SINGLE CLAY LENS ON UPPER SURFACE, SCATTERED CRACKS.
- 9) CL-ML, CLAY, DRY, FIRM, LOW PLASTICITY, SCATTERED CRACKS.
- 10) SM-ML, SILTY SAND, DRY, MEDIUM DENSE, MASSIVE, SCATTERED CRACKS AND CLAY-FILLED KROTOVINAS, NOTE SINGLE ELONGATE CUT-AND-FILL STRUCTURE INFILLED BY SILTY SAND WITH GRAVEL.
- 11) SP, CLEAN SAND, DRY, MEDIUM DENSE, SCATTERED CRACKS.
- 12) SP, CLEAN SAND, DRY, MEDIUM DENSE, ABUNDANT 1 INCH INTERBEDS OF SILTY SAND, SCATTERED CRACKS, NOTE SINGLE CLAY-FILLED KROTOVINA.

 = KROTOVINA, FILLED WITH CLAY.

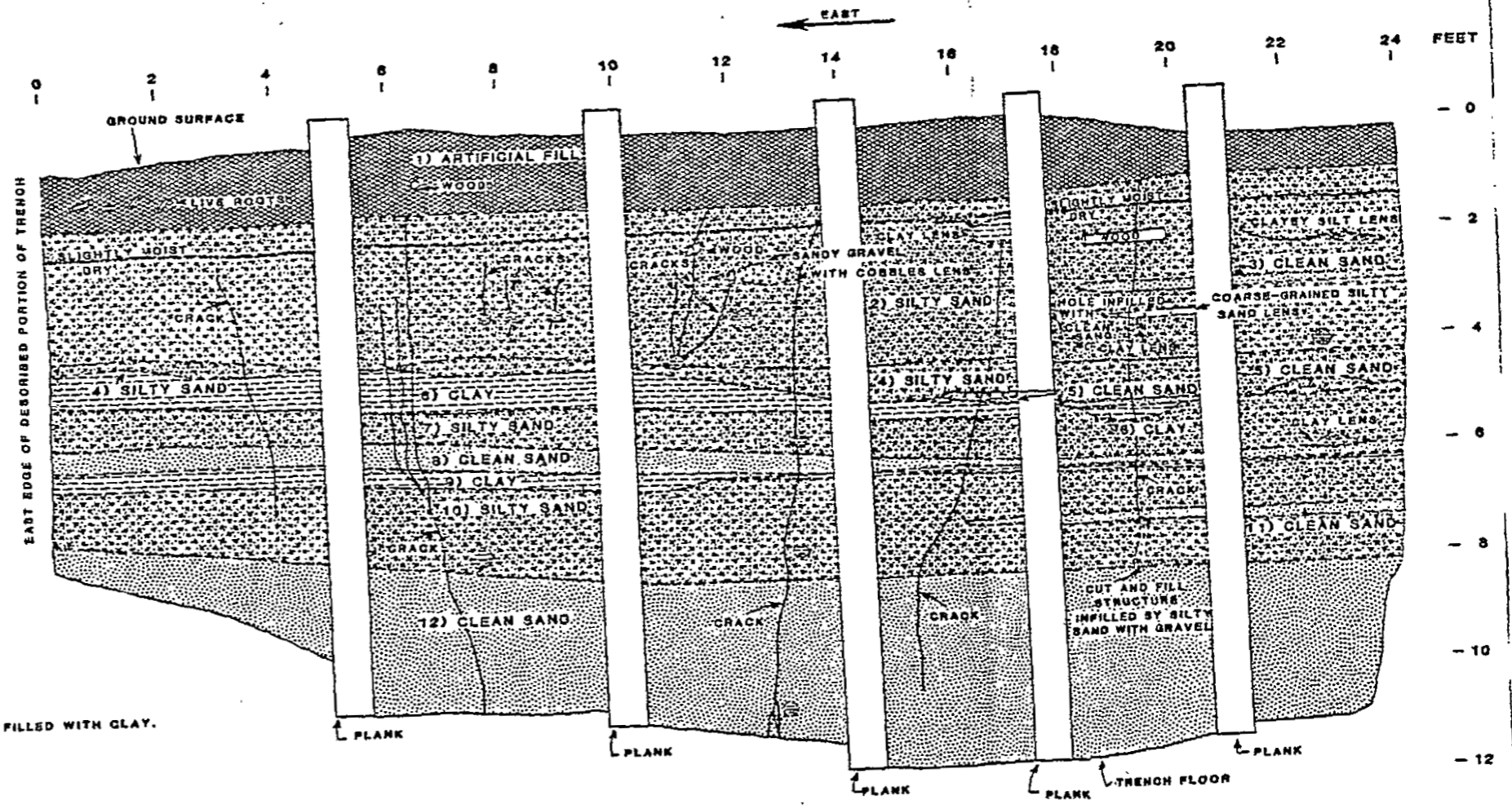


Figure 11

NEW MEXICO BUREAU OF MINES
AND MINERAL RESOURCES
EL LLANO SUBSIDENCE PROJECT
LOG OF TRENCH ESBH-11
FINAL 28 JUNE 1985

LOGGED BY G. JOHNSPER AND M. HEMINGWAY.
1-21-85
SEE ACTIVITY LOCATION MAP FOR TRENCH LOCATION

APPENDIX IV

Contour and crack maps of GGSS Areas 1-4

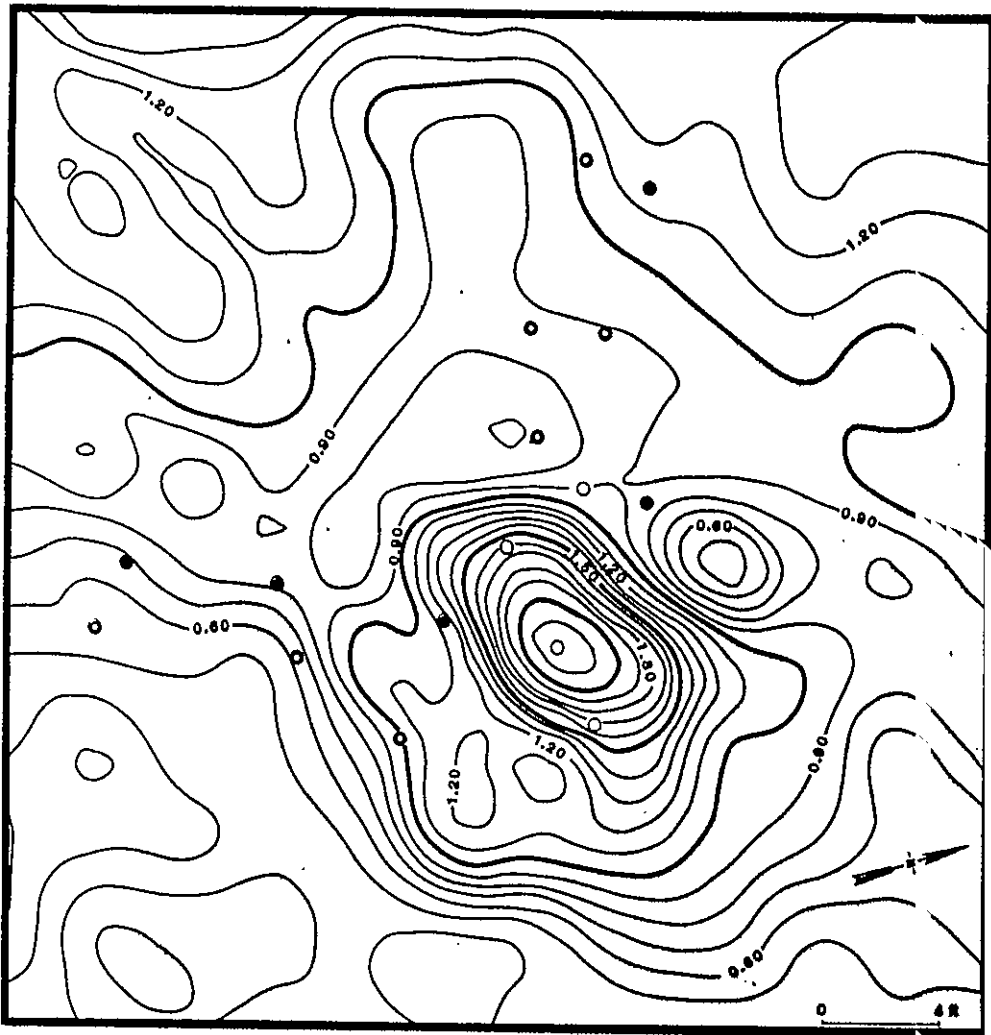


Figure 1 Contour map of GGSS-Area 1.
 Contours represent depth below datum elevation of 5733 feet.

Contour Interval 0.1 feet
 Monitoring Wells
 ○ injection and water
 ● moisture and density
 ● settlement

28 JUNE 1985

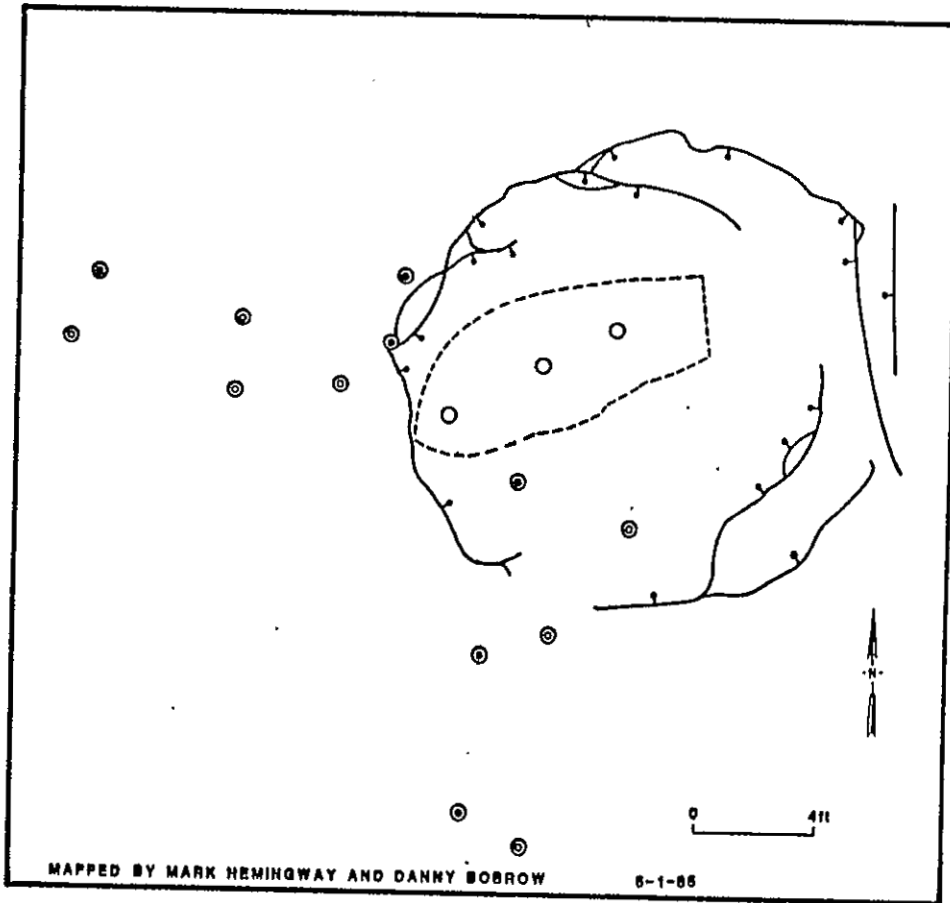







Figure 2 Crack location map of GGSS-Area 1.

28 JUNE 1985

-  Crack location with ball on downthrown side
-  Berm for ponding water
- Monitoring Well Symbols
 -  Water injection
 -  Moisture and density
 -  Settlement

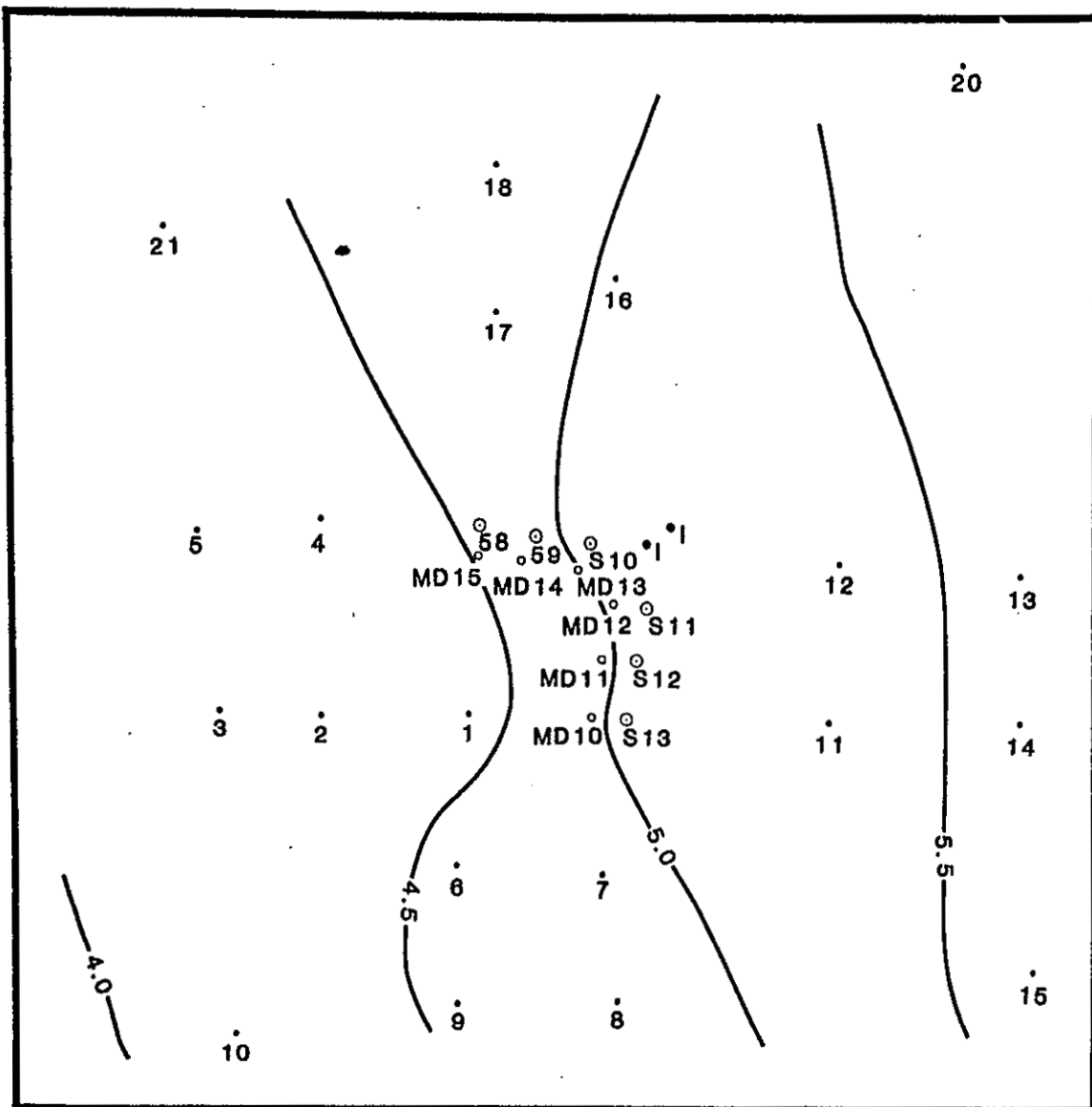
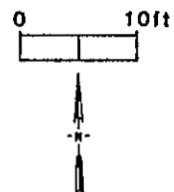


Figure 3 Detailed contour map of GGSS-Area 2.

EXPLANATION

- 4.5— 0.5 foot contour line (equal elevation)
 - S8 ○ settlement monitoring well
 - injection well
 - MD ○ moisture and density monitoring well
 - 8 • rebar control point
- Reduced from survey data obtained on 3-21-85.



See Appendix XII for location of GGSS Areas.

28 JUNE 1985

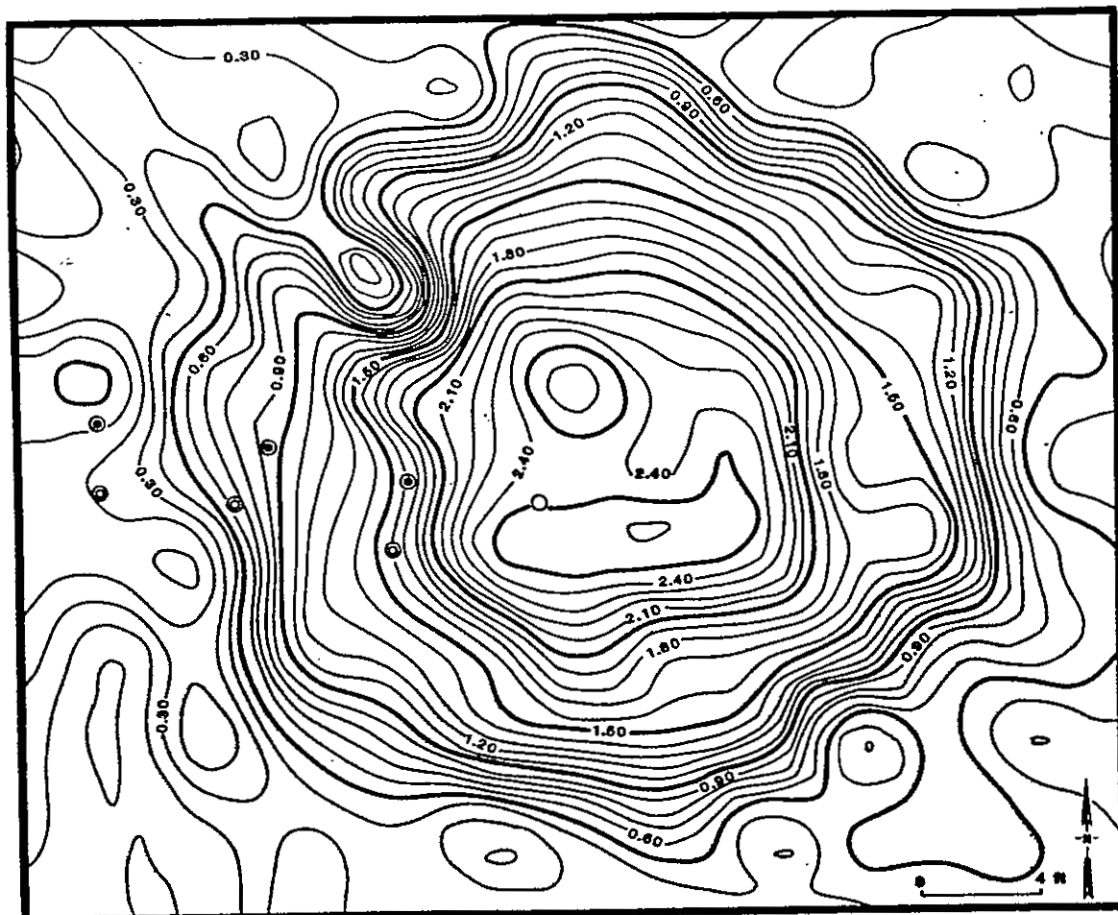


Figure 4 Contour map of GGSS-Area 3.
Contours represent depth below
datum elevation of 5733 feet.

Contour interval 0.1 feet
Monitoring Wells

- injection and water
- moisture and density
- settlement

28 JUNE 1985

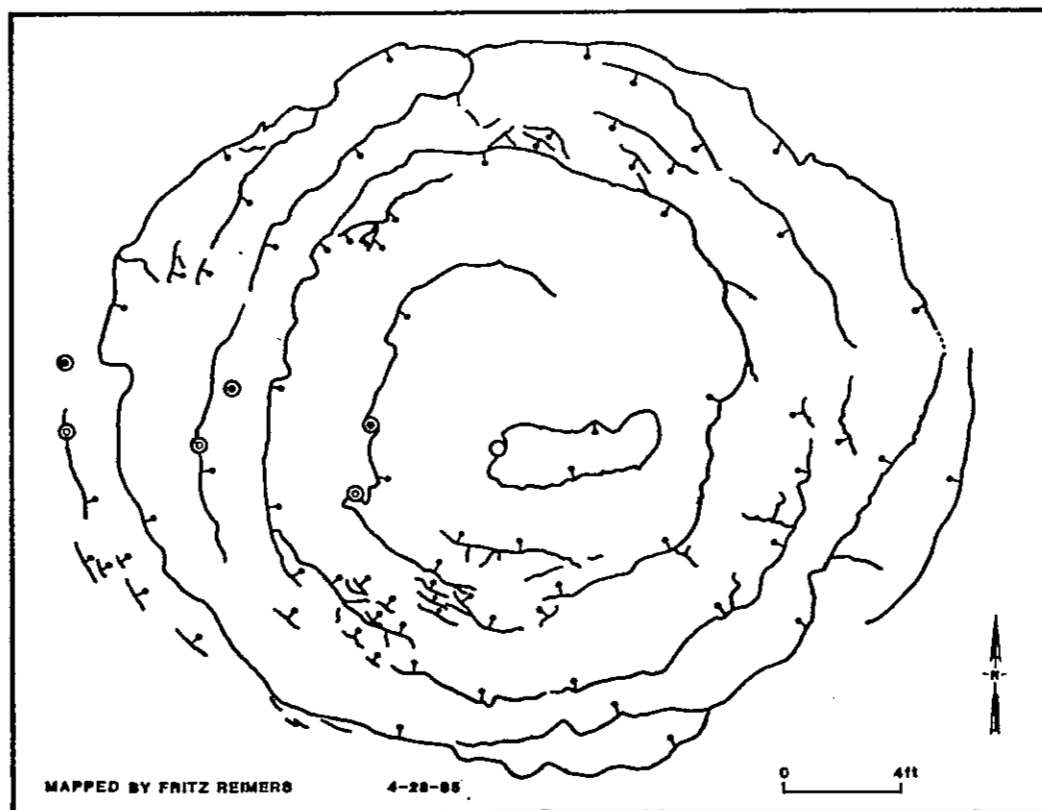


Figure 5 Crack location map
of GGSS-Area 3.

28 JUNE 1985

- Crack location with ball
on downthrown side
- Monitoring Well Symbols:
- Water Injection
 - ⊙ Moisture and density
 - ⊗ Settlement

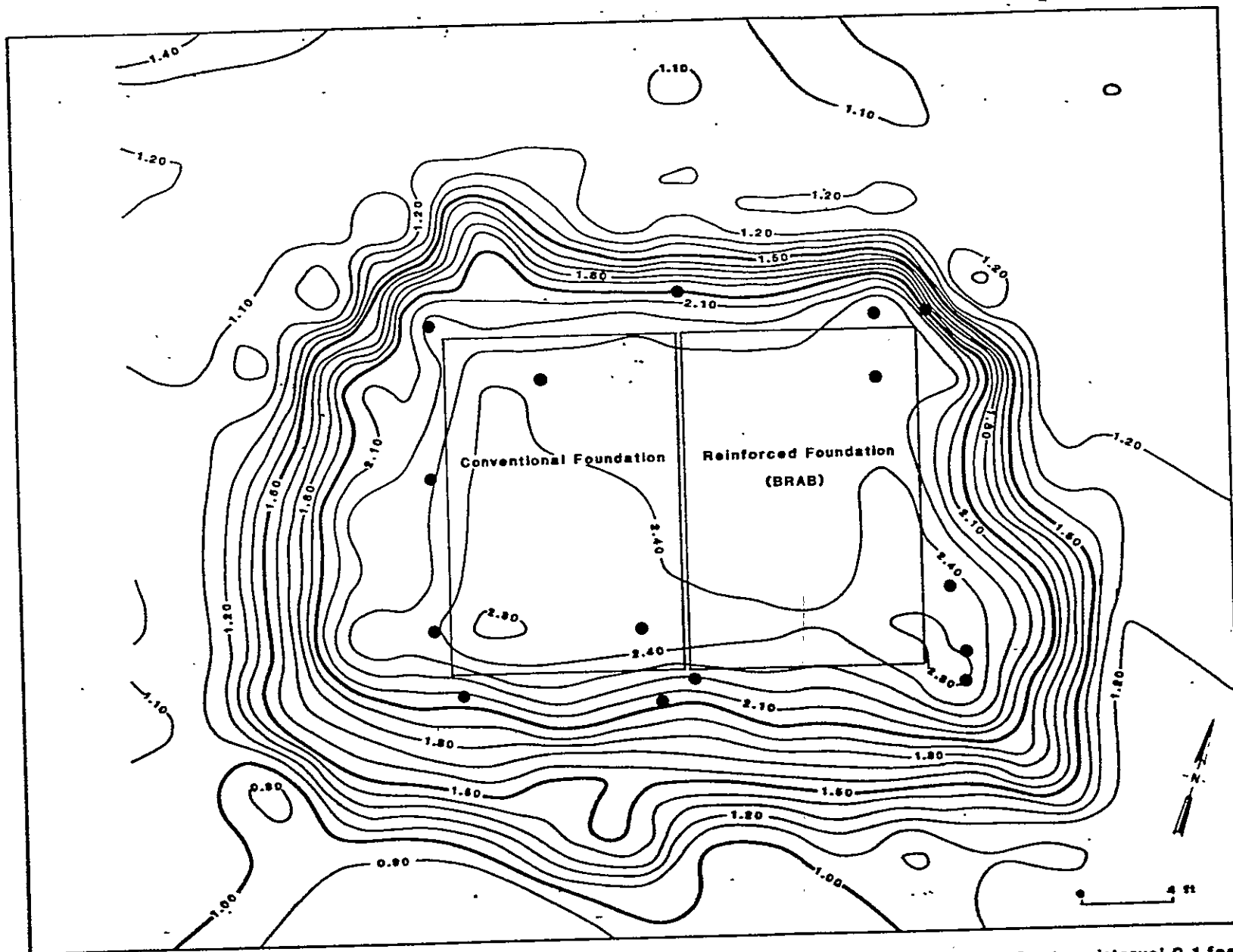


Figure 6 Contour map of GGSS-Area 4.

Contour interval 0.1 feet
 Contours represent depth below
 datum elevation of 5,734.5 feet.

● Drill Holes

28 JUNE 1985

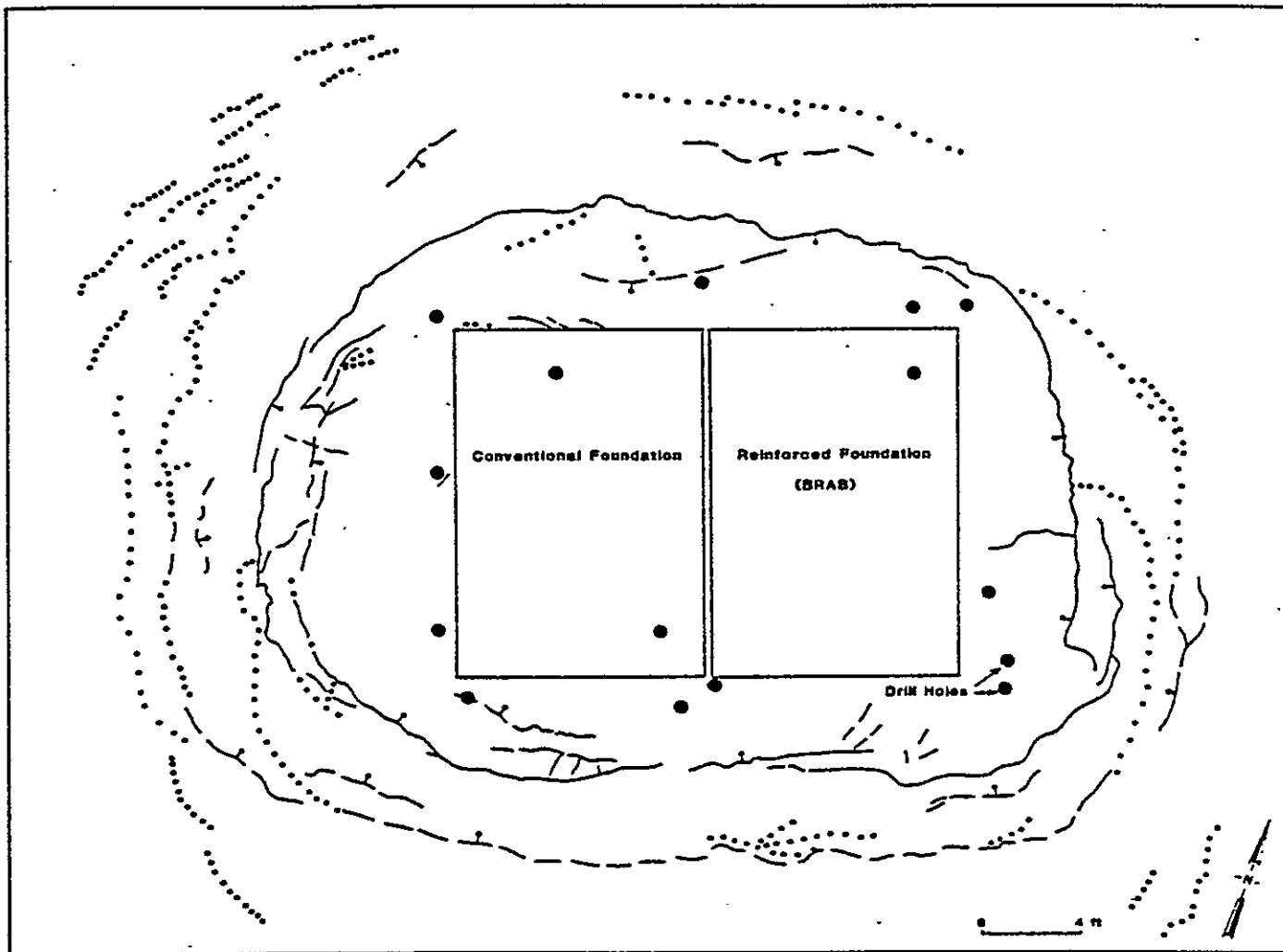


Figure 7 Crack development map of GGSS-Area 4.

28 JUNE 1985

Cracking Key

- - - May 28, 1985
- — — May 31, 1985
- · · · June 10, 1985
- · · · June 15, 1985

APPENDIX V

Pearson correlations of soil properties

	R	DEN	MC	LL	PI	GR	SAND	FINES	CLAY	CONW	CP	CONW	BC
R	1.0000 (202) P=*****	-0.1055 (202) P=.135	-0.4717 (202) P=.000	-0.7451 (201) P=.000	-0.7722 (93) P=.000	-0.2060 (202) P=.001	-0.2587 (201) P=.000	-0.5982 (202) P=.000	-0.5294 (18) P=.023	-0.1107 (11) P=.701	0.2999 (16) P=.467	-0.9691 (4) P=.018	-1.0000 (2) P=*****
DEN	-0.1055 (202) P=.135	1.0000 (370) P=*****	-0.3378 (370) P=.000	-0.3593 (283) P=.000	-0.1341 (94) P=.198	-0.1894 (348) P=.000	-0.3989 (348) P=.000	-0.5166 (348) P=.000	0.0424 (19) P=.863	-0.5293 (24) P=.008	-0.5880 (21) P=.005	-0.1927 (9) P=.618	0.8992 (5) P=.029
MC	-0.4717 (202) P=.000	-0.3378 (370) P=.000	1.0000 (830) P=*****	0.6463 (258) P=.000	0.5378 (124) P=.000	0.1381 (478) P=.003	0.2341 (474) P=.000	0.5966 (478) P=.000	-0.3783 (27) P=.051	-0.1632 (24) P=.446	-0.2468 (21) P=.280	0.3123 (9) P=.411	-0.2235 (24) P=.000
LL	-0.7451 (201) P=.000	-0.3593 (283) P=.000	0.6463 (258) P=.000	1.0000 (258) P=*****	0.9543 (124) P=.000	0.1671 (258) P=.007	0.2588 (257) P=.000	0.7236 (258) P=.000	-0.4174 (21) P=.059	0.2408 (11) P=.475	-0.1682 (10) P=.642	0.9293 (4) P=.051	-0.1655 (5) P=.227
PI	-0.7722 (93) P=.000	-0.1341 (94) P=.198	0.5378 (124) P=.000	0.9543 (124) P=.000	1.0000 (124) P=*****	0.1587 (124) P=.078	0.2286 (124) P=.011	0.5777 (124) P=.000	0.2814 (13) P=.351	0.0908 (7) P=.836	-0.3076 (6) P=.549	1.0000 (2) P=*****	-0.2805 (7) P=.126
GR	-0.2060 (202) P=.001	-0.1894 (348) P=.000	0.1381 (478) P=.003	0.1671 (258) P=.007	0.1587 (124) P=.078	1.0000 (478) P=*****	0.7247 (475) P=.000	0.2690 (478) P=.000	0.2785 (27) P=.159	-0.3255 (21) P=.137	-0.3588 (20) P=.120	0.0674 (8) P=.874	0.4064 (124) P=.000
SAND	-0.2587 (201) P=.000	-0.3989 (348) P=.000	-0.2341 (474) P=.000	0.2588 (257) P=.000	0.2286 (124) P=.011	0.7247 (475) P=.000	1.0000 (475) P=*****	0.5105 (475) P=.000	0.3048 (27) P=.122	-0.3129 (6) P=.167	-0.1969 (20) P=.405	0.1627 (5) P=.756	-0.4462 (124) P=.000
FINES	-0.5982 (202) P=.000	-0.5166 (348) P=.000	0.5966 (478) P=.000	0.7236 (258) P=.000	0.5777 (124) P=.000	0.2690 (478) P=.000	0.5105 (475) P=.000	1.0000 (478) P=*****	0.6829 (27) P=.000	0.2027 (5) P=.379	-0.0453 (20) P=.850	0.4306 (8) P=.284	-0.3823 (9) P=.000
CLAY	-0.5294 (18) P=.023	0.0424 (19) P=.863	-0.3783 (27) P=.051	0.4174 (21) P=.059	0.2814 (13) P=.351	0.2785 (27) P=.159	0.3048 (27) P=.122	0.6829 (27) P=.000	1.0000 (27) P=*****	0.0000 (6) P=1.000	-0.7220 (5) P=.155	0.1147 (3) P=.922	-0.5400 (8) P=.000
CONW	-0.1307 (11) P=.701	-0.5293 (24) P=.008	0.1632 (24) P=.446	0.2408 (11) P=.475	0.0908 (7) P=.438	-0.3355 (21) P=.137	-0.3129 (6) P=.167	0.2027 (5) P=.379	0.0000 (6) P=1.000	1.0000 (24) P=*****	0.5293 (21) P=.013	0.5248 (5) P=.278	99.0000 (0) P=*****
CP	0.2999 (16) P=.467	-0.5880 (21) P=.005	-0.2468 (21) P=.280	-0.1682 (10) P=.642	-0.3076 (6) P=.549	-0.3588 (20) P=.120	-0.1969 (20) P=.405	-0.0453 (20) P=.850	-0.2220 (5) P=.155	0.5292 (21) P=.013	1.0000 (21) P=*****	-0.3946 (5) P=.504	99.0000 (0) P=*****
CONW	-0.9694 (4) P=.018	-0.1927 (9) P=.618	0.3123 (9) P=.411	0.9293 (4) P=.051	1.0000 (2) P=*****	0.0674 (8) P=.874	0.1627 (6) P=.756	0.4306 (8) P=.284	0.1147 (3) P=.922	0.5248 (5) P=.278	-0.3946 (5) P=.504	1.0000 (2) P=*****	99.0000 (0) P=*****
BC	-1.0000 (2) P=*****	0.8992 (5) P=.029	-0.2235 (24) P=.000	-0.1655 (5) P=.227	-0.2805 (7) P=.126	-0.4064 (124) P=.000	-0.4462 (124) P=.000	-0.3823 (9) P=.000	-0.5400 (8) P=.000	99.0000 (0) P=*****	99.0000 (0) P=*****	99.0000 (0) P=*****	1.0000 (256) P=*****

(COEFFICIENT / (CASES) / SIGNIFICANCE) (A VALUE OF '99.0000' IS PRINTED IF A COEFFICIENT CANNOT BE COMPUTED)

TABLE1--Pearson correlations of the collapse ratio, R, and all other soil property values.

	R	DEN	MC	LL	PI	GR	SAND	FINES	CLAY	CONWW
R	1.0000 (202) P=*****	-0.1055 (202) P=.135	-0.4717 (202) P=.000	-0.7451 (201) P=.000	-0.7722 (93) P=.000	-0.2060 (202) P=.003	-0.2587 (201) P=.000	-0.5982 (202) P=.000	-0.5294 (18) P=.023	-0.1307 (11) P=.701
DEN	-0.1055 (202) P=.135	1.0000 (370) P=*****	-0.3378 (370) P=.000	-0.3593 (203) P=.000	-0.1341 (94) P=.198	-0.1894 (348) P=.000	-0.3989 (346) P=.000	-0.5166 (348) P=.000	0.0424 (19) P=.863	-0.5293 (24) P=.008
MC	-0.4717 (202) P=.000	-0.3378 (370) P=.000	1.0000 (630) P=*****	0.5463 (258) P=.000	0.5978 (124) P=.000	0.1381 (476) P=.003	0.2341 (474) P=.000	0.5966 (478) P=.000	0.3783 (27) P=.051	0.1632 (24) P=.446
LL	-0.7451 (201) P=.000	-0.3593 (203) P=.000	0.5463 (258) P=.000	1.0000 (258) P=*****	0.9643 (124) P=.000	0.1671 (258) P=.007	0.2588 (257) P=.000	0.7236 (258) P=.000	0.4174 (21) P=.059	0.2408 (11) P=.475
PI	-0.7722 (93) P=.000	-0.1341 (94) P=.198	0.5878 (124) P=.000	0.9643 (124) P=.000	1.0000 (124) P=*****	0.1587 (124) P=.078	0.2286 (124) P=.011	0.5777 (124) P=.000	0.2814 (13) P=.351	0.0258 (11) P=.836
GR	-0.2060 (202) P=.003	-0.1894 (348) P=.000	0.1381 (476) P=.003	0.1671 (258) P=.007	0.1587 (124) P=.078	1.0000 (478) P=*****	0.7247 (475) P=.000	0.2690 (478) P=.000	0.2785 (27) P=.159	-0.3355 (21) P=.137
SAND	-0.2587 (201) P=.000	-0.3989 (346) P=.000	0.2341 (474) P=.000	0.2588 (257) P=.000	0.2286 (124) P=.011	0.7247 (475) P=.000	1.0000 (475) P=*****	0.5105 (475) P=.000	0.3048 (27) P=.122	-0.3129 (21) P=.379
FINES	-0.5982 (202) P=.000	-0.5166 (348) P=.000	0.5966 (476) P=.000	0.7236 (258) P=.000	0.5777 (124) P=.000	0.2690 (478) P=.000	0.5105 (475) P=.000	1.0000 (478) P=*****	0.6829 (27) P=.000	0.2022 (21) P=.379
CLAY	-0.5294 (18) P=.023	0.0424 (19) P=.863	0.3783 (27) P=.051	0.4174 (21) P=.059	0.2814 (13) P=.351	0.2785 (27) P=.159	0.3048 (27) P=.122	0.6829 (27) P=.000	1.0000 (27) P=*****	0.0000 (6) P=1.000
CONWW	-0.1307 (11) P=.701	-0.5293 (24) P=.008	0.1632 (24) P=.446	0.2408 (11) P=.475	0.0968 (7) P=.836	-0.3355 (21) P=.137	-0.3129 (21) P=.167	0.2022 (21) P=.379	0.0000 (6) P=1.000	1.0000 (24) P=*****
CP	0.2599 (10) P=.467	-0.5880 (21) P=.005	-0.2468 (21) P=.280	-0.1682 (10) P=.642	-0.3076 (6) P=.549	-0.3588 (20) P=.120	-0.1969 (20) P=.405	-0.0453 (20) P=.850	-0.7220 (6) P=.155	0.5292 (21) P=.013
CONWOW	-0.9694 (4) P=.018	-0.1927 (9) P=.618	-0.3123 (8) P=.411	0.9293 (4) P=.051	1.0000 (2) P=*****	0.0674 (8) P=.874	0.1627 (6) P=.756	0.4306 (8) P=.284	0.1147 (3) P=.922	0.5248 (6) P=.278
BC	-1.0000 (2) P=*****	0.8992 (5) P=.029	-0.2235 (256) P=.000	-0.1655 (58) P=.227	-0.2805 (31) P=.126	-0.4064 (124) P=.000	-0.4462 (124) P=.000	-0.3823 (124) P=.000	-0.5400 (8) P=.163	99.0000 (0) P=*****

(COEFFICIENT / (CASES) / SIGNIFICANCE) (A VALUE OF 99.0000 IS PRINTED IF A COEFFICIENT CANNOT BE COMPUTED)

	lnR	DEN	MC	LL	PI	GR	SAND	FINES	CLAY	CONHW	CP	CONWOD	BC
lnR	1.0000 (.2021) P=*****	-0.1203 (.202) P=.078	-0.5129 (.202) P=.000	-0.8339 (.201) P=.000	-0.8534 (.201) P=.000	-0.1553 (.202) P=.011	-0.2374 (.201) P=.000	-0.6204 (.202) P=.000	-0.5647 (.18) P=.007	-0.1294 (.11) P=.353	0.2692 (.10) P=.225	-0.9401 (.9) P=.013	-1.0000 (.2) P=*****
DEN	-0.1003 (.202) P=.078	1.0000 (.370) P=*****	-0.3379 (.370) P=.000	-0.3591 (.401) P=.000	-0.1341 (.309) P=.000	-0.1394 (.300) P=.000	-0.3989 (.348) P=.000	-0.5166 (.16) P=.000	0.0424 (.24) P=.431	-0.5293 (.24) P=.004	-0.5390 (.21) P=.002	-0.1927 (.9) P=.309	0.8992 (.5) P=.015
MC	-0.5129 (.202) P=.000	-0.3379 (.370) P=*****	1.0000 (.640) P=*****	0.0463 (.258) P=.000	0.5078 (.124) P=.000	0.1381 (.490) P=.001	0.2341 (.474) P=.000	0.5906 (.27) P=.000	0.3783 (.21) P=.026	0.1632 (.11) P=.223	-0.2166 (.140) P=.140	0.5123 (.9) P=.200	-0.2735 (.256) P=.000
LL	-0.8339 (.201) P=.000	-0.3591 (.401) P=.000	0.0463 (.258) P=.000	1.0000 (.258) P=*****	0.9043 (.124) P=.000	-0.1671 (.478) P=.004	0.2588 (.250) P=.000	0.7236 (.25) P=.000	0.4174 (.21) P=.030	0.2408 (.11) P=.237	-0.1682 (.10) P=.321	0.9297 (.4) P=.025	-0.1655 (.55) P=.114
PI	-0.8534 (.201) P=.000	-0.1341 (.309) P=.000	0.0463 (.258) P=.000	0.9043 (.124) P=.000	1.0000 (.124) P=*****	0.1587 (.478) P=.005	0.2286 (.257) P=.005	0.5777 (.25) P=.000	0.2814 (.13) P=.175	0.0988 (.7) P=.418	-0.3076 (.8) P=.275	1.0000 (.2) P=*****	-0.2805 (.31) P=.063
GR	-0.1553 (.202) P=.011	-0.1394 (.300) P=.000	0.1381 (.490) P=.001	0.1671 (.478) P=.004	0.1587 (.124) P=.039	1.0000 (.478) P=*****	-0.2247 (.475) P=.000	0.2690 (.478) P=.000	0.2785 (.27) P=.040	-0.3355 (.21) P=.088	-0.3588 (.20) P=.000	0.0674 (.8) P=.437	-0.4064 (.124) P=.000
SAND	-0.2374 (.201) P=.000	-0.3989 (.348) P=.000	0.2341 (.474) P=.000	0.2588 (.250) P=.000	0.2286 (.257) P=.005	0.7247 (.475) P=.000	1.0000 (.475) P=*****	0.5105 (.27) P=.000	0.3048 (.27) P=.061	-0.3129 (.71) P=.083	-0.1909 (.29) P=.293	0.1677 (.6) P=.378	-0.4462 (.124) P=.000
FINES	-0.6204 (.202) P=.000	-0.5166 (.348) P=.000	0.5966 (.476) P=.000	0.7236 (.258) P=.000	0.5777 (.124) P=.000	0.2690 (.478) P=.000	0.5105 (.475) P=*****	1.0000 (.27) P=.000	0.6929 (.27) P=.000	0.2022 (.21) P=.190	-0.0453 (.20) P=.425	0.4306 (.8) P=.147	-0.3823 (.124) P=.000
CLAY	-0.5647 (.18) P=.007	0.0424 (.24) P=.431	0.3783 (.21) P=.026	0.4174 (.21) P=.030	0.2408 (.11) P=.237	0.2785 (.27) P=.040	0.3048 (.27) P=.061	0.6829 (.27) P=.000	1.0000 (.27) P=*****	0.0000 (.6) P=.500	-0.7220 (.5) P=.078	0.1147 (.11) P=.461	-0.5100 (.2) P=.082
CONHW	-0.1284 (.11) P=.353	-0.5293 (.24) P=.004	0.1632 (.24) P=.223	0.2408 (.11) P=.237	0.0988 (.7) P=.418	-0.3355 (.21) P=.068	-0.3129 (.21) P=.083	0.2022 (.21) P=.190	0.0000 (.6) P=.500	1.0000 (.24) P=*****	0.5292 (.21) P=.007	0.5248 (.6) P=.139	99.0000 (.0) P=*****
CP	0.2692 (.10) P=.225	-0.5889 (.21) P=.002	-0.2468 (.21) P=.140	-0.1687 (.10) P=.321	-0.3076 (.6) P=.275	-0.3588 (.20) P=.060	-0.1969 (.20) P=.203	-0.0453 (.20) P=.425	-0.7220 (.4) P=.078	0.5792 (.41) P=.007	1.0000 (.21) P=*****	-0.3946 (.5) P=.252	99.0000 (.0) P=*****
CONWOD	-0.9461 (.9) P=.018	-0.1927 (.9) P=.309	0.3123 (.9) P=.200	0.9297 (.4) P=.025	1.0000 (.2) P=*****	0.0674 (.8) P=.437	0.1627 (.6) P=.378	0.4306 (.8) P=.142	0.1147 (.11) P=.461	0.5248 (.6) P=.139	-0.3946 (.5) P=.252	1.0000 (.9) P=*****	99.0000 (.0) P=*****
BC	-1.0000 (.2) P=*****	0.8992 (.5) P=.015	-0.2735 (.256) P=.000	-0.1655 (.55) P=.114	-0.2805 (.31) P=.063	-0.4064 (.124) P=.000	-0.4462 (.124) P=.000	-0.3823 (.124) P=.000	-0.5400 (.256) P=.082	99.0000 (.0) P=*****	99.0000 (.0) P=*****	99.0000 (.0) P=*****	1.0000 (.256) P=*****

TABLE 2--Pearson correlations of the log of collapse ratio, lnR, and all other soil property values.

APPENDIX VI

Laboratory data compilation tables

Laboratory data compilation tables

Test Hole No.	Depth of Sample (ft.)	Tested By B=Bureau F=Fox H=Hay Depr	Sample Type Undisturbed Disturbed	Density (pcf) Dry	Moisture Content (%)	Atterberg Limits LL PI	Sieve Analysis (% Passing)											Clay <2µ	USCS Soil Description
							3/4"	1/2"	3/8"	No. 4	No. 10	No. 20	No. 40	No. 60	No. 80	No. 100	No. 140		
GCSSHP-10	4	B	D		3														- slightly silty sand (SP-SM)*
	14	B	D		5														- slightly silty sand (SP-SM)*
	24	B	D		5														- sand (SP-SM)* - clayey sand (SC)*
GCSSHP-11	4	B	D		3														- slightly silty sand (SP-SM)*
	14	B	D		4														- silty sand (SM)*
	24	B	D		5														- silty clayey sand (SC-SM)*
GCSSHP-12	4	B	D		5														- slightly silty sand (SP-SM)*
	14	B	D		8														- clayey sand (SC)*
	24	B	D		5														- clayey sand (SC)*
GCSSHP-13	4	B	D		4														- slightly silty sand (SP-SM)*
	14	B	D		4														- silty sand (SM)*
	24	B	D		8														- clayey sand (SC)*
GCSSHP-14	4	B	D		3														- sand (SP)*
	14	B	D		5														- silty sand (SM)*
	24	B	D		6														- silty sand (SM)*
GCSSHP-15	4	B	D		4														- slightly silty sand (SP-SM)*
	14	B	D		4														- silty sand (SM)*
	24	B	D		5														- silty sand (SM)*

* = USGS Soil description is based on field classification of soil sample; not on the limited laboratory data shown here.

Laboratory data compilation tables

Test Hole No.	Depth of Sample (ft.)	Tested By B=Bureau F=Fox H=Hy Dep't	Sample Type Undisturbed	Density (pcf) Dry	Moisture Content (%)	Atterberg Limits		Sieve Analysis (% Passing)											Clay $\leq 2\mu$	USCS Soil Description	
						LL	PI	3/4"	1/2"	3/8"	No. 4	No. 10	No. 20	No. 40	No. 60	No. 65	No. 80	No. 100			No. 140
GCSSS-17	4-6	B	U	94	6	21	1	100	100	100	95	95	94	93	86	77	68	45	23.70	2.5	silty sand (SM)
	14-16	B	U	97	4	16	NP	100	100	100	88	84	80	73	62	52	43	26	13.60	-	silty sand (SM)
	24-26	B	U	101	6	NV	NP	81	-	-	70	67	60	43	27	20	15	9	4.35	-	sand (SP)
GCSSS-18	4-6	B	U	88	7	25	5	100	100	100	100	99	98	95	87	78	67	44	23.58	3.1	silty-clayey sand (SM-SC)
	9	B	D	-	-	-	-	-	-	-	-	-	-	-	-	-	-	-	-	-	sand (SP)*
	14-16	B	U	94	6	20	NP	100	100	100	100	100	98	94	85	75	64	42	23.78	1.8	silty sand (SM)
	19	B	D	-	-	-	-	-	-	-	-	-	-	-	-	-	-	-	-	-	silty sand (SM)*
	29-31	B	U	95	8	29	7	100	100	100	100	100	99	97	87	74	63	45	31.11	6.9	clayey sand (SC)
GCSSS-19	4-6	B	U	91	6	21	1	100	100	100	100	100	99	97	90	81	71	47	24.38	-	silty sand (SM)
	9	B	D	-	-	-	-	-	-	-	-	-	-	-	-	-	-	-	-	-	sand (SP)*
	14-16	B	U	92	6	24	6	100	100	100	100	98	96	93	87	81	74	55	35.66	2.6	silty-clayey sand (SM-SC)
	24-26	B	U	92	5	16	NP	100	100	100	93	91	88	79	66	55	43	23	10.64	-	slightly silty sand (SP-SM)
	29	B	D	-	-	-	-	-	-	-	-	-	-	-	-	-	-	-	-	-	clayey sand (SC)*
GCSSS-20	4-6	B	U	101	4	20	NP	100	100	100	86	82	77	70	61	53	43	25	11.05	-	slightly silty sand (SP-SM)
	9	B	D	-	-	-	-	-	-	-	-	-	-	-	-	-	-	-	-	-	sand (SP)*
	14-16	B	U	93	5	19	NP	100	100	100	100	99	98	97	87	75	62	35	17.58	-	silty sand (SM)
	24-26	B	U	95	4	20	NP	100	100	100	100	99	97	89	72	58	46	27	13.35	-	silty sand (SM)*
	29	B	D	-	-	-	-	-	-	-	-	-	-	-	-	-	-	-	-	-	sandy clay (CL)*
GCSSS-21	4-6	B	U	94	5	19	1	100	100	100	97	96	92	83	68	56	45	26	13.80	2.1	silty sand (SM)*
	9	B	D	-	-	-	-	-	-	-	-	-	-	-	-	-	-	-	-	-	silty sand (SM)*
	14-16	B	U	98	6	20	NV	-	-	-	-	-	-	-	-	-	-	-	-	-	slightly silty sand (SP-SM)*
	24-26	B	U	94	5	19	1	100	100	100	97	96	92	83	68	56	45	26	13.80	2.1	silty sand (SM)*
	29	B	D	-	-	-	-	-	-	-	-	-	-	-	-	-	-	-	-	-	silty sand (SM)*
GCSSNP-1	4	B	D	6	-	-	-	-	-	-	-	-	-	-	-	-	-	-	-	-	silty sand (SM)*
	9	B	D	5	-	-	-	-	-	-	-	-	-	-	-	-	-	-	-	-	slightly silty sand (SP-SM)*
	14	B	D	8	-	-	-	-	-	-	-	-	-	-	-	-	-	-	-	-	silty sand (SM)*
	19	B	D	14	-	-	-	-	-	-	-	-	-	-	-	-	-	-	-	-	silty sand (SM)*
	24	B	D	18	-	-	-	-	-	-	-	-	-	-	-	-	-	-	-	-	silty sand (SM)*
GCSSNP-2	4	B	D	4	-	-	-	-	-	-	-	-	-	-	-	-	-	-	-	-	silty sand (SM)*
	9	B	D	4	-	-	-	-	-	-	-	-	-	-	-	-	-	-	-	-	silty sand (SM)*
	14	B	D	6	-	-	-	-	-	-	-	-	-	-	-	-	-	-	-	-	sand (SP)*
	19	B	D	8	-	-	-	-	-	-	-	-	-	-	-	-	-	-	-	-	slightly silty sand (SP-SM)*
	24	B	D	6	-	-	-	-	-	-	-	-	-	-	-	-	-	-	-	-	silty sand (SM)*
GCSSNP-3	4	B	D	6	-	-	-	-	-	-	-	-	-	-	-	-	-	-	-	-	silty sand (SM)*
	9	B	D	5	-	-	-	-	-	-	-	-	-	-	-	-	-	-	-	-	silty sand (SM)*
	14	B	D	5	-	-	-	-	-	-	-	-	-	-	-	-	-	-	-	-	silty sand (SM)*
	19	B	D	6	-	-	-	-	-	-	-	-	-	-	-	-	-	-	-	-	silty sand (SM)*
	24	B	D	4	-	-	-	-	-	-	-	-	-	-	-	-	-	-	-	-	silty sand (SM)*
GCSSNP-4	4	B	D	7	-	-	-	-	-	-	-	-	-	-	-	-	-	-	-	-	slightly silty sand (SP-SM)*
	9	B	D	7	-	-	-	-	-	-	-	-	-	-	-	-	-	-	-	-	slightly silty sand (SP-SM)*
	14	B	D	19	-	-	-	-	-	-	-	-	-	-	-	-	-	-	-	-	silty sand (SM)*
	19	B	D	17	-	-	-	-	-	-	-	-	-	-	-	-	-	-	-	-	clayey sand (SC)*
	24	B	D	12	-	-	-	-	-	-	-	-	-	-	-	-	-	-	-	-	clayey sand (SC)*
GCSSNP-5	4	B	D	5	-	-	-	-	-	-	-	-	-	-	-	-	-	-	-	-	silty sand (SM)*
	9	B	D	6	-	-	-	-	-	-	-	-	-	-	-	-	-	-	-	-	silty sand (SM)*
	14	B	D	6	-	-	-	-	-	-	-	-	-	-	-	-	-	-	-	-	sandy silt (MC)*
	19	B	D	6	-	-	-	-	-	-	-	-	-	-	-	-	-	-	-	-	sandy clay (CL)*
	24	B	D	7	-	-	-	-	-	-	-	-	-	-	-	-	-	-	-	-	sandy clay (CL)*
GCSSNP-6	4	B	D	-	-	-	-	-	-	-	-	-	-	-	-	-	-	-	-	-	silty sand (SM)*
	9	B	D	6	-	-	-	-	-	-	-	-	-	-	-	-	-	-	-	-	silty sand (SM)*
	14	B	D	6	-	-	-	-	-	-	-	-	-	-	-	-	-	-	-	-	sandy silt (ML)*
	19	B	D	-	-	-	-	-	-	-	-	-	-	-	-	-	-	-	-	-	sandy clay (CL)*
	24	B	D	15	-	-	-	-	-	-	-	-	-	-	-	-	-	-	-	-	sandy clay (CL)*

* * USGS Soil description is based on field classification of soil sample; not on the listed laboratory data shown here.

Laboratory data compilation tables

Test Hole No.	Depth of Sample (ft.)	Tested By B=Bureau F=Fox H=Hy Dept.	Sample Type Undisturbed Disturbed	Density (pcf) Dry	Moisture Content (%)	Atterberg Limits		Sieve Analysis (% Passing)										Clay <2µ	USCS Soil Description		
						LL	PI	3/4"	1/2"	3/8"	No. 4	No. 10	No. 20	No. 40	No. 60	No. 65	No. 80			No. 100	No. 140
GSSS-10	2-4	B	U	91	8	19	NP	100	100	100	100	100	100	98	90	77	65	41	25.18	-	silty sand (SM)
	4	B	D		6																slightly silty sand (SP-SM)*
	9-11	B	U	100	3	18	NP	100	100	100	100	100	100	98	90	76	61	32	13.25	-	silty sand (SM)
	14	B	D		3																sand (SP)*
	19-21	B	U	103	3	NV	NP	100	100	100	99	97	89	77	61	47	37	20	9.11	-	slightly silty sand (SP-SM)
	24	B	D		8																slightly silty sand (SP-SM)*
	29-31	B	U	103	9	18	NP	100	100	100	100	100	100	97	89	76	63	38	21.15	-	silty sand (SM)
	34	B	D		8																sand (SM)*
	39	B	D		8																silty sand (SM)*
44	B	D		7																sand (SP)*	
GSSS-11	2-4	B	U	94	3	23	3	100	100	100	100	100	100	98	90	78	67	45	30.95	-	silty sand (SM)
	4	B	D		9																slightly silty sand (SP-SM)*
	9-11	B	U	101	4	16	NP	100	100	100	100	99	99	97	87	70	54	25	10.44	-	slightly silty sand (SP-SM)
	14	B	D		4																sand (SP)*
	19-21	B	U	85	8	21	NP	100	100	100	99	98	97	96	84	69	51	24	7.86	-	slightly silty sand (SP-SM)
	24	B	D		4																sand (SW)*
	29-31	B	U		7	NV	NP	100	100	100	100	100	99	94	82	68	55	30	13.83	-	silty sand (SM)
34	B	D		7																sand (SW)*	
39	B	D		12																clayey sand (SC)*	
GSSS-12	2-4	B	U	79	11	32	3	100	100	100	100	100	100	98	93	86	80d	65	54.47	-	sandy silt (ML)
	4	B	D		8																clayey sand (SC)*
	9-11	B	U	101	4	18	NP	100	100	100	100	100	100	97	86	70	56	31	16.18	-	silty sand (SM)
	14	B	D		4																slightly silty sand (SP-SM)*
	19-21	B	U	105	4	NV	NP	100	100	100	86	75	62	40	18	10	6	5	2.44	-	sand (SP)
	24	B	D		6																sand (SP)*
	29-31	B	U	101	7	NV	NP	100	100	100	100	100	99	97	82	72	57	29	14.23	1.4	silty sand (SM)
34	B	D		9																sand (SP-SM)*	
39-41	B	U	96	10	20	1	100	100	100	100	100	99	97	87	73	60	36	21.11	-	silty sand (SM)	
44	B	D		8																sand (SP)*	
GSSS-13	2-4	B	U	93	4	18	NP	100	100	100	99	98	96	91	78	62	47	23	9.93	-	slightly silty sand (SP-SM)
	4	B	D		9																slightly silty sand (SP-SM)*
	9-11	B	U	96	7	20	NP	100	100	100	100	100	100	98	90	75	61	34	17.51	-	silty sand (SM)*
	14	B	D		5																sand (SP)*
	19-21	B	U	96	5	NV	NP	55	-	52	49	46	43	34	21	15	11	6	2.79	-	gravel (GP)
	24	B	D		8																sand (SP)*
	29-31	B	U	92	18	17	NP	100	100	100	98	97	95	94	81	68	54	26	10.71	-	slightly silty sand (SP-SM)
	34	B	D		10																slightly silty sand (SP-SM)*
GSSS-14	4	B	D		3																silty sand (SM)*
	9	B	D		5																silty sand (SM)*
	14	B	D		6																sand (SP)*
	19	B	D		9																silty sand (SM)*
	24	B	D		9																silty sand (SM)*
	29	B	D		7																silty sand (SM)*
34	B	D		7																sandy silt (ML)*	
GSSS-15	4	B	D		3																sand (SP)*
	9	B	D		6																silty sand (SM)*
	14	B	D		6																sand (SP)*
	19	B	D		8																silty sand (SM)*
	24	B	D		8																sandy silt (ML)*
	29	B	D		6																silty sand (SM)*
34	B	D		11																silty sand (SM)*	
GSSS-16	4	B	D		3																sand (SP)*
	9	B	D		3																silty sand (SM)*
	14	B	D		9																silty sand (SM)*
	19	B	D		7																silty sand (SM)*
	24	B	D		8																sandy silt (ML)*
	29	B	D		7																silty sand (SM)*
34	B	D		8																silty sand (SM)*	

* = USGS Soil description is based on field classification of soil sample; not on the limited laboratory data shown here.

Laboratory data compilation tables

Test Hole No.	Depth of Sample (ft.)	Tested By P=Bureau F=Fox H=Hy Dept	Sample Type Undisturbed	Density (pcf) Dry	Moisture Content (%)	Atterberg Limits		Sieve Analysis (% Passing)										Clay <2µ	USCS Soil Description					
						LL	PI	3/4"	1/2"	3/8"	4	10	20	40	60	65	80			100	140	200		
GCSSS-4	2-4	B	U	88	7																	-	silty sand (SM)*	
	4	B	D		13																		-	slightly silty sand (SP-SM)*
	9-11	B	U	86	7																		-	slightly silty sand (SP-SM)*
	14	B	D		6																		-	gravelly sand (SM)*
	19-21	B	U	92	6																		-	silty sand (SM)*
	29-31	B	U	93	8																		-	clayey silt (ML)*
	34	B	D		10																		-	silty sand (SM)*
	44	B	D		24																		-	silty clay (CL)*
GCSSS-5	2-4	B	U	86	7																		-	silty sand (SM)*
	4	B	D		7																		-	clayey sand (SC)*
	9-11	B	U	104	6	20	NP	100	100	100	99	99	98	95	87	78	68	44	21.50				-	silty sand (SM)*
	14	B	D		3																		-	sand (SM)*
	19-21	B	U	99	6	20	2	100	100	100	100	100	100	96	85	74	64	45	27.69	3.1			-	silty sandy (SM)
	24	B	D		6																		-	silty sand (SM)*
	29-31	B	U	87	7																		-	silty sand (SM)*
	34	B	D		11																		-	clayey silt (ML)*
GCSSS-6	2-4	B	U	84	8																		-	slightly silty sand (SP-SM)*
	4	B	D		11																		-	clayey sand (SC)*
	9-11	B	U	95	6																		-	sand (SP)*
	14	B	D		7																		-	sand (SP)*
GCSSS-7	2-4	B	U	89	5																		-	slightly silty sand (SP-SM)*
	4	B	D		13																		-	clayey sand (SC)*
	9-11	B	U	94	8	20	NP	100	100	100	100	99	99	97	90	82	72	48	24.77	3.9			-	silty sand (SM)
	14	B	D		7																		-	sand (SP-SM)*
	19-21	B	U	92	6																		-	silty sand (SM)*
	24	B	D		5																		-	silty sand (SM)*
	29	B	D		7																		-	sand (SP)*
	34-36	B	U	91	7	19	NP	100	100	100	100	100	100	98	90	78	68	48	31.52				-	silty sand (SM)
GCSSS-8	2-4	B	U	94	3	15	NP	100	100	100	100	100	99	98	89	74	58	30	12.95	1.5			-	slightly silty sand (SP-SM)*
	4	B	D		4																		-	sand (SP-SM)*
	9-11	B	U	102	4	13	NP	100	100	100	100	100	100	98	88	71	56	28	11.75	1.8			-	silty sand (SM)
	14	B	D		3																		-	gravelly sand (SM)*
	19-21	B	U	101	7	15	NP	100	100	100	94	93	92	87	71	54	41	21	9.52				-	slightly silty sand (SP-SM)*
	24	B	D		12																		-	silty sand (SM)*
	29-31	B	U	110	3	NV	NP	100	100	100	100	100	94	76	60	45	33	15	6.09				-	slightly silty sand (SP-SM)*
	34	B	D		12																		-	silty sand (SM)*
GCSSS-9	2-4	B	U	95	4	30	9	100	100	100	100	100	100	99	92	79	66	37	18.19				-	clayey sand (SC)
	4	B	D		4																		-	sand (SP)*
	9-11	B	U	104	3	17	NP	100	100	100	99	99	98	96	85	68	52	24	8.89				-	slightly silty sand (SP)*
	14	B	D		3																		-	silty sand (SM)
	19-21	B	U	108	6	18	NP	100	100	100	100	99	97	92	80	67	55	34	18.44	2.0			-	slightly clayey sand (SP-SM)*
	24	B	D		6																		-	silty sand (SM)
	29-31	B	U	102	9	18	NP	100	100	100	100	100	98	90	78	63	49	26	12.80				-	slightly clayey sand (SP-SM)*
	34	B	D		8																		-	silty-clayey sand (SM-SC)

* = USCS Soil description is based on field classification of soil sample; not on the limited laboratory data shown here.

Laboratory data compilation tables

Test Hole No.	Depth of Sample (ft.)	Tested By B=Bureau F=Fox H=Hy Dept	Sample Type Undisturbed Disturbed	Density (pcf) Dry	Moisture Content (%)	Atterberg Limits		Sieve Analysis (% Passing)										Clay (>2µ)	USCS Soil Description		
						LL	PI	3/4"	1/2"	3/8"	No. 4	No. 10	No. 20	No. 40	No. 60	No. 80	No. 100			No. 140	No. 200
GCSSM-7	1.5	B	D		7															- silty sand (SM)*	
	4	B	D		5															- silty sand (SM)*	
	6.5	B	D		7															- silty sand (SM)*	
	9	B	D		6															- silty sand (SM)*	
	11.5	B	D		7															- silty sand (SM)*	
	14	B	D		5															- silty sand (SM)*	
	16.5	B	D		6															- sand (SP)*	
	19	B	D		3															- gravelly sand (Sw)*	
	20.5	B	D		8															- silty sand (SM)*	
	22	B	D		6															- silty sand (SM)*	
	23.5	B	D		11															- silty sand (SM)*	
	25	B	D		14															- silty sand (SM)*	
	26.5	B	D		9															- gravelly sand (Sw)*	
	28	B	D		14															- silty sand (SM)*	
	33	B	D		22															- clayey sand (SC)*	
	38	B	D		23															- silty sand (SM)*	
	43	B	D		16															- sandy clay (CL)*	
GCSSM-8	1.5	B	D		14															- silty sand (SM)*	
	4	B	D		7															- sandy silt (ML)*	
	6.5	B	D		7															- silty sand (SM)*	
	9	B	D		6															- slightly silty sand (SP-SM)*	
	11.5	B	D		8															- sand (SP)*	
	14	B	D		5															- slightly silty sand (SP-SM)*	
	16.5	B	D		5															- silty sand (SM)*	
	19	B	D		6															- silty sand (SM)*	
	20.5	B	D		5															- sand (Sw)*	
	22	B	D		6															- sand (SP)*	
	23.5	B	D		3															- sand (SP)*	
	26	B	D		4															- sand (SP)*	
	28.5	B	D		7															- sand (SP)*	
	34	B	D		17															- silty sand (SM)*	
	36.5	B	D		14															- silty sand (SM)*	
	39	B	D		16															- silty sand (SM)*	
	41.5	B	D		27															- silty sand (SM)*	
GCSS-1	2-4	B	U	83	9	21	4	100	100	100	100	100	100	99	92	84	74	52	29.71	4.6	- silty-clayey sand (SM-SC)
	4	B	D		13																- silty sand (SM)*
	9-11	B	U	82	7	25	6	100	100	100	100	100	99	97	87	79	72	55	26.78		- silty-clayey sand (SM-SC)
	14	B	D		14																- silty sand (SM)*
	19	B	D		15																- clay (CH)*
	24	B	D		16																- clay (CH)*
	29	B	D		20																- clay (CH)*
	34	B	D		15																- clay (CH)*
	39	B	D		9																- sandy gravel (Gw)*
	44	B	D		15																- silty clay (CL)*
	49	B	D		15																- silty clay (CL)*
GCSS-2	2-4	B	U	95	11																- silty sand (SM)*
	4	B	D		7																- sandy silt (ML)*
	9-11	B	U	95	5	19	NP	100	100	100	100	100	100	97	86	75	64	40	19.87		- silty sand (SM)*
	14	B	D		7																- sand (SP)*
	19-21	B	U	92	6																- silty sand (SM)*
	24	B	D		6																- silty sand (SM)*
	29-30	B	U																		- silty sand (SM)*
	34	B	D		8																- sandy silt (ML)*
	39	B	D		13																- sandy clay (CL)*
	44	B	D		15																- silty clay (CL)*
GCSS-3	2-4	B	U	85	7																- slightly silty sand (SP-SM)*
	4	B	D		11																- sandy silt (ML)*
	9-11	B	U	91	8																- sand (SP)*
	14	B	D		5																- sand (Sw)*
	19-21	B	U	90	5																- silty sand (SM)*
	24	B	D		7																- silty sand (SM)*
	29-31	B	U	85	10																- clayey silt (ML)*
	34	B	D		10																- sandy silt (ML)*
	39	B	D		16																- sandy clay (CL)*
	44	B	D		18																- slightly silty clay (CH-CL)*

* - USCS Soil description is based on field classification of soil sample; not on the limited laboratory data shown here.

Laboratory data compilation tables

Test Hole No.	Depth of Sample (ft.)	Tested By B=Bureau F=Fox H=Hy Depr	Sample Type Undisturbed Disturbed	Density (pcf) Dry	Moisture Content (%)	Atterberg Limits LL PI	Sieve Analysis (% Passing)										Clay <2µ	USCS Soil Description
							3/4"	1/2"	3/8"	No. 4	No. 10	No. 20	No. 40	No. 60	No. 80	No. 100		
GCSSM-2	4	B	D	5														
	9	B	D	3														silty sand (SM)*
	14	B	D	4														slightly silty sand (SP-SM)*
	19	B	D	6														sand (SP)*
	24	B	D	4														sand (SP)*
	29	B	D	7														sand (SP)*
GCSSM-3	34	B	D	6														slightly silty sand (SP-SM)*
	34.3	B	D	6														silty sand (SM)*
GCSSM-3	1	B	D	14														silty sand (SM)*
	2.5	B	D	3														silty sand (SM)*
	4	B	D	6														silty sand (SM)*
	5.5	B	D	7														silty sand (SM)*
	7	B	D	7														silty sand (SM)*
	8.5	B	D	7														silty sand (SM)*
	10	B	D	7														silty sand (SM)*
	11.5	B	D	6														silty sand (SM)*
	13	B	D	9														silty sand (SM)*
	14.5	B	D	4														silty sand (SM)*
	16	B	D	7														slightly silty (SP-SM)*
	17.5	B	D	7														silty sand (SM)*
	19	B	D	6														slightly silty sand (SP-SM)*
	20.5	B	D	6														silty sand (SM)*
	22	B	D	7														silty sand (SM)*
	23.5	B	D	12														silty sand (SM)*
	25	B	D	20														silty sand (SM)*
	26.5	B	D	22														clayey sand (SC)*
28	B	D	22														silty sand (SM)*	
29.5	B	D	20														silty sand (SM)*	
31	B	D	20														silty sand (SM)*	
32.5	B	D	18														clayey sand (SC)*	
34	B	D	21														clayey sand (SC)*	
35.5	B	D	21														clayey sand (SC)*	
37	B	D	21														silty sand (SM)*	
38.5	B	D	20														sandy clay (CL)*	
GCSSM-4	4	B	D	6														clay (CH)*
	9	B	D	5														silty sand (SM)*
	14	B	D	5														silty sand (SM)*
	19	B	D	7														sand (SP)*
	21.5	B	D	7														slightly silty sand (SP-SM)*
	24	B	D	6														silty sand (SM)*
	26.5	B	D	6														silty sand (SM)*
	29	B	D	7														silty sand (SM)*
	31.5	B	D	9														silty sand (SM)*
	34	B	D	11														clayey sand (SC)*
GCSSM-5	4	B	D	7														clayey sand (SC)*
	9	B	D	7														silty sand (SM)*
	14	B	D	6														silty sand (SM)*
	19	B	D	2														silty sand (SM)*
	19.2	B	D	4														gravelly sand (SW)*
	21.5	B	D	15														slightly silty sand (SP-SM)*
	23	B	D	18														silty sand (SM)*
	24.5	B	D	24														silty sand (SM)*
	26	B	D	23														silty sand (SM)*
	27.5	B	D	21														silty sand (SM)*
	29	B	D	23														silty sand (SM)*
	30.5	B	D	23														silty sand (SM)*
32	B	D	24														silty sand (SM)*	
GCSSM-6	4	B	D	8														silty sand (SM)*
	14	B	D	5														sandy silt (ML)*
	24	B	D	7														silty sand (SM)*
	29	B	D	8														silty sand (SM)*
	34	B	D	8														sandy silt (ML)*

* * USGS Soil description is based on field classification of soil sampler, not on the limited laboratory data shown here.

Laboratory data compilation tables

Test Hole No.	Depth of Sample (ft.)	Tested By B=Bureau F=Fox H=Hwy Dept	Sample Type Undisturbed	Density (pcf) Dry	Moisture Content (%)	Atterberg Limits		Sieve Analysis (# Passing)											Clay <2µ	USCS Soil Description				
						LL	PI	3/4"	1/2"	3/8"	No. 4	No. 10	No. 20	No. 40	No. 60	No. 80	No. 100	No. 140			No. 200			
CGSSI-1	2-4	B	U	81	34	24	2	100	100	100	100	100	99	98	97	-	92	86	68	44.40	-	silty sand (SM)		
	4	B	D		6			100	100	100	100	100	97	94	86	19	-	16	14	8	3.9	-	sand (SP)	
	9-11		U	83	6	NV	NP	-	-	-	-	0	-	-	-	-	-	-	-	-	31.6	-	silty sand (SM)*	
	14	B	D		7	20	11	100	100	100	99	98	95	92	69	-	21	19	4	1.7	-	sand (SP)		
	19-21	B	U	88	6	NV	NP																silty sand (SM)*	
	24	B	D		8			100	100	100	100	100	99	95	68	-	42	38	16	7.9	-	slightly silty sand (SP-SM)*		
	29-31	B	U	85	8	NV	NP																sand (SP)*	
	34	B	D		9			100	100	100	100	100	98	84	70	-	61	53	30	14.8	-	silty sand (SM)*		
	CGSSI-2	2-4	B	U	92	3	NV	NP																silty sand (SM)*
		4	B	D		4			100	100	100	100	100	100	98	90	-	74	55	24	11.7	-	clayey sand (SC)*	
9-11			U	96	2	NV	NP	-	-	-	-	100	-	99	-	-	64	-	-	-	6.3	-	slightly silty sand (SP-SM)	
14		B	D		6			88	88	87	82	72	56	45	31	-	21	15	7	3.2	-	gravelly sand (SM)		
19-21		B	U	88	9																		clayey sand (SC)*	
24		B	D		10																		silty sand (SM)*	
29-31		B	U	105	7																			
34	B	D		6			100	100	90	84	76	64	49	30	-	19	13	6	2.6	-	gravelly sand (SM)			
CGSSI-3	0-2	B**	U																				silty sand (SM)*	
	2-4	B**	U																				sand (SP)*	
	4-6	B**	U																				gravelly sand (SM)*	
	6-8	B**	U																				silty sand (SM)*	
	8-10	B**	U																				slightly silty sand (SP-SM)	
CGSSI-4	2	B	D																				silty clayey sand (SM-SC)*	
	4	B	D																				silty sand (SM)*	
	9	B	D																				slightly silty sand (SP-SM)*	
CGSSI-5	2	B	D																				silty sand (SM)*	
	4	B	D																				gravelly sand (SM)*	
	9	B	D																				sand (SP)*	
CGSSI-6	2	B	D																				silty sand (SM)*	
	4	B	D																				sand (SP)*	
	9	B	D																				sand (SP)*	
CGSSI-7	2	B	D																				silty sand (SM)*	
	4	B	D																				slightly silty sand (SP-SM)*	
	9	B	D																				silty sand (SM)*	
CGSSI-8	4	B	D																				silty sand (SM)*	
	9	B	D																				silty sand (SM)*	
CGSSI-1	1	B	D		10																		silty sand (SM)*	
	2.5	B	D		5																		slightly silty sand (SP-SM)*	
	4	B	D		4																		slightly silty sand (SP-SM)*	
	5.5	B	D		4																		silty sand (SM)*	
	7	B	D		5																		sand (SP)*	
	8.5	B	D		6																		silty sand (SM)*	
	10	B	D		18																		silty sand (SM)*	
	11.5	B	D		7																		silty sand (SM)*	
	13	B	D		5																		sand (SM)*	
	14.3	B	D		7																		silty sand (SM)*	
	16	B	D		4																		sand (SM)*	
	17.5	B	D		4																		silty sand (SM)*	
	20.5	B	D		12																		silty sand (SM)*	
	22	B	D		10																		silty sand (SM)*	
	23.5	B	D		9																		silty sand (SM)*	
	25	B	D		11																		silty sand (SM)*	
	26.5	B	D		17																		clayey sand (SC)*	
	28	B	D		13																		slightly silty sand (SP-SM)*	
	29.5	B	D		33																		silty sand (SM)*	
	31	B	D		20																		sandy clay (CL)*	
31.8	B	D		5																		sand (SM)*		
32.5	B	D		17																		sandy clay (CL)*		
34	B	D		8																		sand (SM)*		

* = USCS Soil description is based on field classification of soil sample; not on the limited laboratory data shown here.
 ** = Analyzed by Dan Stephens and Assoc.

Laboratory data compilation tables

Test Hole No.	Depth of Sample (ft.)	Tested By B=Bureau F=Fox Heavy Dept.	Sample Type Undisturbed Disturbed	Density (pcf) Dry	Moisture Content (%)	Atterberg Limits					Sieve Analysis (% Passing)										Clay <2µ	USCS Soil Description				
						LL	PI	3/4"	1/2"	3/8"	No. 4	No. 10	No. 20	No. 40	No. 60	No. 80	No. 100	No. 140	No. 200							
ESPON-44	2-4	F	U	80	8	26	8	100	100	100	100	99	-	97	-	-	83	-	-	42.0	-	clayey sand (SC)				
	7	B	D	-	7																	-	silty sand (SM)*			
	12	B	D	-	-	1																	-	gravelly sand (SW)*		
	17-19	F	U	92	4	NV	NP	97	95	93	86	79	-	71	-	-	52	-	-	19.1	-	silty sand (SM)				
	22-24	B	U	107	4	18	NP	100	100	100	100	100	98	90	75	-	60	47	27	14.19	-	silty sand (SM)				
	27-29	F	U	99	6	16	NP	100	100	100	100	100	-	98	-	-	78	-	-	22.3	-	silty sand (SM)				
	32	B	D	-	4																		-	silty sand (SM)*		
	37	B	D	-	8																			-	silty sand (SM)*	
42	B	D	-	6																				-	silty sand (SM)*	
ESPON-45	4	B	D	-	4																			-	slightly silty sand (SP-SM)*	
	14	B	D	-	4																				-	silty sand (SM)*
	24	B	D	-	6																				-	sand (SP)*
	34	B	D	-	13																				-	silty sand (SM)*
	44	B	D	-	8																				-	sand (SP)*
	54	B	D	-	7																				-	gravelly sand (SW)*
	64	B	D	-	14																				-	slightly silty sand (SP-SM)*
	74	B	D	-	17																				-	silty sand (SM)*
84	B	D	-	22																				-	silty sand (SM)*	
99	B	D	-	21																				-	silty sand (SM)*	

* USCS Soil Description is based on field classification of soil sample; not on the limited laboratory data shown here.

Laboratory data compilation tables

Test Hole No.	Depth of Sample (ft.)	Tested By B=Bureau F=Fox H=Hy Dept	Sample Type Undisturbed Disturbed	Density (pcf) Dry	Moisture Content (%)	Atterberg Limits		Sieve Analysis (1" Passing)													Clay (%)	USCS Soil Description
						LL	PI	3/4"	1/2"	3/8"	No. 4	No. 10	No. 20	No. 40	No. 60	No. 80	No. 100	No. 140	No. 200			
ESP01-39	2-4	F	U	90	4	NV	NP	100	100	100	100	100	-	99	-	-	77	-	-	21.9	-	silty sand (SM)
	4-6	F	U	92	6	23	NP	100	100	100	100	100	-	98	-	-	87	-	-	40.4	-	silty sand (SM)
	8-10	F	U	95	3	21	NP	100	100	100	91	90	87	79	60	-	48	39	34	13.12	-	silty sand (SM)
	13-15	B	U	74	14	46	19	100	100	100	100	100	-	100	-	-	97	-	-	86.4	-	silt (ML)
	18-20	B	U	97	5	20	NP	100	100	100	100	100	100	97	78	-	62	50	28	12.43	-	silty sand (SM)
	23-25	F	U	86	10	37	14	100	100	100	100	100	-	95	-	-	83	-	-	52.4	-	sandy clay (CL)
	28-30	F	U	78	12	35	13	100	100	100	100	100	-	99	-	-	93	-	-	79.1	-	silty clay (CL)
	33	B	D	-	1	-	-	-	-	-	-	-	-	-	-	-	-	-	-	-	-	silty sand (SM)*
	38	B	D	-	5	-	-	-	-	-	-	-	-	-	-	-	-	-	-	-	-	silty sand (SM)*
	43	B	D	-	1	-	-	-	-	-	-	-	-	-	-	-	-	-	-	-	-	slightly silty sand (SP-SM)*
	48	B	D	-	2	-	-	-	-	-	-	-	-	-	-	-	-	-	-	-	-	silty sand (SM)*
	58	B	D	-	8	-	-	-	-	-	-	-	-	-	-	-	-	-	-	-	-	silty sand (SM)*
	68	B	D	-	1	-	-	-	-	-	-	-	-	-	-	-	-	-	-	-	-	silty sand (SM)*
	80	B	D	-	14	-	-	-	-	-	-	-	-	-	-	-	-	-	-	-	-	slightly silty sand (SP-SM)*
90	B	D	-	12	-	-	-	-	-	-	-	-	-	-	-	-	-	-	-	-	sand (SP)*	
100	B	D	-	-	-	-	-	-	-	-	-	-	-	-	-	-	-	-	-	-	sand (SP)*	
ESP01-40	2-4	F	U	95	6	NV	NP	100	100	100	100	-	94	-	-	57	-	-	22.6	-	silty sand (SM)	
	5-7	F	U	103	25	48	28	100	97	97	95	94	-	87	-	-	70	-	-	50.8	-	sandy clay (CL)
	9-11	B	U	89	29	59	26	100	100	100	100	100	100	100	100	-	100	100	98.51	-	clay (CH)	
	14-16	F	U	99	10	24	NP	100	100	100	100	-	88	-	-	48	-	-	25.9	-	silty sand (SM)	
	19-21	B	U	94	19	19	NP	100	100	100	100	100	95	71	57	-	42	12	16	8.36	-	slightly silty sand (SP-SM)
	24-26	F	U	88	34	82	47	100	100	100	100	100	-	100	-	-	93	-	-	84.8	-	clay (CH)
	29-31	F	U	92	32	61	30	100	100	100	100	100	-	100	-	-	99	-	-	97.8	-	clay (CH)
	34	B	D	-	18	-	-	-	-	-	-	-	-	-	-	-	-	-	-	-	-	clay (CH)*
	39	B	D	-	26	-	-	-	-	-	-	-	-	-	-	-	-	-	-	-	-	clay (CH)*
	44	B	D	-	7	-	-	-	-	-	-	-	-	-	-	-	-	-	-	-	-	clay (CH)*
	49	B	D	-	18	-	-	-	-	-	-	-	-	-	-	-	-	-	-	-	-	clay (CH)*
	50.5	B	D	-	23	-	-	-	-	-	-	-	-	-	-	-	-	-	-	-	-	clayey sand (SC)*
	ESP01-41	2-4	B	U	96	4	18	NP	100	100	100	100	97	93	84	-	66	52	28	13.02	-	silty sand (SM)*
		8-10	B	U	105	2	21	NP	100	80	-	78	74	67	56	42	33	28	19	11.60	-	slightly silty sand (SP-SM)*
18-20		B	U	91	5	32	4	100	100	100	100	100	98	89	-	82	77	69	58.15	-	sandy silty (ML)	
20		B	D	-	17	-	-	-	-	-	-	-	-	-	-	-	-	-	-	-	-	sandy clay (CL)*
28-30		B	U	95	7	18	NP	100	100	100	100	100	99	94	77	63	52	33	16.20	-	silty sand (SM)*	
38-40		B	U	87	15	39	11	100	100	100	100	100	99	94	77	85	81	71	55.81	-	silty sand (ML)	
48		B	D	-	3	-	-	-	-	-	-	-	-	-	-	-	-	-	-	-	-	silty sand (SM)*
58		B	D	-	3	-	-	-	-	-	-	-	-	-	-	-	-	-	-	-	-	silty sand (SM)*
68		B	D	-	4	-	-	-	-	-	-	-	-	-	-	-	-	-	-	-	-	silty sand (SM)*
78		B	D	-	11	-	-	-	-	-	-	-	-	-	-	-	-	-	-	-	-	silty sand (SM)*
88		B	D	-	19	-	-	-	-	-	-	-	-	-	-	-	-	-	-	-	-	slightly silty sand (SP-SM)*
98		B	D	-	16	-	-	-	-	-	-	-	-	-	-	-	-	-	-	-	-	silty sand (SM)*
108		B	D	-	-	-	-	-	-	-	-	-	-	-	-	-	-	-	-	-	-	silty clay (CL)*
ESP01-42		2-4	F	U	101	7	NV	NP	100	100	100	99	98	-	82	-	-	39	-	-	12.3	-
	5-7	B	U	90	8	21	NP	100	100	100	100	100	100	95	75	-	55	40	18	7.24	-	slightly silty sand (SP-SM)
	9-11	F	U	96	3	NV	NP	100	100	99	99	98	-	79	-	-	22	-	-	5.8	-	slightly silty sand (SP-SM)
	14-16	B	U	109	2	15	NP	100	100	100	100	99	94	74	41	27	19	10	4.67	-	sand (SP)	
	19-21	F	U	98	5	NV	NP	100	100	100	100	100	-	98	-	-	79	-	-	21.6	-	silty sand (SM)
	24-26	F	U	106	3	NV	NP	100	100	100	100	100	-	97	-	-	49	-	-	10.0	-	slightly silty sand (SP-SM)
	29	B	D	-	14	-	-	-	-	-	-	-	-	-	-	-	-	-	-	-	-	sandy clay (CL)*
	34-36	F	U	103	4	NV	NP	100	100	100	100	100	-	89	-	-	40	-	-	15.3	-	silty sand (SM)
	39-41	B	U	107	2	20	NP	100	100	100	100	100	98	81	49	34	25	15	8.88	-	slightly silty sand (SP-SM)	
	44-46	F	U	96	8	21	NP	100	100	100	100	100	-	95	-	-	65	-	-	32.4	-	silty sand (SM)
	49	B	D	-	20	-	-	-	-	-	-	-	-	-	-	-	-	-	-	-	-	slightly sandy clay (CH)*
	59	B	D	-	26	-	-	-	-	-	-	-	-	-	-	-	-	-	-	-	-	clay (CH)*
	64	B	D	-	25	-	-	-	-	-	-	-	-	-	-	-	-	-	-	-	-	sand (SP)*
	ESP01-43	2-4	F	U	92	9	NV	NP	100	100	100	99	99	-	97	-	-	71	-	-	25.9	-
4-6		F	U	91	5	16	NP	100	100	100	100	100	-	98	-	-	68	-	-	24.8	-	silty sand (SM)
8-10		B	U	101	4	17	NP	100	100	100	100	100	99	98	84	66	51	28	14.34	-	silty sand (SM)	
13-15		F	U	98	7	NV	NP	100	100	100	100	100	-	98	-	-	71	-	-	16.7	-	silty sand (SM)
18-20		F	U	103	4	NV	NP	100	100	100	100	100	-	99	-	-	50	-	-	10.5	-	slightly silty sand (SP-SM)
23-25		U	U	98	4	16	NP	85	-	80	78	76	75	72	60	44	32	14	6.40	-	slightly silty sand (SP-SM)	
28-30		F	U	95	9	17	NP	100	100	100	100	99	-	96	-	-	64	-	-	21.2	-	silty sand (SM)
33-35		F	U	99	6	NV	NP	100	100	100	100	99	-	94	-	-	71	-	-	19.9	-	silty sand (SM)
38-40		B	U	98	7	23	3	100	100	100	100	100	99	97	87	74	62	41	27.66	-	silty sand (SM)*	
40		B	D	-	6	-	-	-	-	-	-	-	-	-	-	-	-	-	-	-	-	silty sand (SM)*
41		B	D	-	2	-	-	-	-	-	-	-	-	-	-	-	-	-	-	-	-	sand (SP)*

* USCS Soil Description is based on field classification of soil sample; not on the limited laboratory data shown here.

Laboratory data compilation tables

Test Hole No.	Depth of Sample (ft.)	Tested By B=Bureau F=Fox H=Hay Dept.	Sample Type Undisturbed	Density (pcf) Dry	Moisture Content (%)	Atterberg Limits		Sieve Analysis (% Passing)											Clay <2>	USCS Soil Description				
						LL	PI	3/4"	1/2"	3/8"	No. 4	No. 10	No. 20	No. 40	No. 60	No. 80	No. 100	No. 140			No. 200			
ESPDH-33	2-4	F	U	79	11	37	10	100	100	100	100	100	100	99	-	-	97	-	-	81.2	-	slightly sandy silt (ML)		
	5-7	F	U	80	15	40	12	100	100	100	100	100	100	97	-	-	88	-	-	66.2	-	sandy silt (ML)		
	9-11	B	U	80	10	27	2	100	100	100	100	100	100	98	94	-	86	78	60	40.13	-	silty sand (SM)		
	14-16	F	U	91	5	NV	NP	100	100	100	100	100	99	-	-	-	51	-	-	21.1	-	silty sand (SM)		
	19-21	F	U	98	4	NV	NP	100	100	100	100	100	100	-	-	-	41	-	-	9.9	-	slightly silty sand (SP-SM)		
	24-26	B	U	105	7	20	NP	100	100	100	100	100	100	100	97	84	-	70	57	34	17.55	-	silty sand (SM)	
	29-31	F	U	110	7	NV	NP	100	100	100	100	100	99	-	-	-	27	-	-	9.2	-	slightly silty sand (SP-SM)		
34	B	D	-	29	-	-	-	-	-	-	-	-	-	-	-	-	-	-	-	-	-	sand (SP)*		
ESPDH-34	2-4	F	U	92	18	29	10	100	100	100	100	100	100	98	-	-	83	-	-	40.4	-	clayey sand (SC)		
	5-7	B	U	106	18	22	4	100	100	100	98	96	94	89	77	-	66	57	42	29.61	-	slightly clayey sand (SP-SC)		
	9-11	F	U	88	17	NV	NP	100	100	100	100	100	100	97	-	-	88	-	-	42.6	-	silty sand (SM)		
	14-16	F	U	94	8	19	NP	100	98	97	96	94	-	-	-	-	69	-	-	23.4	-	silty sand (SM)		
	19-21	B	U	96	9	27	3	100	100	100	100	100	100	96	89	-	82	76	58	35.54	-	silty sand (SM)		
	24	B	D	-	14	-	-	-	-	-	-	-	-	-	-	-	-	-	-	-	-	-	clayey sand (SC)*	
	29-31	F	U	101	9	17	NP	100	100	100	100	99	-	-	-	59	-	-	22.6	-	silty sand (SM)			
39-41	F	U	94	20	31	11	100	100	100	100	100	100	-	-	-	84	-	-	62.2	-	sandy clay (CL)			
ESPDH-35	2-4	F	U	94	4	23	NP	100	100	100	100	100	100	92	-	-	56	-	-	16.6	-	silty sand (SM)		
	4-6	F	U	105	3	NV	NP	100	100	100	100	100	100	88	-	-	45	-	-	12.5	-	silty sand (SM)		
	8-10	B	U	93	10	22	3	100	100	100	100	100	100	96	83	-	71	62	42	26.57	5.3	silty sand (SM)		
	13-15	F	U	75	15	40	15	100	100	100	100	100	100	-	-	-	98	-	-	88.2	-	clay (CL)		
	19	B	D	-	1	-	-	-	-	-	-	-	-	-	-	-	-	-	-	-	-	slightly silty sand (SP-SM)*		
	24	B	D	-	10	-	-	-	-	-	-	-	-	-	-	-	-	-	-	-	-	silty clay (CL)*		
	28-30	F	U	96	5	20	NP	100	100	100	100	100	100	97	-	-	79	-	-	28.3	-	silty sand (SM)		
	33-35	B	U	100	3	19	NP	100	100	100	100	100	100	98	84	-	69	43	34	15.42	-	silty sand (SM)		
	38-40	F	U	86	9	31	7	100	100	100	100	100	100	99	-	-	95	-	-	63.3	-	sandy silt (ML)		
	43-44.5	F	U	98	4	24	NP	97	97	96	96	94	-	-	-	81	-	-	60	-	23.5	-	silty sand (SM)	
48	B	D	-	4	-	-	-	-	-	-	-	-	-	-	-	-	-	-	-	-	-	slightly silty sand (SP-SM)*		
ESPDH-36	2-4	F	U	95	3	NV	NP	100	100	100	100	99	-	-	-	85	-	-	42	-	15.2	-	silty sand (SM)	
	5-7	B	U	91	11	38	12	100	100	100	100	100	100	99	96	-	92	87	77	58.42	-	clay (CL)		
	9-11	F	U	92	5	20	NP	100	100	100	100	100	100	97	-	-	72	-	-	25.1	-	silty sand (SM)		
	14-16	B	U	105	3	23	NP	100	100	100	100	100	99	89	68	-	58	53	42	25.06	4.2	silty sand (SM)		
	19-21	F	U	94	13	27	NP	100	100	100	100	100	100	91	-	-	78	-	-	36.7	-	silty sand (SM)		
	24-26	F	U	99	15	28	NP	100	100	100	100	100	100	-	-	-	88	-	-	37.1	-	silty sand (SM)		
	29	B	D	-	33	-	-	-	-	-	-	-	-	-	-	-	-	-	-	-	-	-	clay (CH)*	
	34-36	F	U	93	29	NV	NP	100	100	100	100	100	100	98	-	-	80	-	-	30.3	-	silty sand (SM)		
	39	B	D	-	17	-	-	-	-	-	-	-	-	-	-	-	-	-	-	-	-	-	clay (CH)*	
	44	B	D	-	12	-	-	-	-	-	-	-	-	-	-	-	-	-	-	-	-	-	silty sand (SM)*	
49	B	D	-	16	-	-	-	-	-	-	-	-	-	-	-	-	-	-	-	-	-	silty sand (SM)*		
ESPDH-37	2-4	F	U	102	4	18	NP	100	100	100	100	99	-	-	-	87	-	-	62	-	25.8	-	silty sand (SM)	
	4-6	F	U	91	5	NV	NP	100	100	100	99	98	-	-	-	86	-	-	58	-	24.8	-	silty sand (SM)	
	6	B	D	-	10	-	-	-	-	-	-	-	-	-	-	-	-	-	-	-	-	-	silty sand (SM)*	
	8	B	D	-	3	-	-	-	-	-	-	-	-	-	-	-	-	-	-	-	-	-	silty sand (SM)*	
	13-15	B	U	98	7	24	3	100	100	100	100	100	98	92	76	-	63	54	36	20.59	-	silty sand (SM)		
	18-20	F	U	93	6	NV	NP	100	100	100	100	100	100	-	-	-	100	-	-	87	-	27.7	-	silty sand (SM)
	21	B	D	-	1	-	-	-	-	-	-	-	-	-	-	-	-	-	-	-	-	-	slightly silty sand (SP-SM)*	
28	B	D	-	4	-	-	-	-	-	-	-	-	-	-	-	-	-	-	-	-	-	sand (SP)*		
ESPDH-38	2-4	F	U	95	18	77	45	100	100	100	100	100	100	99	-	-	83	-	-	61.4	-	silty clay (CH)		
	5-7	F	U	86	27	78	43	100	100	100	100	100	100	95	-	-	69	-	-	48.0	-	clayey sand (SC)		
	9-11	B	U	105	6	NV	NP	100	100	100	100	100	98	87	57	-	38	27	13	5.15	-	slightly silty sand (SP-SM)		
	14-16	F	U	107	6	NV	NP	100	100	100	100	100	100	89	-	-	38	-	-	9.7	-	slightly silty sand (SP-SM)		
	19-21	B	U	87	34	79	37	100	100	100	100	100	100	100	100	100	100	99	99.0	4.3	clay (CH)			
	24-26	F	U	103	19	21	NP	100	100	100	100	100	100	-	-	-	77	-	-	17.0	-	silty sand (SM)		
	29	B	D	-	35	-	-	-	-	-	-	-	-	-	-	-	-	-	-	-	-	-	slightly silty sand (SP-SM)*	
	34	B	D	-	32	-	-	-	-	-	-	-	-	-	-	-	-	-	-	-	-	-	clay (CH)*	
	39	B	D	-	28	-	-	-	-	-	-	-	-	-	-	-	-	-	-	-	-	-	clay (CH)*	
44	B	D	-	23	-	-	-	-	-	-	-	-	-	-	-	-	-	-	-	-	-	clayey sand (SC)*		

* USCS Soil Description is based on field classification of soil sample; not on the limited laboratory data shown here.

Laboratory data compilation tables

Test Hole No.	Depth of Sample (ft.)	Tested By B=Bureau F=Fox H=Hwy Dept	Sample Type Undisturbed	Density (pcf) Dry	Moisture Content (%)	Atterberg Limits			Sieve Analysis (% Passing)										Clay <2µ	USCS Soil Description														
						LL	PI	3/4"	1/2"	3/8"	No. 4	No. 10	No. 20	No. 40	No. 60	No. 80	No. 100	No. 140			No. 200													
ESP04-28	2-4	F	U	103	4	NV	NP	100	100	100	100	99	-	77	-	-	35	-	-	9.3	-	slightly silty sand (SP-SM)												
	5-7	F	U	101	2	NV	NP	100	100	180	100	98	-	51	-	-	18	-	-	5.6	-	slightly silty sand (SP-SM)												
	9-11	B	U	99	9	20	NP	100	100	100	100	100	99	91	73	-	63	56	40	24.77	-	slightly silty sand (SM)												
	14-16	F	U	87	11	NV	NP	100	100	100	100	100	-	98	-	-	84	-	-	35.1	-	slightly silty sand (SM)												
	19-21	B	U	104	2	19	NP	100	100	100	100	100	99	88	57	-	43	34	20	10.08	-	slightly silty sand (SP-SM)												
	24-26	F	U	106	3	NV	NP	100	100	100	100	99	-	74	-	-	29	-	-	-	7.8	-	slightly silty sand (SP-SM)											
	29	B	D	-	23	-	-	-	-	-	-	-	-	-	-	-	-	-	-	-	-	-	clayey silt (MH)*											
	34	B	D	-	28	-	-	-	-	-	-	-	-	-	-	-	-	-	-	-	-	-	-	clayey silt (MH)*										
	39	B	D	-	8	-	-	-	-	-	-	-	-	-	-	-	-	-	-	-	-	-	-	-	sandy clay (CH)*									
	44-46	F	U	93	20	37	16	100	100	100	100	100	-	100	-	-	99	-	-	-	-	-	-	-	slightly silty sand (SP-SM)*									
	49	B	D	-	29	-	-	-	-	-	-	-	-	-	-	-	-	-	-	-	84.1	-	-	-	slightly silty sand (SP-SM)*									
	ESP04-29	1-2.5	F	U	94	14	22	NP	100	100	100	100	100	-	97	-	-	84	-	-	-	-	-	-	-	49.9	-	slightly silty sand (SM)						
5-7.5		B	U	-	-	-	-	-	-	-	-	-	-	-	-	-	-	-	-	-	-	-	-	-	-	-	slightly silty sand (SM)							
10		B	D	-	17	-	-	-	-	-	-	-	-	-	-	-	-	-	-	-	-	-	-	-	-	-	slightly silty sand (SM)							
11-13.5		F	U	100	12	23	NP	100	100	100	100	99	-	97	-	-	72	-	-	-	-	-	-	-	-	30.1	-	slightly silty sand (SM)						
15-17.5		B	U	-	-	-	-	-	-	-	-	-	-	-	-	-	-	-	-	-	-	-	-	-	-	-	-	slightly silty sand (SM)						
20		B	D	-	19	-	-	-	-	-	-	-	-	-	-	-	-	-	-	-	-	-	-	-	-	-	-	sandy clay (CL)*						
20.5-23		F	U	105	17	29	9	100	100	100	100	100	-	88	-	-	67	-	-	-	-	-	-	-	-	-	-	sandy clay (CL)*						
25-27.5		B	U	-	-	-	-	-	-	-	-	-	-	-	-	-	-	-	-	-	-	-	-	-	-	-	-	slightly silty sand (SM)						
30-32.5		F	U	108	15	19	NP	100	100	100	100	100	-	97	-	-	75	70	-	-	-	-	-	-	-	-	-	slightly silty sand (SP-SM)*						
35		B	D	-	13	-	-	-	-	-	-	-	-	-	-	-	-	-	-	-	-	-	-	-	-	-	-	-	slightly silty sand (SM)					
35.5-38		F	U	111	13	NV	NP	100	99	98	98	97	-	89	-	-	65	-	-	-	-	-	-	-	-	-	-	-	slightly silty sand (SM)					
40-42.5		B	U	-	-	-	-	-	-	-	-	-	-	-	-	-	-	-	-	-	-	-	-	-	-	-	-	-	slightly silty sand (SM)					
45-47.5	F	U	106	11	NV	NP	100	100	100	100	100	-	87	-	-	40	35	-	-	-	-	-	-	-	-	-	-	slightly silty sand (SM)						
47.5	B	D	-	4	-	-	-	-	-	-	-	-	-	-	-	-	-	-	-	-	-	-	-	-	-	-	-	slightly silty sand (SM)						
50	B	D	-	24	-	-	-	-	-	-	-	-	-	-	-	-	-	-	-	-	-	-	-	-	-	-	-	sand (SP)*						
51-53.5	F	U	110	11	NV	NP	100	97	97	97	96	-	94	-	-	80	69	-	-	-	-	-	-	-	-	-	-	sandy clay (CL)*						
53.5-56	B	D	-	1	-	-	-	-	-	-	-	-	-	-	-	-	-	-	-	-	-	-	-	-	-	-	-	slightly silty sand (SM)						
ESP04-30	2-4	F	U	92	4	NV	NP	100	100	100	100	100	-	92	-	-	60	-	-	-	-	-	-	-	-	-	-	-	23.2	-	slightly silty sand (SM)			
	5-7	B	U	98	8	19	NP	100	100	100	100	99	98	96	85	-	70	56	31	-	-	-	-	-	-	-	-	-	15.03	-	slightly silty sand (SM)			
	9-11	F	U	84	19	57	29	100	100	100	100	100	-	98	-	-	79	-	-	-	-	-	-	-	-	-	-	-	57.9	-	sandy clay (CL)			
	14-16	F	U	89	6	24	NP	100	100	100	100	100	-	99	-	-	89	-	-	-	-	-	-	-	-	-	-	-	-	49.1	-	slightly silty sand (SM)		
	19-21	B	U	97	3	18	NP	100	96	93	87	84	81	75	62	-	51	42	24	-	-	-	-	-	-	-	-	-	-	11.51	-	slightly silty sand (SP-SM)		
	24	B	D	-	2	-	-	-	-	-	-	-	-	-	-	-	-	-	-	-	-	-	-	-	-	-	-	-	-	slightly silty sand (SM)*				
	29-31	F	U	83	14	40	17	100	100	100	100	100	-	99	-	-	95	-	-	-	-	-	-	-	-	-	-	-	-	74.8	-	slightly clay (CL)		
	34-36	F	U	103	3	17	NP	100	100	100	99	98	-	85	-	-	61	-	-	-	-	-	-	-	-	-	-	-	-	18.3	-	slightly silty sand (SM)		
	39	B	D	-	1	-	-	-	-	-	-	-	-	-	-	-	-	-	-	-	-	-	-	-	-	-	-	-	-	-	gravelly sand (Sw)*			
	ESP04-31	1-2.5	F	U	84	21	55	27	100	100	100	100	100	-	100	-	-	96	-	-	-	-	-	-	-	-	-	-	-	-	80.1	-	slightly silty clay (CL)	
		5-7.5	B	U	-	-	-	-	-	-	-	-	-	-	-	-	-	-	-	-	-	-	-	-	-	-	-	-	-	-	-	slightly silty sand (SM)*		
		10-12.5	F	U	103	5	NV	NP	100	100	100	100	100	-	97	-	-	70	-	-	-	-	-	-	-	-	-	-	-	-	20.9	-	slightly silty sand (SM)	
15-17.5		F	U	113	2	NV	NP	100	97	97	91	86	-	50	-	-	21	-	-	-	-	-	-	-	-	-	-	-	-	-	8.3	-	slightly silty sand (SP-SM)	
20-22.5		F	U	105	17	44	22	100	100	100	100	100	-	99	-	-	92	-	-	-	-	-	-	-	-	-	-	-	-	-	66.7	-	slightly silty clay (CL)	
25-27.5		B	U	-	-	-	-	-	-	-	-	-	-	-	-	-	-	-	-	-	-	-	-	-	-	-	-	-	-	-	slightly silty sand (SM)*			
30-32.5		F	U	107	5	NV	NP	100	100	100	99	98	-	90	-	-	44	-	-	-	-	-	-	-	-	-	-	-	-	-	14.1	-	slightly silty sand (SM)	
33		B	D	-	4	NV	NP	100	100	100	100	100	100	95	80	-	64	-	-	-	-	-	-	-	-	-	-	-	-	-	13.9	-	slightly silty sand (SM)	
39-41		F	U	103	6	NV	NP	100	100	100	100	99	-	79	-	-	33	-	-	-	-	-	-	-	-	-	-	-	-	-	-	13.1	-	slightly silty sand (SM)
49-51		F	U	105	5	NV	NP	100	97	95	94	91	-	67	-	-	31	-	-	-	-	-	-	-	-	-	-	-	-	-	-	8.4	-	slightly silty sand (SP-SM)
59		B	D	-	-	-	-	-	-	-	-	-	-	-	-	-	-	-	-	-	-	-	-	-	-	-	-	-	-	-	-	slightly silty sand (SM)*		
69		B	D	-	6	NV	NP	100	100	100	100	100	93	71	50	-	39	32	20	-	-	-	-	-	-	-	-	-	-	-	-	10.9	-	slightly silty sand (SP-SM)
79	B	D	-	24	32	12	100	100	100	100	100	98	90	72	-	59	50	38	-	-	-	-	-	-	-	-	-	-	-	-	29.1	-	clayey sand (SC)	
89	B	D	-	18	NV	NP	100	100	100	100	100	99	95	86	-	74	61	36	-	-	-	-	-	-	-	-	-	-	-	-	18.5	-	slightly silty sand (SM)	
99	B	D	-	17	20	NP	100	100	100	100	98	93	83	70	-	61	55	42	-	-	-	-	-	-	-	-	-	-	-	-	30.6	-	slightly silty sand (SM)	
109	B	D	-	24	-	-	-	-	-	-	-	-	-	-	-	-	-	-	-	-	-	-	-	-	-	-	-	-	-	-	-	sandy clay (CL)*		
109.5	B	D	-	15	NV	NP	69	66	66	45	35	29	22	15	-	12	10	8	-	-	-	-	-	-	-	-	-	-	-	-	5.8	-	gravelly sand (Sw)	
ESP04-32	2-4	F	U	83	6	28	4	100	100	100	100	100	-	98	-	-	93	-	-	-	-	-	-	-	-	-	-	-	-	-	53.6	-	sandy silt (ML)	
	5-7	B	U	94	4	19	NP	100	100	100	100	100	98																					

Laboratory data compilation tables

Test Hole No.	Depth of Sample (ft.)	Tested By B=Bureau F=Fox H=Hy Dept	Sample Type Undisturbed Disturbed	Density (pcf) Dry	Moisture Content (%)	Atterberg Limits					Sieve Analysis (% Passing)										USCS Soil Description	
						LL	PI	3/4"	1/2"	3/8"	No. 4	No. 10	No. 20	No. 40	No. 60	No. 80	No. 100	No. 140	No. 200	Clay <2μ		
ESPCH-24	2-4	F	U	82	10	28	7	100	100	100	100	100	100	100	-	95	-	-	65.9	-	sandy silt (ML)	
	5-7	B	U	93	4	18	NP	100	100	100	99	99	99	95	80	64	51	29	15.52	-	silty sand (SM)	
	9-11	F	U	72	18	58	28	100	100	100	100	100	-	99	-	-	93	-	-	67.7	-	silty sand (CL)
	14-16	F	U	99	3	NV	NP	100	100	100	100	99	-	83	-	-	27	-	-	5.6	-	slightly silty sand (SP-SM)
	19-21	B	U	87	13	29	10	100	100	100	100	100	100	83	-	-	72	63	45	26.77	-	clayey sand (SC)
	24-26	F	U	103	2	NV	NP	100	98	98	97	96	-	83	-	-	49	-	-	13.7	-	silty sand (SM)
	26	B	D	-	1	-	-	-	-	-	-	-	-	-	-	-	-	-	-	-	-	sand (SP)
	34-36	F	U	95	4	NV	NP	100	100	100	100	99	-	93	-	-	64	-	-	23.7	-	silty sand (SM)
	ESPCH-25	1	B	D	-	14	-	-	-	-	-	-	-	-	-	-	-	-	-	-	-	silty sand (SM)*
5		B	D	-	4	-	-	-	-	-	-	-	-	-	-	-	-	-	-	-	silty sand (SM)*	
8		B	D	-	1	-	-	-	-	-	-	-	-	-	-	-	-	-	-	-	sand (SP)*	
14		B	D	-	2	-	-	-	-	-	-	-	-	-	-	-	-	-	-	-	slightly silty sand (SP-SM)*	
15-17		F	U	117	3	NV	NP	97	95	93	88	79	-	48	-	-	22	20	-	10.7	-	slightly silty sand (SP-SM)
17		B	D	-	1	-	-	-	-	-	-	-	-	-	-	-	-	-	-	-	silty sand (SM)*	
20-22.5		B	U	-	-	-	-	-	-	-	-	-	-	-	-	-	-	-	-	-	silty sand (SM)*	
22.5		B	D	-	1	-	-	-	-	-	-	-	-	-	-	-	-	-	-	-	silty sand (SM)*	
25-27.5		F	U	102	4	20	NP	100	100	99	98	96	-	84	-	-	60	-	-	22.2	-	silty sand (SM)
27.5		B	D	-	3	-	-	-	-	-	-	-	-	-	-	-	-	-	-	-	sand (SP)*	
30-32.5		F	U	96	4	NV	NP	100	100	100	100	100	-	96	-	-	80	-	-	22.8	-	silty sand (SM)
32.5		B	D	-	1	-	-	-	-	-	-	-	-	-	-	-	-	-	-	-	silty sand (SM)*	
35-37.5		B	U	-	-	-	-	-	-	-	-	-	-	-	-	-	-	-	-	-	silty sand (SM)*	
37.5		B	D	-	1	-	-	-	-	-	-	-	-	-	-	-	-	-	-	-	silty sand (SM)*	
40-42.5		F	U	114	3	NV	NP	98	97	97	95	92	-	74	-	-	48	-	-	17.4	-	silty sand (SM)
42.5		B	D	-	1	-	-	-	-	-	-	-	-	-	-	-	-	-	-	-	silty sand (SM)*	
45-47.5		F	U	105	7	NV	NP	100	100	100	100	100	-	100	-	-	86	67	-	22.9	-	silty sand (SM)
47.5		B	D	-	4	-	-	-	-	-	-	-	-	-	-	-	-	-	-	-	-	slightly silty sand (SP-SM)*
50-52.5		B	U	-	-	-	-	-	-	-	-	-	-	-	-	-	-	-	-	-	-	silty sand (SM)*
52.5		B	D	-	4	-	-	-	-	-	-	-	-	-	-	-	-	-	-	-	-	slightly silty sand (SP-SM)*
60-62.5		F	U	115	3	NV	NP	100	100	100	100	100	-	97	-	-	61	-	-	23.5	-	silty sand (SM)
62.5	B	D	-	3	-	-	-	-	-	-	-	-	-	-	-	-	-	-	-	-	silty sand (SM)*	
65-67	F	U	115	2	NV	NP	100	100	100	100	100	-	86	-	-	47	-	-	18.9	-	silty sand (SM)	
67.5	B	D	-	2	-	-	-	-	-	-	-	-	-	-	-	-	-	-	-	-	silty sand (SM)*	
80	B	D	-	10	-	-	-	-	-	-	-	-	-	-	-	-	-	-	-	-	silty sand (SM)*	
90	B	D	-	2	-	-	-	-	-	-	-	-	-	-	-	-	-	-	-	-	sand (SP)*	
100	B	D	-	12	-	-	-	-	-	-	-	-	-	-	-	-	-	-	-	-	sand (SP)*	
110	B	D	-	15	-	-	-	-	-	-	-	-	-	-	-	-	-	-	-	-	slightly silty sand (SP-SM)*	
120	B	D	-	19	-	-	-	-	-	-	-	-	-	-	-	-	-	-	-	-	sandy gravel (Gh)*	
ESPCH-26	2-4	F	U	95	9	20	NP	100	100	100	100	100	-	96	-	-	78	-	-	29.4	-	silty sand (SM)
	5-7	B	U	86	16	24	5	100	100	100	100	100	100	98	90	82	73	54	34.11	-	silty clayey sand (SM-SC)	
	9-11	F	U	93	8	32	11	100	100	100	100	100	-	97	-	-	87	-	-	53.3	-	sandy silt (ML)
	14-16	B	U	98	2	17	NP	100	100	100	96	95	90	72	43	-	29	22	12	5.78	-	slightly silty sand (SP-SM)
	19-21	F	U	96	5	19	NP	100	98	97	94	92	-	84	-	-	64	-	-	30.3	-	silty sand (SM)
	24-26	F	U	103	2	NV	NP	100	100	100	99	98	-	70	-	-	26	-	-	5.5	-	slightly silty sand (SP-SM)
	29	B	D	-	1	-	-	-	-	-	-	-	-	-	-	-	-	-	-	-	-	silty sand (SM)*
ESPCH-27	1-2.0	F	U	90	6	22	NP	100	100	100	100	100	-	95	-	-	58	49	-	21.7	-	silty sand (SM)
	2-4.5	F	U	94	2	NV	NP	100	100	100	100	100	-	96	-	-	67	-	-	20.0	-	silty sand (SM)
	5-7.5	B	U	-	-	-	-	-	-	-	-	-	-	-	-	-	-	-	-	-	silty sand (SM)*	
	10	B	D	-	8	-	-	-	-	-	-	-	-	-	-	-	-	-	-	-	-	silt (ML)*
	10.5-12	F	U	88	20	NV	NP	100	99	98	98	98	-	87	-	-	38	27	-	10.3	-	slightly silty sand (SP-SM)
	16-18.5	B	U	-	-	-	-	-	-	-	-	-	-	-	-	-	-	-	-	-	-	silty sand (SM)*
	18.5	B	D	-	9	-	-	-	-	-	-	-	-	-	-	-	-	-	-	-	-	silty sand (SM)*
	20	B	D	-	10	-	-	-	-	-	-	-	-	-	-	-	-	-	-	-	-	silty sand (SM)*
	20.5-23	F	U	109	13	20	NP	100	100	100	100	99	-	92	-	-	71	-	-	36.1	-	silty sand (SM)
	23	B	D	-	1	-	-	-	-	-	-	-	-	-	-	-	-	-	-	-	-	slightly silty sand (SP-SM)*
	25-28	F	U	98	20	33	11	100	100	100	100	99	-	95	-	-	86	-	-	58.1	-	sandy clay (CL)
	28	B	D	-	9	-	-	-	-	-	-	-	-	-	-	-	-	-	-	-	-	silty sand (SM)*
	30-31.5	B	U	-	-	-	-	-	-	-	-	-	-	-	-	-	-	-	-	-	-	silty sand (SM)*
	31.5	B	D	-	6	-	-	-	-	-	-	-	-	-	-	-	-	-	-	-	-	silty sand (SM)*
	35.5	B	D	-	11	-	-	-	-	-	-	-	-	-	-	-	-	-	-	-	-	clayey sand (SC)*
	36-38.5	F	U	102	5	NV	NP	100	100	100	100	100	-	91	-	-	54	-	-	18.6	-	silty sand (SM)
	38.5	B	D	-	1	-	-	-	-	-	-	-	-	-	-	-	-	-	-	-	-	slightly silty sand (SP-SM)*
	40-42.5	F	U	110	3	NV	NP	100	100	100	98	97	-	79	-	-	45	-	-	16.4	-	silty sand (SM)
42.5	B	D	-	3	-	-	-	-	-	-	-	-	-	-	-	-	-	-	-	-	silty sand (SM)*	
45	B	D	-	3	-	-	-	-	-	-	-	-	-	-	-	-	-	-	-	-	silty sand (SM)*	
45.5-48	F	U	106	3	NV	NP	100	100	100	100	100	-	93	-	-	52	-	-	18.8	-	silty sand (SM)	
48	B	D	-	4	-	-	-	-	-	-	-	-	-	-	-	-	-	-	-	-	silty sand (SM)*	

* USCS Soil Description is based on field classification of soil sample; not on the limited laboratory data shown here.

Laboratory data compilation tables

Test Hole No.	Depth of Sample (ft.)	Tested By	Sample Type	Density (pcf)	Moisture Content (%)	Atterberg Limits	Sieve Analysis (% Passing)													Clay <2µ	USCS Soil Description	
							LL	PI	3/4"	1/2"	3/8"	No. 4	No. 10	No. 20	No. 40	No. 60	No. 65	No. 80	No. 100			No. 140
ESPOH-18	2-4	F	U	87	9	31 12	100	100	100	99	98	-	90	-	-	71	-	-	42.0	-	very clayey sand (SC)	
	5-7	B	U	102	2	19 NP	100	100	100	94	93	92	86	70	58	49	31	16.00	2.3	silty sand (SM)		
	9	B	D	-	12	100	100	100	100	99	91	81	73	-	67	63	53	41.8	-	clayey sand (SC)*		
	14-16	F	U	94	9	NV NP	100	100	100	100	100	-	97	-	82	-	-	29.4	-	silty sand (SM)		
	19	B	D	-	7	100	100	100	100	100	100	100	96	80	66	55	32	15.5	-	clayey sand (SC)*		
	24-26	F	U	95	8	NV NP	100	100	100	100	100	-	99	-	78	-	-	20.1	-	silty sand (SM)		
	29	B	D	-	13	100	100	100	100	100	100	100	89	75	65	58	43	30.1	-	silty sand (SM)*		
ESPOH-19	1.5-4	F	U	112	14	27 7	100	100	100	100	100	-	96	-	-	69	-	-	36.5	-	clayey sand (SC)	
	7.5-10	B	U	-	-	-	-	-	-	-	-	-	-	-	-	-	-	-	-	-	silty sand (SM)*	
	12.5-15	F	U	104	3	NV NP	-	-	-	100	100	-	96	-	-	64	-	-	21.7	-	silty sand (SM)	
	17.5-20	F	U	112	5	18 NP	100	100	100	100	99	-	88	-	-	54	-	-	20.3	-	silty sand (SM)	
	22.5-25	B	U	-	-	-	-	-	-	-	-	-	-	-	-	-	-	-	-	-	silty sand (SM)*	
	27.5-30	F	U	98	5	NV NP	100	100	100	100	100	-	93	-	-	67	-	-	19.8	-	silty sand (SM)	
	32.5-35	F	U	113	5	NV NP	-	-	-	-	-	-	100	-	97	-	-	20.1	-	silty sand (SM)		
	37.5-40	B	U	-	-	-	-	-	-	-	-	-	-	-	-	-	-	-	-	-	slightly silty sand (SP-SM)*	
	42.5-45	F	U	107	7	NV NP	100	100	100	100	100	-	94	-	-	42	-	-	11.7	-	slightly silty sand (SP-SM)	
	47.5-50	F	U	115	17	NV NP	-	-	-	100	99	-	78	-	-	44	-	-	14.0	-	silty sand (SM)	
	52.5-55	F	U	124	14	NV NP	100	99	99	98	97	-	71	-	-	15	-	-	11.4	-	slightly silty sand (SP-SM)	
	55	B	D	-	13	NV NP	100	100	100	85	80	69	53	36	-	27	22	15	9.7	-	slightly silty sand (SP-SM)	
ESPOH-20	2-4	F	U	108	21	NV NP	100	100	100	100	99	-	94	-	-	68	-	-	30.1	-	silty sand (SM)	
	5-7	F	U	98	12	NV NP	100	100	100	100	100	-	99	-	-	83	-	-	26.8	-	silty sand (SM)	
	9-11	B	U	79	37	38 14	100	100	100	100	100	100	99	97	92	99	97	92	71.86	-	slightly sandy clay (CL)	
	14-16	F	U	102	8	NV NP	100	100	99	99	98	-	83	-	-	49	-	-	8.7	-	slightly silty sand (SP-SM)	
	19-21	B	U	101	14	16 NP	100	100	100	100	100	98	91	72	57	46	26	12.45	-	silty sand (SM)		
	24	B	D	-	9	100	100	100	100	100	98	92	79	-	67	56	36	19.1	-	silty sand (SM)*		
	34-36	F	U	108	7	NV NP	100	100	100	100	89	-	83	-	-	42	-	-	13.3	-	silty sand (SM)	
	49-51	F	U	109	4	NV NP	100	100	99	99	98	-	68	-	-	26	-	-	7.7	-	slightly silty sand (SP-SM)	
ESPOH-21	1	B	D	-	14	29 9	100	100	100	100	100	98	92	84	-	76	69	52	32.1	-	clayey sand (SC)	
	5	B	D	-	10	36 12	100	100	100	100	100	98	90	77	-	70	64	52	38.0	-	silty sand (SM)	
	8	B	D	-	2	18 NP	100	100	100	85	83	82	77	61	-	47	37	23	13.3	-	silty sand (SM)	
	14	B	D	-	15	100	100	100	100	99	98	93	87	-	83	80	67	45.2	-	silty sand (SM)		
	14.5	F	D	-	-	-	-	-	-	-	-	-	-	-	-	-	-	-	-	-	sandy clay (CL)*	
	15-17.5	B	U	-	-	-	-	-	-	-	-	-	-	-	-	-	-	-	-	-	silty sand (SM)*	
	22.5-25	F	U	107	3	NV NP	100	100	100	100	100	-	96	-	-	76	57	-	17.9	-	silty sand (SM)	
	27.5-30	F	U	109	7	18 NP	100	100	100	100	99	-	94	-	-	72	-	-	29.9	-	silty sand (SM)	
	30-32.5	B	U	-	-	-	-	-	-	-	-	-	-	-	-	-	-	-	-	-	silty sand (SM)*	
	37.5-40	F	U	109	6	NV NP	100	100	100	100	100	-	95	-	-	60	45	-	14.3	-	silty sand (SM)	
	44-45	F	U	102	14	NV NP	100	100	99	98	98	-	85	-	-	47	-	-	21.1	-	silty sand (SM)	
	47	B	D	-	24	18 NP	100	100	100	98	98	97	87	64	-	48	38	23	13.1	-	silty sand (SM)	
	47.5-50	F	U	125	5	NV NP	100	100	100	100	99	-	85	-	-	40	34	-	12.5	-	silty sand (SM)	
ESPOH-22	2-4	F	U	90	8	NV NP	100	100	100	100	100	-	96	-	-	74	-	-	32.0	-	silty sand (SM)	
	5-7	B	U	93	6	20 NP	100	100	100	100	100	100	99	91	-	87	74	47	25.62	-	silty sand (SM)	
	9-11	F	U	94	4	NV NP	100	100	100	100	100	-	86	-	-	56	-	-	21.2	-	silty sand (SM)	
	14-16	B	U	86	17	32 11	100	100	100	100	100	99	91	68	-	56	49	38	28.75	-	clayey sand (SC)	
	19-21	F	U	90	11	32 13	100	100	100	100	100	-	96	-	-	84	-	-	45.2	-	clayey sand (SC)	
	24	B	D	-	11	100	100	100	100	100	100	98	91	81	-	75	70	59	46.2	-	silty sand (SM)*	
	29-31	F	U	89	6	NV NP	100	100	100	100	100	-	99	-	-	85	-	-	38.9	-	silty sand (SM)	
ESPOH-23	1	B	D	-	26	41 13	100	100	100	100	96	86	70	53	-	44	38	28	19.9	-	clayey sand (SC)	
	5	B	D	-	9	29 6	100	100	100	100	100	99	86	69	-	59	51	39	28.0	-	silty sand (SM)	
	8	B	D	-	3	NV NP	100	100	100	100	100	96	83	56	-	39	29	16	-	-	slightly silty sand (SP-SM)	
	14	F	D	-	-	-	-	-	-	-	-	-	-	-	-	-	-	-	-	-	sand (SP)*	
	14.5	B	D	-	10	22 NP	100	100	100	100	100	96	90	84	-	79	74	57	37.1	-	silty sand (SM)	
	15-17.5	F	U	-	-	-	-	-	-	-	-	-	-	-	-	-	-	-	-	-	slightly silty sand (SP-SM)*	
	22.5-25	B	U	-	-	-	-	-	-	-	-	-	-	-	-	-	-	-	-	-	slightly silty sand (SP-SM)*	
	25-27	F	U	103	3	NV NP	100	100	100	100	100	-	88	-	-	42	34	-	9.4	-	slightly silty sand (SP-SM)	
	32.5-35	F	U	104	23	18 NP	100	100	100	100	100	-	98	-	-	77	-	-	19.5	-	silty sand (SM)	
	33	B	D	-	24	24 NP	100	100	100	100	100	100	99	96	-	91	84	64	39.6	-	silty sand (SM)	
	40	B	D	-	39	54 11	100	100	100	100	100	95	78	65	-	47	40	30	21.9	-	clayey sand (SC)	
	50	B	D	-	33	56 32	100	100	100	100	100	95	81	65	-	56	50	41	31.1	-	clayey sand (SC)	
	60	B	D	-	8	NV NP	100	100	100	100	86	73	61	53	47	-	42	38	31	24.5	-	silty sand (SM)
	65	B	D	-	3	-	-	-	-	-	-	-	-	-	-	-	-	-	-	-	sandy gravel (GW)*	

* USC Soil Description is based on field classification of soil sample; not on the limited laboratory data shown here.

Laboratory data compilation tables

Test Hole No.	Depth of Sample (ft.)	Tested By Bureau Felix Henry Lepr	Sample Type Undisturbed Disturbed	Density (pcf) Dry	Moisture Content (%)	Atterberg Limits		Sieve Analysis (% Passing)										Clay (%)	USCS Soil Description				
						LL	PI	3/4"	1/2"	3/8"	No. 4	No. 10	No. 20	No. 40	No. 60	No. 65	No. 80			No. 100	No. 140	No. 200	
ESP04-8	2-4	F	U	78	16	61	30	100	100	100	100	100	-	99	-	-	93	-	-	86.6	-	clayey silt (ML)	
	5-7	F	U	92	22	75	40	100	100	100	100	100	-	98	-	-	85	-	-	69.8	-	clayey silt (ML)	
	10	B	D	-	1	NV	NP	100	100	100	79	76	68	52	34	-	26	20	12	6.8	0.9	slightly silty sand (SP-SM)	
	14-16	B	U	105	1	16	NP	100	100	100	100	100	100	97	78	-	60	49	29	15.03	-	silty sand (SM)*	
	19	B	D	-	1	NV	NP	100	100	100	78	65	47	33	21	-	14	11	6	3.8	0.5	gravelly sand (SW)	
	24-26	F	U	96	6	24	J	100	100	100	100	100	-	94	-	-	79	-	-	37.9	-	silty sand (SM)	
	29-31	F	U	95	6	26	NP	100	100	100	100	100	-	95	-	-	64	-	-	38.1	-	silty sand (SM)	
	34-36	F	U	95	9	29	9	100	100	100	100	100	-	95	-	-	80	-	-	54.1	-	sandy silt (ML)	
	39-41	F	U	99	4	NV	NP	100	100	100	99	96	-	71	-	-	50	-	-	18.3	-	silty sand (SM)	
	44	B	D	-	1	NV	NP	100	100	100	98	95	86	67	45	-	34	28	18	11.2	2.4	slightly silty sand (SP-SM)	
49	B	D	-	17	NV	NP	100	100	100	88	83	71	57	39	-	30	24	14	8.0	-	slightly silty sand (SP-SM)		
ESP04-9	2-4	F	U	86	5	21	NP	100	98	98	97	97	-	92	-	-	75	-	-	31.9	-	silty sand (SM)	
	5-7	F	U	85	5	NV	NP	100	100	100	97	95	-	88	-	-	66	-	-	22.0	-	silty sand (SM)	
	14-16	F	U	95	2	NV	NP	100	100	100	100	100	-	96	-	-	54	-	-	6.2	-	slightly silty sand (SP-SM)	
	19-21	B	U	111	2	19	NP	90	-	88	79	69	57	44	31	-	24	19	13	8.16	-	slightly silty sand (SP-SM)*	
	24-26	F	U	101	5	NV	NP	100	100	100	100	100	-	92	-	-	58	-	-	28.4	-	silty sand (SM)	
	29-31	F	U	93	2	NV	NP	100	100	100	100	99	-	84	-	-	35	-	-	7.0	-	lightly silty sand (SP-SM)	
	34-36	F	U	107	3	NV	NP	100	100	99	99	99	-	84	-	-	48	-	-	16.2	-	silty sand (SM)	
	39	B	D	-	1	NV	NP	100	100	100	96	87	68	46	26	-	17	13	7	4.0	-	silty sand (SM)	
	44	B	D	-	2	NV	NP	100	100	100	100	100	99	91	68	-	51	39	20	8.8	1.0	slightly silty sand (SP-SM)	
	49	B	D	-	2	NV	NP	100	100	100	94	92	86	74	51	-	37	28	15	7.0	0.8	slightly silty sand (SP-SM)	
	54	B	D	-	2	NV	NP	100	100	100	99	98	92	83	63	-	48	38	21	9.7	-	slightly silty sand (SP-SM)	
	59	B	D	-	3	NV	NP	100	100	100	94	90	86	75	48	-	34	26	14	6.9	-	slightly silty sand (SP-SM)	
	64	B	D	-	4	NV	NP	100	100	100	99	91	73	48	-	35	27	16	8.6	-	slightly silty sand (SP-SM)		
	69	B	D	-	7	19	NP	100	100	100	100	98	92	77	-	67	60	47	32.0	4.9	silty sand (SM)		
	69-5	B	D	-	20	44	17	100	100	100	100	99	94	82	72	-	68	64	56	44.9	7.6	clayey sand (SC)	
	74	B	D	-	5	19	NP	100	100	100	99	98	94	82	58	-	45	36	23	14.2	-	silty sand (SM)	
	79	B	D	-	17	25	7	100	100	100	100	100	99	93	83	-	75	68	55	41.0	-	silty clayey sand (SM-SC)	
	84	B	D	-	15	24	8	100	100	100	93	90	87	77	59	-	46	38	25	15.7	-	clayey sand (SC)	
	89	B	D	-	12	18	NP	100	100	100	100	100	97	86	72	-	62	54	39	26.6	-	silty sand (SM)	
94-5	B	D	-	7	NV	NP	83	72	72	66	57	46	38	27	-	19	15	8	4.7	-	gravelly sand (SW)		
103-5	B	D	-	25	48	21	100	100	100	100	99	98	90	74	-	66	61	51	42.8	-	clayey sand (SC)		
114	B	D	-	2	-	-	-	-	-	-	-	-	-	-	-	-	-	-	-	-	gravel (GW)*		
124	B	D	-	5	-	-	-	100	100	100	100	100	97	79	51	-	38	31	21	13.4	-	silty sand (SM)*	
ESP04-10	2-4	F	U	82	9	26	5	100	100	100	100	100	-	98	-	-	86	-	-	57.7	-	sandy silt (ML)	
	5-7	F	U	87	13	28	8	100	100	100	100	98	-	86	-	-	79	-	-	63.3	-	silty clay (CL)	
	9	B	D	-	1	NV	NP	100	100	100	100	100	99	94	71	-	51	38	20	8.8	-	slightly silty sand (SP-SM)	
	14-16	F	U	86	4	NV	NP	100	100	100	100	100	-	97	-	-	80	-	-	19.7	-	silty sand (SM)	
	19	B	D	-	1	NV	NP	100	100	100	97	93	81	67	44	-	29	20	10	4.9	-	silty sand (SM)	
	24-26	F	U	96	4	NV	NP	100	100	100	100	100	-	96	-	-	74	-	-	22.5	-	silty sand (SM)	
	29-30	F	U	88	6	25	NP	100	100	100	100	100	-	97	-	-	85	-	-	39.7	-	silty sand (SM)	
	34	B	D	-	6	24	5	100	100	100	100	100	100	96	90	-	82	75	58	38.6	-	silty sand (SM)	
	39	B	D	-	1	NV	NP	100	100	100	88	85	82	70	50	-	38	30	18	9.0	-	slightly silty sand (SP-SM)	
	ESP04-11	2-4	F	U	92	18	26	7	100	100	100	100	99	-	98	-	-	67	-	-	35.6	-	silty-clayey sand (SM-SC)
5-7		F	U	95	21	22	NP	100	100	100	100	100	-	98	-	-	95	-	-	58.8	-	sandy silt (ML)	
9-11		F	U	101	9	21	NP	100	100	100	100	99	-	95	-	-	75	-	-	51.9	-	sandy silt (ML)	
14-16		F	U	88	7	NV	NP	100	100	100	100	100	-	99	-	-	77	-	-	20.9	-	silty sand (SM)	
19-21		F	U	105	8	22	NP	96	94	94	92	92	-	90	-	-	76	-	-	30.4	-	silty sand (SM)	
24-26		B	U	105	6	18	NP	100	100	100	100	100	100	95	75	-	57	44	23	10.95	-	slightly silty sand (SM)*	
29-31		F	U	112	3	28	NP	100	100	100	100	100	100	-	97	-	-	97	-	-	73.1	-	sandy silt (ML)
34-36		F	U	112	3	69	41	100	100	100	100	100	-	98	-	-	89	-	-	68.7	-	sandy clay (CI)	
39-41		F	U	89	28	NV	NP	100	100	100	98	95	-	54	-	-	15	-	-	3.3	-	silty sand (SM)	
41		B	D	-	5	-	-	-	-	-	-	-	-	-	-	-	-	-	-	-	-	-	
44-46		F	U	98	9	NV	NP	100	100	100	100	94	-	49	-	-	23	-	-	13.5	-	silty sand (SM)	
49-51		B	U	99	19	20	NP	100	100	100	100	99	97	89	71	-	59	50	34	20.05	-	silty sand (SM)	
54-56		F	U	107	7	NV	NP	100	100	100	99	99	-	86	-	-	54	-	-	19.2	-	silty sand (SM)	
59-61		F	U	104	3	NV	NP	100	100	99	98	97	-	86	-	-	41	-	-	9.1	-	slightly silty sand (SP-SM)	
61		B	D	-	4	NV	NP	100	100	100	100	99	91	78	55	-	41	32	18	9.0	-	slightly silty sand (SP-SM)	
65-67		F	U	107	6	NV	NP	100	100	96	94	92	-	79	-	-	47	-	-	16.6	-	silty sand (SM)	
67	B	D	-	1	NV	NP	100	95	95	84	75	58	38	18	-	11	7	4	2.0	-	silty sand (SM)		
70	B	D	-	12	NV	NP	100	100	100	100	99	91	77	55	-	41	32	19	10.3	-	slightly silty sand (SP-SM)		
79	B	D	-	8	-	-	-	100	100	100	100	98	90	74	54	-	43	36	24	15.4	-	silty sand (SM)*	

* USCS Soil description is based on field classification of soil sample; not on the limited laboratory data shown here;

Laboratory data compilation tables

Test Hole No.	Depth of Sample (ft.)	Tested By B=Bureau F=Fox H=Hy Dept	Sample Type Undisturbed Disturbed	Density (pcf) Dry	Moisture Content (%)	Archer-Liatsis		Sieve Analysis (% Passing)										Clay <2µ	USCS Soil Description				
						LL	PI	3/4"	1/2"	3/8"	No. 4	No. 10	No. 20	No. 40	No. 60	No. 80	No. 100			No. 140	No. 200		
ESPDI-1	2.5	F	D	-	12	19	NP	100	96	96	96	96	-	91	-	-	66	-	-	23.3	-	silty sand (SM)	
	5	F	D	-	10	NP	NP	100	100	100	99	99	-	94	-	-	64	-	-	17.1	-	silty sand (SM)	
	7.5	F	D	-	15	20	NP	100	100	100	98	98	-	92	-	-	68	-	-	30.6	-	silty sand (SM)	
	10	F	D	-	22	19	NP	100	100	100	100	100	-	97	-	-	78	-	-	37.6	-	silty sand (SM)	
	10.5	F	D	-	39	69	34	100	100	100	100	100	-	100	-	-	87	-	-	65.9	-	sandy silt (MH)	
	12.5	F	D	-	31	32	12	100	100	100	100	100	-	94	-	-	72	-	-	44.6	-	clayey sand (SC)	
	15	F	D	-	26	45	20	100	100	100	100	100	-	95	-	-	81	-	-	56.1	-	sandy clay (CL)	
	17.5	F	D	-	23	28	6	100	100	100	100	100	-	97	-	-	89	-	-	59.8	-	sandy silt (ML)	
	20	F	D	-	16	22	NP	78	78	78	78	78	-	77	-	-	62	-	-	29.4	-	silty sand (SM)	
	22.5	F	D	-	17	45	20	100	100	100	100	99	-	95	-	-	80	-	-	40.4	-	clayey sand (SC)	
	25	F	D	-	10	NV	NP	100	100	100	99	99	-	94	-	-	63	-	-	16.8	-	silty sand (SM)	
	27.5	F	D	-	13	26	6	100	100	100	100	100	-	91	-	-	54	-	-	24.2	-	silty-clayey sand (SM-SC)	
	30	F	D	-	15	20	NP	100	100	100	100	99	-	93	-	-	72	-	-	31.6	-	silty sand (SM)	
	32.5	F	D	-	7	NV	NP	100	100	100	98	95	-	70	-	-	34	-	-	9.0	-	slightly silty sand (SP-SM)	
	35	F	D	-	10	NV	NP	100	100	100	99	97	-	75	-	-	38	-	-	9.5	-	slightly silty sand (SP-SM)	
	37.5	F	D	-	24	NV	NP	100	100	100	100	100	-	99	-	-	90	-	-	34.7	-	silty sand (SM)	
	38	F	D	-	14	19	NP	100	100	100	100	99	-	91	-	-	56	-	-	24.7	-	silty sand (SM)	
	40	F	D	-	10	NV	NP	100	100	100	100	99	-	73	-	-	40	-	-	10.9	-	slightly silty sand (SP-SM)	
	42.5	F	D	-	10	NV	NP	100	100	97	94	91	-	69	-	-	39	-	-	20.3	-	silty sand (SM)	
	45	F	D	-	10	NV	NP	100	98	93	90	87	-	62	-	-	27	-	-	15.3	-	silty sand (SM)	
	47.5	F	D	-	13	NV	NP	100	100	100	100	99	-	83	-	-	45	-	-	25.5	-	silty sand (SM)	
	50	F	D	-	24	33	L3	100	100	100	100	99	-	97	-	-	85	-	-	33.6	-	sandy clay (CL)	
	55	F	D	-	11	NV	NP	100	100	100	99	99	-	90	-	-	61	-	-	26.1	-	silty sand (SM)	
	57.5	F	D	-	6	22	NP	100	100	100	100	100	-	99	-	-	85	-	-	31.1	-	silty sand (SM)	
	60	F	D	-	9	15	L3	100	100	98	97	97	-	94	-	-	77	-	-	44.6	-	clayey sand (SC)	
	62.5	F	D	-	-	-	-	-	-	-	-	-	-	-	-	-	-	-	-	-	-	sandy clay (CL)*	
	63	F	D	-	9	NV	NP	100	100	100	100	100	-	96	-	-	66	-	-	30.9	-	silty sand (SM)	
	65	F	D	-	4	NV	NP	100	100	100	100	100	-	96	-	-	64	-	-	17.5	-	silty sand (SM)	
	67.5	F	D	-	5	NV	NP	100	100	100	100	100	-	81	-	-	36	-	-	10.4	-	slightly silty sand (SP-SM)	
	ESPDI-2	2.5	F	D	-	8	28	NP	100	100	100	100	100	-	96	-	-	86	-	-	47.5	-	silty sand (SM)
		5	F	D	-	7	25	4	100	100	100	100	100	-	99	-	-	88	-	-	49.6	-	silty sand (SM)
		7.5	F	D	-	4	NV	NP	100	100	100	100	100	-	92	-	-	63	-	-	25.1	-	silty sand (SM)
		10	F	D	-	7	29	8	100	100	100	100	100	-	98	-	-	89	-	-	45.6	-	clayey sand (SC)
12.5		F	D	-	4	17	NP	100	100	100	100	100	-	92	-	-	67	-	-	23.6	-	silty sand (SM)	
15		F	D	-	6	NV	NP	100	100	100	100	100	-	98	-	-	92	-	-	34.2	-	silty sand (SM)	
17.5		F	D	-	7	27	10	100	100	100	100	100	-	95	-	-	72	-	-	34.1	-	clayey sand (SC)	
20		F	D	-	8	26	NP	100	100	99	99	99	-	97	-	-	93	-	-	64.5	-	sandy silt (ML)	
22.5		F	D	-	14	54	26	100	100	100	100	100	-	100	-	-	92	-	-	68.5	-	sandy clay (CH)	
23		F	D	-	-	-	-	-	-	-	-	-	-	-	-	-	-	-	-	-	-	-	
25		F	D	-	6	24	NP	100	100	100	100	100	-	99	-	-	92	-	-	39.0	-	silty sand (SM)	
27.5		F	D	-	3	NV	NP	100	100	100	99	99	-	92	-	-	62	-	-	19.4	-	silty sand (SM)	
30		F	D	-	3	NV	NP	100	100	100	100	100	-	99	-	-	79	-	-	23.4	-	silty sand (SM)	
32.5		F	D	-	6	24	NP	100	96	96	95	94	-	91	-	-	82	-	-	47.2	-	silty sand (SM)	
35		F	D	-	6	31	10	100	100	100	100	99	-	97	-	-	91	-	-	34.2	-	clayey sand (SC)	
37.5		F	D	-	3	NV	NP	100	100	100	100	100	-	97	-	-	77	-	-	23.0	-	silty sand (SM)	
40		F	D	-	1	NV	NP	100	100	100	100	99	-	72	-	-	28	-	-	7.4	-	slightly silty sand (SP-SM)	
42.5		F	D	-	2	NV	NP	83	83	81	74	68	-	45	-	-	29	-	-	10.2	-	slightly silty sand (SP-SM)	
45		F	D	-	5	NV	NP	100	100	100	100	99	-	92	-	-	72	-	-	28.9	-	silty sand (SM)	
47.5		F	D	-	2	NV	NP	100	100	100	99	96	-	68	-	-	23	-	-	6.0	-	slightly silty sand (SP-SM)	
50		F	D	-	2	NV	NP	86	79	77	71	62	-	46	-	-	32	-	-	13.4	-	silty sand (SM)	
52.5		F	D	-	8	30	10	100	100	100	100	99	-	96	-	-	85	-	-	53.1	-	sandy clay (CL)	
55		F	D	-	16	55	26	100	100	100	100	100	-	99	-	-	92	-	-	69.2	-	sandy clay (CH)	
57.5	F	D	-	4	17	NP	100	100	100	100	99	-	89	-	-	63	-	-	26.1	-	silty sand (SM)		
60.5	B	D	-	-	-	-	100	100	100	93	89	77	61	35	-	19	16	6	1.3	-	sand (SP)		
62.5	B	D	-	-	-	-	-	-	-	-	-	-	-	-	-	-	-	-	-	-	silty clay (CL)*		
65	B	D	-	-	-	-	100	100	100	100	96	89	75	40	-	25	20	7	2.6	-	sand (SP)		
70	B	D	-	-	-	-	-	-	-	-	-	-	-	-	-	-	-	-	-	-	slightly silty sand (SP-SM)*		

* USCS Soil description is based on field classification of soil sample; not on the limited laboratory data shown here.

This thesis is accepted on behalf of the faculty
of the Institute by the following committee:

John R. MacMillan

Advisor

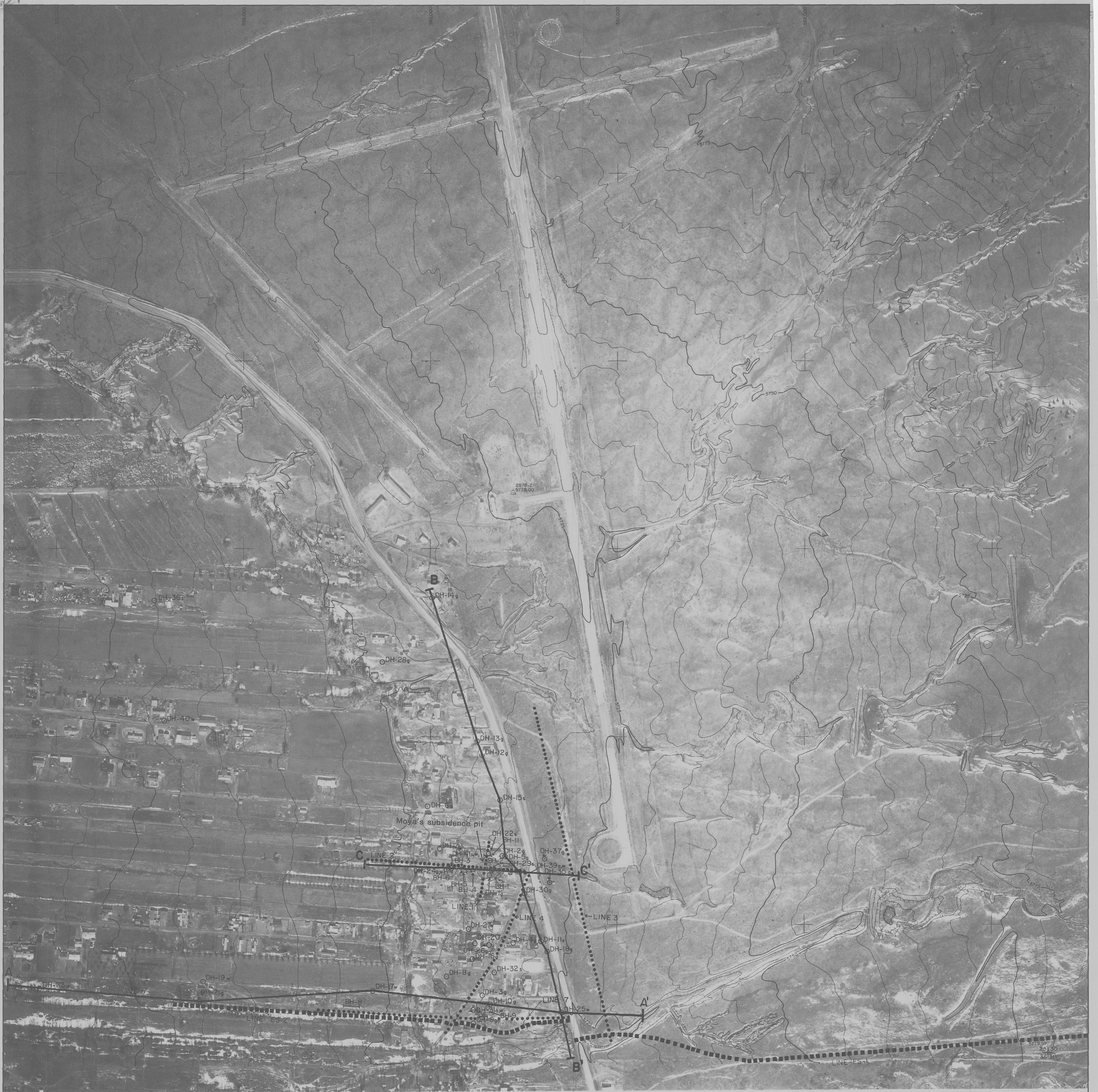
Gary D. J. J. J.

Catherine T. Airone

Jan. 23, 1986

Date

OF 239



28 JUNE 1985

PLATE 1: GEOTECHNICAL ACTIVITY LOCATION MAP

RECTIFIED PHOTO - TOPOGRAPHIC MAP
 OF
 ESPAÑOLA, NEW MEXICO & VICINITY
 FOR
 NEW MEXICO BUREAU OF MINES
 FEBRUARY 1985

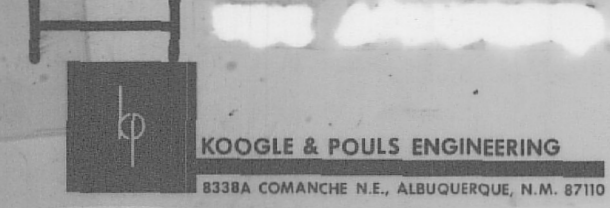
SECTION 25, T. 21 N., R. 8 E.

Reimers, 1986

EXPLANATION

- o DRILL HOLE
- s SETTLEMENT MONITORING WELL
- w WATER MONITORING WELL
- g GEOTECHNICAL WELL
- EXPLORATION TRENCHES
- SEISMIC REFRACTION LINE
- SEISMIC REFLECTION LINE
- GROUND VIBRATION MONITOR

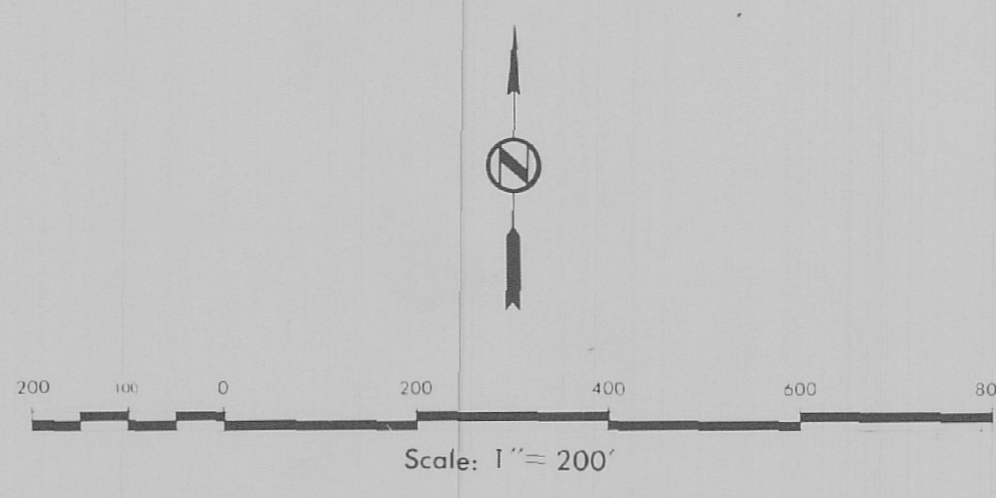
GEOLOGIC CROSS SECTION



- LEGEND
- 1000' NEW MEXICO STATE PLANE GRID COORDINATE, CENTRAL ZONE
 - FIELD CONTROL POINT
 - RECOVERED SECTION CORNER
 - GRAPHICALLY PROJECTED SECTION CORNER
 - INDEX CONTOUR
 - INTERMEDIATE CONTOUR
 - DEPRESSION CONTOUR
 - SPOT ELEVATION

SHEET INDEX

23	24	19
26	25	30
35	36	31
2	1	



CONTOUR INTERVAL 5 FEET
 COMPILED BY PHOTOGRAMMETRIC METHODS
 DATE OF PHOTOGRAPHY JANUARY 15, 1985
 ELEVATIONS ARE BASED ON
 CITY OF ESPANOLA BM 5625.95
 NEW MEXICO STATE PLANE GRID BASED ON
 U.S.C. & G.S. STATIONS JOSE AND JOSE AZ MK
 THIS MAP COMPLIES WITH THE
 NATIONAL MAP ACCURACY STANDARDS

OF 239

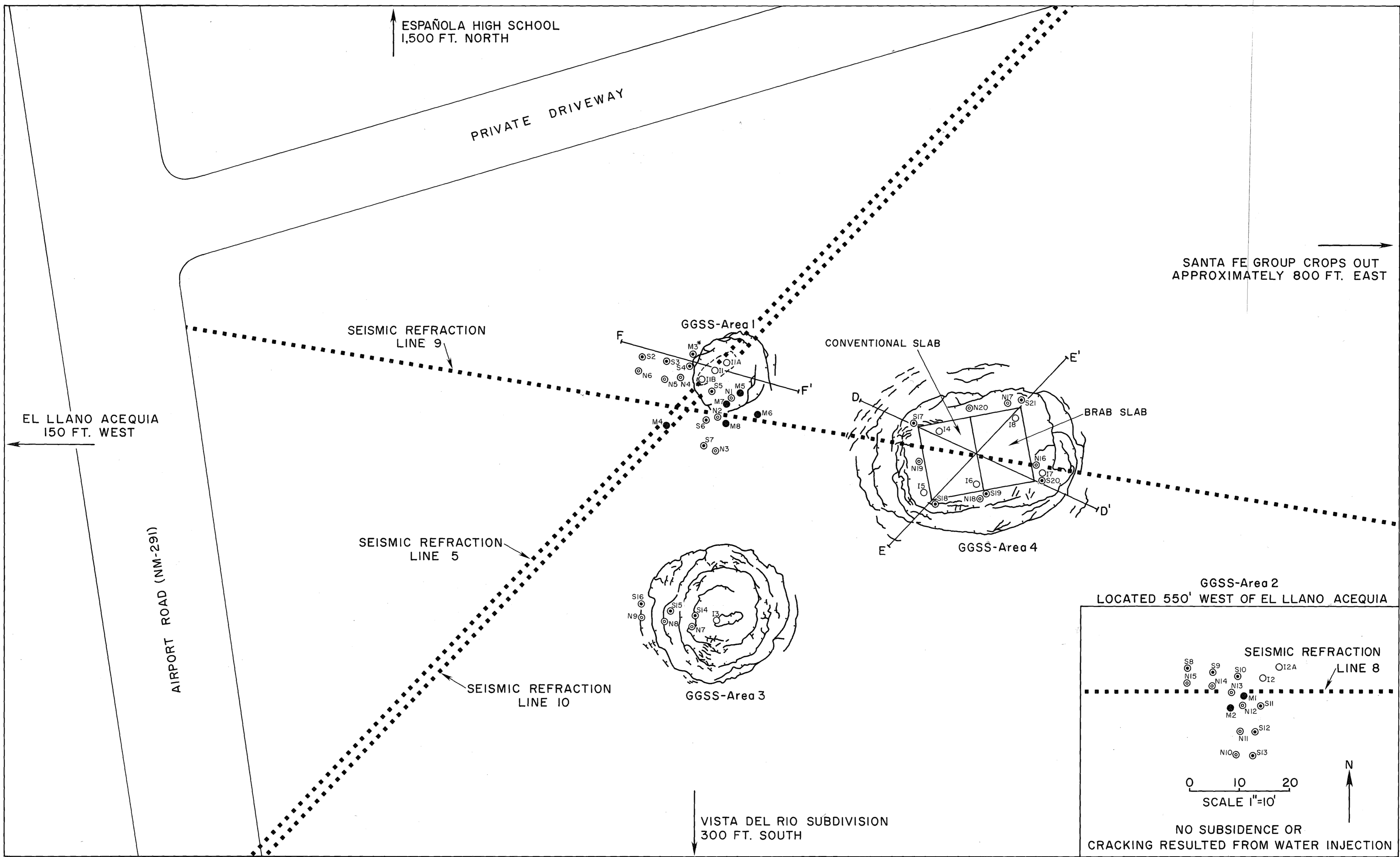
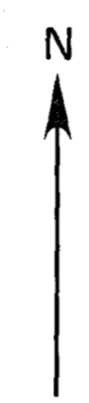


PLATE 2:
Geotechnical Activity Location Map of GGSS-Areas 1-4

0 10 20
SCALE 1"=10'



EXPLANATION

- I13 INJECTION WELL
- ⊙S2 SETTLEMENT MONITORING WELL
- ⊙N18 NEUTRON PROBE MOISTURE AND DENSITY MONITORING WELL
- M6 MOISTURE SAMPLING WELL
- SEISMIC REFRACTION LINE
- F—F' GEOLOGIC CROSS-SECTION
- ~ CRACK WITH BALL ON DOWNTHROWN SIDE
- AREA OF PONDED WATER

*ALTHOUGH M3 WAS ORIGINALLY DRILLED AS A MOISTURE WELL, THEREBY GAINING THE "M" DESIGNATION, A SETTLEMENT MONUMENT WAS SUBSEQUENTLY INSTALLED AND MONITORED.